

Modelling catchment sensitivity to rainfall
resolution and erosional parameterisation in
simulations of flash floods in the UK

A THESIS SUBMITTED TO THE UNIVERSITY OF MANCHESTER
FOR THE DEGREE OF DOCTOR OF PHILOSOPHY
IN THE FACULTY OF SCIENCE AND ENGINEERING

2017

Declan A. Valters

School of Earth and Environmental Sciences

Contents

Abstract	16
Declaration	17
Copyright Statement	18
Acknowledgements	19
1 Introduction	20
1.1 Overview	20
1.1.1 Spatial variability in intense rainfall	21
1.1.2 Numerical modelling of hydrogeomorphic processes	22
1.1.3 Technical and methodological needs	23
1.2 Thesis aims and structure	24
1.2.1 Aims	24
1.2.2 Structure	25
2 Modelling landscape evolution	27
2.1 Introduction	27
2.1.1 Scope	29
2.2 Fundamentals of Landscape Evolution Models	30
2.2.1 Governing Equations	30
2.2.2 Realism and Prediction	31
2.3 Technical Implementation	32
2.3.1 Grid and Discretisation	33
2.3.2 Surface Flow Routing	35
2.3.3 Data Input Sources	36

2.3.4	Boundary Conditions	36
2.4	Current Models	37
2.4.1	CAESAR-Lisflood	37
2.4.2	CHILD	38
2.4.3	FastScape-based LEMs	39
2.4.4	LAPSUS	40
2.4.5	Other LEMs	41
2.5	Uncertainty, Sensitivity, and Calibration	44
2.5.1	Uncertainty	44
2.5.2	Sensitivity and Calibration	45
2.6	Validation & Confirmation	45
2.6.1	Field Confirmation	46
2.6.2	Topographic Metrics	47
2.7	Limitations	47
2.8	Conclusions	48
3	Rainfall representation in current landscape evolution models	50
3.1	Introduction	50
3.2	One-dimensional models	51
3.3	Two-dimensional models	54
3.3.1	Hydrological models	54
3.3.2	Landscape erosion and evolution models	58
3.3.3	Summary of current model capabilities	62
3.4	Research needs for hydrogeomorphology	63
3.4.1	Technological advances and needs	65
3.5	Model choice for further development: CAESAR-Lisflood	66
4	Integration of rainfall radar data with a landscape evolution model	68
4.1	Introduction	68
4.1.1	Rainfall data sources	69
4.1.2	Advantages of radar for hydrological applications	71
4.1.3	Basic principles of Radar	71
4.1.4	Processing and error correction	72

4.2	Rainfall radar in Britain and Ireland	73
4.3	UK 1km Radar Composite Product	74
4.4	Use in landscape evolution models	75
4.4.1	Linking gridded rainfall data with the CAESAR-Lisflood model	75
4.5	Summary	79
5	Development of a numerical landscape evolution model for high-performance computing	80
5.1	Introduction	80
5.2	Model description and parallelisation	82
5.2.1	Origins: CAESAR-Lisflood	82
5.2.2	HAIL-CAESAR	82
5.2.3	Process representation	86
5.2.4	Parallelisation implementation	88
5.2.5	Potential speed up from parallelisation	93
5.3	Testing and benchmarking	94
5.3.1	Regression testing	95
5.3.2	Differences in sediment flux and yields between models and compilers	96
5.3.3	Performance comparison with CAESAR-Lisflood	101
5.3.4	HPC profiling and speed-up	102
5.3.5	Performance scaling on HPC compute nodes	102
5.3.6	Strong scaling	102
5.3.7	Weak scaling	106
5.3.8	Thread profiling	109
5.4	Discussion	110
5.4.1	Parallel scaling	110
5.4.2	Load balancing issues	112
5.4.3	Loop scheduling	113
5.5	Conclusions	114
6	Model setup and parameterisation of two flash flood events in the UK	115

6.1	Background	115
6.2	Meteorological setting	116
6.2.1	Boscastle, Cornwall storm 2004	118
6.2.2	Ryedale, North York Moors storm 2005	119
6.3	Flooding and geomorphic change	120
6.3.1	Boscastle, Cornwall, 2004	120
6.3.2	Ryedale, North Yorkshire, 2005	121
6.4	Experiment design	122
6.4.1	Model initialisation and configuration	123
6.5	Summary	127
7	Sensitivity of a flood-inundation model to rainfall distribution and erosional parameterisation	129
7.1	Introduction	129
7.2	Method	132
7.2.1	Sensitivity analysis of the TOPMODEL m parameter	132
7.3	Results	134
7.3.1	Model sensitivity to the m parameter	134
7.3.2	Catchment hydrographs	138
7.3.3	Flood inundation and river levels	143
7.3.4	Spatial variation in flood inundation	150
7.4	Discussion	158
7.4.1	Rainfall spatial resolution	158
7.4.2	Hydrograph calibration and choice of m parameter value	160
7.4.3	Erosional parameterisation	161
7.5	Conclusions	163
8	Hydrometeorological controls on landscape erosion modelling	166
8.1	Introduction	166
8.1.1	Theory	167
8.1.2	Objectives	169
8.2	Results	170
8.2.1	Catchment sediment flux	170

8.2.2	Spatial variations in channel erosion	173
8.2.3	Local variation in erosion patterns	175
8.3	Discussion	185
8.3.1	Sensitivity to erosion law and rainfall heterogeneity	185
8.3.2	Comparison with observed geomorphic change post-flood	186
8.3.3	Implications for longer-term landscape evolution	189
8.4	Conclusion	190
9	Conclusions	192
9.1	Review of aims and overview of results	192
9.1.1	Flood-inundation model sensitivity	193
9.1.2	Erosion and sediment flux sensitivity	193
9.2	Key themes and synthesis	194
9.3	Technical advances	195
9.4	Future research and applications	196
9.5	Future development of HAIL-CAESAR	197
9.6	Summary	199
A	Software availability	232
A.1	Radar data processing code	232
A.2	HAIL-CAESAR landscape evolution model code	232
A.3	Figure plotting software	232
B	Paper reprint	233

Word count 74333

List of Tables

2.1	Feature comparison of widely used landscape evolution models. Process representation shown by model in blue/pink/white matrix.	43
3.1	User defined parameters in the Han et al. (2015) orographic rainfall model implemented in CHILD.	62
5.1	Summary of most expensive program functions, using a test case of a 48 hour flood simulation, with the model run in hydrology-only mode . The test case is based on the flooding that took place in the Boscastle (River Valency) catchment in August 2004, in Cornwall, UK (Golding et al., 2005).	89
5.2	Summary of most expensive program functions, with erosion processes enabled , using a test case of a 48 hour flood simulation. The test case is based on the flooding that took place in the Boscastle (River Valency) catchment in August 2004, in Cornwall, UK (Golding et al., 2005).	89
5.3	Idealised potential speed-up according to Amdahl's law (equation 5.8). Value for P calculated using profiling results from the Boscastle (River Valency) flood test simulation after 48 hours simulated time.	94
5.4	Initial performance and compilation comparison with CAESAR-Lisflood, using the River Swale test case, 50m DEM, 10 year simulation	102
5.5	Strong scaling test cases used to benchmark the HAIL-CAESAR model, using Swaledale and Boscastle DEMs.	103

5.6 Weak scaling test cases with the Boscastle DEM resampled at increasing resolutions from 0.5m to 5m. The absence of run-time results for certain erosion simulations is due to memory limitations preventing higher resolution simulations from running.	108
6.1 Table showing key characteristics of each storm event.	117
6.2 Outline of the simulations carried out for both the Ryedale and Boscastle case studies.	123
6.3 Start and end times (UTC) for each 72 hour simulation. The major rainfall event occurs during the second day in each simulation.	125
7.1 TOPMODEL m parameter values used to run sensitivity simulations for each type of rainfall input types (Uniform and Gridded) for the Ryedale catchment.	133
7.2 Peak water discharges and corresponding times at peak flow for each of the simulation cases. Discharge is calculated at the outlet of the catchment model domain. Time is given in UTC on the day of the storm.	143

List of Figures

2.1	The evolution of landscape evolution models.	28
2.2	Conservation of mass in a soil mantled landscape or sediment covered channel (after Dietrich et al. (2003) and Tucker and Hancock (2010)). η is the surface elevation, B is the boundary (base-level) change, q_s the sediment transport term, and dx the grid cell size in a discretised landscape (assuming regular grid-spacing in this example).	31
2.3	Main components and boundary conditions of a landscape evolution model. Boundary conditions include the climatic, tectonic and base-level conditions (rainfall and uplift), as well as the conditions specified on the model domain edges, such as where water and sediment can leave the model domain (shown by the red line). Channel network shown by blue lines. Erosion rate (red-yellow) is shown as a grid cell variable in this example.	33
2.4	A comparison of two terrain-discretisation approaches. (Top) Regular, rectangular gridded discretisation. (Bottom) TIN, (Triangulated Irregular Network), with adaptive re-meshing. (Re-drawn from Tucker, et al. 2001b).	34
2.5	Comparison of single- and multiple flow direction routing methods. (Re-drawn from Schäuble et al. (2008)).	36
2.6	CAESAR-Lisflood simulating the flooding of Carlisle, UK, 2005. Hydrogeomorphic effects of single floods can be simulated in this LEM due to the implementation of a non-steady flow hydrological component (Bates et al., 2010). Blue to pink colouring represents water depth, with pink indicating the deepest water depths. Model domain 5 km across.	38

4.1	Network of weather radar stations in the British Isles and Ireland. <i>Source: National Meteorological Library, Met Office, UK.</i>	74
4.2	From the UK composite radar product (a), subgrids of the study area extracted for the time period of interest (b). The number of radar image pixels in each subgrid determines the number of hydroindex zones used in the model initialisation.	77
4.3	(a) Using the extracted radar data subgrids, a timeseries file is created mapping each radar image pixel to a hydroindex zone, for every time step. The hydroindex grid file must be the same dimensions and grid-spacing as the input terrain DEM (b). Numbering each radar image pixel in one of the extracted subgrids (c), the hydroindex file (d), is created from mapping the pixel indexes to the same resolution grid as the terrain input DEM.	78
5.1	Flow chart showing a simplified outline of the HAIL-CAESAR program flow. Grey shaded boxes indicate sections of the code parallelised with OpenMP. Rounded rectangles indicate output and input files.	85
5.2	Water discharge rates over first 250 days of simulation. Outputs from the Swale 10 year at 50m resolution test case, showing results from the original CAESAR-Lisflood model and HAIL-CAESAR model compiled under two different compilers: Intel and GCC. The inset highlights the typical magnitude of difference in water discharge where the hydrographs diverge.	98
5.3	Catchment sediment flux over first 250 days of simulation. Outputs from the Swale 10 year at 50 m resolution DEM test case, showing results from the original CAESAR-Lisflood model and HAIL-CAESAR model compiled under two different compilers: Intel and GCC. The inset is to highlight the typical magnitude in sediment flux difference where the outputs diverge.	99
5.4	Cumulative catchment sediment flux over full duration of simulation. Outputs from the Swale 10 year at 50 m DEM resolution test case, showing results from the original CAESAR-Lisflood model and HAIL-CAESAR model compiled under two different compilers: Intel and GCC.	100

5.5	Speed-up achieved relative to serial code on 2, 4, 8, 12, 16, 20, 24, 30, 36, 42, and 48 cores. Four sets of simulations are used representing a range of model uses from short, single event episodes (48–72hr) to 1 year simulations.	105
5.6	Weak scaling with the Boscastle DEM at increasing resolution (see Table 5.6). Hydrological and erosion-enabled simulations shown. Each simulation uses c.150 000 grid cells per CPU. The absence of results for certain erosion simulations is due to memory limitations preventing higher resolution simulations from running.	107
5.7	Thread profiling of the Swale 1 year simulation with 50m DEM. Data from major functions only displayed.	110
6.1	Location of the two case study catchments in Britain, marked by the main settlement within each catchment.	117
6.2	Total accumulated radar rainfall (24 hours) over the Valency (Boscastle) catchment during the 16th August 2004.	119
6.3	Total accumulated radar rainfall (24 hours) over the Ryedale catchment during the 19th June 2005.	120
7.1	Hydrograph sensitivity to the m parameter under uniform rainfall inputs. Discharge over time at the Ryedale catchment outlet for varying values of the m parameter. The measured discharge at the catchment gauging station is overlaid in dashed line. The results from the simulations with $m > 0.008$ are omitted for clarity due to the low discharges they produced.	136
7.2	Hydrograph sensitivity to the m parameter under gridded rainfall inputs. Discharge over simulation time at the Ryedale catchment outlet for varying values of the m parameter. The measured discharge at the catchment gauging station is overlaid in dashed line. The results from the simulations with $m > 0.008$ are omitted for clarity due to the low discharges they produced.	137

7.3	Boscastle hydrographs (discharge over time at catchment outlet) for each simulation of the 2004 Boscastle event listed in Table 6.2. Inset shows detail of main flood peaks around hour 40 of the simulation.	141
7.4	Ryedale hydrographs (discharge over time at catchment outlet) for each simulation of the 2005 Ryedale event listed in Table 6.2.	142
7.5	Total inundation area (km^2) covered by floodwaters in the Boscastle (top) and Ryedale (bottom) catchments throughout the duration of the each storm. Inundation area is shown for each combination of flood-only, erosion-enabled, gridded rainfall input, and uniform rainfall input simulation. The erosion-enabled simulations use the transport-limited erosion law (TLIM). Detachment limited erosion cases were omitted for clarity.	147
7.6	Mean floodplain water depth (metres) in the Boscastle (top) and Ryedale (bottom) catchments throughout the duration of the each storm. Floodplain is defined using the Clubb et al. (2017) floodplain delineation algorithm.) Water depth is shown for each combination of flood-only, erosion-enabled, gridded rainfall input, and uniform rainfall input simulation. The erosion-enabled simulations use the transport-limited erosion law (TLIM). Detachment limited erosion cases were omitted for clarity. .	148
7.7	Main channel mean water depth (metres) in the Boscastle (top) and Ryedale (bottom) catchments throughout the duration of the each storm. The main channel is defined as the highest-order stream in each catchment (Strahler, 1957) and excludes all minor tributaries. Water depth is shown for each combination of flood-only, erosion-enabled, gridded rainfall input, and uniform rainfall input simulation. The erosion-enabled simulations use the transport-limited erosion law (TLIM). Detachment limited erosion cases were omitted for clarity.	149
7.8	Location map of the Boscastle catchment and Valency river valley, with the village of Boscastle shown. Location of the zoom-in images in Figures 7.9 (A) and 7.10 (B) shown in rectangular outlines.	151

7.9	Flood extents in the Boscastle catchment around the village area (location A on the overview map in Figure 7.8) at the time of maximum river discharge for each simulation.	152
7.10	Flood extents in the Boscastle catchment around the upstream confluence area (location B on the overview map in Figure 7.8) at the time of maximum river discharge for each simulation.	153
7.11	Location map of the Ryedale catchment and Rye river valley, with the village of Helmsley shown. Location of the zoom-in images in Figures 7.12 (A), 7.13 (B), and 7.14 (C) shown in rectangular outlines.	154
7.12	Flood extents in the Ryedale catchment in the floodplain area south of Helmsley (location C on the overview map in Figure 7.11) at the time of maximum river discharge for each simulation.	155
7.13	Flood extents in the Ryedale catchment in the area surrounding Helmsley village (location B on the overview map in Figure 7.11) at the time of maximum river discharge for each simulation.	156
7.14	Flood extents in the Ryedale catchment in the gorge area west of Helmsley village (location A on the overview map in Figure 7.11) at the time of maximum river discharge for each simulation.	157
8.1	Ryedale sediment flux (Total sediment volume output per hour at catchment outlet) for each erosion-enabled simulation of the 2005 Ryedale event listed in Table 6.2.	171
8.2	Boscastle sediment flux (total sediment volume output per hour at catchment outlet for each erosion-enabled simulation of the 2004 Boscastle event listed in Table 6.2.	172
8.3	Channel averaged elevation difference along the main river channel in the Valency catchment. Simulation using the transport limited erosion parametrisation. Longitudinal profile is averaged over bins spaced every 50m. Transverse averaging (across the channel) is done over a 10m wide section centred on the channel midpoint. Results from the GRIDDED_TLIM simulation shown in blue and the UNIFORM_TLIM simulation shown in green.	174

8.4	Channel averaged elevation difference along the main river channel in the Ryedale catchment. Simulation using the transport limited erosion parametrisation. Longitudinal profile is averaged over bins spaced every 200m. Transverse averaging (across the channel) is done over a 10m wide section centred on the channel midpoint. Results from the GRIDDED_TLIM erosion simulation shown in blue and the UNIFORM_TLIM simulation shown in green.	175
8.5	Boscastle. River Valency main channel in vicinity of Boscastle village. Net difference in elevation after 72 hours simulation, showing the gridded and uniform rainfall simulations, for each of the two erosion law end-members (transport-limited and detachment-limited). Elevation change smaller than $\pm 0.2\text{m}$ in magnitude is not shown for clarity. Boscastle harbour is located in the upper left corner of each figure.	177
8.6	Boscastle. South-east section of catchment showing the Lesnewth Stream tributary channel. Net difference in elevation after 72 hours simulation, showing the gridded and uniform rainfall simulations, for each of the two erosion law end-members (transport-limited and detachment-limited). Elevation change smaller than $\pm 0.2\text{m}$ in magnitude is not shown for clarity.	178
8.7	Ryedale. South-east section of Ryedale catchment showing the area around the village of Helmsley. Net difference in elevation after 72 hours simulation, showing the gridded and uniform rainfall simulations, for each of the two erosion law end-members (transport-limited and detachment-limited). Elevation change smaller than $\pm 0.2\text{m}$ in magnitude is not shown for clarity.	179
8.8	Boscastle. Map of extent of catchment change in elevation greater than 0.02m. Change in elevation shown after 72 hours of model simulation using gridded rainfall and the transport limited erosion law. Output from the gridded rainfall input, transport-limited erosion simulation (GRIDDED_TLIM). Logarithmic scale for erosion.	180

8.9	Boscastle. Map of extent of catchment change in elevation greater than 0.02m. Change in elevation shown after 72 hours of model simulation using uniform rainfall and the transport limited erosion law. Output from the uniform rainfall, transport-limited simulation (UNIFORM_TLIM). Logarithmic scale for erosion.	181
8.10	Ryedale. Map of extent of catchment change in elevation greater than 0.02m. Change in elevation shown after 72 hours of model simulation using uniform rainfall and the transport limited erosion law. Output from the uniform rainfall, transport-limited simulation (GRIDDED_TLIM). Logarithmic scale for erosion.	182
8.11	Ryedale, upper Rye channel. Map of extent of erosion and deposition greater than 0.02m in magnitude. Change in elevation shown after 72 hours of model simulation using gridded rainfall and the transport-limited erosion law (GRIDDED_TLIM). Logarithmic scale for erosion. .	183
8.12	Ryedale, upper Rye channel. Map of extent of erosion and deposition greater than 0.02m in magnitude. Change in elevation shown after 72 hours of model simulation using gridded rainfall and the detachment-limited erosion law (GRIDDED_DLIM). Logarithmic scale for erosion. .	184

The University of Manchester

Declan A. Valters

Doctor of Philosophy

Modelling catchment sensitivity to rainfall resolution and erosional parameterisation in simulations of flash floods in the UK

31st August 2017

The contribution of this thesis is twofold: 1) the development of a hydrodynamic landscape evolution model for use on high-performance computing systems and 2) assessing the sensitivity of hydrogeomorphic processes to high-resolution rainfall input data and erosional parameterisation using the model.

The thesis addresses a limitation in numerical landscape evolution models regarding how spatial variation in rainfall is represented or parameterised within such models. Typically, landscape evolution models forsake a realistic representation of rainfall patterns in favour of a simpler treatment of rainfall as being spatially homogeneous across the model domain. This simplification of rainfall spatial variability is still made despite the fact that many geomorphological processes are sensitive to thresholds of sediment entrainment and transport, driven by the distribution and movement of water within the landscape.

The thesis starts by exploring current limitations in rainfall representation in landscape evolution models, and assesses various precipitation data sources that could be potentially used as more realistic rainfall inputs to landscape evolution models. A numerical model of landscape evolution is developed for deployment on high-performance parallel computing systems, based on the established CAESAR-Lisflood model (Coulthard et al., 2013). The new model code is benchmarked, showing performance benefits compared with the original CAESAR-Lisflood model it is based on.

The model is applied to assessing the sensitivity of flood-inundation predictions, sediment flux, and erosion distribution within river catchments to spatial variation in rainfall during extreme storm events. Two real storm events that caused localised flash flooding in the UK are used as test cases: the Boscastle storm of 2004 and the North York Moors storm of 2005.

Flood extent predictions and river discharges are found to be sensitive to the use of spatially variable input rainfall data, with high-resolution rainfall data leading to larger peak flood discharges. However, the differences are less pronounced in smaller catchments. The role of sediment erosion during large floods is also assessed, but it is found to play a minor role relative to spatially variable rainfall data. In contrast, the geomorphological response of catchments to single storm events is shown to be less sensitive to the spatial heterogeneity of rainfall input and controlled more strongly by the choice of erosional process parameterisation within the model. Nonetheless, spatial variability in rainfall data is shown to increase sediment yields during flash flood simulations.

Declaration

No portion of the work referred to in the thesis has been submitted in support of an application for another degree or qualification of this or any other university or other institute of learning.

Copyright Statement

- i. The author of this thesis (including any appendices and/or schedules to this thesis) owns certain copyright or related rights in it (the “Copyright”) and s/he has given The University of Manchester certain rights to use such Copyright, including for administrative purposes.
- ii. Copies of this thesis, either in full or in extracts and whether in hard or electronic copy, may be made **only** in accordance with the Copyright, Designs and Patents Act 1988 (as amended) and regulations issued under it or, where appropriate, in accordance with licensing agreements which the University has from time to time. This page must form part of any such copies made.
- iii. The ownership of certain Copyright, patents, designs, trade marks and other intellectual property (the “Intellectual Property”) and any reproductions of copyright works in the thesis, for example graphs and tables (“Reproductions”), which may be described in this thesis, may not be owned by the author and may be owned by third parties. Such Intellectual Property and Reproductions cannot and must not be made available for use without the prior written permission of the owner(s) of the relevant Intellectual Property and/or Reproductions.
- iv. Further information on the conditions under which disclosure, publication and commercialisation of this thesis, the Copyright and any Intellectual Property and/or Reproductions described in it may take place is available in the University IP Policy (see <http://documents.manchester.ac.uk/DocuInfo.aspx?DocID=24420>), in any relevant Thesis restriction declarations deposited in the University Library, The University Library’s regulations (see <http://www.manchester.ac.uk/library/about/regulations>) and in The University’s Policy on Presentation of Theses.

Acknowledgements

This work was funded by the Natural Environment Research Council doctoral training grant number NE/L501591/1.

Data was provided by the British Atmospheric Data Centre, the Environment Agency (England), Ordnance Survey Open Data, and the UK National River Flow Archives.

This work used the ARCHER UK National Supercomputing Service (<http://www.archer.ac.uk>) and the Centre for Environmental Data Analysis JASMIN computing facility (<http://www.jasmin.ac.uk/>).

1

Introduction

1.1 Overview

Intense rainfall has the power to cause flash flooding and drive rapid landscape change in a single storm. Rainfall input to river catchments is one of several controls on runoff generation, flood inundation, and sediment dynamics during storms. Understanding how river catchments are sensitive to rainfall patterns during severe storms is important for improving our ability to predict flood events and the impact they have on the landscape. Flash floods and the geomorphic effects they have on the landscape pose a risk to communities living in the vicinity of rivers and their floodplains. The majority of the world's population live in temperate or sub-tropical climate regions on the Earth, where water is one of the main forces acting on the landscape and presents a risk to large populations living in proximity to rivers and their floodplains (Plate, 2002). Flash flooding from intense rainfall can lead to catastrophic consequences for the communities it affects, including loss of life, economic impacts, and damage to the environment (Barredo, 2009; Bennett, 2014). The economic damages in years with substantial flooding events can be costly to residents, businesses, and government. The average economic cost of flooding is estimated at around £1.1 billion annually in England, which could rise to as much as £27 billion by 2080 (Bennett, 2014). The year-to-year impacts from flooding are highly variable, for example, the total costs of the 2007 flooding in the UK was estimated at £3 billion. Outwith the UK, global economic costs due to flooding in the same year were approximately £40 billion (Pitt, 2008). The variability in the severity of flooding from year-to-year can make mitigation

planning difficult, as there is a large degree of natural variability as well as a general increase in likelihood of intense rainfall events in the UK (Kendon et al., 2014).

Storm events also drive landscape evolution over longer timescales through the cumulative effects of flash flood events over decades and centuries, as well as global changes in the Earth's atmosphere and tectonic activity (Molnar and England, 1990; Molnar, 2001; Whipple and Meade, 2006). Understanding the sensitivity of catchment-scale erosional processes to rainfall variability is therefore important to increasing our knowledge of landscape evolution theory. The duration and intensity of storms is known to have an effect on the long term morphological evolution of landscapes (Sólyom and Tucker, 2004; Sólyom and Tucker, 2007), as is the effect of orographic precipitation on mountain range morphology (Han et al., 2015).

Improving predictions of how catchments respond to intense rainfall, and its impacts on the landscape, is of critical importance to society, as well as for advancing hydrological and geomorphological theory.

1.1.1 Spatial variability in intense rainfall

Rainfall is perhaps the most straightforward and direct cause of flooding. Where more rain falls in a period of time than can be transported by a river channel, or stored in other parts of the river catchment, flooding will occur. Indeed, the “absurdly simple” concept known as the First Law of Quantitative Precipitation states that the highest rainfall totals are observed where the rainfall rate is highest for the longest period of time (Doswell et al., 1996). Despite its apparent simplicity, rainfall spatial and temporal patterns can be highly variable down to the catchment scale. The susceptibility of catchments to flash flooding from intense rainfall is dependent on the spatial and temporal distribution of rainfall inputs, as well as the physical characteristics of a river catchment, such as its vegetation cover, soil saturation, sediment dynamics, channel morphology, and catchment hydromorphometry.

During rain storms, the distribution of rainfall varies in time and space. The spatial distribution of rainfall in a storm is dependent on atmospheric conditions such as the distribution and content of moisture in the atmosphere, wind direction and speed, as well as topography, which can lead to the orographic enhancement of rainfall (Roe, 2003; Roe, 2005; Houze, 2012). Spatial variability in rainfall patterns is relative to the

size of the catchment over which rain falls and the size of the rainfall feature. From the perspective of the stationary river catchment, rainfall spatial variability is also determined by how a rain cell or cells move across a catchment during the course of the storm (Willems, 2001). Typically, rainfall events associated with convective activity, such as occurring in the summer months of the UK, have the potential to create the most spatial variability relative to river catchments, due to their geographically focused characteristics. Convective-style rainfall events are also typically associated with the short intense rainfall events that have led to flash flooding in UK catchments (Gray and Marshall, 1998; Bell and Moore, 2000; Browning et al., 2007; Blackburn et al., 2008; Kendon et al., 2014), as well as other catchments further afield (Doswell, 1993; Doswell et al., 1996). Spatial variability in convective rain cells can vary considerably; generalised models of rain cell structure shows their spatial distribution of rainfall intensities to be described by a Gaussian distribution (Luyckx et al., 1998; Willems, 2001), or to put it more evocatively, the shape of a “wizard’s cap” (Sólyom and Tucker, 2007, p. 86), with rainfall intensities peaking sharply in the centre of the cell and then decaying rapidly towards the edges.

In summary, there are many sources of rainfall spatial variability during intense rainfall events at a range of scales, yet from a numerical modelling perspective these are often overlooked in favour of more simplistic treatments of rainfall input. Though some research has been directed at understanding the sensitivity of purely hydrological models to rainfall spatial variability (Krajewski et al., 1991; Nicótina et al., 2008; Segond et al., 2007), in hydrodynamic landscape erosion and evolution models it remains to be fully investigated.

1.1.2 Numerical modelling of hydrogeomorphic processes

Studying the impact of flash flooding on the landscape has been of interest to the hydrological, meteorological, and geomorphological communities for centuries. (e.g. Dana, 1882; Schumm, 1979; Costa and O’Connor, 1995). Hydrological models designed to understand and predict flooding in river channels and catchments have existed for over 150 years (Mulvaney, 1851), originally arising from civil engineering needs to determine the capacity of culverts and other man-made structures transporting water within river catchments. Mulvaney’s model, later termed *the Rational Method*,

was a simple equation designed to capture the key components of the catchment water sources and the resulting peak discharge. The peak discharge, Q_p , is given as follows:

$$Q_p = CA\bar{R} \quad (1.1)$$

The Mulvaney equation captures two important components of catchment hydrology: the total catchment area, A , and the maximum catchment-averaged rainfall, \bar{R} , as well as an empirically-derived parameter, C .

Numerical models have enabled us to address many questions in the theoretical understanding of landscape response to intense rainfall events, such as the influence of stochastic variability in storm intensity and duration (Tucker and Bras, 2000) and the relative importance of storms in runoff production (Darby et al., 2013). Numerical landscape evolution models have proved useful, if imperfect, tools for the prediction of flooding and landscape change (Tucker and Hancock, 2010) both in the short term (Beven et al., 1984), and in response to longer-duration changes in rainfall events associated with climate change (e.g. Coulthard et al., 2000; Coulthard et al., 2012a; Hancock et al., 2017).

Predicting the impacts of flash flooding has been aided greatly by the use of numerical models. However, most models, particularly those incorporating landscape erosion processes, typically assume a uniform input of rainfall across the area being studied or simulated. In many meteorological situations, this is unrealistic and does not capture the true spatial and temporal variation in rainfall patterns. As many erosional processes are both a) strongly coupled to hydrological processes (Sidle and Onda, 2004; Loague et al., 2006; Beven and Carling, 1989) and b) threshold dependent (Snyder et al., 2003b) or non-linear (Coulthard et al., 1998; Phillips, 2003), it follows that numerical models which do not realistically capture heterogeneity in rainfall inputs will not accurately predict the distribution of floodwaters and the distribution of erosion during spatially heterogeneous rainfall events.

1.1.3 Technical and methodological needs

To investigate whether hydro-geomorphic processes are sensitive to the spatial detail of rainfall patterns, we first need a numerical model that can capture heterogeneity in rainfall inputs, either through the input of rainfall data from external sources, such

as weather radar or numerical weather prediction model output, or through synthetic rainfall data generation (e.g. Peleg and Morin, 2014). The model should be capable of simulating flood inundation and sediment dynamics as well as representing both spatially variable and spatially uniform rainfall inputs. The choice of model could be made from the existing range of landscape evolution models available (Chapter 2), from developing a new numerical model from scratch, or taking an existing model and extending its functionality beyond simple rainfall representation. A review of rainfall representation in existing landscape evolution models is discussed in Chapter 3, where the current limitations in existing modelling approaches are highlighted.

1.2 Thesis aims and structure

1.2.1 Aims

The aims of this thesis are twofold: firstly to address the technological and methodological needs outlined previously through the development of a suitable numerical landscape evolution model, secondly, to use this model to investigate the sensitivity of flood inundation predictions to rainfall heterogeneity and erosional parameterisation within the model. In the context of this thesis, sensitivity to rainfall spatial variability is evaluated in terms of comparing spatially uniform rainfall data with high-resolution rainfall radar data (Chapter 4). Sensitivity to erosion law parameterisation, for the purposes of the simulations carried out is assessed through varying the choice of erosion and sediment transport laws available in the numerical model, described in Chapter 5. The thesis aims can be summarised as follows:

1. Develop and test a landscape evolution model capable of simulating landscape erosion and flood inundation, incorporating high-resolution rainfall data inputs such as rainfall radar or numerical weather prediction model output.
2. Assess the sensitivity of flood inundation predictions during intense rainfall events to two competing factors:
 - (a) The spatial variability of input rainfall data.
 - (b) The choice of erosion law parameterisation.

3. Assess the sensitivity of sediment yields and spatial distribution of erosion during intense rainfall events to the spatial resolution of rainfall input data. The same two factors in are assessed as sources of sensitivity:
 - (a) The spatial variability of input rainfall data.
 - (b) The choice of erosion law parameterisation.

1.2.2 Structure

Following this introductory chapter, Chapter 2¹ presents an overview of landscape erosion and evolution models (LEMs), their underlying principles and implementation including a discussion of the capabilities and limitations of current landscape evolution models. Chapter 3 reviews the current approaches in the numerical modelling literature to represent rainfall and rainfall spatial variability in landscape evolution models, and highlights the current limitations in such approaches. The current research questions in hydro-geomorphological sensitivity to rainfall spatial variability are discussed in tandem with the technical developments required in numerical models to better address these questions. Chapter 4 presents an overview of rainfall radar data sources, with a focus on data products available in the UK. Based on the discussion and conclusions in Chapter 3, it was decided to re-develop an existing model and extend its functionality to enable ensemble simulations on high-performance computing (HPC) services, using high-resolution rainfall radar as input data to the model. The technical development of the model is discussed in Chapter 5 and the performance and parallel scalability of the model code is assessed. The investigation of aims 2) and 3) is presented in the remaining chapters: Chapter 6 presents two case studies of flash flooding in the UK, which are used in the following chapters to investigate hydro-geomorphic sensitivity to rainfall spatial heterogeneity and erosion process parameterisation. The meteorological background and impact of the two events is described and the set-up of the numerical modelling experiments is presented. Chapter 7 assesses how the flood-inundation component of the model is sensitive to the choice of erosional process parameterisation and to the resolution of rainfall input data. Chapter 8 focuses on

¹An extended version of Chapter 2 was published in the British Society for Geomorphology's *Geomorphological Techniques* collection of technical review papers (Valters, 2016). A reprint of the article is presented in Appendix B.

how sediment flux and the spatial distribution of erosion during an intense rainfall event is sensitive to both the choice of erosion law and the resolution of rainfall input data. A further discussion and conclusion, synthesising the results of the preceding chapters is presented in Chapter 9.

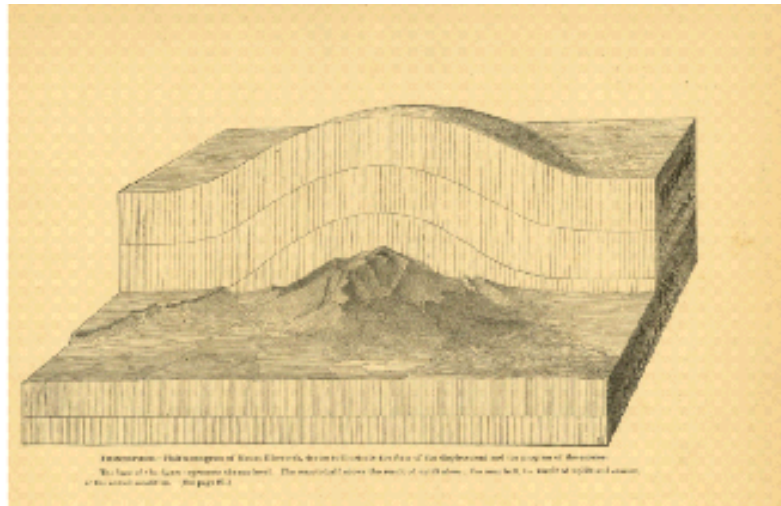
2

Modelling landscape evolution

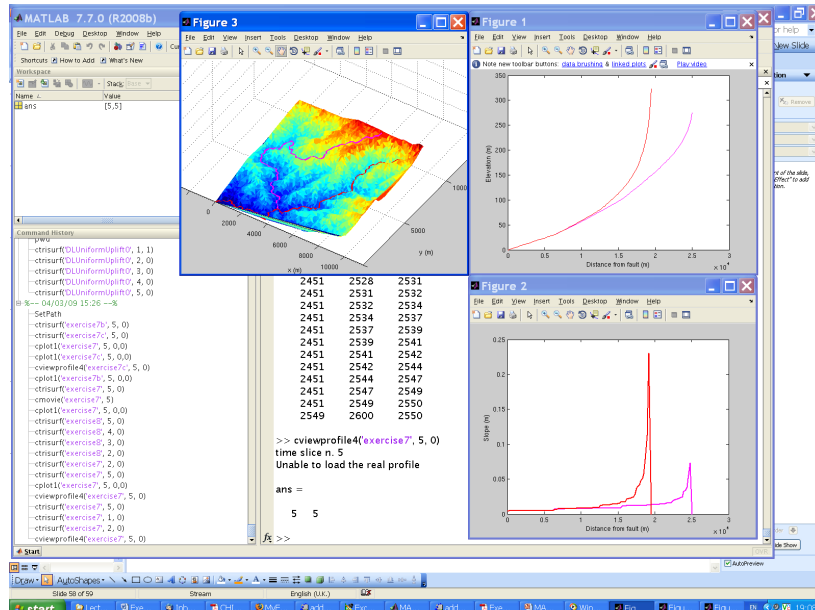
2.1 Introduction

¹Landscape evolution models (LEMs) are quantitative tools used to simulate Earth surface processes and the evolution of the land surface. LEMs can be used to deduce whether hypotheses about landscape evolution are likely to be valid, by making quantitative predictions about their development. The earliest LEMs were conceptual and largely qualitative, such as the early pictorial landscape evolution diagrams by Gilbert and Dutton (1877), Figure 2.1a. Gilbert's model contains many of the key components in a modern LEM. The background schematic depicts the effect of an uplift field alone on the landscape, and the foreground depicts the combined effects of uplift and erosion. Gilbert also recognised the important concept of boundary conditions in LEMs, stating that the base of the diagram represents a fixed sea-level in this case. These early models offered insight into the potential course of landscape evolution, and sowed the seeds for the later development of LEMs that abound today. In Figure 2.1b, a computer-based LEM (CHILD, Tucker et al., 2001a) is shown, with the components of boundary conditions, uplift, and other process representations that are still core concepts in modern LEMs. The advent of computerised, numerical LEMs, such as those in Figure 1b, along with high-resolution digital topographic data provide important quantitative tools for investigating landscape process and form.

¹An extended version of this chapter was published in the British Society for Geomorphology's *Geomorphological Techniques* article series. (Valters, 2016)



(a) The diagrammatic LEM of Gilbert and Dutton (1877).



(b) A computer numerical landscape evolution model (CHILD, Tucker et al., 2001a).

Figure 2.1: The evolution of landscape evolution models.

2.1.1 Scope

This chapter provides a practical guide to the usage of numerical LEMs. Readers interested in detailed theoretical aspects of landscape evolution modelling should refer to other detailed literature reviews, such as those by Pazzaglia (2003), Martin and Church (2004), Willgoose (2005), and Tucker and Hancock (2010). Other reviews focus on the use and application of LEMs, such as Willgoose and Hancock (2011), Van De Wiel et al. (2011), and Temme et al. (2013). This chapter is not solely a software-type review of different LEMs (e.g. Coulthard, 2001), though comparisons between the features of various LEMs will be made to aid the prospective landscape evolution modeller. In short, the chapter aims to provide an overview of the usage, theoretical background, and software features of mainstream LEMs at the present time.

Physical analogue models of landscape evolution are outwith the scope of this chapter, although numerical LEMs have not replaced their analogue counterparts – nor are they intended to. Physical models are actively used in landscape evolution studies (Hancock et al., 2002; Bonnet and Crave, 2006; Bonnet, 2009; Sweeney et al., 2015), but such experiments are usually custom-designed to meet the particular needs of a specific research question, and the materials available to construct the analogue model. In numerical landscape evolution modelling, there is more of a collective move (perhaps subconsciously) towards using a small number of community-developed numerical models, which are freely available to the modelling community.

The LEMs discussed in this chapter are primarily designed to simulate processes in humid–temperate sub-aerial environments. The role of glacial or aeolian processes are undoubtedly important in landscape evolution, but are frequently overlooked by the current range of available models, though a range of glacial-specific models exist (e.g. Braun et al., 1999; Tomkin, 2007; Herman and Braun, 2008; Egholm et al., 2011; Egholm et al., 2012). Coastal, glacial, and aeolian processes are currently better catered for in environment-specific models. However, the range of geomorphic process representation in more generic LEMs continues to expand and develop.

2.2 Fundamentals of Landscape Evolution Models

2.2.1 Governing Equations

LEMs are ultimately driven by a set of mathematical equations: the *geomorphic transport functions*, often termed ‘laws’ (Dietrich et al., 2003; Tucker and Hancock, 2010). These laws may be derived from physical first principles, empirical evidence, or sometimes a combination of both. When implemented in a model, these laws are applied to a series of discretised cells or nodes representing the landscape. Conservation of mass is applied when calculating the fluxes in and out of neighbouring cells or nodes. The most common assumption made in most LEMs with respect to conservation of mass is that each column of rock or regolith has discrete boundaries between layers of different densities (Figure 2.2), i.e. there is no allowance for a dynamic variation of density throughout each column in the model. Some models may further assume a uniform layer of substrate with no separate regolith layer. With these assumptions in mind, the majority of LEMs use a mass balance equation of the form:

$$\frac{\partial \eta}{\partial t} = B - \nabla q_s$$

where η is the surface elevation, t is time, B is a source such as the rate of sediment production, uplift or subsidence rate, and ∇q_s is the divergence of flux of material – what comes in minus what goes out – in the x and y directions (after Tucker and Hancock (2010), eq. (3).)

The modeller must be aware of which equations are implemented in the chosen LEM. Simpler models may be based on a single equation for each process represented, or even a single geomorphic transport function representing bulk processes, such as the hillslope diffusion equation (Culling, 1960). More complex models offer the user a wide range of governing equations to select from – this allows comparisons to be made from using different theoretical models of sediment erosion and transport. The Channel-Hillslope Integrated Landscape Development (CHILD) model (Tucker et al., 2001b), for example, allows the user to select from several different governing equations for sediment transport, fluvial incision, and hillslope erosion.

Each of these laws is based on a set of assumptions about the environments that they represent. The selection of the appropriate geomorphic transport law may be

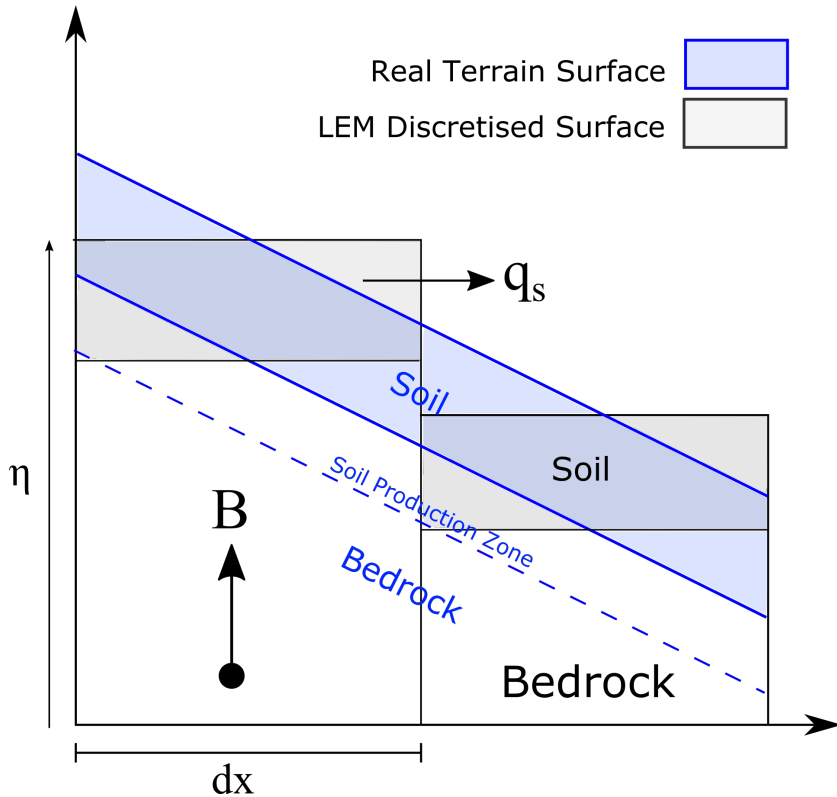


Figure 2.2: Conservation of mass in a soil mantled landscape or sediment covered channel (after Dietrich et al. (2003) and Tucker and Hancock (2010)). η is the surface elevation, B is the boundary (base-level) change, q_s the sediment transport term, and dx the grid cell size in a discretised landscape (assuming regular grid-spacing in this example).

scale dependent. The basic stream power law, for example, does not scale well when applied to drainage basins below around 1 km^2 in area (Hergarten et al., 2015; Stock and Dietrich, 2003).

2.2.2 Realism and Prediction

An important question to ask in the selection of an LEM is what degree of physical realism is sufficient and appropriate for the hypothesis being tested. Models with a strong physical basis, for example those based on computational fluid dynamics (CFD) such as OpenFOAM (Jasak et al., 2007), or SPHysics (Gomez-Gesteira et al., 2012), may be appropriate for studying landscape evolution on very small scales, at the level where forces from multi-directional fluid flow and particle motion form part of the hypothesis (e.g. Bates and Lane, 1998; Jackson et al., 2015). The trade-off in using such models is the increased computational expense, which is why they are infrequently

used in studies of landscape evolution beyond small scales.

The question is often posed whether LEMs can be used as truly predictive tools to make quantitative, accurate, and confirmable predictions about how landscapes will respond to future environmental changes at human timescales (Hooke, 2003; Pelletier et al., 2015). Recently, however, some authors have used LEMs to make quantitative forecasts about the evolution of landscapes in very specific environments, such as the response of coastal cliff erosion to climate change over the next century (Hackney et al., 2013), and the evolution and remediation of former quarries and tailings from mining operations (Hancock and Willgoose, 2004; Hancock et al., 2015).

2.3 Technical Implementation

LEMs are designed to simulate the evolution of topography over a discretised x, y, z landscape surface, as shown in Figure 2.3. Often, this type of model is referred to as a 3D or ‘whole-landscape’ model (Willgoose, 2005). The term ‘2.5D’ is sometimes used as most LEMs do not explicitly use a vertical coordinate representing the position of terrain in the vertical. Instead, the vertical dimension is modelled implicitly as a variable for each (x, y) grid cell. LEMs are implemented over a fixed spatial extent (the model domain), with pre-defined boundaries, as denoted by the x and y directions in Figure 2.3.

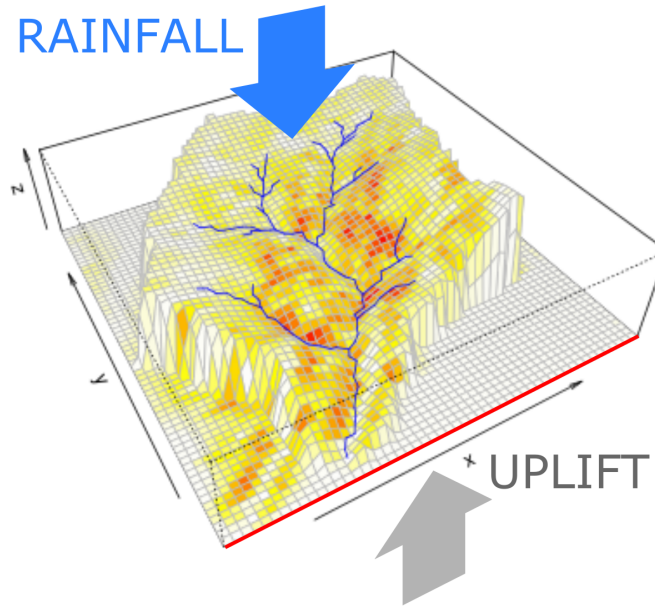


Figure 2.3: Main components and boundary conditions of a landscape evolution model. Boundary conditions include the climatic, tectonic and base-level conditions (rainfall and uplift), as well as the conditions specified on the model domain edges, such as where water and sediment can leave the model domain (shown by the red line). Channel network shown by blue lines. Erosion rate (red-yellow) is shown as a grid cell variable in this example.

2.3.1 Grid and Discretisation

The grid or mesh representing the land surface may be regular (rectilinear cells) or irregular, such as a triangular irregular network (TIN). The discretisation method of the terrain, and for rectilinear gridded domains the grid-cell size, dictates the length scale of landscape features that can be resolved in the model. Figure 2.4 depicts a typical regular gridded model domain. In this case, the maximum resolution of the river channel (in blue) is limited to the grid cell size of the model domain, or digital elevation model (DEM) used to initialise the model. Consideration should be given to whether the input data and model domain are of fine enough grid-spacing to resolve geomorphic features of interest.

The advantage of irregular gridded models is that they allow adaptive re-meshing

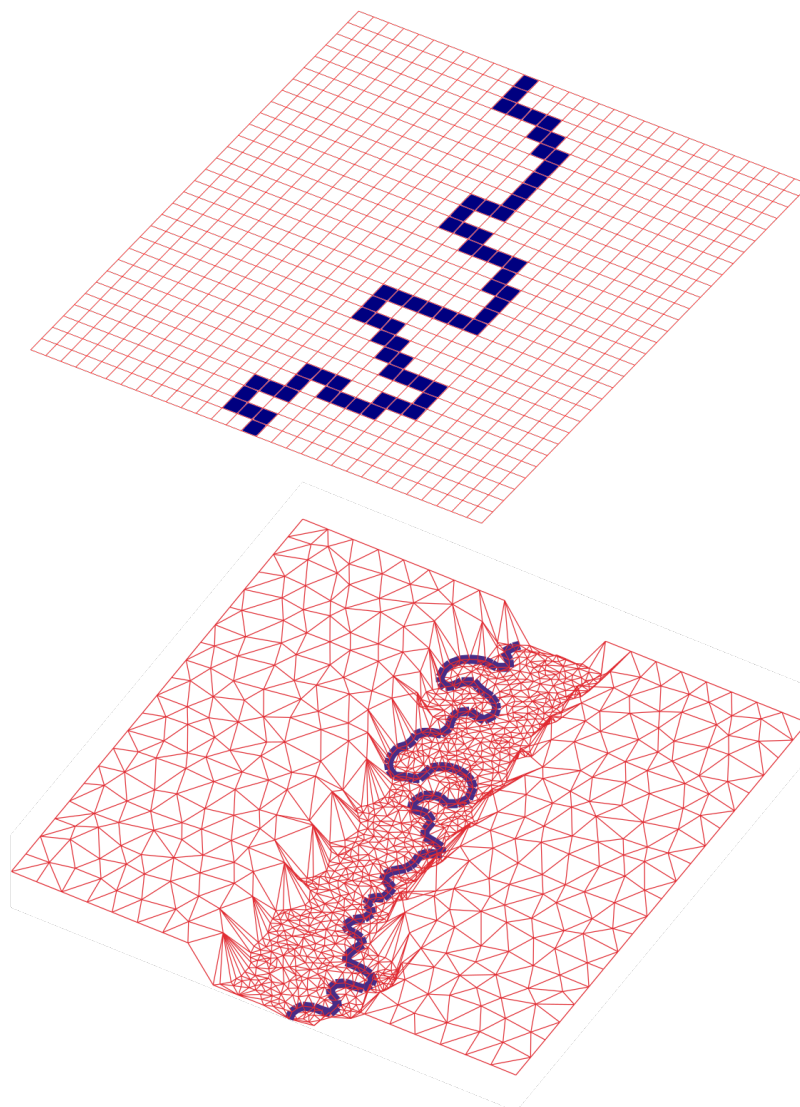


Figure 2.4: A comparison of two terrain-discretisation approaches. (Top) Regular, rectangular gridded discretisation. (Bottom) TIN, (Triangulated Irregular Network), with adaptive re-meshing. (Re-drawn from Tucker, et al. 2001b).

to finer grid-spacing (Figure 2.4) where detailed resolution of certain geomorphic features is advantageous, such as in river channels or gullies (Braun and Sambridge, 1997; Tucker et al., 2001b). Triangular irregular networks also have advantages for the representation of drainage networks – flow routing is not restricted to 45 degree increments as it is in regular, square-gridded models (Figure 2.5 Tucker et al., 2001b). In regular gridded LEMs, the grid cell size is uniform across the entire model domain. Regular gridded models dominate the current range of models, being computationally less expensive, and having a source code structure that is often easier to understand, if modifications need to be made. Regular gridded models are more easily compatible

with the common raster formats of DEMs, such as TIFF and ASCII raster data, as well as other data inputs derived from remote sensing such as land-use, soil moisture, and vegetation cover.

2.3.2 Surface Flow Routing

In real landscapes surface water may flow in multiple directions over terrain, but in LEMs flow direction is limited by a flow-routing algorithm and the discretisation scheme representing the land surface. The simplest square-gridded models route water from a single cell into one of either 4 or 8 adjacent cells, based on the path of steepest descent (Figure 2.5), known as the D4 or D8 algorithms (O'Callaghan and Mark, 1984). D8 algorithms, though simple, tend to be too convergent – resulting in a channel network with each stream the width of a single grid-cell (Wilson et al., 2008). More complex algorithms use a scheme where water can be routed in multiple flow directions (MFD) and the total water flux can be apportioned over multiple cells (Figure 2.5). However, this class of algorithm tends to be overly dispersive in water flow routing (Wilson et al., 2008).

The D-infinity scheme (Tarboton, 1997) is a single flow direction method aimed at addressing some of the limitations of the standard D8 algorithm. The appropriate scheme depends on the level of realism required for the hypothesis being tested. Simulations of complex riverine processes, incorporating braided channel networks, for example, would require a model with a multiple-direction flow-routing model. Flow routing models, with the notable exception of the FastScape algorithm (Braun and Willett, 2013), are typically the most computationally expensive part of a landscape evolution model, involving many iterative calculations per grid cell or node.

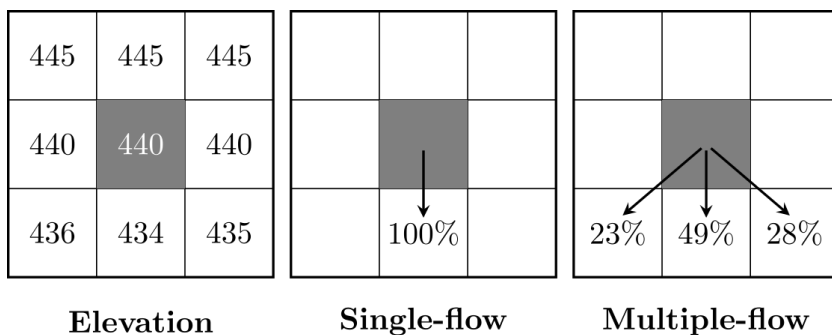


Figure 2.5: Comparison of single- and multiple flow direction routing methods. (Redrawn from Schäuble et al. (2008)).

2.3.3 Data Input Sources

For modelling of real landscapes, thought must be given to the source data used to initialise the landscape surface in the model. In simulations of large-scale landscape evolution (model domains of tens to hundreds of kilometres), input data resolution can be relatively coarse, such as a 90 m SRTM-derived (Shuttle Radar Topography Mission) DEM. Even this resolution may be higher than necessary and DEMs may be coarsened through resampling with GIS software in order to reduce the total number of grid cells and hence computational expense. Higher resolution DEMs are necessary for modelling small-scale features, such as gully formation or hillslope erosion (Nearing and Hairsine, 2010). It may be necessary to acquire sufficiently high resolution data, on the order of metres to centimetres, from sources such as airborne LiDAR (Gallay, 2013), terrestrial laser scanning (Lemmens, 2011), or structure from motion techniques (Micheletti et al., 2015). In short, the appropriate resolution of input data is dictated by the length scales at which the geomorphic processes of interest operate.

2.3.4 Boundary Conditions

Thought must also be given to the boundary conditions of the model domain. Boundary conditions refer to any input or constraint on the x, y, z minima and maxima of the model domain (Figure 2.3), including tectonic or base-level change, and climatic input, such as precipitation. Most models will operate on the principle of having at least one open boundary where water or sediment can flow out. In some models the placement of boundary outlets is customisable by the user (e.g. CHILD, FastScape).

The LEM user should also consider the possibility that these boundary conditions may not be fixed over time, such as variation in rainfall rate or uplift rate. In some situations, the boundary conditions may exhibit feedback with the internal processes of the model domain (Raymo and Ruddiman, 1992; Willett, 1999).

2.4 Current Models

LEM development has bloomed in the previous two decades, in part due to significant and continued computational advancement, and there is now a wide variety of models to choose from. The range of models available vary in their complexity, applicability to different timescales, and different process representation. In this section, some of the existing LEMs currently in common use are briefly reviewed.

2.4.1 CAESAR-Lisflood

A family of related models have developed from the original CAESAR LEM (Coulthard et al., 1996; Coulthard et al., 2002). The original CAESAR model is a cellular automaton model that simulates water flow across the landscape, fluvial erosion, sediment deposition, and hillslope processes. CAESAR-Lisflood (Coulthard et al., 2013), the current iteration of the model, uses a more physical-based surface water flow component based on a simplified numerical solution to the shallow water equations (LISFLOOD-FP Bates et al., 2010). The non-steady hydrological component of the model allows effects such as tidal flows, lake filling, and the blocking of valley floors by alluvial fans to be represented in LEMs (Coulthard et al., 2013).

CAESAR-Lisflood is suited to simulation of entire drainage basins (in ‘catchment mode’) or sub-sections of a river channel (in ‘reach mode’), e.g. Coulthard and Wiel (2006) and Van De Wiel et al. (2007). CAESAR-Lisflood is an appropriate tool for timescales ranging from modelling the effects of a single storm over a few hours, through seasonal, to annual, and millennial time scales of landscape evolution. Process representation in CAESAR-Lisflood is focussed primarily on hydrodynamics and sediment transport, including the simulation of multiple-sized grain fractions.

Though there is theoretically no upper limit to the time periods that can be simulated with CAESAR-Lisflood, existing studies have focused on shorter scales from

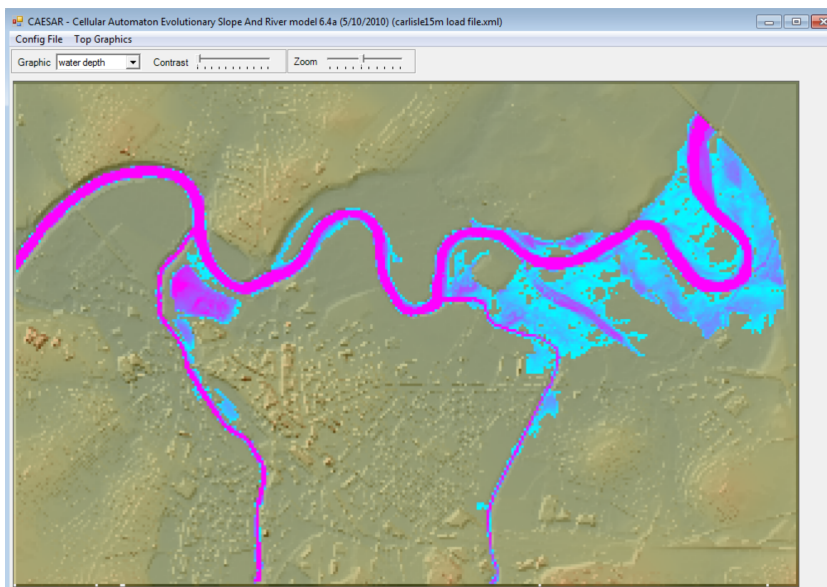


Figure 2.6: CAESAR-Lisflood simulating the flooding of Carlisle, UK, 2005. Hydrogeomorphic effects of single floods can be simulated in this LEM due to the implementation of a non-steady flow hydrological component (Bates et al., 2010). Blue to pink colouring represents water depth, with pink indicating the deepest water depths. Model domain 5 km across.

decades up to thousands of years, such as simulating sediment output of a small basin under short term climate predictions (Coulthard et al., 2012b), simulating storm and tidal surge dynamics on coastal environments (Skinner et al., 2015), and forecasting the short term geomorphic evolution of former mine-workings and excavations (Pascullo and Audisio, 2015).

CAESAR-Lisflood uses a graphical user interface (GUI) to set model parameters and display output (Figure 2.6). The GUI makes model set-up quick and easier for users with less familiarity with command-line operations or code modification. The current version is limited to running in a Windows-only environment. The integration of visualisation with the core model code also allows the user to view model output as the simulation progresses (Figure 2.6); this has the advantage of letting the user monitor output without having to wait for a full simulation to complete and visualise the output in a separate step.

2.4.2 CHILD

The Channel Hillslope Integrated Landscape Development model (CHILD, Tucker et al., 2001b) is another widely-used model for investigating landscape evolution in a

variety of environments, on temporal scales from decades to millions of years. The modular design of the LEM has facilitated its expansion over recent years and it now supports various types of geomorphic process representation. CHILD supports initialisation of the terrain surface from DEM data or generating synthetic topographies from scratch. A wide range of fluvial incision processes can be simulated with CHILD, including both detachment- and transport-limited erosion models, sediment transport, and a range of hydrological and rainfall-runoff generation routines. Recent development of modules has extended process representation to include, for example, modules of dynamic vegetation growth (Collins and Bras, 2004), floodplain evolution (Clevis et al., 2006b), dynamic adjustment of channel width (Attal et al., 2008), representation of sediment grain size (Gasparini et al., 2004), debris flows (Lancaster et al., 2003), and stochastic rainfall generation (Tucker and Bras, 2000).

CHILD differs from many of the other models described in this section, as it eschews a traditional grid-based spatial discretisation in favour of a triangular mesh, or TIN. As previously discussed in Section 2.3, this allows the model resolution to vary spatially across the domain, becoming higher in regions where smaller scale features and processes operate, such as river meanders, and coarser where features are much larger in spatial extent, such as floodplains and hillslopes (Tucker et al., 2001a).

The CHILD model's TIN-based approach is advantageous in its flexibility at representing different scale features within a landscape (Braun and Sambridge, 1997; Tucker et al., 2001b), but adds an extra layer of complexity when working with typical raster data formats, requiring conversion between raster and TIN data at the input and output stages of the modelling workflow. A series of MATLAB scripts are provided with the CHILD model for visualising output. The open-source RCHILD package is also available for output visualisation with the R programming language (Dietze, 2014). The CHILD model is platform-independent (it will run on multiple computer operating systems).

2.4.3 FastScape-based LEMs

FastScape is an algorithm based on an efficient implicit numerical scheme to solve variants of the stream power law for modelling large scale landscape evolution (Braun and Willett, 2013). The major advance made by the FastScape algorithm was to

increase the efficiency of the flow routing calculation – a bottleneck in most LEMs – and hence the model is useful for rapidly testing hypotheses of landscape evolution. Several related LEMs have been based on an implementation of the FastScape algorithm, including:

- The ‘original’ FastScape LEM (Braun and Willett, 2013)
- DAC – the Divide and Capture model (Castelltort et al., 2012; Goren et al., 2014)
- LSDTopoTools: Raster Model (<http://lsdtopotools.github.io>)

Recent applications of FastScape-based LEMs have focused on the simulation of synthetic landscapes under differing tectonic, lithological, and climatic boundary conditions (Braun and Willett, 2013; Braun and Guillocheau, 2014; Castelltort et al., 2012; Yang et al., 2015). The FastScape LEM also allows for the use of DEM data to set the initial surface topography in the model. An optional GUI interface is also included with the FastScape LEM, though this is currently only functional in Linux-based environments. The underlying FastScape algorithm is generic, and not necessarily tied to any particular LEM – users may choose to implement the algorithm in other open source models.

2.4.4 LAPSUS

The LAPSUS model (Landscape Modelling at Multi-dimensions and Scales) is a modular, multi-process model suited to studying catchment-scale erosional processes and landscape evolution at a range of temporal scales from years to hundreds of thousands of years (Schoorl et al., 2000; van Gorp et al., 2015). LAPSUS is suited to studying landscape evolution by means of soil and sediment redistribution through processes of fluvial erosion, surface wash, landsliding, tillage, creep, and tectonics. Applications include studying the interaction of non-linear processes in landscape evolution (Temme and Veldkamp, 2009; Schoorl et al., 2014), the role of tillage and changing land-use in decadal to millennial scale landscape evolution (Schoorl and Veldkamp, 2001; Baartman et al., 2012b), the sensitivity of soil erosion to rainfall intensity (Baartman et al., 2012a), and exploring uncertainty and parameter choice in landscape evolution

modelling (Temme et al., 2011). LAPSUS features a graphical user interface similar in appearance to the CAESAR interface in Figure 2.6, allowing a similar visual monitoring of model outputs to take place without further post-processing required.

2.4.5 Other LEMs

Landscape evolution modellers have a vast choice of models at their disposal: the organisation CSDMS (Community Surface Dynamics Modelling System: <http://csdms.colorado.edu>) operates as a de facto model repository for developers and users of LEMs. The terrestrial model section lists well over one hundred different models that have been published to the site. CSDMS is a useful starting place for potential modellers to select an LEM based on their own requirements.

Some LEMs extend the functionality (and often complexity) of existing models. For example, the CAESAR-Lisflood-DESC model (Barkwith et al., 2015) features, in addition to the core components of CAESAR-Lisflood, modules for distributed surface and soil hydrology, groundwater hydrology and a more physically realistic representation of landsliding. Applications of CLiDE have included the prediction of geomorphic and environmental hazards over human timescales (e.g. Tye et al., 2013; Barkwith et al., 2015).

The current range of LEMs includes well established software packages such as the SIBERIA and CASCADE models. SIBERIA (Willgoose et al., 1991) is a square gridded model originally developed to investigate the feedbacks between hydrology, catchment form, and tectonics (Willgoose et al., 1994). CASCADE (Braun and Sambridge, 1997) was an early implementation of a TIN-based model designed to simulate long-term landscape evolution as a function of fluvial and hillslope processes. Though the deployment of these two models has declined in recent years somewhat, they continue to be used as a benchmark for inter-model comparison in some studies (e.g. Hancock et al., 2015).

Recent developments within the modelling community have extended traditional modelling functionality with other elements of geomorphic analysis. The LSDTopo-Tools software (<http://lsdtopotools.github.io>), for example, features an LEM based on the FastScape algorithm, integrated within a set of powerful topographic

analysis tools. This allows easy transition between modelling and analysis of the results using common and novel topographic metrics.

Another recent development is the Landlab software package (Hobley et al., 2017), which takes a highly modular approach to numerical modelling of landscapes. The user can rapidly create their own bespoke LEM from a set of existing components. This results in a high degree of user control over the complexity of the model configuration, not only in terms of process representation, but also the effect that technical aspects, such as grid type and flow routing algorithm have on model performance and output. The modular design avoids the usual expenditure of re-writing commonly used codes for process representation, model gridding, and standardised file input and output. A key strength of Landlab is its accessibility to users who do not have significant prior experience in designing and implementing numerical codes, but wish to embark on model development. Examples of Landlab’s applications include the study of impact cratering on landscape evolution (Hobley et al., 2013), the impacts of wildfires on hydrologic response (Adams et al., 2017), quantifying the link between regolith production and subsurface temperatures (Barnhart and Anderson, 2014), investigating the response of landscape evolution under non-steady state hydrology (Adams et al., 2017), and as a basis for developing a stochastic cellular automaton model (Tucker et al., 2015).

The selection of LEMs discussed here range from those that have already established a wide user-base in landscape evolution research (e.g. CHILD, CAESAR, LAPSUS), to newer developments that offer novel functionality or process representation for modellers (e.g. Landlab, CLiDE, DAC, LSDTopoTools). This chapter is not an exhaustive list of landscape evolution models, and some previously popular models have been omitted as it was felt they have been superseded or subsumed by newer offerings. The range of LEMs discussed here should nevertheless provide a starting point for tackling a wide range of modelling endeavours. A table summarising the main features and processes represented in each LEM is given in Table 2.1.

Model	Time scale applicability (years)	Input types	Landscape Type [¶]	Grid type	Language	Bedrock variation		Vegetation		GUI		Parallelisation		Open Source	
						#	#	#	#	#	#	#	#	#	#
CHILD	$10^3 - 10^7$	DEM/ Synth*	Basin/ Range	TIN	C++										
FastScape	$10^4 - 10^7$	DEM/ Synth.	Range	Square	Fortran										
CAESAR- Lisflow	$10^2 - 10^4$	DEM	Basin/ Reach	Square	C#										
CLiDE [§]	$10^2 - 10^4$	DEM	Basin	Square	C#										
SIBERIA	$10^3 - 10^7$	DEM/ Synth.	Range	Square	Fortran										
LSDTopoTools [¶]	$10^{-2} - 10^7$	Synth.	Range /Basin	Square	C++										
Landlab	$10^3 - 10^7$	DEM/ Synth.	Range	TIN/Sqr.	Python										
LAPSUS	$10^{-1} - 10^5$	DEM	Basin	Square	C#										

* – ‘Synthetic’ DEM. I.e. the model will initialise itself to a synthetic terrain based on certain initial conditions without an external DEM file.

† – Transport limited

‡ – Detachment limited

§ – Based on the CAESAR-Lisflow model, with further coupled components for groundwater.

¶ – Contains a FastScape-based landscape evolution model, and a CAESAR-based hydrodynamic model.

– On request of the authors.

|| – Range: multiple basins, mountain range evolution; Basin: singular drainage basin/river catchment; Reach: sections of river catchment

* – Spatial distribution of rainfall/climate input

Featured/Yes	
Caveat	
Not featured/Unknown	

Table 2.1: Feature comparison of widely used landscape evolution models. Process representation shown by model in blue/pink/white matrix.

2.5 Uncertainty, Sensitivity, and Calibration

2.5.1 Uncertainty

Uncertainty in modelling describes our inability to know precisely the initial conditions of a model, to represent in a model all the processes that govern landscape evolution, and ultimately to know with certainty the accuracy of the predicted outcome (Beven, 1996; Pelletier et al., 2015). All LEMs make simplifications regarding process representation, partly due to a lack of detailed knowledge in how certain processes work, and partly due to limitations about how these processes can be represented in computer models. Uncertainty may also stem from inaccuracies in input data sources, the choice of model parameters, and the boundary conditions of the model (and whether these parameters and boundary conditions might change through time). Uncertainty in LEMs may lead to errors that propagate through the simulation and increase in magnitude as a simulation progresses.

Ideally, one should address uncertainty by first assessing which parameters the model is most sensitive to – it may be that large uncertainties in one parameter have relatively little effect on the model outcome, whereas small uncertainties in a different parameter produce unexpectedly large variation in the model outcome (Pelletier et al., 2015).

Methods such as ensemble analysis should be considered, whereby multiple instances of the same simulation are run, with a range of parameters chosen from a probability distribution to assess the most likely outcomes from a model. While uncertainty cannot be removed entirely from modelling studies, it is useful to be able to state the most probable outcome(s), based on a probabilistic distribution of input conditions.

Uncertainty is a particular challenge in landscape evolution modelling as many processes are threshold dependent (Snyder et al., 2003b), or scale non-linearly (Schumm, 1979). In choosing parameter values, guidance can be taken from published values of such parameters derived for similar environments, particularly when they have been calibrated with field data, where available (e.g Temme et al., 2011; Hancock et al., 2015; Mudd et al., 2014).

2.5.2 Sensitivity and Calibration

Following earlier definitions (Oreskes et al., 1994; Trucano and Swiler, 2006), calibration is defined here as the selection and modification of input parameters of a model in order that they maximise agreement with observed data in real landscapes. Such parameters in LEMs might include the coefficient terms in fluvial erosion laws, for example the K , m , and n parameters in the stream power law (Seidl and Dietrich, 1992), hydrological parameters such as Manning's n (Manning et al., 1890), or the threshold shear stresses required to initiate erosion (Snyder et al., 2003b). Many such parameters are not directly quantifiable by field measurement, and model users should consult similar studies for recommended values, or conduct their own sensitivity analyses to constrain uncertainty in parameter choice. Other parameters may lend themselves to more rigorous methods of calibration, where they link directly or indirectly to measurable values in the field. Examples would include the calibration of hydrological parameters to produce a 'best fit' with observed discharge values at river gauging stations (Coulthard et al., 2013; Wong et al., 2015) and constraining stream power law parameters using statistical models and sensitivity analyses (Croissant and Braun, 2014; Mudd et al., 2014).

2.6 Validation & Confirmation

Validation is the process of assessing the legitimacy of a model set-up. Results from a model may or may not be valid depending on the quality of input data and model parameter choice (Oreskes et al., 1994). Moreover, validation does not necessarily establish the truth or accuracy of model predictions, only that the model is internally consistent. In practice, it can be thought of as a 'sanity check' on the input to the LEM before beginning the simulation. For example, is the input DEM of sufficient resolution to represent the scale of geomorphic features expected to be formed? Do the input parameters conform to observed or realistic ranges? If the answer to these types of question is 'no', the model predictions will be invalid.

Geomorphologists use LEMs to deduce whether hypotheses about landscape evolution are likely to be valid, which requires a method for assessing how the model output supports the hypothesis. Confirmation refers to the assessment of how model

predictions – after selecting suitable input parameters – match observations in nature (Oreskes et al., 1994). Directly observing landscape evolution is challenging at human timescales, as whole-landscape change occurs at slow pace, making direct confirmation of model predictions difficult in many situations (Hasbargen and Paola, 2003; Hoey et al., 2003). Some predictions made by LEMs, however, can be directly or indirectly confirmed to a certain extent with field observations. This includes short term phenomena such as gully formation, coastal erosion, and river bank incision. At short timescales, direct monitoring and quantification of erosion rates, particularly in rapidly eroding fluvial settings, becomes feasible.

2.6.1 Field Confirmation

Techniques to indirectly measure the rates of landscape change are wide-ranging, and include measuring sediment flux at catchment outlets, using traps to measure bedload erosion and deposition (Bunte et al., 2004), bedload impact sensors (Rickenmann and McArdell, 2007; Turowski et al., 2010), suspended sediment measurements at gauging stations (Brazier, 2004), and the use of radio frequency identification-tagged sediment particles to track sediment movement (Chapuis et al., 2015; Beer et al., 2015).

Through the rise of digital photogrammetric techniques, such as airborne and terrestrial laser scanning, direct measurement of whole-landscape morphological change is now possible at high enough resolutions to quantify small differences in topographic features, particularly in rapidly evolving landscapes (Rosser et al., 2005; Vaaja et al., 2011). Using these methods to aid model confirmation would be limited to small scale studies, as processing of point cloud data from these sources can be highly computationally expensive (Axelsson, 1999).

At longer, geomorphologically significant timescales, a range of techniques becomes available to assist in the calibration of LEMs and confirmation of hypotheses. Optically stimulated luminescence dating uses a property of quartz and feldspar minerals that records the amount of time they have sat in a sedimentary or soil deposit, which can be used for dating landforms (Aitken, 1998; Stokes, 1999; Murray and Wintle, 2000). The applicability of this technique to different temporal scales is site-specific and ranges from years to upwards of hundreds of thousands of years. Cosmogenic radionuclide (CRN) dating is a technique based on the interaction of cosmic rays with certain

isotopes in minerals in the Earth's surface (Anderson et al., 1996; Dunai, 2010). The production rate of certain isotopes can then be used to determine absolute ages and erosion rates in the landscape. A recent application combining an LEM with a model of CRN production rates is found in Mudd (2017), where it is used to explore the detection of transience in landscapes. The method is suitable for determining ages up to about 4 million years (Burbank and Anderson, 2011).

2.6.2 Topographic Metrics

In the past, looser forms of qualitative assessment have been used where LEMs are applied in an exploratory manner, such as to test mathematical models of geomorphic processes, or make speculative predictions of landscape evolution. In this sense, topographies generated by LEMs can be compared to real landscapes that they are intended to represent. Visual inspection of real versus simulated terrains can provide some degree of hypothesis confirmation (Bras et al., 2003; Hooke, 2003). However, it is recommended that this approach be extended to quantitative analysis by using a range of topographic metrics to compare simulated topographies with their natural counterparts. Such metrics include: mean relief, slope, river profile concavity, channel steepness indices (e.g. Wobus et al., 2006), terrain curvature, hypsometry, and roughness. A similar technique of comparing LEM output to physical analogue models has also been implemented by Hancock et al. (2002).

A range of techniques is available to assist the modeller in assessing model predictions and confirming hypotheses of landscape evolution. The most appropriate methods will depend on the time-scale of the study, and the type of predictions made by the hypothesis.

2.7 Limitations

Landscape evolution models are based on a body of existing theoretical models describing geomorphic processes. Arguably, one of the greatest limitations in landscape evolution modelling is the lack of unified theories describing key processes in the landscape, such as fluvial incision or hillslope form (Dietrich et al., 2003). This forces the user to select from an often wide (and still expanding) range of geomorphic transport

laws, without sufficient knowledge of the particular landscape equation in question to select the most appropriate law. Sensitivity analyses may help to quantify the uncertainty stemming from this issue.

Long term landscape evolution modelling (on the order of thousands to millions of years) suffers from the issue of how to upscale micro-scale geomorphic processes to the macro-scale. The extent to which quasi-random fluctuations in geomorphic processes, such as turbulent flow in rivers and small-scale heterogeneity in soil or bedrock composition, should be incorporated into long-term laws of landscape evolution laws is not yet fully developed (Tucker and Hancock, 2010). Many LEMs have relied on statistical approaches to deal with this issue (Hovius et al., 1997; Lague, 2005; Lague, 2013). However, the scaling exponents and statistical distributions in these parameterisations are often based on limited empirical evidence from field observation.

Numerical landscape evolution modelling is also bound by limitations of computing power available to the user. Considerations have to be made when designing LEM experiments in order that the simulations can be carried out in reasonable compute time. Higher grid resolutions and less parameterisation of key processes may lead to more physically realistic simulations, but at increased computational expense. Recent releases of some LEMs have begun to tackle this by incorporating parallelisation techniques into the model code, taking advantage of multi-core processors that have now proliferated into most personal computers as well as supercomputers.

2.8 Conclusions

When considering the use of landscape evolution models in geomorphological research, the modeller must make key decisions at certain stages of the modelling process. The modelling process can be summarised as follows:

1. Definition of the research aim and purpose of the model.
2. Selection of appropriate model and components.
3. Choice of input data if applicable.
4. Selection and calibration of model parameters, possibly including sensitivity analysis to address uncertainty.

5. Validation of model set-up – is the choice of parameters and input data logical and internally consistent?
6. Confirmation of model predictions against observed data.
7. Interpretation of model predictions.

There are two factors that should be considered at each of these stages: scale and process representation. The intended scale of the experiment, both temporal and spatial, has implications for LEM selection (e.g. is the model suitable for the time-scale of interest?). Process representation should also strongly guide decisions at each stage. The user needs to know which laws are implemented in their chosen LEM, and what parameters are associated with them that need to be selected and calibrated. If the model offers a choice of geomorphic process laws to choose from, which is the most appropriate for the environment that the experiment is intended to emulate?

Landscape evolution models are powerful tools for the geomorphologist. Like all powerful tools, however, care must be used to avoid unintended consequences from misuse. Numerical LEMs have heralded a new era in geomorphic research, and are increasingly used to address important research questions in geomorphology. They aid both our understanding of how geomorphic processes work, and our ability to make quantitative predictions about landscape change in the future.

3

Rainfall representation in current landscape evolution models

3.1 Introduction

In the context of numerical landscape evolution models, rainfall input is defined as the quantity of water added to a surface cell or node, or to the whole model domain, over a given time period. In practise, no landscape evolution or hydrological models represent rainfall in the sense of it falling from the sky and hitting the ground. The model is only ‘aware’ of rainfall input once it is added as quantity to the hydrological component of the model. While this may seem a somewhat trivial point, the impact of individual rain drops on the land surface is known to be an important contributor to surface erosion, yet omitted from most numerical models. Rain-splash erosion, as it is termed, is a well-studied phenomenon (Morgan, 1978; Meyer, 1981). The interaction of raindrops with the surface is complex; it depends on the size of raindrop (Morgan et al., 1998), falling velocity (Park et al., 1983), angle of attack (Pedersen and Hasholt, 1995), soil exposure, soil mineralogy, and cohesion of the soil surface (Luk, 1979). All of these factors could affect both erosion on the landscape hillslopes, as well as the route that water takes before it enters rivers, where fluvial erosion can occur.

In physical analogue models of landscapes, the generation of rainfall implicitly accounts for some of the above factors in rainsplash erosion, such as drop size, because of the physical need to generate a rainfall source from a position above the surface,

such as through a fine-meshed sprinkler (e.g. Hancock and Willgoose, 2001). Geomorphologists using physical analogue models of landscape evolution attempt a degree of rainfall realism by ensuring the raindrops they generate are reasonably well scaled to the size of their landscape analogue (Meyer, 1994). By contrast, numerical models of landscape evolution begin their representation of rainfall input at the surface; effectively ignoring any effects of rainfall travel through the atmosphere or its impact on the surface. Conceptually, rainfall input in numerical models is the amount of water that would be added at the surface from one or more (usually many more!) raindrops, once they have reached the ground. It ignores any effects from the physical collision raindrops make with the ground. This simple conceptual model of rainfall input is used throughout the rest of this chapter when referring to rainfall input in numerical landscape evolution models.

3.2 One-dimensional models

Isolated aspects of landscape evolution and hydrology can be studied using one dimensional models of features such as hillslope profiles and longitudinal river profiles, or storm hydrographs in the case of hydrology. Although the work in this thesis focuses on 2D models, it is useful to consider the work done by others investigating the feedback from rainfall variability on 1D models of landscape evolution, before progressing to fully 2D or 2.5D¹ models.

One dimensional models simplify aspects of the landscape system, isolating key components such as the longitudinal profile of a river or hillslope. Roe et al. (2002) modify a simple 1D model for river profile evolution (Seidl and Dietrich, 1992; Howard, 1994) to incorporate a feedback for orographic precipitation based on increasing elevation along a steepening river profile. Their precipitation feedback model accounts for two precipitation regimes: the first typical of midlatitude, shallower, and narrower

¹Occasionally, the terms 2D and 2.5D are used interchangeably when referring to landscape evolution models, although in effect they both produce what looks like a ‘3D’ terrain surface from their output. The ‘third’ dimension (or extra 0.5D in 2.5D terminology) comes from the fact that the elevation variable can be used to reconstruct a 3D picture of the landscape based on the value for each grid cell or node. In practice, nearly all of the process models in landscape evolution models are 2D, e.g. water routing over the surface does not account for turbulent flow in x , y and z directions, such as in computational fluid dynamic models. Sediment transport does not account directly for 3D particle motion or collisions between particles.

mountain ranges such as the West coast of North America, and one for broader and taller ranges such as the Sierra Nevada, European Alps or the Southern Alps of New Zealand. The former represents rainfall patterns that are dominated by the prevailing upslope winds, increasing precipitation with distance upstream, whereas the latter represents environments where atmospheric moisture content exerts more control over precipitation, resulting in decreasing rainfall at higher elevations, and a rainfall shadow on the leeward side of the range. In a later work (Roe, 2003) the 1D model incorporating orographic rainfall feedback is extended to the 1D relief structure over a transect of a mountain range. The maximum relief is found to be strongly dependent on the type of precipitation regime chosen; the prevailing upslope wind regime favouring lower relief, symmetric mountain ranges, and the atmospheric moisture-limited regime favouring higher relief mountain ranges.

Further 1D models have been developed to determine the relative importance of rainfall variability compared to other boundary conditions, such as tectonic uplift or base level fall. The 1D river profile model of Wobus et al. (2010) uses a transport-limited formulation of river profile evolution (Meyer-Peter and Müller, 1948) with a simple parameterisation of rainfall based on modifying the exponent to the discharge-area approximation given by:

$$q_w = k_q A^c \quad (3.1)$$

where q_w is the water discharge, k_q a dimensional coefficient, A the contributing drainage area, and c the exponent that relates which portions of the drainage basin contribute to gathering precipitation and converting it to water discharge. A decrease in c represents a shift to more rainfall being gathered in the upper reaches of the stream. An increase in c represents rainfall being gathered in the lower reaches. The situation where $c = 1$ implies rainfall input is equal along all sections of the river profile. The end result of this formulation is perhaps intuitive: more rainfall input in the upper reaches of the stream (decrease in c) results in more incision in the headwaters. However, the study reveals a key difference in the way that climatic and tectonic signals propagate along a river channel. Numerical results show that rainfall-driven perturbations propagate from the channel head downstream, whereas tectonic perturbations invariably propagate from base-level upwards towards the channel head. The authors,

however, reach this conclusion without simulating the scenario where there is more contributing rainfall from the lower reaches, i.e. the value of c is higher. However, given the setting of the study (streams draining a mountain front) it is perhaps reasonable to assume an increasing precipitation rate as elevation increases with distance into the mountain range.

River channel profiles are not the only markers of landscape evolution, though they do dominate the range of 1D modelling studies investigating sensitivity to the spatial distribution of rainfall (Tucker and Hancock, 2010). Hillslope erosion rates are known to be sensitive to the spatially averaged rainfall rate, especially where vegetation cover is low (Owen et al., 2011). Hillslope bedrock erosion decreases according to a power law as mean rainfall rates decrease, from semi-arid to hyperarid environments. In general though, the study of hillslope sensitivity to the spatial distribution of rainfall remains under-studied, particularly in the case of 1D profile evolution.

In the one-dimensional modelling studies discussed, there is a key limitation, which is often acknowledged by the authors. Channel profiles in 1D form are modelled without their tributary streams. The main stem of the channel is assumed to be representative of the entire catchment as a whole. This implies that tributary channels, and hillslopes feeding the main channel, experience the same precipitation patterns, or that differences between the main channel and its contributing water sources can be ignored. Rainfall spatial variability from tributary channels, or from runoff over hillslopes is lost, or smeared-out (Roe et al., 2002). The effects of water routing within a drainage network are also lost, and interesting relationships between rainfall distribution, river network connectivity and erosion are potentially overlooked. Complex parameterisations of rainfall production are often reduced to a single number or exponent in an equation describing the evolution of the landform profile of interest. Rainfall spatial patterns are often complex over correspondingly complex terrain, and only 2D models may suffice to fully explore the sensitivity of landscape process and form to rainfall spatial distribution.

3.3 Two-dimensional models

Two-dimensional models are grid-cell based (or based on a grid of connected ‘nodes’) and allow certain variables to vary spatially across the model domain, from cell-to-cell or node-to-node. There are comparatively few landscape evolution models that allow spatially variable rainfall input across the model domain, and some of the examples discussed here are from purely hydrological models. However, the principle of modelling spatially variable rainfall remains the same and there are potential applications in hydrological modelling that can be extended to landscape evolution modelling purposes.

3.3.1 Hydrological models

In the world of hydrological modelling, distributed² rainfall inputs are more commonplace. A range of meteorological input data sources have been used to drive distributed hydrological models. Three main sources of spatial rainfall data commonly used are dense-network rainfall-gauge data, precipitation radar, and precipitation outputs from numerical weather prediction models. Each one of these sources has a range of merits and demerits as a raw data source (further discussed in Chapter 4), but the discussion here focuses on their suitability as spatially heterogeneous rainfall datasets for numerical landscape evolution models, rather than an appraisal of their relative merits in reporting precipitation distribution.

Precipitation data generated by numerical weather prediction models has been successfully used in distributed hydrological models to make hydrological forecasts, as well as to analyse historic flooding events. Hay et al. (2006) use the MM5 model (Mesoscale Meteorological model)³ to generate gridded rainfall data over a five-year period. The rainfall data is used to drive the PRMS distributed hydrological model (the Precipitation Runoff Modelling System) over a corresponding five-year period. The numerical weather prediction model is run at grid cell spacings of 20 km, 5 km,

²Distributed hydrological models take into account the spatial distribution of meteorological inputs like rainfall, and other distributed variables such as soil moisture, vegetation, and land use. ‘Distributed’ is a term usually applied to hydrological models and less so to landscape evolution models, though in practice both can be said to be types of distributed model if inputs are spatially variable across the model domain.

³A precursor to the Weather Research and Forecasting model, WRF.

and 1.7 km, the finest of which resolves individual valleys and massifs, and captures the resulting rainfall patterns over the catchment at high resolution. The study also compares the way that rainfall input zones in the hydrological model are represented. In the hydrological model, different zones of rainfall input can be defined along natural topographic boundaries, which are termed *Hydrological Response Units*. These rainfall zone units tend to follow sub-catchment boundaries within the main catchment watershed. Alternatively, the catchment can be divided up more simply into rainfall input zones corresponding to a regularly spaced grid at a cell-spacing that matches the resolution of the input data. In general, increasing rainfall input resolution in the Hay et al. (2006) study results in a greater accuracy when compared with observed river discharge values. Using irregular-shaped hydrological response units based on natural sub-catchments, rather than a regular gridding of input data, results in better agreement with observed river discharges. However, as resolution increases towards the 1.7 km grid-cell spacing, the difference seen in discharges from using irregular shaped hydrological response units and regular grids of comparable resolution decreases.

In a study that uses high resolution numerical weather prediction model data to drive a hydrological model, Younger et al. (2008) test the suitability of rainfall forecast data for making hydrological predictions and improving flood forecasting. High resolution (250 m grid spacing) simulations using the United Kingdom Met Office Unified Model are used to generate input rainfall data to drive a TOPMODEL-based hydrological model (*Dynamic-TOPMODEL*) of Beven and Freer (2001a). The semi-distributed hydrological model *Dynamic-TOPMODEL* of Beven and Freer (2001a) groups topographically similar regions of the catchment and calculates runoff-prediction for each of the these self-similar zones. The amount of runoff calculated is then assigned to each node in that particular zone. Computationally, this is more efficient than performing runoff calculations for every single grid cell in the catchment domain. The Younger et al. (2008) study considers two events, a summer convective rainfall event and a winter stratiform rainfall event. Although the hydrological simulation using the dense-network of rainfall gauge data produced outputs more closely matched to discharge observations, simulations with the numerical weather model rainfall forecast also produce accurate results. Younger et al. (2008) highlight the potential of using high resolution rainfall forecast data to improve flood forecasting in the future, giving greater prediction lead-in times

compared to nowcasting from rainfall radar or real time raingauge measurements.

Rainfall data from numerical weather prediction models lends itself well to use as input data for hydrological modelling; it is typically written in a gridded data output format, and if the user has control over both the generation of the numerical weather prediction model output as well as the hydrological or landscape evolution model, generating compatible data formats can be straightforward.

A consensus has yet to emerge on whether distributed hydrological models are sensitive to the spatial distribution of rainfall input. Even when comparing catchments of similar sizes and environments, many studies are in disagreement (Nicótina et al., 2008). In terms of the peak discharge and the time to the peak from the onset of heavy rainfall during a flood, the use of spatially heterogeneous rainfall input data appears to have little impact on the predicted hydrographs (Krajewski et al., 1991; Shah et al., 1996a; Shah et al., 1996b). Antecedent conditions may determine some of the relative sensitivity in catchment hydrological response (Shah et al., 1996b), but only when initial water saturation levels are low. Variability in runoff production mechanisms are thought to be an important control on runoff response (Shah et al., 1996b; Segond et al., 2007). Whether variability in rainfall heterogeneity also contributes to the runoff response depends on antecedent conditions, as catchments may be able to dampen spatial heterogeneities in rainfall (Segond et al., 2007). In the simulations run by Nicótina et al. (2008), the source of rainfall data is from a network of rain gauges. Rainfall resolution is varied by first interpolating the rain gauge data with a kriging⁴ method to 100 m resolution. The 100 m resolution data is then upscaled to coarser resolutions of 10 km and 50 km, giving three sets of simulations, one for each data resolution. Their study uses two catchments of 1560 km² and 8000 km² in area. Nicótina et al. (2008) select catchments of relatively large size compared to previous studies. The choice of larger catchments is based on one of their hypotheses being that smaller catchments are closer in size to mesoscale rainfall features, and therefore less likely to experience truly heterogeneous spatial rainfall patterns. The results of the Nicótina et al. (2008) study show small differences between flood hydrograph peaks, which are more pronounced for the larger (8000 km²) catchment. A further

⁴Using a weighted average of neighbouring samples to estimate the unknown rainfall value at a given grid cell location.

set of simulations also compares a conservative upscaling of rainfall resolution to a non-conservative upscaling, i.e. the total volume of rainfall is not necessarily the same post-upscaling. The non-conservative upscaled rainfall resolutions display a greater difference in maximum flood discharge over the three rainfall resolutions than the conservative upscaling method. Nicótina et al. (2008) assert that catchments are more sensitive to the total volume of precipitation than its spatial heterogeneity, although this is perhaps to be expected if the non-conservatively upscaled experiments simply add more water to the catchment at coarser rainfall resolutions. Further experiments in the Nicótina et al. (2008) study with different runoff-generation mechanisms show a much more marked sensitivity in hydrograph response, compared to rainfall spatial heterogeneity.

From a hydrological perspective, accurate representation of the total rainfall volume and runoff-generating mechanisms in a hydrological model are more important than the spatial pattern of rainfall distribution (Gabellani et al., 2007; Nicótina et al., 2008). However, the approach of previous studies has been to focus primarily on the flood hydrograph during these simulations, which is essentially the water discharge modelled (or measured) at a single point at the catchment outlet. Few studies have properly addressed the sensitivity of the areal extent of floodwaters in response to spatially variable rainfall inputs to a catchment. To aid understanding and prediction of the risk posed to communities by flash flooding, knowing to what degree flood waters are sensitive to spatial variation in rainfall inputs would be a useful development in flood forecasting, in addition to just predicting the peak discharge for a given point in the catchment.

Intuitively, one might expect that in a river catchment system with its well defined boundaries and singular outlet point, that any mass-conserving model would produce similar results given water inputs of equal volume⁵. The details of interest may lie in what goes on inside the model domain, rather than what comes out the catchment outlet point. In other words, the spatial distribution of floodwaters should be just as important as the water discharge at the outlet. Nevertheless, the work done by the hydrological modelling community has laid some of the foundations for using spatially variable rainfall data in two-dimensional landscape evolution models. A range of

⁵Excluding the non-conserving rainfall upscaling method used by Nicótina et al. (2008)

data input sources and interpolation methods that have been successfully tested in hydrological modelling and should be transferable to models that also simulate the erosional processes within catchments. Some of the basic findings will also help guide the research in the later chapters, and in extending the development of an existing landscape evolution model in Chapter 5.

3.3.2 Landscape erosion and evolution models

Few of the currently available numerical landscape erosion and evolution models explicitly allow the user to vary the spatial distribution of rainfall across the model domain. At longer timescales, spatial variation in climatic conditions such as rainfall will eventually be averaged out over centuries and millennia, in effect negating any variation in rainfall spatial patterns (Sólyom and Tucker, 2007; Tucker and Hancock, 2010). However, this assumption only holds true if we believe that storm location and rainfall patterns bear no relation to the underlying topography of a landscape or river catchment. In other words, the assumption is that on the short term there is no orographic influence, and on the longer term, that there is no link between evolving topography and evolving weather patterns in a region. Only in recent years, and in a select few studies, have geomorphologists begun to question this assumption. As interest in this question has grown, models have been developed to accommodate this functionality. At the short-term end of the landscape modelling spectrum (days to centuries), the latest releases of the CAESAR-Lisflood model (Coulthard, 2017) now allow for spatially variable rainfall input data.

Landscape evolution models have been used to show that erosional processes are sensitive to spatial variation in rainfall inputs over timescales of decades to centuries. In a sensitivity study that systematically varied the rainfall input data spatial resolution to the CAESAR-Lisflood model, Coulthard and Skinner (2016) assessed landscape evolution model sensitivity in terms of sediment and water flux, and the spatial distribution of erosion in a mid-sized upland catchment (415 km^2). Rainfall input data was sourced from precipitation radar, and rainfall data resolution is varied at 5 km, 10 km, 20 km resolutions, as well as a ‘lumped’ input where rainfall is averaged spatially across the whole catchment. When the source data was upscaled to coarser resolution, the total volume of rainfall was conserved (in contrast to the

non-conserving upscaling methods used by Nicótina et al. (2008)). The simulations were run with 10-years of continuous rainfall data from rainfall radar records, looped over a 30-year period. Compared to the uniform (lumped) precipitation data, increasing the rainfall data grid resolution increased sediment flux from the catchment. In the case of the highest resolution rainfall simulation (5 km), sediment flux increased by over 100% compared to the uniform rainfall case. Natural spatial variation in rainfall patterns was removed by randomising the rainfall cell ‘tiles’ from the precipitation radar data, in an attempt to remove any rainfall patterns from orography in the catchment. In essence, Coulthard and Skinner (2016) focused solely on the effects of rainfall data resolution alone, rather than the spatial patterns of rainfall in nature, which are often influenced by topography. The rainfall field randomising technique minimises biases from naturally occurring organisation in storm cells and orographic rainfall enhancement.

Fluvial processes and flooding are not the only geomorphic processes potentially sensitive to the spatial distribution of rainfall. Numerical models of whole-landscape evolution have a recognized bias towards temperate–humid landscapes (Pazzaglia, 2003; Tucker and Hancock, 2010) and tend to focus on a limited range of geomorphic processes: hydrology, fluvial erosion, hillslope evolution, and sediment transport. Landsliding is an often overlooked, yet important process in landscape evolution, although it frequently goes unrepresented in numerical models of whole-landscape evolution (Tucker and Hancock, 2010). Landslide triggering is generally addressed in more domain-specific models, such as von Ruette et al. (2014), who investigate the sensitivity of shallow landslide initiation to the spatial distribution of rainfall in a catchment. A catchment-scale landscape evolution model designed specifically for investigating landslide triggering (the *CHLT* model von Ruette et al., 2013) was used to investigate the initiation of shallow landslides under both spatially uniform rainfall and a coarse grid-based spatially variable rainfall input. The rainfall input data was a product of integrated rain gauge data and rainfall radar measurements. As the coarseness of the data is high relative to the size of the study catchment, an inverse distance weighting interpolation method⁶ was used to downscale the data to a 2.5 m grid cell size, the

⁶An interpolation that gives preferential weighting to points that are closer to each other. The measured values closest to the prediction point of interest have more weighting, which diminishes with distance from the point of prediction.

same resolution as the digital elevation model data used in the study. A further set of simulations was carried out with a set of artificial rainfall input grids at 500 m grid cell size. The simulations reveal the main sensitivity to landslide initiation is the rainfall intensity and the infiltration capacity of the soil. If rainfall intensity is too high, water will run off before it can fully infiltrate the soil; there exists a ‘sweet-spot’ where rainfall intensities are low enough that the soil will become saturated more readily, and more landslides will be initiated. In the simulations run with equivalent rainfall intensities, spacial heterogeneity exerts some control over the distribution of landslides, as certain grid cells experience high rainfall rates, whereas others experience lower rainfall rates, closer to the rainfall rate ‘sweet-spot’, and consequently more landslide initiation. The findings of von Ruette et al. (2013) show that sensitivity of landsliding initiation to rainfall spatial heterogeneity is dependent on a number of other conditions such as soil moisture capacity, infiltration rate, rainfall rate, and rainfall intermittency. Rainfall spatial distribution in a catchment exerts a control on whether these conditions will be optimal for landslide initiation, since rainfall distribution controls local water inputs at the surface. It is by concluded by von Ruette et al. (2013) that both the spatial distribution of landslides and the total number of landslides triggered are sensitive to the spatial distribution of rainfall in a catchment, assuming other conditions such as infiltration capacity are near-uniform across the catchment.

Longer term landscape evolution

Landscape evolution sensitivity to rainfall detail over much longer timescales, on the order of 100 000 years and greater, has been explored to a limited extent in a few studies. The ratio of storm cell size to catchment shape and size is one factor believed to control the long term evolution of catchment topography and drainage network morphology (Sólyom and Tucker, 2007). In the Sólyom and Tucker (2007) model, storm cells are represented as perfectly circular features with peak rainfall intensities at the centre of the circle, decaying exponentially from the centre:

$$I = I_0 \exp(-L_s/L_0) \quad (3.2)$$

where I is the rainfall intensity at a given point in the storm cell, I_0 is the rainfall intensity in the centre of the storm, L_s is the distance from the centre of the storm to

a given point in the storm cell and L_0 is a characteristic length scale associated with the spatial decline of rainfall intensity.

Orographic effects on rainfall enhancement are not represented in the model. In Solyom and Tucker's simulations, a set of idealised diamond-shaped catchments are varied in their elongation (length-width ratio), while being subjected to a steady non-uniform rainfall field described by the exponential decay function, centred at the middle of the diamond-shaped catchment. (The exact implementation details of the model code are not revealed within the paper.) In general, non-uniform rainfall patterns introduce a catchment-shape sensitivity to rainfall-runoff production, which in theory should affect the magnitude and distribution of erosional processes throughout the catchment as well. Examples of topographies generated by the model are not presented in the study, but shown instead is the total catchment discharge in non-dimensionalised form compared to non-dimensionalised catchment length. The simulations indicate that the greatest sensitivity occurs when the size of the storm decline rate, L_0 , is about half of the catchment radius. Solyom and Tucker's interpretation of this is that if storm intensity declines very rapidly over space, i.e. the storm cell is small and focused, then the majority of runoff production occurs in the vicinity of the storm cell, and is therefore sensitive to the shape of the catchment (assuming the storm falls near the centre of the catchment.) If the storm intensity decline rate is gradual, or intensity does not decline at all within the cell, then in contrast the runoff generation is relatively insensitive to catchment shape and storm size.

A more detailed look at the way topography is influenced by spatial variation in rainfall patterns – including the effect of orographic rainfall gradients – is found in the recent work of Han et al., 2015. Building on earlier work by Roe et al. (2002), who found the geometry of river long profiles to exhibit sensitivity to an orographic rainfall feedback mechanism, they explore the sensitivity of the whole landscape over a 2D domain. Modifying the CHILD landscape evolution model (Tucker et al., 2001a), they develop a parameterisation scheme for orographic rainfall based on the model of Smith and Barstad (2004). In their implementation of Smith and Barstad's model, the user-controlled variables governing rainfall production are given in Table 3.3.2. The model offers considerable control over many meteorological variables determining orographic rainfall. In a series of simulations under differing rainfall conditions, the authors find

Parameter	Units
Initial cloud water column density	kg m^{-2}
Initial hydrometeor column density	kg m^{-2}
Time constant for conversion from cloud water to hydrometeors	seconds
Time constant for hydrometeor fallout	seconds
Wind speed	m s^{-1}
Mountain half width	metres

Table 3.1: User defined parameters in the Han et al. (2015) orographic rainfall model implemented in CHILD.

only a slight sensitivity of the concavity of the main trunk channels under spatially variable rainfall. They conclude that channel concavity is not generally sensitive to orographic rainfall patterns, in contrast to the 1D profile model of Roe et al. (2002), which showed much greater sensitivity. The more revealing topographic metrics were found in planform study; both the hypsometric integral⁷ and the channel steepness index⁸ were found to be more strongly linked to the orographic rainfall gradient.

In the model domain, rainfall input values for each node are now calculated individually, rather than the uniform rainfall field used in standard versions of CHILD. The calculation is based on a number of factors including the elevation of the current grid node, the direction of the prevailing wind, and factors relating to water content in the atmosphere. As the elevation of grid nodes can change as topography evolves throughout the simulation, and rainfall inputs depend on the elevation of each node, there is an explicit feedback mechanism between orographic precipitation and landscape evolution represented in the model.

3.3.3 Summary of current model capabilities

The technical capabilities of landscape evolution models have evolved in tandem with research needs in a piecemeal fashion. As climate change has become an important factor in driving research needs and interests, landscape evolution models have evolved themselves to cater for a range of climatic parameterisations at a range of time scales.

⁷A measure of the fraction of a catchment above a given elevation, describing the distribution of elevations over the catchment. See Brocklehurst and Whipple (2004) and Cohen et al. (2008).

⁸A measure of channel steepness normalised to drainage area (Wobus et al., 2006).

Two-dimensional⁹ numerical models are increasingly used for forecasting and predictive purposes, as well as just answering theoretical research-driven questions. Despite their potential however, 2D models of landscape evolution are only beginning to be developed to allow detailed spatial variation in many of the climatic variables, such as rainfall. This is seen in the CHILD landscape evolution model work of Han et al. (2015) as well of the development of CAESAR-Lisflood (Coulthard and Skinner, 2016; Coulthard, 2017) to simulate spatially variable rainfall input fields.

Recent advances in landscape evolution modelling have coupled hydrological model components with erosional process modules to produce hydrodynamic landscape evolution models that do not assume steady state discharge and runoff in a catchment. For example, the CAESAR-Lisflood model (Coulthard et al., 2013), Landlab modelling framework (Hobley et al., 2017), and tRIBS model (Vivoni et al., 2011) all contain forms of distributed hydrological models to simulate the transfer of water as well as sediment between grid cells or nodes. At longer timescales, the meteorological processes representing rainfall over a landscape have been parameterised, though the detail of these parameterisation schemes can be quite sophisticated (e.g. Han et al., 2015), incorporating established models of rainfall production and enhancement in mountainous regions (Roe et al., 2002; Roe, 2003; Smith and Barstad, 2004).

3.4 Research needs for hydrogeomorphology

The sensitivity of hydro-geomorphic processes to the spatial details of climate and precipitation is still relatively unexplored. Hydro-geomorphology is key to understanding long-term landscape evolution as well as the shorter-term risks faced by communities in proximity to rivers, floodplains, and landslide-prone areas. Although the field is more advanced in purely hydrological studies (Krajewski et al., 1991; Smith et al., 2005; Segond et al., 2007; Nicótina et al., 2008) there is still a lack of agreement on when sensitivities to rainfall heterogeneities become most pronounced, given the dependence on other aspects of catchment hydrology. The role of runoff generating mechanisms, the influence of vegetation, the influence of groundwater routing pathways, are all

⁹Or 2.5-dimensional, if the elevation variable is considered a limited 3rd dimension, in the sense that elevation can go up or down in landscape evolution models, though the underlying process representation remains restricted two-dimensions in the x, y plane. For example water flow and sediment transport is not fully realised in 3D in any current landscape evolution model.

affected by the spatial distribution of rainfall in a catchment, yet further investigations into these competing factors are required to reach more consensus among the hydrological community. Although in some hydrological studies there is an insensitivity of hydrological processes to rainfall heterogeneity over a catchment (Krajewski et al., 1991; Smith et al., 2005), a key difference in landscape erosion evolution modelling is that many erosional processes are threshold dependent (Snyder et al., 2003b). Findings by Coulthard and Skinner (2016) find a pronounced sensitivity to rainfall data resolution in term of sediment flux from a catchment (up to a 100% increase), in contrast to the relatively small differences observed in purely hydrological models (e.g. Nicótina et al., 2008). Apart from the Coulthard and Skinner (2016), no other studies have been found that systematically explore landscape evolution model response to rainfall data resolution. Studies have yet to explore the effect of different spatial patterns of rainfall on the hydrogeomorphic impacts of single severe storms.

With regards to data sources for rainfall input into landscape evolution models, the most typical source is rainfall gauge data, for single sites or sparse networks across a catchment. Rainfall radar has also been explored as a potential source offering higher spatial resolution than most rain gauge data typically available (Coulthard and Skinner, 2016). Other potential sources include output from numerical weather prediction (NWP) models, or the use of artificial weather generators (e.g. Peleg and Morin, 2014). These two sources offer the potential to explore a variety of different spatial patterns of rainfall data, without having to source them directly from historic events. With approaches using NWP models to simulate idealised weather conditions, or using weather generators, or data from rainfall radar archives, researchers have the potential to explore sensitivity to the spatial patterns of rainfall for a variety of meteorological conditions, and the potential to systematically explore the effects of different distributions of rainfall on landscape erosion and evolution.

There is still a great deal of unexplored ground for developing landscape evolution models beyond their current capabilities. Developments are needed to accommodate further types of spatially variable climatic input data and their interpolation to different scales (e.g. von Ruette et al., 2014; Coulthard and Skinner, 2016), to develop new feedback models between topography and rainfall generation (e.g. Han et al., 2015), new parameterisations of storm cell morphology (e.g. Sólyom and Tucker, 2007), and

to develop models to take advantage of high-performance computing facilities.

3.4.1 Technological advances and needs

Landscape evolution modellers have in general been reluctant to take advantage of emerging technology or high-performance computing (HPC) systems to explore bigger problems, or to explore uncertainty in model output through ensemble simulations. By way of contrast, in fields such as meteorology, mineralogy, particle physics, and engineering, the use of high-performance computing facilities is commonplace. In part, this is due to many problems in landscape evolution modelling stemming from a lack of agreement over geomorphic process laws. There is still considerable uncertainty over which geomorphic ‘laws’ are best suited to represent certain natural processes, and the answer can be dependent on the environment being studied. As such, modelling simulations in landscape evolution have often focused on investigating the big-picture, broad-brushed questions about how landscapes evolve as a supplement to empirical field based studies. Geomorphologists, perhaps quite justifiably, have not yet required large-scale computing facilities used in other fields, as their questions can be answered satisfactorily with reduced complexity, and less computationally demanding numerical models. This is especially true as a large body of numerical landscape evolution modelling is used in an exploratory manner (Hancock, 2003; Lancaster and Grant, 2003; Tucker and Hancock, 2010), or to make observations that are partly qualitative. However, geomorphology is moving away from a purely qualitative era as a range of quantitative methods have been developed and deployed in recent studies incorporating landscape evolution modelling (e.g. Attal et al., 2011; Mudd, 2017), such as absolute dating methods of landforms and sediments, as well as digital topographic analysis. Returning to the comparison with other fields and their use of high-performance computing, these fields often suffer the same problems in uncertainty that geomorphology does in the choice of process law or parameterisation used in a numerical simulation. However, this has not prevented them from judicious use of HPC in carrying out numerical simulations. In fact, one of the strengths of HPC facilities is the capability to assess many hundreds, if not thousands, of modelling scenarios and parameter choices in ensemble simulations. This use of HPC has helped to quantify the uncertainty in process laws and model parameters, a problem which geomorphology is not immune

to (Tucker and Hancock, 2010; Pelletier et al., 2015). A drive towards making use of high-performance computing facilities is needed in geomorphology as problem sizes grow through the continued expansion in data coverage and resolution.

3.5 Model choice for further development: CAESAR-Lisflood

For the aims of this thesis (Chapter 1), a numerical landscape evolution model that satisfies several requirements is needed:

1. Process representation including flood inundation and sediment transport using a variety of sediment transport laws
2. Capable of simulation hourly-scale flood events (individual storms)
3. Ability to utilise temporally and spatially variable rainfall data sources from gridded rainfall data products.
4. Scalability to multi-processor computing environments, for conducting ensemble style simulations across multiple compute-nodes, preferably on high-performance computing systems.

CAESAR-Lisflood, as discussed in previous sections, would appear to meet several of these criteria particularly (1) and (2), though less so for (3) and (4). CAESAR-Lisflood includes a well tested flood-inundation module, based on the established LISFLOOD 2D hydraulic model (Bates and Lane, 1998). It is therefore capable of representing water flow dynamics within the context of individual storms, when a river catchment is not at hydrological steady state¹⁰. The hydrodynamic nature of CAESAR-Lisflood can be contrasted to many other landscape evolution models which assume a hydrological steady state across a catchment during storm events (e.g. CHILD). CAESAR-Lisflood also features two sediment transport laws, though neither of them are a bedrock incision-based erosion law, such as found in CHILD. CAESAR-Lisflood therefore lacks a range of erosion laws covering the full spectrum or erosional

¹⁰Water inputs are not equal to water outputs due to the transient movement of water through the catchment.

processes, instead focusing on what are termed ‘transport-limited’ erosion laws, i.e. those limited by the rate of sediment transport that can be transported by flowing water.

From a technical implementation perspective, CAESAR-Lisflood is a square-grid based model, which makes for easier interoperability with both terrain input data, and crucially, gridded rainfall datasets, such as from numerical weather prediction model output or rainfall radar data sources. Although there are advantages to using other grid meshes (as discussed in Chapter 2), such as the triangular irregular grid in CHILD-based models, they come with an increased difficulty in interoperability with common square grid-based data formats, as the gridded data inputs need to be interpolated over the grid points of the irregular terrain mesh. If the input data changes rapidly through time, as rainfall data may do during a storm, then frequent re-interpolation is needed, increasing the computational cost of the simulation.

Moreover, the CAESAR-Lisflood model has a large existing community and support network, and is well established having been used in many landscape evolution modelling studies for over two decades (Valters, 2016). The model’s original implementation (in the form of ‘CAESAR’) was tested using upland catchments in the UK (Coulthard, 1999), and as will be presented in more detail in Chapter 6, this thesis will also be based on case studies from upland UK catchments.

For the reasons discussed above, CAESAR-Lisflood will be used as the basis for and implementation of a landscape evolution model for use in a high-performance computing environment, which is not currently possible with the existing model due to its implementation in the C# programming language. The functionality of the model will be extended further to work on multiprocessor parallel computing systems, and with an improved range of erosion laws. The development of this model is presented in Chapter 5. A software framework for processing rainfall radar data from the UK rainfall radar system for use in CAESAR-Lisflood and derived models is presented in Chapter 4.

4

Integration of rainfall radar data with a landscape evolution model

4.1 Introduction

Measuring and predicting rainfall has been a central activity to meteorological and hydrological sciences for centuries. The importance of having good estimates of rainfall for understanding hydrological processes was recognised by Perrault (1674), particularly for understanding the role of rainfall in the water cycle (Biswas, 1970). Historically, the earliest hydrometeorological observations in Britain were recorded by Bede the Venerable (AD 672–735) (McCulloch and Robinson, 1993). Quantitative measurement of rainfall with instrumentation in the UK is attributed to Christopher Wren and Robert Hooke (Biswas, 1970), who developed a precursor to the modern tipping-bucket raingauge, although numerous records of rainfall measurement have been noted in other societies predating efforts in Britain (Strangeways, 2010). Quantifying the amount of rainfall that has fallen in a given area over a period of time is referred to formally as *quantitative precipitation estimation* (Fabry, 2015) and its prediction ahead of time as *quantitative precipitation forecasting* (Golding, 2000; Browning, 2003).

In the context of landscape evolution and erosion modelling, realistic rainfall input sources are often a secondary consideration, with many models using a uniform rainfall rate across the model domain, or generating rainfall inputs artificially from stochastic rainfall generators (Chapter 3, Tucker and Bras, 2000). Despite the paucity of realistic rainfall data use in landscape evolution modelling, there is no shortage of rainfall data

at the disposal of the landscape evolution modeller. This chapter explores some of the potential meteorological data sources that could be incorporated into numerical models of landscape erosion and evolution, and presents a software framework for processing rainfall radar data for use in the CAESAR-Lisflood landscape evolution model, and its derivative models.

4.1.1 Rainfall data sources

Direct measurement of rainfall is accomplished through the use of rainfall gauges, which provide *in situ* measurement of rainfall totals, and in some cases, instantaneous rainfall rates, at a fixed-point location. In the UK, the density and spacing of rainfall gauges is heterogeneous at the individual catchment scale, though there is good coverage at regional to national scale. At catchment and sub-catchment scale, however, most rainfall gauge networks are too sparse to provide detailed information about the distribution of rainfall variability within a catchment. Exceptional coverage is sometimes found in catchments that have been instrumented as ‘research catchments’, where a high-density network of gauges has been established for monitoring of specific catchments, (e.g. the Plynlimon research catchment, Newson, 1979) but this is atypical. Though raingauges are reliable for point totals of rainfall, common types of gauge (such as the widespread tipping-bucket raingauge) have a tendency to underestimate true rainfall rates during very high rainfall intensities (Habib et al., 2001; Ciach, 2003). Nonetheless, the rain gague data is used extensively for verifying and calibrating other indirect measurements of rainfall, such as satellite or radar (Harrison et al., 2000; Ebert, 2007), or predictions from numerical weather forecast models (Golding, 2000).

Indirect measurements of precipitation can be either *active* or *passive* in their mode of measurement. Active sensors emit a pulse of electromagnetic radiation, usually in the microwave–radiowave band depending on the application, and measure the amount of energy reflected back from hydrometeors (Fabry, 2015). A mathematical function is used to convert the measurement of reflected electromagnetic radiation into a rainfall rate or rainfall amount, the choice of function depending on the particular method used. Passive sensors, as their name implies, do not actively emit any kind of electromagnetic radiation directly, but measure only the radiation emitted naturally from

the Earth's surface. When precipitation is present over the surface, passive sensors measure the brightness temperature¹ from the surface, and use this measurement to determine the phase and intensity of rainfall present based on a number of physical and empirical conversion formulae. Many satellite precipitation measurement missions combine active and passive sensing to build a complete picture of rainfall on the Earth's surface (e.g. the *Tropical Rainfall Measurement Mission*, TRMM, Simpson et al. (1988), the *Global Precipitation Measurement Mission*, Hou et al. (2014)). The advantage of satellite precipitation measurements lies in their ability to cover large regions of the globe, which would be infeasible with a network of ground-based measurements. Satellite precipitation measurements are particularly useful at increasing the coverage of rainfall measurement over the oceans, where there is a particular paucity of other measurement sources. Limitations in satellite precipitation measurement include its lower resolution compared to ground based measurements, due to the distance between the surface and the orbiting sensor, as well as the lack of coverage around polar regions on most satellites. Due to the orbiting nature of satellites, they cannot currently take measurements with the same frequency as ground-based methods. Typical temporal resolution of satellite measurements is on the order of 1.5–3 hours, whereas ground-based methods can take measurements up to every few minutes. Consequently, space-borne measurements are not usually suitable for applications requiring high-frequency, high-resolution measurements of rainfall, but lend themselves well to providing consistent, near-global coverage (with the exception of polar regions).

Ground-based precipitation radars are active sensors, emitting pulses of electromagnetic radiation in a 360° field of view through a rotating antenna. They measure the intensity of the beam that is reflected and use this to derive a rainfall rate through a series of empirical formulae (Wilson and Brandes, 1979). The scanning beam is angled slightly above level (typically 5°) allowing a near-surface measurement of rainfall at close range, which gradually becomes higher as the beam extends in range. Rainfall radars have a large variety of ranges depending on application, but national weather service radar stations typically have a range of 200–500 km in diameter (Fabry, 2015).

¹Brightness Temperature is a descriptive measure of radiation in terms of the temperature of a hypothetical blackbody emitting an identical amount of radiation at the same wavelength.

4.1.2 Advantages of radar for hydrological applications

Weather radar is particularly well suited to use in hydrological applications, and for the purposes of this thesis, by extension, to landscape erosion models that feature a hydrological component. There are two principal hydrological applications (Harrison et al., 2012): 1) routine monitoring of precipitation for climatological data collection, day-to-day river management, weather forecasting, and model validation; 2) early detection and prediction of floods for civil protection purposes. Both applications have common requirements such as data accuracy, but early flood detection has the added need for rapid estimation and dissemination of rainfall rates in order to give as much lead time as possible to authorities responsible for flood prediction and mitigation (Fabry, 2015).

Rainfall radar is particularly useful in small catchments, where response times to intense rainfall events are short, and where rapid rises in river level can quickly overcome infrastructure such as flood defences, reservoirs, and dams. With smaller catchments, the likelihood of having other sources of rainfall and hydrological information diminishes, such as rainfall and river flow gauges (Fabry, 2015). In larger catchments with adequate gauging facilities, precipitation may have large variability in spatial patterns, necessitating the use of other methods to determine the distribution of rainfall inputs into a river catchment. Large, mountainous catchments also benefit from rainfall radar as they may experience intense localised rainfall and quickly channel the rain from steep hillslopes into gorges and river channels.

4.1.3 Basic principles of Radar

Radar works on the principle of emitting microwaves and measuring the intensity and time taken of waves reflected back from distant hydrometeors. The use of radar to detect distant rainfall was alluded to by Marshall et al. (1947) who wrote:

“It may be possible therefore to determine with useful accuracy the intensity of rainfall at a point quite distant (say 100km) by the radar echo from that point”.

The basic principle of rainfall radar remains the same to this day, though technological advances have increased the quality and speed of dissemination of rainfall

measurements. Specifically, meteorological radar measures the reflectivity, and uses this value to determine the intensity of rainfall through an empirical formula relating reflectivity intensity to a rainfall rate. This is referred to as the Z–R relationship, where Z is the reflectivity and R is the rainfall rate. Many variants of the formula exist, taking the general form of:

$$Z = aR^b \quad (4.1)$$

where a and b are empirically-derived constants (Gunn and Kinzer, 1949; Joss and Waldvogel, 1969).

4.1.4 Processing and error correction

The reflectivity returns measured at any individual radar site are a combination of the radar waves reflected off hydrometeors at the scan level at a given moment in time, plus any other objects or obstacles in the path of the radar, plus a level of background noise from the atmosphere and instrument. From receiving raw radar return signals, there follow several steps to process this data and convert it into a usable rainfall product, giving an accurate estimate of surface rainfall. Post-processing steps can be summarised as follows:

1. Noise removal. Background noise may come from instrumental sources or sources in the atmosphere. A typical approach to noise removal is to estimate the mean noise from scans taken on precipitation-free periods and subtract this from the measured return reflectivity.
2. Removal of non-precipitation echoes. Sources of non-precipitation echoes include insects, birds, air and shipping traffic, and interference from other radar emitters. There are several approaches to removing this type of echo, some combining several techniques into one (Germann et al., 2006; Rico-Ramirez and Cluckie, 2008).
3. Removal of blocking obstacles such as terrain. Radar scans made at low elevations suffer from blocking of the emitted signals by topography. The effects of blocking on radar reflectivity can be modelled using a high resolution digital

elevation map and a model of radar beam propagation (Pellarin et al., 2002). Another approach is to use long term records of reflectivity and rainfall rate to extrapolate rainfall rates in the blocked regions.

4.2 Rainfall radar in Britain and Ireland

Britain and Ireland are covered by a network of C-band (5 cm wavelength) radar stations. Fifteen of these stations are located in the UK and maintained by the UK Met Office, two in Ireland are maintained by Met Éireann. A further radar is located on the island of Jersey, maintained by Jersey Met. Combined, these sites give coverage of the whole of Britain, Ireland, and surrounding waters (Figure 4.1). The scanning pattern of the radar network returns radar reflectivity data at four elevations every five minutes, at a resolution of 600 m by 1°, extending to 250 km in range (Harrison et al., 2012).

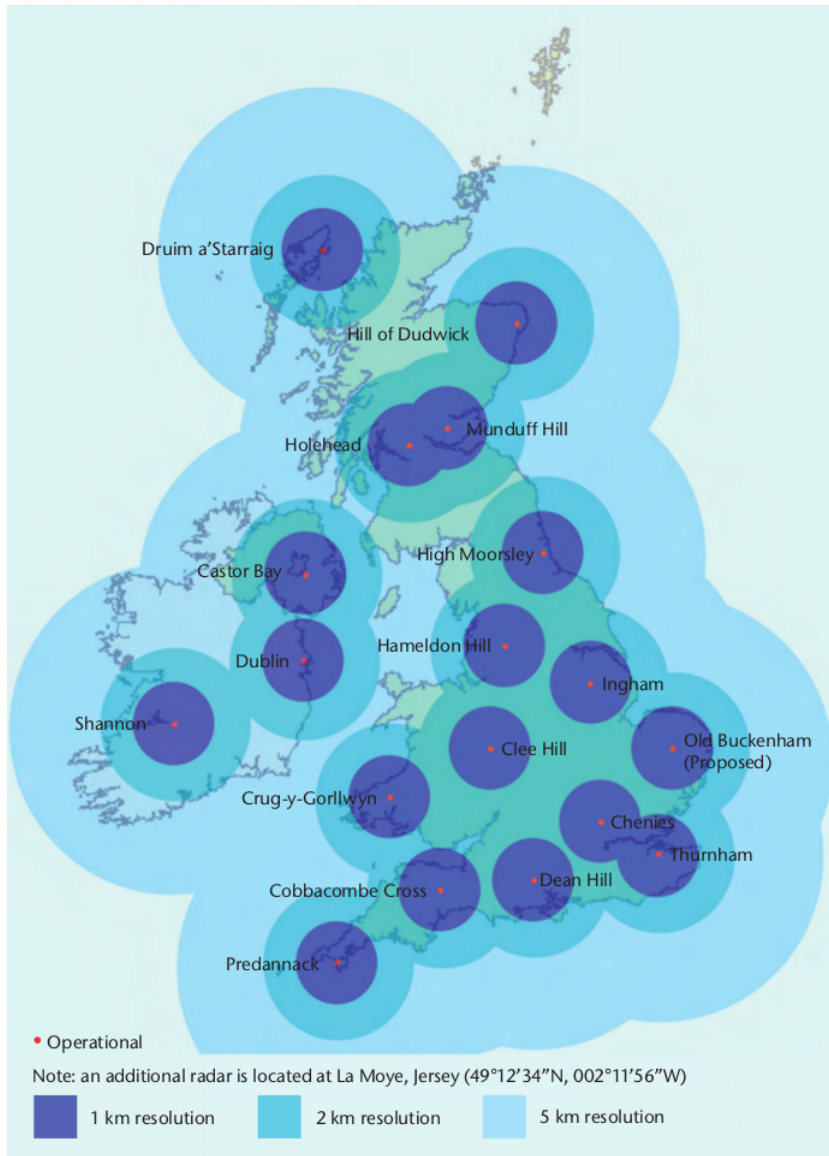


Figure 4.1: Network of weather radar stations in the British Isles and Ireland. *Source: National Meteorological Library, Met Office, UK.*

4.3 UK 1km Radar Composite Product

After processing and error correction of raw radar returns, the rainfall data still exist in a non-gridded format for each individual radar site and the surrounding scan-area. This intermediate format is unsuitable for many applications in environmental modelling and climatology, as adjacent radar sites may report different rainfall rates at locations covered by the overlap of neighbouring radar coverages. To produce a national-scale gridded rainfall data product for the UK, single-site rainfall estimates are composed into a unified data product with a domain covering 47°–62.7°N,

13.47°W–4°E (Met Office, 2003). Where grid points are covered by overlapping rainfall estimates, the radar with the highest ‘quality index’ – a function based on the height of the lowest usable radar scan – is used in the composite data product (Harrison et al., 2009). Other approaches for generating composite radar data products use weighted inputs based on the quality of all radars that provide coverage for a given location (Peura and Koistinen, 2007). The finalised UK radar composite product consists of five-minute data at 1 km grid spacing on a regular Cartesian grid. The data is supplied in a proprietary binary format and requires further data processing for ingestion into other models or subsequent analysis.

4.4 Use in landscape evolution models

No currently available landscape evolution models have the capability to directly ingest spatially variable rainfall data from meteorological data sources, such as radar composite products or rainfall data from numerical weather prediction model output. This was a key limitation of current landscape evolution models identified in Chapter 3. The CAESAR-Lisflood model is capable of ingesting spatially variable rainfall data, but not directly from meteorological data formats, though previous efforts have been made to manually process radar data for the CAESAR-Lisflood model using GIS (Geographic Information System) software (e.g. Coulthard and Skinner, 2016). The current lack of an automated framework for processing gridded meteorological data for landscape evolution modelling studies substantially slows down research workflows and brings the potential for introducing error or inconsistency between similar studies. Current best-practice advice is to devise automated tools to ensure data processing workflows are reproducible (Wilson et al., 2014).

4.4.1 Linking gridded rainfall data with the CAESAR-Lisflood model

A software framework is presented for processing gridded meteorological rainfall data for ingestion into a landscape evolution model.

Radar data from the UK 1 km composite data product is provided in binary format covering the whole UK (Met Office, 2003). To extract the data for the study area and

convert it to a suitable format for the CAESAR-Lisflood model, a further series of post-processing steps are required. The required inputs to the CAESAR-Lisflood model for spatially variable rainfall are:

- A **hydroindex grid** file used to mark zones of the catchment that receive different amounts of rainfall throughout the simulation. The hydroindex file has the same dimensions and grid-cell size as the main input terrain DEM in the model.
- A **rainfall timeseries** file. This file lists the rain rate at each time step (by row) for each one of the hydroindex zones (by column).

The workflow for producing these input files from the radar composite product is:

1. Convert the composite data from binary format to a human-readable text format.
2. Crop and extract the set of radar images for the time period and geographical extent required. (Figure 4.2.)
3. From the extracted radar images, compile the rainfall rate timeseries. The number of ‘hydroindex zones’ corresponds to the number of radar pixels in the extracted radar data subgrids. (Figure 4.3 a.)
4. Produce the hydroindex file at the correct grid-spacing, dimension, and geographical extent. (Figure 4.3 d.)

Details of how to access the code for the radar data processing software are given in Appendix A.

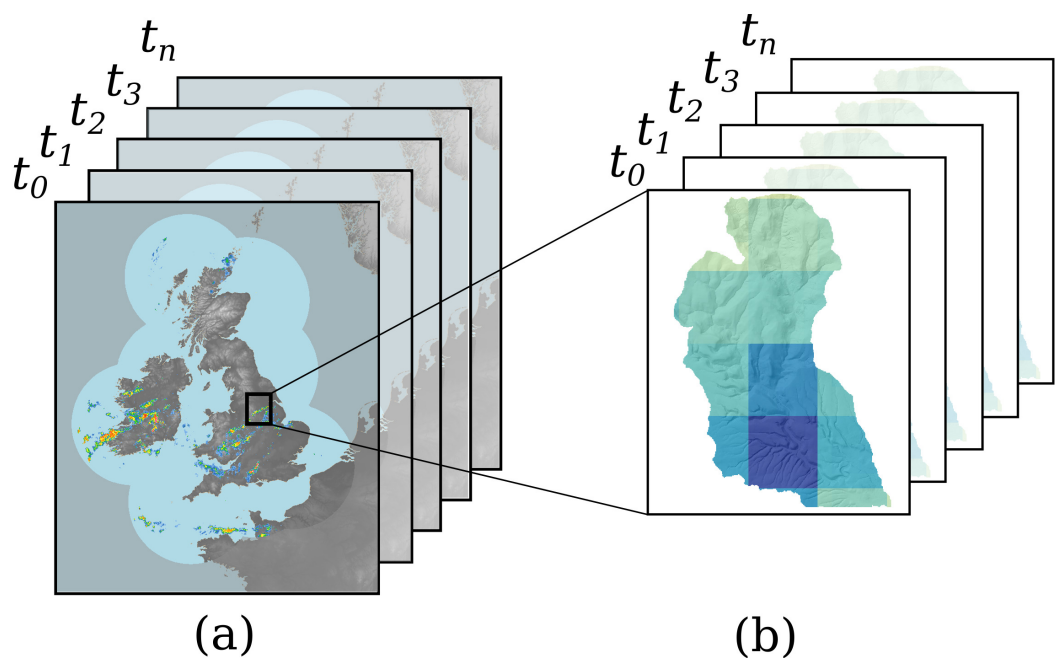


Figure 4.2: From the UK composite radar product (a), subgrids of the study area extracted for the time period of interest (b). The number of radar image pixels in each subgrid determines the number of hydroindex zones used in the model initialisation.

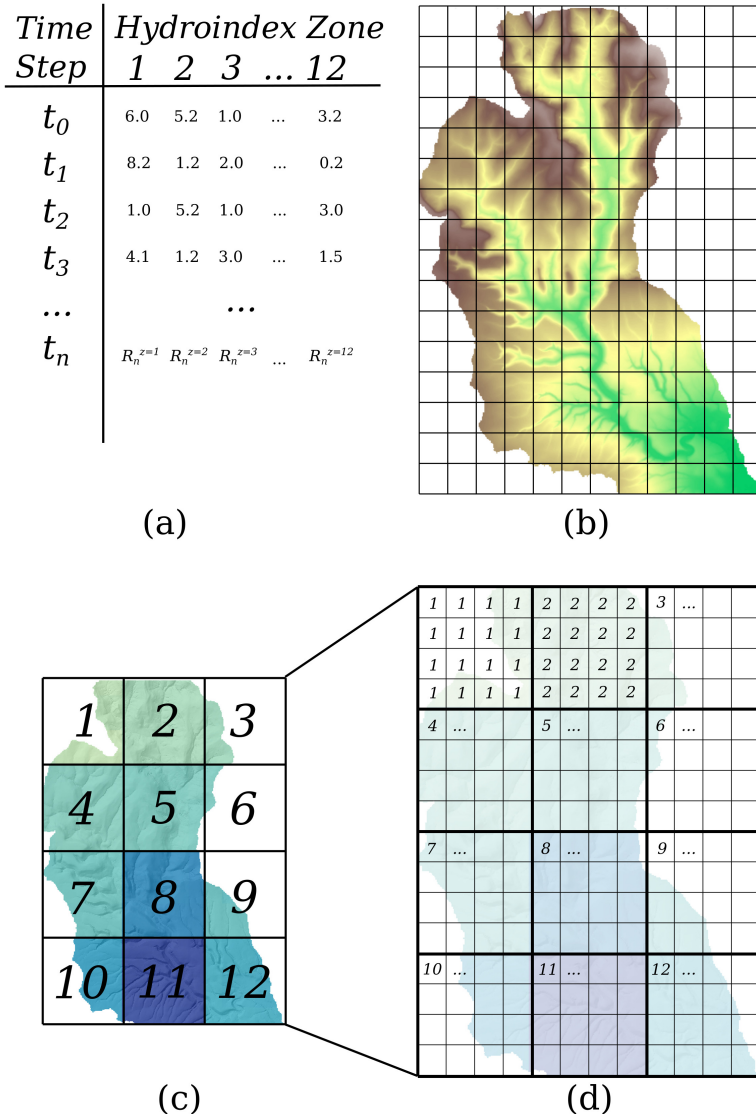


Figure 4.3: (a) Using the extracted radar data subgrids, a timeseries file is created mapping each radar image pixel to a hydroindex zone, for every time step. The hydroindex grid file must be the same dimensions and grid-spacing as the input terrain DEM (b). Numbering each radar image pixel in one of the extracted subgrids (c), the hydroindex file (d), is created from mapping the pixel indexes to the same resolution grid as the terrain input DEM.

4.5 Summary

Rainfall radar is one of many potential sources of rainfall data that can be incorporated with landscape evolution models. Rainfall radar data has several advantages that make it appropriate for use in combination with landscape evolution modelling, particularly the CAESAR-Lisflood model. Both model and data source are based on regular, square gridded domains, which makes the translation of rainfall data source to the model input relatively straightforward. The use of other numerical models based on irregular grids, such as the CHILD model, (Tucker et al., 2001a), would require further interpolation steps at the data preparation stage, and possibly at model runtime if the model domain permits adaptive re-meshing (Clevis et al., 2006a; Tucker et al., 2001b). The CHILD model for example allows the density and location of model grid points to be recalculated during a simulation to better resolve transient geomorphological features such as river meanders or braided rivers. Fixed gridded models such as CAESAR-Lisflood do not require any grid re-meshing during the model simulation, and the computational costs are potentially reduced for this reason.

For studies using multiple sites and case studies, having a single data source such as a national composite radar product provides a degree of comparability between different sites over different time periods, though upgrades to radar equipment and post-processing algorithms (e.g. Harrison et al., 2012) may negate this advantage if there are large time gaps between case studies, or for long-term studies using rainfall radar data. Rainfall radar's availability in gridded format, and its national coverage availability for the UK since 2004 make it an ideal source of rainfall input data for hydrological and landscape evolution modelling studies.

The processing framework presented in this chapter provides an automated and reproducible method for extracting sub-regions of gridded rainfall data from the UK 1km composite radar data product and preparing it for ingestion into the CAESAR-Lisflood landscape evolution model and its derivative models.

5

Development of a numerical landscape evolution model for high-performance computing

5.1 Introduction

Computer-based numerical models of landscapes have evolved since their introduction in the late 1970s, (e.g., Ahnert, 1976) to a point where they are now used to investigate a range of interacting processes in landscape systems including catchment hydrology, sediment transport, hillslope mass movement, and biological processes (Pazzaglia, 2003; Willgoose, 2005; Tucker and Hancock, 2010). Such models have developed over time to become useful tools not only for understanding how landscapes have formed in the past, but also how they will evolve in the future, such as in response to climatic or environmental change (Bras et al., 2003; Church, 2003; Pelletier et al., 2015). Landscape evolution models, as they are often collectively termed, enable catchment scientists, hydrologists, and geomorphologists to investigate landscape change on a range of timescales and spatial resolutions. They address societal needs to forecast the landscape's response to environmental change, as well as further the understanding of individual geomorphological processes and their interaction in forming whole landscapes (Dietrich et al., 2003).

The data driving landscape evolution models, such as the digital elevation models (DEMs) used to represent the landscape surface, and other inputs such as climatic

data, have increased rapidly in spatial resolution in recent years (e.g., Gesch et al., 2002; Rabus et al., 2003; Tarolli et al., 2009; Casas et al., 2006; Krishnan et al., 2011). Topographic datasets have increased in resolution to sub-metre scales, particularly since the advent of terrestrial LiDAR-derived digital elevation models, which are now a common data source in geomorphological analyses and modelling studies (Bates et al., 2003; Passalacqua et al., 2010; Clubb et al., 2014). The growth of high resolution input data is a double-edged sword: it presents the numerical modeller with the opportunity of studying processes at finer scales, often allowing sub-grid processes such as channel morphology to be resolved at the grid-cell scale (Schoorl et al., 2000). However, higher-resolution data also increases the computational cost of model simulations, as the number of calculations at a given model timestep increases with increasing number of grid cells used to represent the model domain. Decreasing the grid cell size of an input dataset causes the total problem size – the number of grid cells in the model domain – to increase non-linearly. Rising demand to study landscape and catchment processes at a regional or even continental scale also increases the computational cost of a model simulation by increasing the total number of grid cells in a model domain. Process representation has also grown in complexity, with many LEMs now supporting a range of rainfall-runoff, flow routing, erosion and slope process laws in a single model (Coulthard, 2001; Tucker and Hancock, 2010; Hobley et al., 2016), further increasing the computational demands made by modelling studies.

Rapid growth in computing power has occurred in tandem with the computational demands made by the hydrological and landscape evolution modelling communities. Individual processor power has steadily increased in following with the predictions made by Moore’s law (Schaller, 1997; Moore, 1998), through a continued increase in the number of transistors on integrated circuitry. As the rate of increase in individual processor speed has slowed in recent years (Mann, 2000; Colwell, 2013), parallel processing – the use of multiple processors to tackle larger computational problems – has become a indispensable tool in the scientific computing community. The uptake of parallelisation methods by the numerical landscape evolution modelling community is still in its infancy (Valters, 2016). However, disciplines with a close affinity to geomorphology have explored the use of parallel computing technologies in order to study larger problem sets, such as in the hydraulic modelling community (e.g., Ivanov et al.,

2004; Neal et al., 2009; Kollet et al., 2010; Smith and Liang, 2013; Liang and Smith, 2015; Smith et al., 2015). The increasing demand for environmental model codes capable of exploiting the parallelism offered by high-performance computing technologies has lead to the development of the HAIL-CAESAR landscape evolution model.

This thesis presents an implementation of the CAESAR-Lisflood model (Coulthard et al., 2013), re-written and adapted to be compatible for shared-memory parallel computing environments. The version presented here, termed HAIL-CAESAR¹, provides an operating-system independent, open source, hydrodynamic landscape evolution model suitable for deployment on various computing environments, including high performance computing architectures.

5.2 Model description and parallelisation

5.2.1 Origins: CAESAR-Lisflood

The porting and modification of HAIL-CAESAR is based on the CAESAR-Lisflood model (Coulthard et al., 2013), a cellular automaton numerical model of landscape evolution integrated with a hydrodynamic flow model (Bates et al., 2010). CAESAR-Lisflood is an open-source, GUI-based landscape evolution model written in the C# programming language, and distributed as a Windows™ executable file. As of version 1.9b (Coulthard, 2017), there was no platform-independent version of the code, and users are required to run the model in GUI-mode on a Windows-based desktop computer. The model was therefore unsuitable for running on Unix-based operating systems, such as those typically found on cluster computing facilities. High performance computing systems, beyond those of typical desktop computers, could not be taken advantage of to run computationally expensive simulations.

5.2.2 HAIL-CAESAR

HAIL-CAESAR, much like the original CAESAR-Lisflood model it is based upon, is a cellular automaton, landscape evolution model for simulating hydrological and sediment transport processes at the river catchment scale. The key components of

¹High-performance Architecture Independent Lisflood-CAESAR model, where *CAESAR* was originally the Cellular Automaton Evolutionary Slope and River model

the model are a hydrodynamic water flow-routing model, and a sediment erosion and transport model (Figure 5.1). The model is designed to simulate catchment processes on timescales of hours, years, and hundreds of years. The HAIL-CAESAR model is an open source, platform-independent C++ implementation of the algorithms in the CAESAR-Lisflood model described in the next section. The model is run from a command line or terminal interface, with the user supplying a parameter file that initialises the variables within the model, and specifies the supplementary input files such as terrain DEM and rainfall input data. The user controls the majority of the model’s operation by changing the parameter file variables. An outline of the program flow, file inputs and outputs is shown in Figure 5.1.

Object-oriented framework The HAIL-CAESAR model is designed within an object-oriented framework, enabling more advanced users to make modifications to the general model structure (Figure 5.1) by modifying the supplied *HAIL-CAESAR-driver.cpp* file. The modular approach to the model’s functionality allows advanced users to create their own custom versions of the model in a structured way using object-oriented principles. The model is also integrated with the LSDTopoTools topographic analysis framework, a C++ software package for the analysis and modelling of landscapes using raster input data. In the object-oriented framework, model simulations are created as object instances, and then methods can be called upon the model object, for example:

```
LSDCatchmentModel mySim("parameters.txt")
// Create an instance of the model
// using an input parameter file.

mySim.loaddata();
mySim.water_inputs();
mySim.depth_update();
mySim.flow_route();
mySim.erode();
```

The flexibility of the object-oriented framework allows the user finer control over the complexity of the simulation in terms of process representation, adding and removing landscape processes as necessary. This modularity in landscape evolution modelling codes is also seen in the CHILD (Tucker et al., 2001a) and Landlab (Hobley et al., 2016) modelling frameworks.

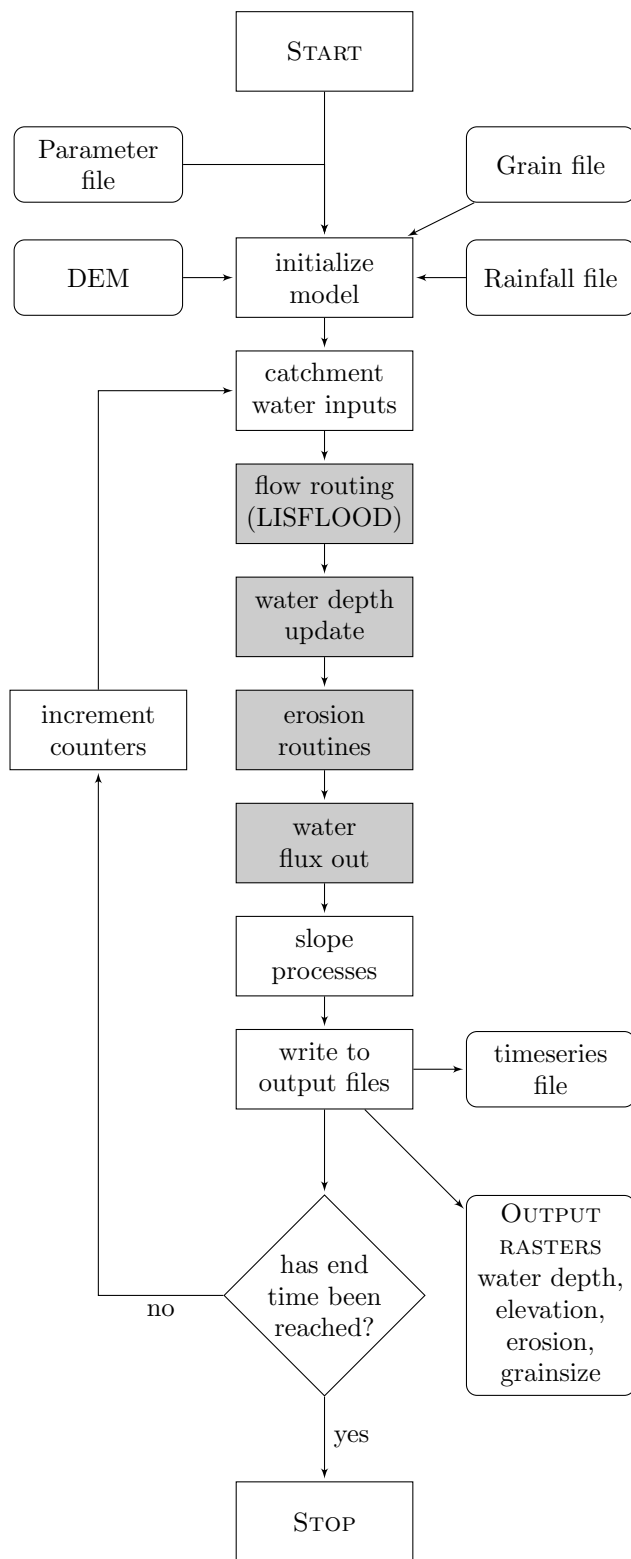


Figure 5.1: Flow chart showing a simplified outline of the HAIL-CAESAR program flow. Grey shaded boxes indicate sections of the code parallelised with OpenMP. Rounded rectangles indicate output and input files.

5.2.3 Process representation

Catchment hydrology

Runoff from rainfall inputs to the catchment is generated using an adaptation of the TOPMODEL hydrological model (Beven and Kirkby, 1979). The TOPMODEL approach first calculates a combined surface and subsurface discharge for the cells within a ‘wetted’ zone of the catchment (Coulthard et al., 2002). The wetted cells approach has the advantage of reducing the number of cells that must be scanned every model iteration, lowering computational cost of the model run. When local rainfall rate in a given grid cell is greater than zero, the total runoff, Q_{tot} , for a grid cell is given by:

$$Q_{tot} = \frac{m}{T} \log \left(\frac{(r - j_t) + \exp \left(\frac{rT}{m} \right)}{r} \right) \quad (5.1)$$

where m is a parameter that controls the rise and fall of the soil moisture store, j_t , T is the time step in seconds, and r the rainfall rate in metres per hour. The soil moisture store, j_t , is given by the formula:

$$j_t = \frac{r}{\left(\frac{r-j_{t-1}}{j_{t-1}} \exp \left(\left(\frac{(0-r)T}{m} \right) + 1 \right) \right)} \quad (5.2)$$

When rainfall rate is zero during the current iteration, the total runoff, Q_{tot} , is given by the equation:

$$Q_{tot} = \frac{m}{T} \log \left(1 + \left(\frac{j_t T}{m} \right) \right) \quad (5.3)$$

with the soil moisture store, j_t , given by:

$$j_t = \frac{j_{t-1}}{1 + \left(\frac{j_{t-1} T}{m} \right)} \quad (5.4)$$

Total runoff, Q_{tot} , is apportioned between surface and subsurface discharge by a user-set threshold for discharge, Q_{min} . When the volume of water for a given cell exceeds this threshold, it is treated as surface runoff and routed according to the flow routing algorithm described in the following section.

Surface flow routing

Surface water and channel flow is an important driver of catchment scale erosional processes. The amount and velocity of water flow is a variable in both the sediment transport and bedrock erosion laws. The surface water flow equations are based on a simplified form of the shallow water flow equations, a simplification first derived by Bates et al. (2010) and later incorporated into the CAESAR-Lisflood landscape evolution model by Coulthard et al. (2013). The flow between cells is calculated by:

$$Q = \frac{q - gh_{flow} \Delta T \frac{\Delta(h+z)}{\Delta x}}{1 + gh_{flow} \Delta t n^2 |q| / h_{flow}^{10/3}} \Delta x \quad (5.5)$$

Sediment transport and erosion

Transport of loose sediment is governed by the Wilcock and Crowe (2003) sediment transport model. The Wilcock and Crowe model represents transport of mixed sand/-gravel fractions based on the surface sediment composition. The rate of sediment transport, q_i , is given as:

$$q_i = \frac{F_i U_*^3 W_i^*}{(s - 1)g} \quad (5.6)$$

where F_i is the fractional volume of sediment, for a given sediment fraction, i , U^* is the shear velocity, s is the ratio of sediment to water density. W_i^* is a function relating fractional transport rate to total transport rate (see Wilcock and Crowe, 2003, for a full derivation of this equation). The usage of this sediment transport model is extrapolated here to account for finer particles such as silts (Van De Wiel et al., 2007), as well as the sand-gravel mixture it was originally designed for.

Bedrock incision

A simple model of bedrock incision based on the excess shear stress model (Tucker et al., 2001b; Tucker, 2004) is implemented in the numerical model. The rate of bedrock incision is determined by the amount of shear stress acting on the bedrock, above a threshold level of stress required to initiate substrate removal (e.g., Snyder et al., 2003a). When bedrock material is removed, it is distributed amongst the sediment

fractions according to the fractional proportions set by the user. The rate of bedrock erosion according to the excess shear stress model is given by:

$$\varepsilon = k_e(\tau_b - \tau_c)^{P_b} \quad (5.7)$$

where k_e is the bedrock erodibility coefficient, τ_b is the basal shear stress on the channel bed, τ_c , is the critical shear stress threshold, P_b is the shear stress exponent (Howard and Kerby, 1983; Whipple and Tucker, 1999).

5.2.4 Parallelisation implementation

The HAIL-CAESAR code is parallelised using a shared-memory parallelisation model. In brief, the shared-memory technique works by distributing the processing load to multiple processing units that all have access to the same memory address space. The HAIL-CAESAR code uses the OpenMP application programming interface (API), which is widely supported on a range of software platforms and computing architectures (Dagum and Menon, 1998). Shared-memory parallel codes such as the one described in this thesis are suitable for any computing system where the physical processors have access to the same memory space. A wide range of systems can avail of shared-memory parallel codes, from multi-core desktop computers, through high-end multi-processor, multi-core workstations, to individual compute nodes on high performance computing services (HPC). The code presented has been tested on a wide range of architectures including desktop computers, small-scale cluster computing facilities, and national scale HPC services.

The main functions in the program that are parallelisable, and most computationally expensive, are the water routing algorithm (*flow_route*), the erosion routines (*erode*), the water depth update function (*depth_update*), and the catchment wetted-area scanning function (*scan_area*). These were identified by profiling the serial version of the code using the *gprof* profiling tool (Graham et al., 1982), and the results are shown in Tables 5.1 and 5.2. Initially, it may appear that using a wetted-cells approach with the *scan_area* function would be a counter-intuitive way to reduce computation time, as the *scan_area* function is computationally expensive itself. However, preliminary experimentation with removing the *scan_area* function (and scanning all cells in the catchment every iteration) showed that in fact the computational expense of

Table 5.1: Summary of most expensive program functions, using a test case of a 48 hour flood simulation, with the model run in **hydrology-only mode**. The test case is based on the flooding that took place in the Boscastle (River Valency) catchment in August 2004, in Cornwall, UK (Golding et al., 2005).

Time (percentage of total)	Function name
77.71	flow_route
17.63	depth_update
3.58	scan_area
1.02	catchment_waterinputs
0.03	water_flux_out

Table 5.2: Summary of most expensive program functions, **with erosion processes enabled**, using a test case of a 48 hour flood simulation. The test case is based on the flooding that took place in the Boscastle (River Valency) catchment in August 2004, in Cornwall, UK (Golding et al., 2005).

Time (percentage of total)	Function name
37.96	erode
25.68	flow_route
15.90	scan_area
11.47	depth_update
3.75	(matrix library functions)
1.84	d50
1.63	slide_GS
0.59	sort_active
0.46	catchment_waterinputs
0.20	sand_fraction

calling this function was far outweighed by the large reduction in cells that had to be scanned every iteration. In practice this is likely due to the fact that catchments are rarely inundated totally, even during flood events, as only the floodplains maintain a significant depth of water. The number of wetted cells is therefore likely to be much smaller than the total number of grid cells in the model domain for the majority of cases, and the wetted cell scanning function (*scan_area*) overall reduces computation time.

flow_route The *flow_route* function is the core water-routing algorithm based on the Bates et al. (2010) algorithm. The *flow_route* function accounts for c. 26% of compute time in a typical erosion-enabled simulation, and 78% of compute time in a flow-only simulation. As one of the most compute-intensive sections of code when the

catchment is in flood, the parallelisation of this section achieved significant overall code speed up for a variety of data inputs. The flow routing algorithm is only performed on those cells in the model domain that have accumulated a water depth, i.e. it is not performed in ‘dry’ cells. This means that only a small subset of cells are accessed during the flow routing section of the code, given a typical scenario where there are significant amounts of flow in the channels and floodplain areas, but little or none on the hillslopes. The code and parallelisation of the *flow_route* function is given in outline form below:

```
#pragma omp parallel for
    schedule(runtime)
for (int y=1; y<=jmax; y++)
{
    int inc = 1;
    while (down_scan[y][inc] > 0)
    {
        // Water routing in x direction...
        // Water routing in y direction...
        inc++;
    }
}
```

depth_update Profiling of the serial code identified the water depth update function as being one of the most compute intensive parts of the code for hydrology-only and erosion-enabled simulations. Updating of water depths is done using the same scanning algorithm as described for *flow_route*, updating depths in cells where there is water, or in neighbouring cells to water-containing cells. An outline of the implementation is presented below:

```
#pragma omp parallel for
    reduction(max:l_maxdepth)
    schedule(runtime)
for (unsigned y = 1; y<= jmax; y++)
```

```

{
    int inc = 1;
    double tempmaxdepth = 0;
    while (down_scan[y][inc] > 0)
    {
        // Update water depths
        // Update suspended sediment
        // concentrations
        // Calculate maximum flow depth
        ...
        inc++;
    }
}

```

scan_area The *scan_area* function analyses the catchment to determine which cells contain water or neighbour water-containing cells and sets an index array based on the current wetted area of the catchment. Further functions that involve updating sediment or water transport amounts then use this array as a mask so that only catchment model cells that contain water will be inspected and have their sediment and water totals updated.

```

#pragma omp parallel for
for (int j=1; j <= jmax; j++)
{
    int inc = 1;
    for (int i=1; i <= imax; i++)
    {
        // zero down_scan array
        down_scan[j][i] = 0;
        // and work out scanned area.
        if (water_depth[i][j] > 0
            || water_depth[i][j - 1] > 0
            || water_depth[i][j + 1] > 0

```

```

    || water_depth[i - 1][j] > 0
    || water_depth[i - 1][j - 1] > 0
    || water_depth[i - 1][j + 1] > 0
    || water_depth[i + 1][j - 1] > 0
    || water_depth[i + 1][j + 1] > 0
    || water_depth[i + 1][j] > 0
)
{
    down_scan[j][inc] = i;
    inc++;
}
}
}

```

erode The most compute-intensive part of the code when run in erosion-enabled mode is the *erode* function. This function performs all sediment entrainment and transport routines. The serial-run test simulation spent c. 38% of its time in this function, plus an additional 5% of time in function calls within the main *erode* routine.

```

#pragma omp parallel for
reduction(max:tempbedloadmax)
schedule(runtime)
for (unsigned int y = 1; y < jmax; ++y)
{
    int inc = 1;
    while (down_scan[y][inc] > 0)
    {
        unsigned x = down_scan[y][inc];
        inc++;
        // Calculate sediment entrainment
        ...
    }
}

```

```

#pragma omp parallel for
{
    // Sediment transport in x-direction
}

#pragma omp parallel for
{
    // sediment transport in y-direction
}

#pragma omp parallel for
{
    // Calculate sediment transport
    // from all 4 edges
    // of the model domain
}

```

5.2.5 Potential speed up from parallelisation

The functions described above, *flow_route*, *depth_update*, *scan_area*, and *erode*, account for 98% and 94% of the compute-time in hydrology-only and erosion-enabled modes, respectively. The model is profiled using a 48 hour test simulation of a flash flood event in the summer of 2004 in the UK, referred to as the ‘Boscastle’ simulation. (Full details of this flood event are described in Chapter 6.) Effective parallelisation of the compute-time dominating functions should result in effective parallel speed-up. The potential speed-up as a result of parallelisation can be estimated using Amdahl’s law (Amdahl, 1967). The law gives the predicted speed up on N processing units based on ideal scaling over multiple cores. Ideal parallel speed-up, S is given by:

$$S = \frac{1}{(1 - P) + (P/N)} \quad (5.8)$$

where P is the proportion of program time that can be run in parallel. (Note that

Table 5.3: Idealised potential speed-up according to Amdahl’s law (equation 5.8). Value for P calculated using profiling results from the Boscastle (River Valency) flood test simulation after 48 hours simulated time.

Number of CPUs	Speed-up (Hydro)	Speed-up (Erosion)
	$P = 0.98$	$P = 0.94$
2	1.94	1.89
4	3.67	3.39
8	6.11	5.63
16	11.03	8.42
32	16.58	11.2
48	19.92	13.4

P may vary slightly between simulations, based on the input data and certain model parameters supplied to the program.) Profiling the program with the Intel VTune amplifier performance analysis tool suggests that the program spends 94% of its time in parallel sections of the code during an erosion-enabled simulation and 98% of compute-time in parallel sections during a hydrology-only simulation. Using Amdahl’s law it is possible to calculate theoretical potential speed-up given in Table 5.3. At the maximum available processor count of 48 cores, speed ups of up to c.20 times are predicted for a hydrology-only simulation, and up to c.13 times for an erosion-enabled simulation. The limitations of Amdahl’s law are that it predicts only idealised speed ups, and does not account for any overheads in parallelisation, such as the creation and synchronisation of threads, nor does it account for performance issues due to the speed of memory access in memory-bound computational problems (Hill and Marty, 2008; Sun and Chen, 2010).

5.3 Testing and benchmarking

Two aspects of model performance are tested in this section. Firstly, tests are carried out to verify that the HAIL-CAESAR model produces comparable scientific results with that of its progenitor, CAESAR-Lisflood. Secondly, benchmarking tests are done to measure any performance gains of HAIL-CAESAR arising from its implementation in C++, parallelisation strategy, and choice of compiler. The HAIL-CAESAR model is tested with two different compilers, to assess any potential differences arising from the choice of compiler. These are the *GCC (GNU compiler collection)* C++ compiler and

the *Intel C++* compiler. The CAESAR-Lisflood model is supplied already compiled with the Microsoft *MSVC C#* compiler. In all cases, compiler optimisation flags are turned on for the compilation process.

5.3.1 Regression testing

Regression testing is a software development practice used to verify that software that has been modified, interfaced with other software, or re-implemented, still performs as expected when compared to the original implementation (Wong et al., 1997). To verify that HAIL-CAESAR produces comparable results to the original CAESAR-Lisflood model, a set of simulations with the same test data and input parameters for both models is carried out. The catchment hydrological and sediment outputs from a 10-year simulation of the River Swale, North Yorkshire, United Kingdom are compared for consistency between both implementations. The Swaledale test case has been well calibrated in previous studies (e.g., Coulthard, 2001) and is supplied with the original CAESAR-Lisflood model as a standard test case. Details of the model testing simulations are shown in Table 5.4.

Three metrics are used to compare the two models (and choice of compiler in HAIL-CAESAR): water discharge rate from the catchment outlet, hourly sediment output, and cumulative sediment output from the catchment over the course of the simulation. Figure 5.2 shows the differences in water discharge comparing HAIL-CAESAR with the original CAESAR-Lisflood model. (For clarity, only the first 250 days are shown.) The flow routing algorithm performs similarly in both models, with the largest discrepancies seen in the first 100 days. An inset in Figure 5.2 shows the typical magnitude and timing of differences in the discharge. The timing and magnitude of the largest flood peaks are comparable, and the largest differences in magnitude on the order of $1\text{--}10\ m^3s^{-1}$. Figure 5.3 shows the sediment flux from the catchment outlet. While there is low-magnitude variation in the sediment flux signal, the main peaks in sediment discharge are at similar times and of similar magnitude in both implementations. Figure 5.4 shows the cumulative sediment output from the catchment. Initially, both implementations show close agreement, until approximately 700 days into the test simulation where the predicted sediment totals begin to diverge. The CAESAR-Lisflood implementation, in this case, predicts an overall lower total

sediment discharge over the 10-year period. The HAIL-CAESAR implementation predicts c. 40% greater total sediment yields after 10 years.

5.3.2 Differences in sediment flux and yields between models and compilers

Several factors may explain the small differences seen between the sediment outputs of the two models (HAIL-CAESAR vs CAESAR-Lisflood) and also in the comparison between the two compilers used to test HAIL-CAESAR. The sediment flux differences are shown in detail for first 250 days of the Swale test simulation in Figure 5.3.

Firstly, floating point numbers cannot be represented exactly in computer memory, due to a finite amount of memory or ‘bits’ that may be used to store each number. In the case of these tests, a *64-bit* data type is used to store numbers. Many calculations using real numbers will produce a result that cannot be represented in the finite number of bits provided by the system ($10 \div 3$, for example, results in 3.333333..., which cannot be stored precisely in a 64-bit data type, or indeed any finite-length data type). Many results such as this must therefore be rounded to fit back into their finite representation (Goldberg, 1991). The rounding error is a characteristic feature of floating-point arithmetic performed by computers. Multiplied over thousands or millions of calculations or iterations of the model, initial error can multiply over time and result in small but noticeable discrepancies within results. Secondly, optimizing compilers are free to evaluate expressions in a different order, so long as it can be shown the optimisation would produce the same mathematical result. However, this does not guarantee that two compilers will produce the exact same *numerical* result, since many floating point calculations do not have an exact result that can be represented with finite precision. If different compilers optimise calculations to be done in different orders, rounding errors may creep into the results at different stages of the calculation, resulting in slightly different final results (Goldberg, 1991; Monniaux, 2008).

Optimisation in compilers can be switched off, and it is possible to force compilers to produce bit-for-bit comparable results, however this results in a significant performance drop in simulation times. Given the relatively small size of the numerical error shown in Figure 5.3 between the two models and the different compilers, it was

not felt warranted to reduce performance significantly to produce exactly comparable sediment fluxes over these timescales.

The effect of compiler and software system choice on the results from numerical models has also been observed in atmospheric models, where different optimisation techniques performed by different compilers resulted in small discrepancies between otherwise identical simulations using models compiled with different compilers. (Hong et al., 2013).

Figure 5.4 shows the cumulative sediment totals over a longer ten-year simulation, which although initially are very close matching across model implementation (HAIL-CAESAR vs CAESAR-Lisflood) and compiler choice for HAIL-CAESAR, a divergence between the HAIL-CAESAR results and the CAESAR-Lisflood results appears around the 750 day mark. The results here would indicate the while HAIL-CAESAR and CAESAR-Lisflood produce comparable results for simulations < 750 days, at longer timescales the differences begin to diverge, producing up to 40% difference after 10 years of simulated sediment output. This again is likely at least partly due to compiler differences producing inexact numerical results. Hong et al. (2013) also find that software system differences produce greater error over longer simulation times, with atmospheric model runs diverging after several days given identical starting conditions but different compiler optimisations. It is believed that a similar effect is evident here. Since the scope of this thesis is to investigate small-scale events at short timescales on the order of days, the diverging results at longer timescales were not deemed to be of great concern for the purpose of this study. Good agreement was found between the two models at much shorter timescales, which is sufficient for this study. However, future work on the HAIL-CAESAR model would ideally investigate these discrepancies further.

A detailed analysis of the differences between the C# compiler used for CAESAR-Lisflood and the Intel and GCC compilers used for HAIL-CAESAR is beyond the scope of this study, but compiler difference remains the most likely source of numerical error based on previously reported study (Hong et al., 2013) and established knowledge regarding numerical error in using floating-point arithmetic (Goldberg, 1991; Monniaux, 2008).

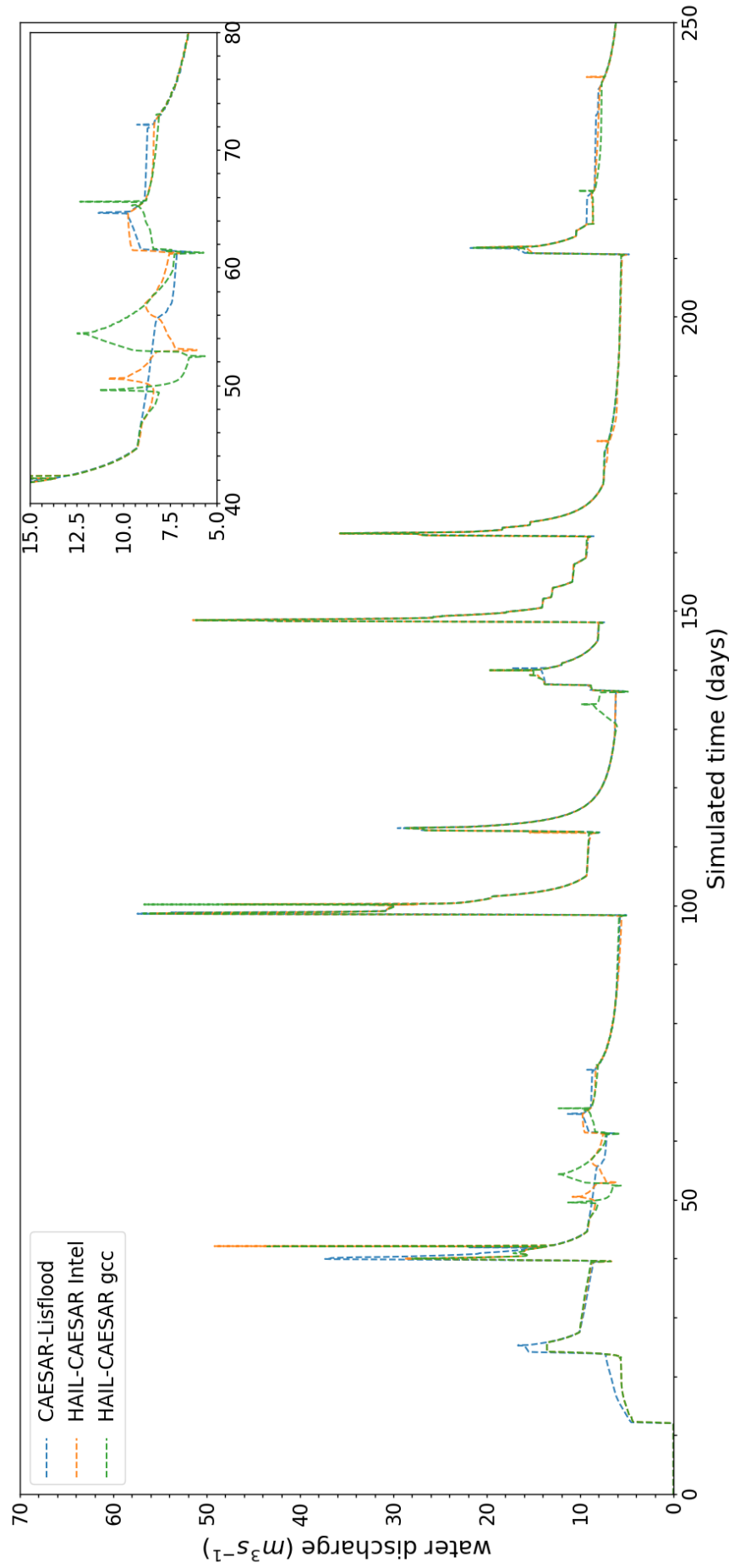


Figure 5.2: Water discharge rates over first 250 days of simulation. Outputs from the Swale 10 year at 50m resolution test case, showing results from the original CAESAR-Lisflood model and HAIL-CAESAR model compiled under two different compilers: Intel and GCC. The inset highlights the typical magnitude of difference in water discharge where the hydrographs diverge.

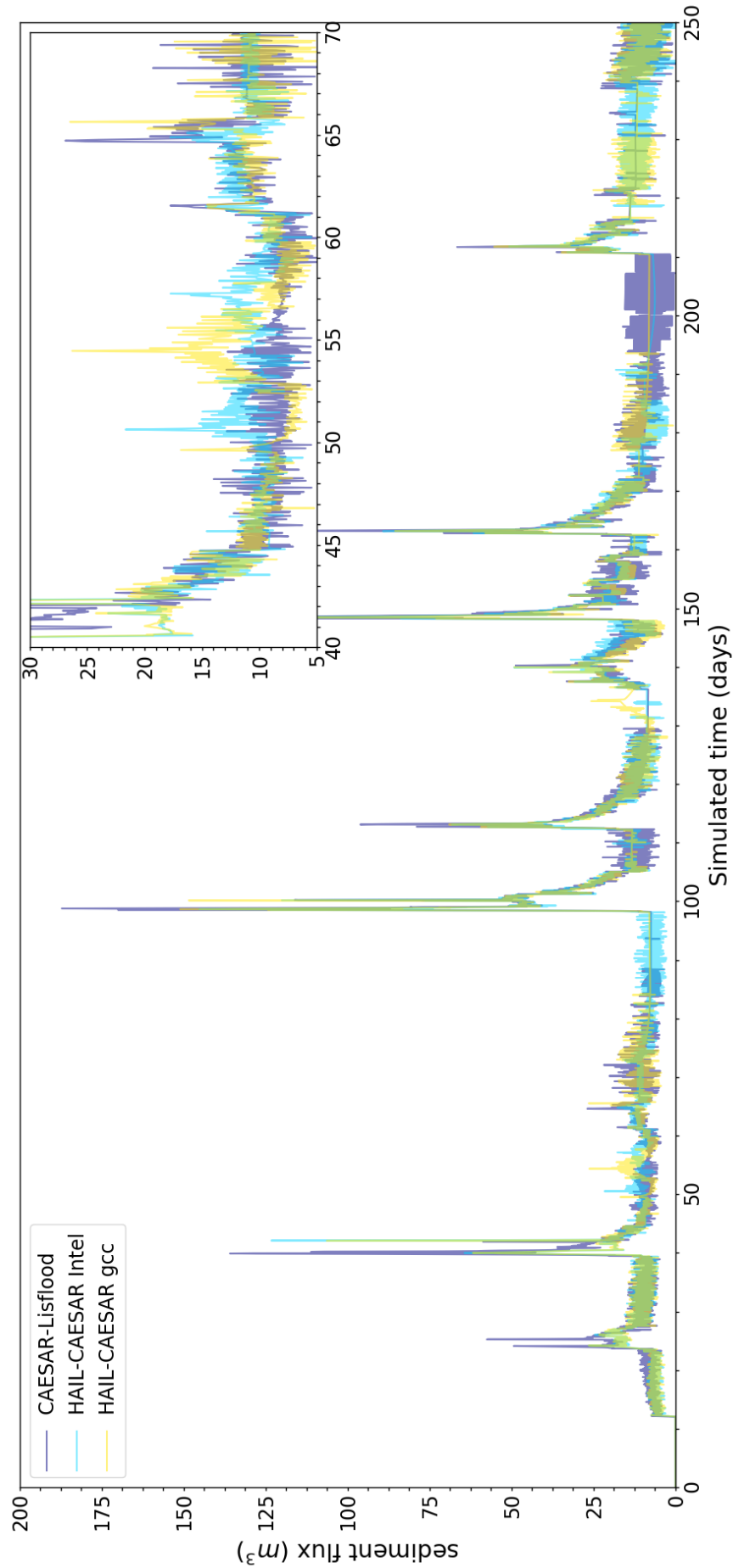


Figure 5.3: Catchment sediment flux over first 250 days of simulation. Outputs from the Swale 10 year at 50 m resolution DEM test case, showing results from the original CAESAR-Lisflood model and HAIL-CAESAR model compiled under two different compilers: Intel and GCC. The inset is to highlight the typical magnitude in sediment flux difference where the outputs diverge.

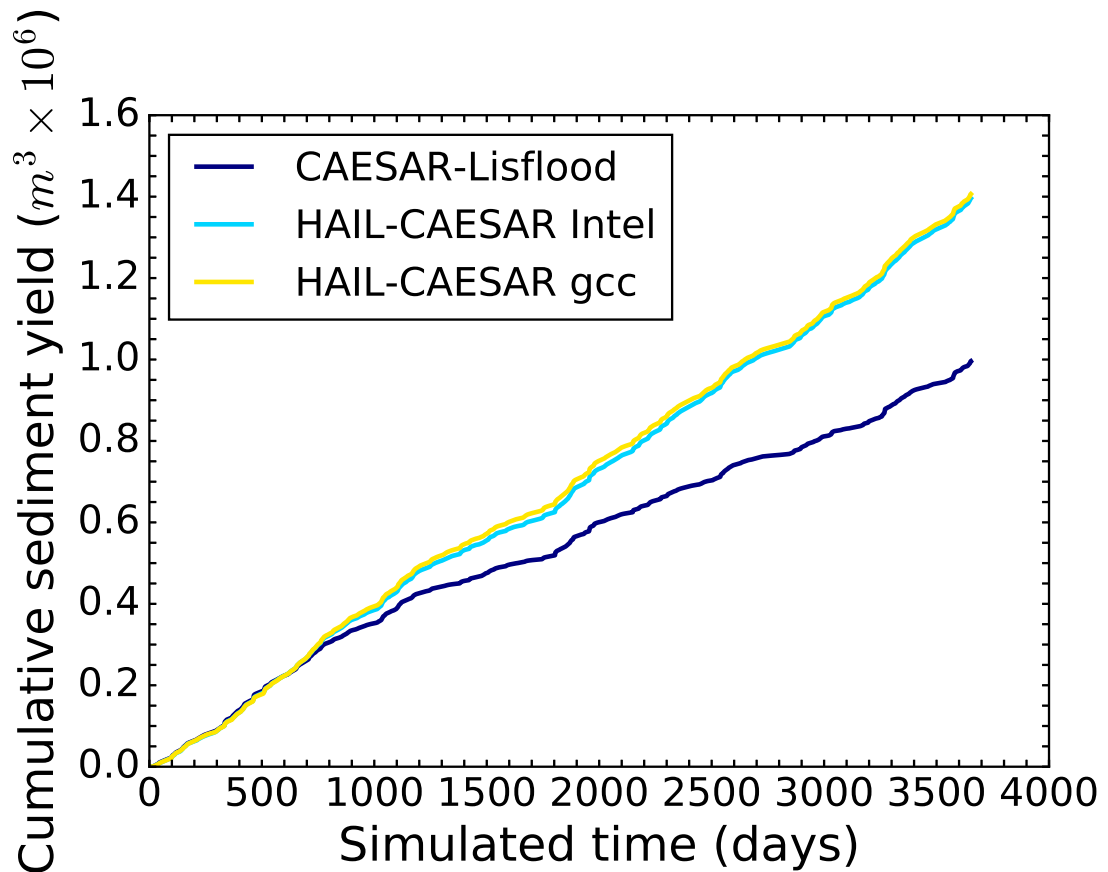


Figure 5.4: Cumulative catchment sediment flux over full duration of simulation. Outputs from the Swale 10 year at 50 m DEM resolution test case, showing results from the original CAESAR-Lisflood model and HAIL-CAESAR model compiled under two different compilers: Intel and GCC.

5.3.3 Performance comparison with CAESAR-Lisflood

Though the code base of HAIL-CAESAR and CAESAR-Lisflood differ somewhat, due to differences in implementation detail between the C# and C++ languages, as well as the parallelisation libraries used, the underlying algorithms remain broadly the same. The two models were compared on similar hardware to assess any gains in speed-up from porting the CAESAR-Lisflood model to a C++ implementation using the OpenMP parallelisation libraries.

The hardware used for this test study was a workstation computer with an Intel i7 8-core processor and 32GiB of memory. The CAESAR-Lisflood test simulations were run on a Windows operating system, as per the requirements of the software; the HAIL-CAESAR model test simulations were run on a Linux operating system on the same machine. The input parameters and input DEM were kept the same for all benchmarking simulations. The details of the test case configurations are shown in Table 5.4.

Using the HAIL-CAESAR implementation, a speed up of c.41% was seen using the open-source GNU C++ compiler (gcc) and a speed-up of 48% using the Intel C++ compiler. As the core algorithms remain the same in both versions of the code, the speed up likely comes from the fewer overheads in the command-line based HAIL-CAESAR model, and potentially through better compiler optimisations available with the C++ compilers. Further speed up may come from the fact that the CAESAR-Lisflood model is executed through a *just-in-time* compiler, translating pre-compiled bytecode into machine code at runtime (Aycock, 2003). In contrast, HAIL-CAESAR runs using a compiled binary executable file, with machine code generated at compile time. The HAIL-CAESAR approach avoids the potential overheads of invoking the dynamic compilation stage in C#/.NET programs.

Model Version	CAESAR-Lisflood 1.9b	HAIL-CAESAR v1.0	
Runtime (hrs:mins)	7:00	4:09	3:39
Programming Language	C#	C++	C++
Compiler	MSVC 14.0	GCC 6.2	Intel v17.0
Optimisation flags	-optimize	-O3, -march=native	-O3, -march=native
Parallel library	C# native parallel library	OpenMP 4.5	OpenMP 4.0
Processor	Intel i7-3770 8 core @ 3.4GHz, 32GiB memory		

Table 5.4: Initial performance and compilation comparison with CAESAR-Lisflood, using the River Swale test case, 50m DEM, 10 year simulation

5.3.4 HPC profiling and speed-up

5.3.5 Performance scaling on HPC compute nodes

The primary aim in developing this software was to have a code that ran on Unix-based high performance computing systems and could be re-compiled for a variety of different platforms and computer architectures. This section demonstrates the scaling potential and optimal hardware configurations using a single compute node on a typical HPC system. Test simulations are run on the ARCHER supercomputer. Each compute node consists of two Intel Ivybridge Xeon processors, each with 12 cores per physical processor. Simultaneous multi-threading allows each core on the processor to effectively act as if it were two separate processing units, giving a total of 48 possible threads/cores per compute node. A single compute node consists of two NUMA²-regions each with access to 16GiB of memory, a total of 32GiB per compute node.

5.3.6 Strong scaling

Strong scaling describes how the performance increase of the code scales as more processors are used to solve a problem of fixed size. We test two typical use case scenarios for the HAIL-CAESAR model. The first case is an extension of the standard test case using the Swale data. The use of the model in this case is typical of longer duration landscape evolution simulations, with periods of predominantly low hydrological flows interspersed with brief (relative to the simulation time) storm events. The second case uses the HAIL-CAESAR model to simulate a single storm event at higher spatial

²Non-uniform memory access

Table 5.5: Strong scaling test cases used to benchmark the HAIL-CAESAR model, using Swaledale and Boscastle DEMs.

Strong scaling benchmarking simulations				
Catchment	Swaledale		Boscastle	
Grid cells	124931	720000	4500000	
DEM cell size	50m	5m	5m	2m
Simulation time	8670 hrs	48 hrs	72 hrs	72 hrs
Catchment Size	150km ²	12km ²	12km ²	12km ²
Number of cores	1, 2, 4, 8, 16, 20, 30, 36, 40, 48			

resolutions, over a much shorter timescale. Two contrasting model applications are chosen to represent the range of timescales the model can be applied to, from short term single storm events to annual and decadal simulations. The simulations are all run with spatially uniform rainfall input.

Multi-event simulation, 1 year The Swaledale test case is run over a 1 year duration, using an input DEM of 50 m resolution. The model is run in hydrology-only and erosion-enabled modes. The input parameters and input DEM are the same for each simulation, as each simulation is repeated on an increasing number of processors (Table 5.5). At the maximum core count of 48 core, results from this simulation show speed up of up to 700% and 550%, for erosion-enabled and hydrology-only modes, respectively. The speed-up shown for erosion-enabled simulations does not always increase in concert as core-counts are increased, although the overall trend is one of increasing speed-up. For example, erosion-enabled simulations with 16, 24, and 36 processors showed a slow down when compared to the preceding benchmark tests using 12, 20, and 30 processors, respectively (Figure 5.5). The hydrological-only simulations showed a more consistent speed-up between benchmark tests (Fig. 5.5), though speed-up potential begins to decline at thread counts around 30 threads and higher, where it is observed the gains from increasing the thread count further diminish.

Single-event simulation, 48–72 hours For this benchmark, two sets of strong scaling experiments are done with two different resolution DEMs. For each set of experiments, the input terrain data and parameters remain the same while increasing

the number of processors over which the problem is shared. The strong scaling benchmark tests use a model domain with a) 720 000 grid cells, and b) 4 500 000 grid cells, representing a 12km² river catchment with 5m and 2m resolution DEMs, respectively. At this resolution of DEM, it is possible to resolve the larger channel geometries at the grid-scale, without resorting to techniques of ‘burning in’ the DEM with a channel. Sub-grid parameterisation of the channel shape, a feature of some models, is also not required.

Since HAIL-CAESAR features both a flood-inundation-only and sediment erosion mode, two further sets of benchmarks were done for both problem sizes, one with the model running in hydrology-only mode, and another running in the erosion-enabled mode.

The results from the single-event scaling benchmark show the greatest speed-up for the 48 hour Boscastle simulation, with a speed-up of almost 16 times at 48 threads/cores, for the hydrology-only simulation. Erosion-enabled simulations also show good speed-up for this problem size (720 000 grid cells), but the linear speed-up trend is lost above around 30 cores, when speed-up gains begin to tail-off. At the larger problem size of 4 500 000 grid cells, the speed-up gains from increasing core counts is much diminished, though still increases linearly through higher core counts. Speed-up here reaches only about 5 times running on 48 cores, in hydrology-only mode, and 3.5 times in erosion-enabled mode.

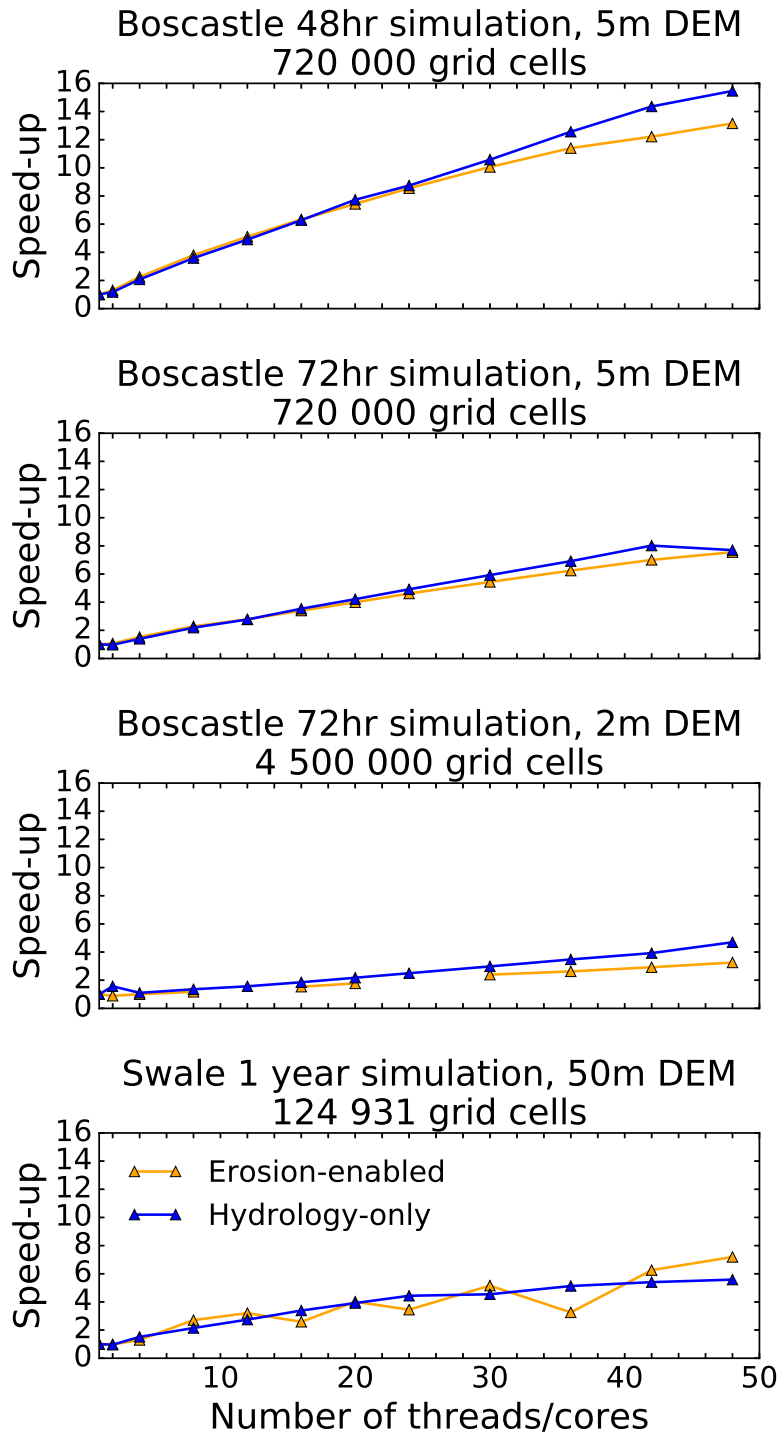


Figure 5.5: Speed-up achieved relative to serial code on 2, 4, 8, 12, 16, 20, 24, 30, 36, 42, and 48 cores. Four sets of simulations are used representing a range of model uses from short, single event episodes (48–72hr) to 1 year simulations.

5.3.7 Weak scaling

Weak scaling is a parallel performance metric used to assess how the code runtime scales as the amount of work per processor is kept the same, but the total problem size – in this case, the number of grid cells in the model domain – is increased (Gustafson, 1988). This mirrors the practice of using larger numbers of processors to tackle model simulations using higher resolution topographic data, or data covering a larger spatial domain. The weak scaling experiments used a set of hydrology-only simulations and a set of erosion-enabled simulations. A series of 72 hour simulations were done using a range of high-resolution topographic datasets, from 0.5 m to 5 m resolution, scaling the number of processors used to maintain the ratio of processors/workload as near as possible. The number of model domain grid cells per core was fixed at approximately 1 500 000. The simulations were repeated for hydrological-mode and erosion-enabled modes, but due to the high memory demands of running very high resolution erosion-enabled simulations, not all simulations could be completed on the available hardware, which has a maximum job runtime of 48 hours.

The simulations in hydrological-only mode show positive weak scaling as the problem size increases in tandem with the number of threads (Figure 5.6). Ideal weak scaling would be expected to show a runtime per number of grid cells/cores remaining approximately constant compared with a single-threaded simulation. The slight increase seen in the weak scaling here is likely due to the overheads experienced with creating and synchronising the extra threads as the problem size is increased.

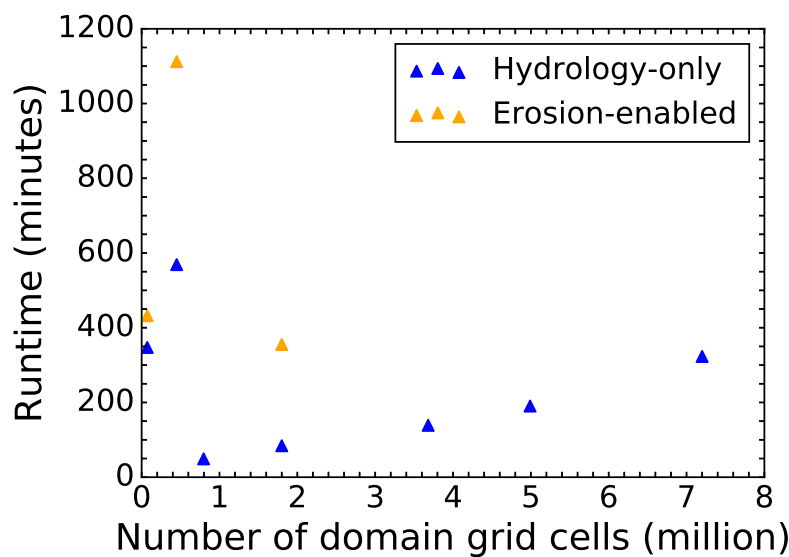


Figure 5.6: Weak scaling with the Boscastle DEM at increasing resolution (see Table 5.6). Hydrological and erosion-enabled simulations shown. Each simulation uses c.150 000 grid cells per CPU. The absence of results for certain erosion simulations is due to memory limitations preventing higher resolution simulations from running.

Table 5.6: Weak scaling test cases with the Boscastle DEM resampled at increasing resolutions from 0.5m to 5m. The absence of run-time results for certain erosion simulations is due to memory limitations preventing higher resolution simulations from running.

Weak scaling simulations, Boscastle DEM, 72 hour simulation						
DEM resolution (m)	Grid cells	Ideal no. of threads	No. of threads	Cells per thread	Run time (Hydro)	Run time (Erosion)
0.5	72 000 000	48	48	1 500 000	323.1	—
0.6	49 900 050	33.3	33	1 512 122	190.4	—
0.7	36 808 200	24.5	26	1 472 328	138.8	—
1.0	18 000 000	12	12	1 500 000	84.3	355.2
1.5	7 960 050	5.3	5	1 592 010	49.0	—
2.0	4 500 000	3	3	1 500 000	568.9	1112.1
5.0	720 000	0.48	1	720 000	347.306	432.3

5.3.8 Thread profiling

Further profiling of the parallelised version of the code was carried out using the Intel® VTune Amplifier performance analyser. Thread profiling shows where the bottlenecks in the code are, including functions that are compute intensive, but also where inefficiencies occur due to overheads from parallelisation and load imbalance. For clarity, a single example using the Boscastle test case is presented, with a simulated model time of 48 hours, running on 8 cores/threads. It is expected that different simulations and domain sizes would produce slightly different results, but this simulation gives a general idea of the parallel performance of specific functions in the code.

The break down of major function overheads is shown in Figure 5.7. Only four of the key parallel-implemented functions, *erode*, *flow_route*, *scan_area*, and *depth_update* are assessed, as other functions collectively amounted to a small proportion of the runtime, or were serial functions. Load imbalance accounts for 22% of the execution time of these four key functions, due to certain threads sitting idle while waiting for other threads to complete. Load imbalance is particularly apparent in the *erode* and *depth_update* functions. Overhead time (from the creation and synchronisation of threads) is minimal across all functions. The issue of load imbalance is discussed further in Section 5.4.2.

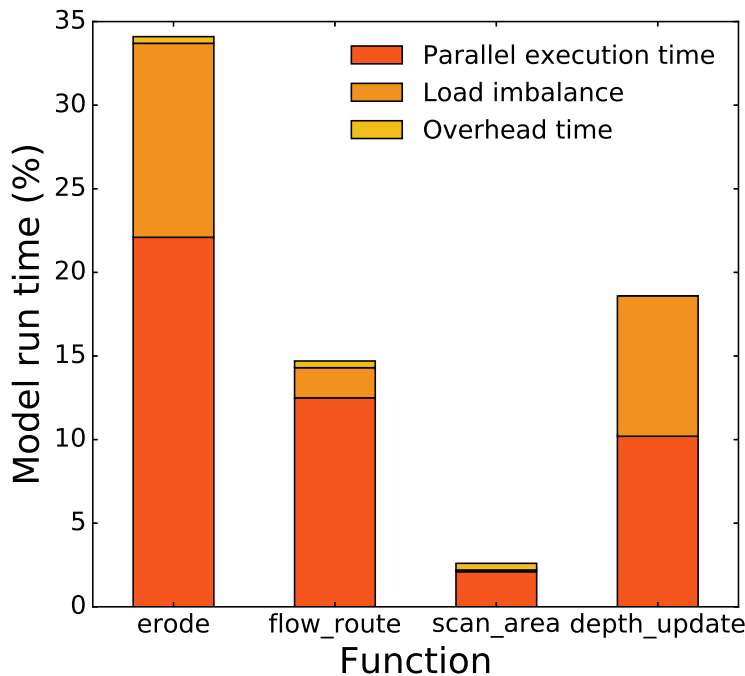


Figure 5.7: Thread profiling of the Swale 1 year simulation with 50m DEM. Data from major functions only displayed.

5.4 Discussion

5.4.1 Parallel scaling

There are three factors that potentially affect the parallel scaling observed in the benchmarking test cases presented.

1. The number of grid cells in a model domain, i.e. the total problem size, which is dependent on the resolution of the DEM input data.
2. The choice of running the simulation as hydrology-only or erosion-enabled model. The erosion option in the model also increases memory demands significantly compared to the hydrology-only mode, as well as computational expense.
3. The hydrological state of the catchment. When the catchment is experiencing flooding due to high rates of rainfall input, the number of cells registered as containing water through the *scan_area* algorithm increases substantially. The location of the water-containing cells in a catchment also determines the amount of load-imbalance in the model. If water-containing cells are concentrated only in a certain area of the catchment, significant load-imbalance will occur.

The most favourable speed-up was observed in the Boscastle 48 hour simulation at 5 m DEM resolution (Figure 5.5.) A speed-up of almost 16x was recorded using the maximum number of cores available on the test hardware. Increasing the length and resolution of the Boscastle simulation appeared to negatively affect the speed-up potential of the simulation. Speed-up gains remained approximately linear into higher core counts, with slight tail-off in speed-up gains observed when approaching 48 cores. The longer-term Swale simulation exhibited poorer scaling, with a gradual drop in speed-up gains as the number of threads/cores was increased.

There is not a clear relationship between number of grid cells in the model domain and speed-up potential. The Swale test case (about 125 000 grid cells), for example, showed almost half as much speed up as the 48 hour Boscastle simulation, despite the latter having 720 000 grid cells in the model domain.

The enabling of erosional processes in simulations did not significantly affect the scaling potential of the simulations. Most benchmark results showed slightly less favourable speed up at higher core counts for erosion-enabled simulations, but this did not appear to be the controlling factor on scaling. In one case (Swale) the erosion-enabled simulation ran 2x faster than the corresponding hydrology-only simulation. The lack of contrast between erosion-enabled and hydrology-only simulations may be explained by the adaptive time stepping feature used in the *erode* function. In erosion-enabled mode, the timestep increases substantially during periods of low water flow and erosion rates, and this may offset the increased computational demands from the *erode* function.

The Boscastle and Swale test cases represent different types of catchment hydrological state. The Boscastle simulations essentially represent a single intense flooding event, where the catchment is in a period of low flow followed by an intense burst of rainfall and erosion for a few hours. The Swale simulation represents a series of storm events, interspersed with ‘dry’ periods, where the model will be able to increase the timestep, but not make heavy use of parallel sections of the code reserved for water routing and erosion routines.

5.4.2 Load balancing issues

Parallel computing problems in which the distribution of workload between each thread or processor is uneven are said to suffer from *load-imbalance*. In other words, although the model domain is divided into equally sized chunks for the number of threads and processors available, each thread will not necessarily receive an equal amount of work to do (Sakellariou, 1996). Threads with little amounts of work to do will therefore remain idle while waiting for heavily-loaded threads complete their assigned work. Numerical simulation of river catchments is inherently load-imbalanced. The load balance problem arises from the nature of catchment processes, where the most rapid rates of geomorphological activity occur in river channels. In river channels, rates of water flow and sediment transport are greatest, relative to the processes operating on hillslopes. The inherent heterogeneity in the nature of catchment processes translates into computational imbalance during model simulations of river catchments. Within the model domain representing a catchment, the grid cells of the domain representing river channel sections will make the greatest computational demand, due to repeated calls to subroutines that calculate or update cell properties. Highly active river channel cells will frequently exceed thresholds set for the calculation of water flows and sediment entrainment, whereas cells representing hillslope areas will be active relatively infrequently.

The mechanism in the model that determines which cells will be updated each iteration is the scanning algorithm described in the *scan_area* section. The algorithm was originally designed (Coulthard et al., 2013) to substantially reduce the number of cells in the model domain that had to be updated each iteration, by isolating the cells that contain water and only performing erosion and sediment transport routines on those ‘wetted’ cells. While the algorithm is effective at reducing compute time this way, it creates a load-imbalance problem for parallel implementations as the location of computationally intensive areas of the model domain cannot be easily predetermined. While threads are assigned equal numbers of iterations, each iteration is not necessarily equally load-balanced in terms of computational expense. In algorithms that perform a global scan of all cells in the model domain, such as the parallel implementation of the flow routing algorithm in Neal et al. (2009), load imbalance is minimalised because threads are kept occupied working on every grid cell, rather than focusing on a subset

of grid cells with discharge or water depth above a given threshold, as is done in the HAIL-CAESAR model. A global scanning algorithm was initially explored in the implementation of HAIL-CAESAR, allowing the removal of the *scan_area* function, but the increase in run-time was so substantial it negated any potential improvements in load balance among the OpenMP threads.

5.4.3 Loop scheduling

The OpenMP application programming interface (API) will automatically partition iterations of a loop between the available number of threads. By default these are assigned statically when a `parallel for` block is entered, with threads receiving an equal number of loop iterations to carry out. The default behaviour can be overridden, however, by explicitly specifying a different scheduling type for parallel for loops. For load imbalanced problems such as discussed in this thesis, the *dynamic* loop scheduling can improve parallel performance by reducing the amount of idle time that threads spend waiting for busy threads to complete their workload (Willebeek-LeMair and Reeves, 1993; Olivier et al., 2012). The default behaviour of the dynamic scheduling type is to assign each loop iteration to one thread, and when the thread finishes it is assigned the next iteration that has yet to be executed. Experiments in finding an ideal loop scheduling set-up to reduce load imbalance in HAIL-CAESAR showed mixed results, with no clear indication that using the dynamic scheduling clause improved run-times in all cases. However, in some test cases, dynamic loop scheduling was shown to offer performance improvement. For this reason, the HAIL-CAESAR model provides users with the option to set the loop scheduling type at run time, by specifying the `OMP_SCHEDULE` environment variable before running the model. It is recommended that users experiment with using dynamic scheduling for their own simulations as it may offer performance increases over default scheduling.

5.5 Conclusions

An implementation of a hydrodynamic landscape evolution model was developed, based on the CAESAR-Lisflood model (Coulthard et al., 2013). The new C++ implementation of the model is modular, cross-platform, and scalable to multi-core computing systems through the implementation of shared-memory parallelism with the OpenMP API. Minimal code changes were required to the serial version of the code to deliver a parallel compute code. The model exhibits a performance increase of c.40% compared to the CAESAR-Lisflood implementation in a like-for-like benchmark. The scaling potential of the model is variable, depending on the size of the problem domain and the likely hydrological state of the river catchment being simulated. In most test cases, linear speed up is achieved at moderate core counts of up to 48 cores, on model domain sizes of up to 4.5 million grid cells. Computational load imbalance was a substantial problem in the model. The causes of the load balancing issues in the model are likely due to the spatially-heterogeneous nature of catchment-scale hydrological and erosional processes. Suggestions are made for minimising load imbalance through dynamic loop scheduling, but the success of these scheduling methods is highly dependent on the input data to the model.

6

Model setup and parameterisation of two flash flood events in the UK

6.1 Background

Intense rainfall events may be short lived, lasting only a few hours, but have the potential to cause substantial and destructive flooding (Lane, 2008; Pitt, 2008). In the UK, many of these storms occur in the summer (Kendon et al., 2014), and their severity is often the result of a combination of meteorological factors. From a meteorological perspective, flash flooding can be predicted through an ingredients-based method; a systematic assessment of the key components present to cause an intense rainfall event likely to lead to flash flooding (Doswell et al., 1996). In the ingredients-based approach, flash flooding occurs when there is a combination of a high rainfall rate for an extended duration of time (usually on the order of hours). Rainfall totals are in turn related to the length of the rainfall event. Factors that lead to high rainfall intensity during an event include the forced ascent of moist air, usually associated with orographically-forced rainfall events (Barros and Lettenmaier, 1994; Houze, 2012). The duration of the event is dependent of the speed of movement and the size of the system bringing rainfall; given equal intensity rainfall rates, a large, slow moving rainfall feature will cause much higher rainfall totals in a river catchment than a fast moving, smaller feature.

Though not essential to the ‘ingredients-based’ method of flash flood prediction, convective-type storms are frequently associated with the type of intense rainfall that

leads to flash flooding (Doswell, 1993), including highly-localised flooding in the UK (Gray and Marshall, 1998; Browning et al., 2007). In certain cases, convective rainfall events may appear stationary or ‘quasi-stationary’ (Chappell, 1986; Warren et al., 2014), leading to prolonged intense rainfall over river catchments.

The combination of these ingredients leads to river catchments being subjected to high-intensity rainfall inputs at a rate faster than a river catchment can transport or store water, leading to river flooding when rivers exceed their bankfull¹ capacity, or surface water flooding if rainfall rates are greater than infiltration rates at the surface. Antecedent conditions, such as soil-moisture content, also play a role in a catchment’s ability to store water, but in cases of the most extreme rainfall events, even catchments with a high potential to store incoming rainfall or slow water flow towards rivers will be overwhelmed with the rate and volume of water input and flooding becomes inevitable.

This chapter describes two intense rainfall and flash flooding events in the UK summers of 2004 and 2005. The cause and impact of the events are described as a background to them being used as case studies in a series of numerical simulations. The series of numerical simulation experiments are designed to investigate the role of rainfall spatial resolution in hydrological and geomorphological processes during severe storms, as described in Chapter 1.

The two events used as case studies took place in 1) the Ryedale catchment, near the town of Helmsley, North Yorkshire, 2005; and 2) the Valency catchment near the village of Boscastle, Cornwall, 2004. Both catchments experienced intense rainfall leading to extensive and damaging flash flooding (Golding et al., 2005; Sibley, 2009). There were significant economic impacts for both communities, as well as geomorphological changes to the river channels and flood plains observed in the aftermath of the flooding (HR Wallingford, 2005; Wass et al., 2008).

6.2 Meteorological setting

The case studies were chosen as they represented infrequent events in each particular catchment. Because there is no commonly agreed definition of what constitutes an extreme or infrequent event (e.g. Wilby et al., 2008; Fowler and Wilby, 2010; Jones et

¹The water level at which a river is at the top of its banks and any further rise would result in water moving into the flood plain.

Catchment Name	Ryedale	Valency
Main settlement	Helmsley	Boscastle
Catchment Area	270km ²	18km ²
Catchment Type	Upland, Moor/Peaty	Upland, Pasture
Storm Date	2005-06-19	2004-08-16
Peak Rainfall (mm hr ⁻¹)	125	c.400
Meteorological Setting	Split-front, convective system	Quasi-stationary convective system
3hr Rainfall Return Period	330yr (Wass et al., 2008)	1300yr (Burt, 2005)

Table 6.1: Table showing key characteristics of each storm event.

al., 2014), for the purpose of this study, flood events likely only to occur approximately once in several hundred years were chosen. (The return period for the 3 hour rainfall event is given in Table 6.1.) Peak river discharges for each of the case study flood events exceeded the 99th percentile for their respective catchments (Hannaford, 2004; National River Flow Archive, 2016). An overview map of the catchment locations is given in Figure 6.1, marked by the location of their main settlements. Table 6.1 summarises the key features of each catchment and its associated storm.

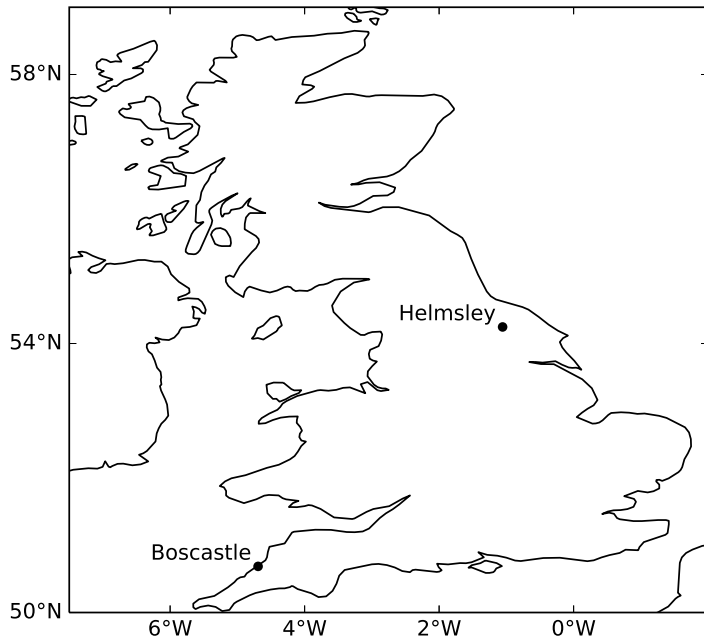


Figure 6.1: Location of the two case study catchments in Britain, marked by the main settlement within each catchment.

6.2.1 Boscastle, Cornwall storm 2004

The Boscastle storm took place on 16 August 2004. The storm led to flooding within the River Valency catchment and the village of Boscastle. In the preceding months March–June, the south-west area of Britain had been drier than usual, although during July the Valency catchment area experienced average rainfall conditions (Golding et al., 2005). The estimated soil moisture deficit² in the area, which had previously been lower than average due to the dry antecedent conditions in March–June, decreased during 1–16 August, due to a return to average rainfall conditions in that month. The soil moisture deficit during this period was estimated to have decreased from approximately 80–220mm to 40–180mm (Golding et al., 2005).

On the day of the storm, rainfall accumulations of up to 184mm from the Lesnewth tipping bucket raingauge (Golding et al., 2005) were recorded in the upper Valency catchment resulted from prolonged rainfall between 1200–1600 UTC. Rainfall rates were thought to have reached almost 400 mm hr^{-1} (Golding et al., 2005), after correcting for under-reporting from rain gauges in the vicinity of the catchment (Burt, 2005). The rainfall accumulations from the 1km gridded composite radar product in the Valency catchment are shown in Figure 6.2. Note that the highest rainfall accumulations from the radar data shown in Figure 6.2 are 115mm, lower than the raingauge totals reported in Golding et al. (2005), likely due to under reporting by precipitation radar.

²The amount of water needed to bring the soil back to field capacity, i.e. a state where the soil is holding the maximum amount of water possible against gravity. (Beven, 2011)

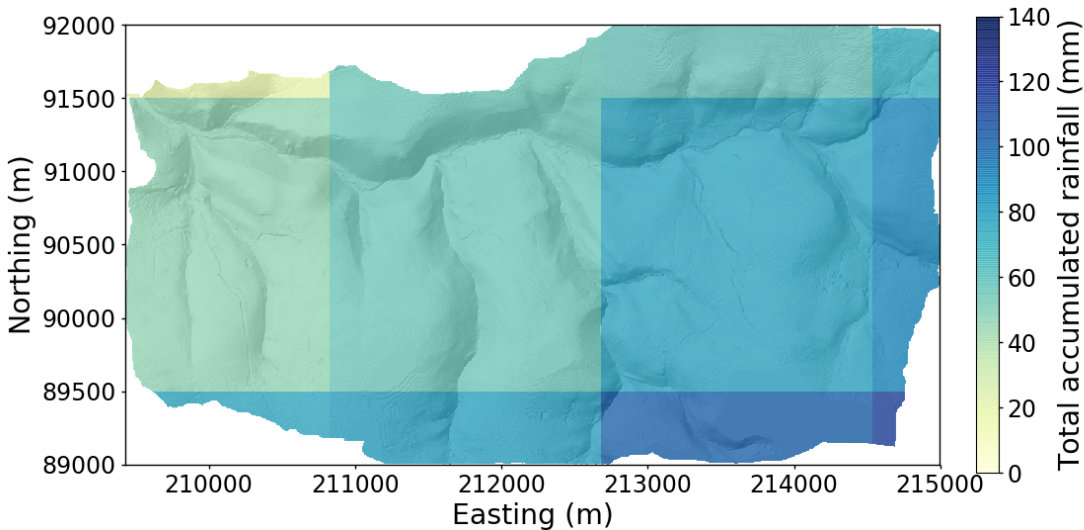


Figure 6.2: Total accumulated radar rainfall (24 hours) over the Valency (Boscastle) catchment during the 16th August 2004.

6.2.2 Ryedale, North York Moors storm 2005

The Ryedale storm occurred on 19 June 2005. Intense rainfall throughout the afternoon led to total accumulated rainfall amounts of up to 89mm in Ryedale between 1400–1800 UTC measured by the Helmsley raingauge. Peak instantaneous rainfall rates were estimated to have been around 32.5mm hr^{-1} (Sibley, 2009) to 59.4 mm hr^{-1} (Hopkins, 2012), though one report states they reached as high as 125 mm hr^{-1} (Cinderey, 2005). Figure 6.3 shows the total accumulated rainfall radar totals from the 1km composite radar product. Most areas of the catchment received total rainfall accumulations similar to the reported raingauge figure (89mm), though up to 131mm is reported in one grid square in the south of the catchment area.

Antecedent conditions before the Ryedale storm of 2005 were dry over a prolonged period over much of the region (Sibley, 2009), leading to cracking of the surface peat in the higher elevations of the catchment. Soil moisture deficit was estimated to be around 60mm in the catchment, higher than usual due to the drier conditions in the preceding months (Wass et al., 2008). With a high soil moisture deficit, thinner soils in the upper reaches of the catchment would have been dry before the intense rainfall.

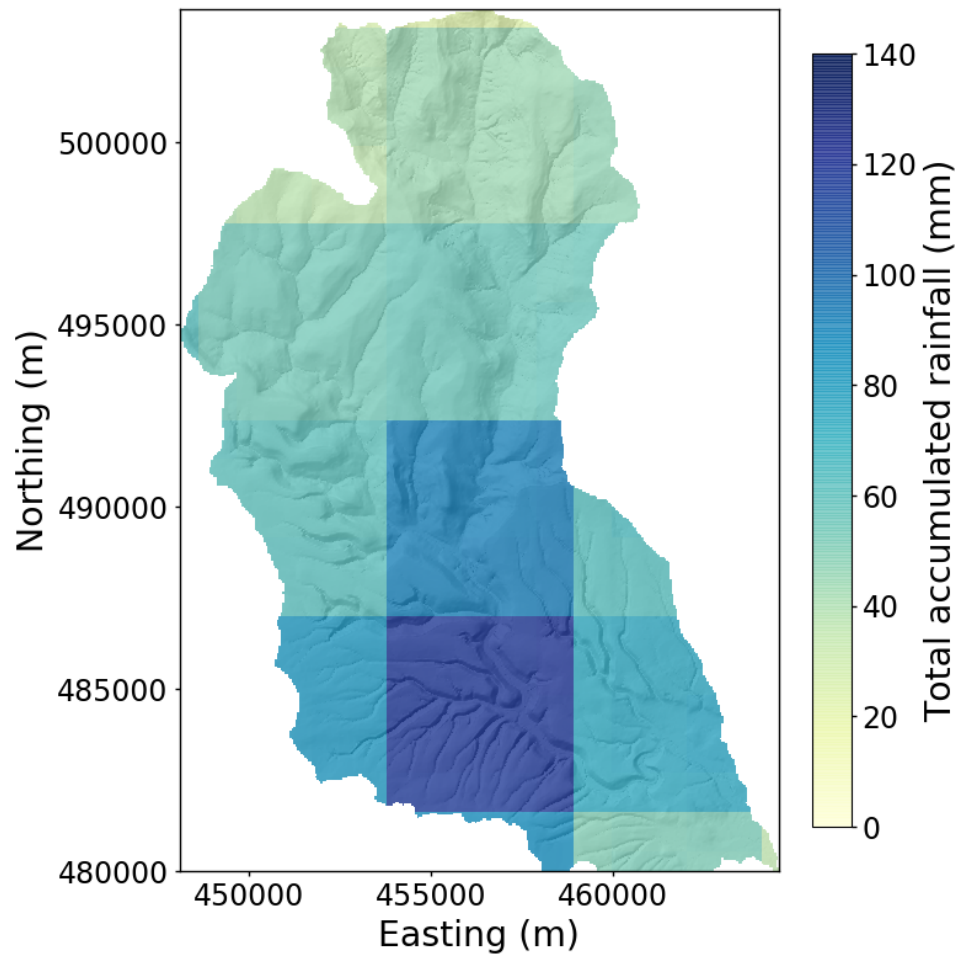


Figure 6.3: Total accumulated radar rainfall (24 hours) over the Ryedale catchment during the 19th June 2005.

6.3 Flooding and geomorphic change

6.3.1 Boscastle, Cornwall, 2004

Flooding was extensive in the area surrounding Boscastle village, with flood levels rapidly exceeding bankfull and flooding several properties to depths of several metres. Water levels in the Valency river and its tributaries began to rise in the early afternoon from approximately 1200 UTC onwards, reaching bankfull around 1430 UTC and peaking at around 1600 UTC, by which point over 70 properties had been flooded, with several destroyed due to the force of the water (HR Wallingford, 2005).

The routing of flood waters in the Boscastle flood was complicated due to the role of large debris blockages ('trash barriers') in the river channels. In particular, a large debris blockage formed under the main bridge in the village crossing the Valency,

which caused a significant backup of water behind the bridge, and re-routing of water through alternate pathways within the village. A reconstruction of the flood based on eyewitness accounts and water mark levels consequently resulted in different reports of the peak water level in the village depending on where the observations were made (HR Wallingford, 2005).

The geomorphological impacts of the flood event were well documented in the aftermath of the event (HR Wallingford, 2005). The Valency river channel and many of its tributaries experienced channel avulsion³ in places, as well as significant downcutting in the upper tributary channels of the catchment. In a number of places the channel avulsion was substantial enough to straighten the channel and increase the local gradient of the river, potentially increasing flow velocities and shear stresses acting on the channel bed. There were large amounts of sediment observed in the river flow at the time, ranging in size from fine silts to boulders. There were some areas of sediment deposition observed along the river channel banks and floodplain, and a sizeable area of sediment deposition in Boscastle harbour. However, most stretches of the main river channel and its tributaries showed net erosion in the form of channel widening (up to 3–4 metres) and deepening (of up to 2 metres) (HR Wallingford, 2005).

6.3.2 Ryedale, North Yorkshire, 2005

Flooding was widespread in the Ryedale catchment, with river levels reaching up to 3.5m at Hawnby, a smaller settlement upstream of Helmsley. At the peak of the flood, the Hawby gauging station building was completely submerged (Wass et al., 2008). In Helmsley, the largest settlement, further downstream, similar river level rises of up to 2m were reported at the peak of the flood in the evening and into the night.

Geomorphologically, the Ryedale catchment saw relatively rapid change considering the short duration of the storm and subsequent flood on 19 June. In the aftermath of the flood, up to 2–3 metres of channel downcutting and erosion were reported to have taken place in the upper reaches of the tributaries of the catchment (Hopkins, 2012; Wass et al., 2008) as well as significant amounts of sediment and debris deposition in the lower reaches of the catchment around Helmsley (Hopkins, 2012). The storm triggered many landslides on hillslopes within the catchment, including 105 reported

³Movement of the original channel to a new position within the flood plain.

shallow landslides in the catchment, as well as two large peat slides in moorland areas covering up to 3.7 ha of mass movement in areal extent (Galiatsatos et al., 2007; Wass et al., 2008). Dry antecedent conditions in the area are believed to have been a main cause of landsliding in the area by weakening the peat moorland within the catchment (Sibley, 2009). Dry conditions preceding summer storms can cause shrinkage and cracking in peatlands, leading to greater risk of erosion in heavy downpours (Warburton et al., 2004). The economic damage was also substantial for a sparsely populated area. Three bridges were destroyed at a cost of £2.9 million, as well as flooding of 121 properties (Wass et al., 2008). Economic loss included agricultural damage such as loss of land and livestock (Sibley, 2009). Many residents were displaced for months during repair and were reported to have suffered illness and psychological trauma from the event (Hopkins, 2012).

6.4 Experiment design

Using the two flash flood events described previously as case studies, an ensemble of simulations was designed to address the questions laid out in Chapter 1 and summarised in the following hypotheses:

- 1. Flood inundation modelling is sensitive to the spatial detail of precipitation inputs.**
 - (a) Catchment hydrology is sensitive to the spatial distribution of rainfall inputs over the catchment area. Resolving the spatial details of a precipitation event, such as during a flash flood, allows the timing and magnitude of flood inundation to be better predicted.
 - (b) Geomorphological change of the river channel and flood plain during a flash flood is substantial enough to alter the patterns of flood inundation. In a model that can account for erosional change during flooding, nuances in flood inundation can be better predicted.
- 2. Erosional processes in river catchments are sensitive to the spatial distribution of rainfall inputs.**

Experiment name	Rainfall input	Erosion law
UNIFORM_HYDRO	Spatially-averaged Radar	(no erosion)
UNIFORM_DLIM	Spatially-averaged Radar	Detachment-limited
UNIFORM_TLIM	Spatially-averaged Radar	Transport-limited
GRIDDED_HYDRO	1km Radar Gridded	(no erosion)
GRIDDED_DLIM	1km Radar Gridded	Detachment-limited
GRIDDED_TLIM	1km Radar Gridded	Transport-limited

Table 6.2: Outline of the simulations carried out for both the Ryedale and Boscastle case studies.

- (a) Erosion and sediment transport processes are sensitive to thresholds determining erosion initiation and sediment entrainment. If item (1a) holds true, then fluvial erosional processes should exhibit sensitivity to the spatial distribution of rainfall inputs of rainfall as well.
- (b) The parameterisation of erosional processes in the model also determines the spatial pattern of erosion and deposition, but does spatial variation in rainfall inputs exert a greater control than the choice of erosion law?

To test the above hypotheses, simulations of the two case studies were repeated, varying the following conditions:

- Rainfall spatial resolution: 1km-gridded/uniform
- Erosion law: transport-limited/detachment-limited

The simulations were parameterised with different erosion law schemes and different rainfall input resolutions to assess which factor exerted the greatest control over flood inundation and sediment transport within the catchment. The same set of experiments was carried out for both the Boscastle and Ryedale events, giving a total of 6 different simulations for each catchment outlined in Table 6.2 – a total of 12 simulations.

6.4.1 Model initialisation and configuration

The numerical landscape evolution model, HAIL-CAESAR was used for all simulations. The equations describing the water routing, sediment erosion and transport laws are described fully in Chapter 5.

Two erosion laws are used in the set of simulations with erosional processes ‘switched-on’ in the model: a transport-limited law and a detachment-limited law. The transport-limited law represents erosion taking place under flowing water, which is limited by the capacity of the water to move away sediment. It assumes a constant supply of sediment is available, and that *transportation* is the effective limiting factor on how much erosion takes place during water flow over hillslopes and in rivers. The transport-limited law in HAIL-CAESAR is based on the Wilcock and Crowe (2003) sediment transport law, which accommodates multiple grain sizes across the sand to gravel particle size range. The equations describing the Wilcock and Crowe model are referred to in Section 5.2.3.

The second type of erosion law used in the simulations is a bedrock incision law based on detachment-limited erosion. A detachment-limited law assumes that erosion is limited by the amount of material that can be *detached* from the bedrock layer, based upon a critical shear stress exerted by water flow being exceeded to detach sediment material. The detachment-limited law is based on the same law used in the CHILD landscape evolution model (Chapter 2) and the equations describing it are given in Section 5.2.3.

The two erosional parameterisations used in these simulations represent two end-members of a spectrum of potential erosion laws that could be used. Upland catchments in the UK, and in these catchments in particular, tend to be a mixture of thin sediment layers and partially exposed bedrock. It was felt that limiting the number of erosion laws used to two end-members would constrain some of the uncertainty in selecting a sediment transport law appropriate for these types of catchment, similar to a landscape evolution modelling approach used by Attal et al. (2008).

Input data

Rainfall input data is taken from the Met Office NIMROD radar rainfall 1km composite dataset (Met Office, 2003). The same 1km rainfall radar product is used to derive the rainfall inputs for the spatially uniform rainfall simulations, by averaging out the gridded rainfall data over the input points of the catchment, thus preserving the total amount of rainfall input in each simulation, and only varying its spatial distribution for the relevant gridded rainfall input simulations.

Topographic data used to initialise the terrain surface for the Boscastle simulation is derived from the Environment Agency (England) 2m LiDAR product. The Boscastle data is resampled to 5m grid spacing to reduce the total number of grid cells and the computational demands of running a complex hydrodynamic model. Environment Agency LiDAR was not available for the whole Ryedale catchment at the time of the simulation, so the Ryedale terrain is initialised using Ordnance Survey ‘Terrain 50’ data, interpolated to 5m grid spacing to enable like-for-like comparison with the Boscastle terrain grid spacing. Resampling the initial topographic data sources to the same terrain grid spacing of 5m for both sets of simulations is done to minimise the potential effects that variation in grid spacing has on model output and subsequent topographic analysis (e.g Chang and Tsai, 1991; Schoorl et al., 2000; Haile and Rientjes, 2005; Zhang et al., 2008)

Simulation duration

The simulations are set to begin 24 hours before the day of each storm event. The model is allowed to run for a further 24 hours after the event, giving a total simulation time of 72 hours. The timing of the simulations is given in Table 6.3.

Event	Start time	End time
Boscastle	2004-08-15 00:00	2004-08-17 23:59
Ryedale	2005-06-18 00:00	2005-06-20 23:59

Table 6.3: Start and end times (UTC) for each 72 hour simulation. The major rainfall event occurs during the second day in each simulation.

Rainfall spatial resolution

In order to assess the sensitivity of hydrogeomorphic processes to the spatial details of precipitation, rainfall spatial inputs were alternated in each simulation between a spatially uniform rainfall input and a 1km gridded rainfall input. Both the spatially uniform and gridded inputs were based on the same original rainfall source data – the UK Met Office Nimrod 1km-composite radar data product (Met Office, 2003). The uniform rainfall input data were created from averaging out the gridded data in space over the model domain. The temporal resolution of the five minute interval data was preserved, giving a time series of spatially averaged rainfall rates for the duration

of the each simulation. To reduce the range of variables within the set of ensemble simulations, only the spatial resolution of rainfall was assessed in this study – other studies had already investigated the effects of the *temporal* resolution of rainfall data on discharge and erosion rates (Nicótina et al., 2008; Coulthard et al., 2013; Coulthard and Skinner, 2016). In all experiments, the temporal resolution of rainfall data was maintained at five minute intervals. To summarise, the two types of rainfall spatial input used were:

- Uniform or ‘lumped’ precipitation: Radar-derived rainfall rates across the catchment are spatially-averaged to produce a catchment-wide rainfall rate. In other words, every grid cell in the model domain receives the same rainfall rate at each five minute rainfall data timestep.
- Gridded rainfall input. The rainfall rate is input from a overlying gridded mesh of raincells, at the same grid spacing as the rainfall radar product (1km).

Erosion-enabled simulations

A variety of erosion laws exist describing how landscapes erode from fluvial erosion. The choice of erosion law for a given catchment depends on a variety of factors, such as the characteristic substrate material in the catchment – is it predominantly loose sediment or cohesive, solid bedrock? In reality, many upland landscapes in the UK are often a mixture of these two extremes, incorporating a thin layer of loose sediment on top of solid bedrock. Streams in such landscapes may be termed mixed-channel systems (Howard, 1998), and many variants on the fluvial incision laws incorporating the role of sediments have been proposed (Lague, 2005; Sklar and Dietrich, 2006). Catchments also often exhibit a transition from rockier upland headwaters, to more thickly soil-mantled floodplains. In order to address the sensitivity to the choice of erosion model for each event simulation (Chapter 2), two erosion model end-members are used, with each one representing a different conceptual model of fluvial erosion and sediment transport. These include: i) a purely sediment transport-limited model (Wilcock and Crowe, 2003), ii) a detachment-limited bedrock erosion model (Howard and Kerby, 1983; Stock and Montgomery, 1999; Whipple and Tucker, 1999). The equations describing the transport-limited and detachment-limited models used in the

model are discussed in detail in Chapter 5. Further erosion laws were considered, such as a hybrid transport- and detachment-limited erosion model, but it was deemed beyond the scope of this study, which is primarily to investigate the role of rainfall heterogeneity, rather than the wide range of erosion and sediment transport models. In keeping with the primary aim of the study, it was opted to use two simple variants of sediment erosion laws to keep the range of model simulations parsimonious.

Flood inundation only simulations

A set of control simulations (suffixed *HYDRO*, for example in Table 6.2) incorporating only rainfall-runoff and surface water routing (with no erosion taking place) were also carried out for comparison against the two erosion end-member simulations. The analysis from these experiments is used to investigate the sensitivity of flood-inundation prediction to geomorphic change during floods, and the results and discussion are presented in Chapter 7.

6.5 Summary

Using case studies from two flash flood events in the UK that took place in recent decades, a series of simulations was designed to investigate the effects of rainfall spatial resolution on flood inundation modelling, and sediment erosion and transport. The simulations are designed to answer the questions laid out in Chapter 1 and the hypotheses summarised in Section 6.4.

The results and analyses from the simulations are discussed in the subsequent chapters. Chapter 7 analyses and discusses the effects that rainfall spatial resolution has on flood inundation prediction in the HAIL-CAESAR numerical model, and also looks at the effects that geomorphic change during a flood has on flood dynamics. This addresses Question 1 laid out in Section 6.4 above.

Chapter 8 analyses the results of the simulations focusing on sediment erosion and transport, discussing whether the spatial patterns of rainfall control the distribution of erosion and deposition in a catchment. The implications for longer-term landscape evolution modelling are also discussed. Chapter 8 addresses Question 2 laid out in Section 6.4 above. Conclusions and links between rainfall inputs, hydrological, and

geomorphological processes are discussed in Chapter 9.

7

Sensitivity of a flood-inundation model to rainfall distribution and erosional parameterisation

7.1 Introduction

The question of whether the hydrological response of a river catchment is sensitive to the spatial detail in rainfall input is unresolved, with a number of different studies arriving at seemingly conflicting conclusions as to the exact role of rainfall spatial variability. One early study using deterministic modelling of river catchments and synthetic rainfall fields (Wilson et al., 1979) suggests that detailed space–time representations of rainfall are needed in distributed hydrological models to produce accurate flood forecasts. Predicting peak discharge in a small catchment (7.5km^2) is sensitive to the temporal resolution of rainfall input data, but less so to the spatial distribution of rainfall inputs during single storm events (Krajewski et al., 1991). Over longer time scales (on the order of decades), a similar conclusion is reached by Coulthard and Skinner (2016), finding that temporal resolution of rainfall input data is a greater control on hydrological outputs over long time periods than spatial resolution.

The catchment size is likely to play a part in determining sensitivity to rainfall spatial distribution, with several studies suggesting smaller catchment sizes can dampen the effect of rainfall spatial variability (Segond et al., 2007; Nicótina et al., 2008). The idea of catchment-size dependence has been developed further (Gabellani et al.,

2007), to suggest that sensitivity to rainfall spatial heterogeneity depends on the characteristic size of the rainfall feature and the catchment size. Systematic investigation of the role of catchment size and morphology have suggested that the ratio between the characteristic hillslope length of the catchment and the rainfall feature determines sensitivity to rainfall spatial heterogeneity (Nicótina et al., 2008). In cases where the rainfall feature is much greater in size than the typical hillslope length, the effects of rainfall spatial heterogeneity on runoff generation and hydrological response are limited.

Modelling catchment hydrological sensitivity to rainfall spatial resolution requires a rainfall data source capable of capturing the spatial variability of rainfall across a catchment. Rainfall radar has been successfully used as a spatially variable rainfall input to a variety of types of catchment hydrology and urban hydrology models, from deterministic flood-inundation models (e.g Coulthard and Skinner, 2016), to probabilistic hydrology models (Bell and Moore, 2000; Cole and Moore, 2008). The use of rainfall radar can be applied to modelling a range of environmental situations. For example, urbanised catchments (Berne et al., 2004; Einfalt et al., 2004; Thorndahl et al., 2014) to small mountain catchments (Borga et al., 2000), as well as large-scale regional hydrological modelling using national rainfall radar networks (Knebl et al., 2005).

Understanding how flood dynamics interact with channel and floodplain morphological change is of growing concern for flood modelling (Fewtrell et al., 2011). Morphological change during flood events has been shown to be a potential control on the extent of flooding during intense rainfall (Schumm, 1979; Stover and Montgomery, 2001; Wong et al., 2015), particularly when river channels undergo geomorphically rapid change during repeated rainfall events of high magnitude (Sear et al., 2010; Slater, 2016). Within the context of a single flood, bedload sediment may become highly mobile, and the forces acting on the boundaries of the river channel are sufficient to alter channel geometry in long profile, cross-section, and channel pattern (Kleinhans et al., 2013; Wong et al., 2015). As a counterargument, during large flood events, the floodplain and river channel may effectively act as one channel unit, dampening any effects brought about by changes to river channel morphology (Bates et al., 2005). The implications of sediment transport and erosion within river catchments has been

highlighted as an important factor in flood inundation modelling (Lane et al., 2007; Lane et al., 2008; Neuhold et al., 2009), and should form part of an effective flood modelling strategy (Wong et al., 2015) in catchments thought to be sensitive to morphological change during large floods. Most numerical modelling approaches to flood inundation prediction are concerned with improving or addressing uncertainties in hydraulic flow (Galland et al., 1991; Bates and De Roo, 2000), rather than considering other boundary conditions such as the morphology of the channel bed and floodplain itself. Numerical models of flood inundation often overlook river channels and their floodplains as a mechanism for controlling flow patterns and inundation extents during flash floods (Neuhold et al., 2009).

Flood inundation prediction studies rarely consider both geomorphological change or spatial heterogeneity in rainfall inputs to the catchment during intense rainfall episodes. Given the reported importance of rainfall resolution on predicting increased erosion rates, sediment yields and channel incision over decades (De Luis et al., 2010; Coulthard and Skinner, 2016), can the same observation be made at the time scale of a single event? In extreme rainfall events that mobilise large amounts of sediment, does this in turn control the dynamics and distribution of the floodwaters? Though there are different conclusions as to importance of rainfall heterogeneity and channel morphological change in flood inundation modelling, there is at least agreement that both have the potential to alter the outcome of flood prediction under certain conditions – yet exactly which conditions is still uncertain. More investigation is needed into which of these uncertainties – spatial heterogeneity of rainfall input or erosional processes – plays the greater role in determining flood inundation patterns during intense rainfall events. The simulations and analysis presented in this chapter attempts to address this by comparing flood inundation model predictions under different rainfall spatial resolution scenarios and erosion law parameterisations.

The following questions are explored through the use of numerical modelling experiments set out in Chapter 6.

1. Are predicted flood inundation extents during a storm sensitive to the spatial resolution of rainfall inputs to the catchment?
2. Is morphological change of the floodplain and channel during a storm event

substantial enough to affect flood inundation predictions?

7.2 Method

An ensemble of numerical simulations detailed in Chapter 6 is used to investigate catchment hydrological response to different parameterisations of spatial variability of rainfall data and erosional process representation. The ensemble simulations use the HAIL-CAESAR landscape evolution model developed in Chapter 5. The results of the simulations were then analysed in terms of the hydrological outputs of the model: water discharge, average water depths, and spatial distribution of floodwaters. The set of simulations used in this chapter are laid out in Table 6.2 in Chapter 6. In addition to the simulations described in Chapter 6, a further set of hydrological simulations is carried out to assess the model sensitivity to the m hydrological parameter that controls how rapidly the catchment responds to rainfall events (Beven and Kirkby, 1979).

7.2.1 Sensitivity analysis of the TOPMODEL m parameter

There are numerous user-defined parameters in the HAIL-CAESAR model (and in landscape evolution models in general) that have a wide range of potential values. Parameter selection in environmental modelling comes with a degree of uncertainty, and resulting outputs from models can be highly sensitive to the user's choice of input parameters for a given simulation (Pelletier, 2012). Initial testing of the HAIL-CAESAR model, and studies using the CAESAR-Lisflood model that it is based upon, show it is particularly sensitive to the m parameter (Coulthard et al., 2002; Welsh et al., 2009). The m parameter in HAIL-CAESAR is based upon an adaptation of the semi-distributed hydrological model TOPMODEL (Beven and Kirkby, 1979). The parameter represents the rate of the rise and fall of the soil moisture store, determining how quickly a catchment responds to rainfall inputs – sometimes referred to as the ‘flashiness’ of a catchment. A high value of m reduces the transmissivity of the soil, leading to slower response times in the catchment, whereas a lower value of m increases soil transmissivity leading to quicker response times to rainfall input and a ‘flashier’ hydrograph. The m value imitates the factors associated with water movement and

Catchment	<i>m</i> parameter
Ryedale	0.003, 0.004, 0.005, 0.006, 0.007, 0.008, 0.009, 0.01, 0.015, 0.02

Table 7.1: TOPMODEL m parameter values used to run sensitivity simulations for each type of rainfall input types (Uniform and Gridded) for the Ryedale catchment.

storage in relation to the vegetation cover of a catchment; it is sometimes termed the *land-use parameter* (Welsh et al., 2009) to reflect this. Typical values used for m range from 0.002–0.005 (grassland) to around 0.02 (dense forest) with the range of values in between representing a full range of vegetation covers (Beven et al., 1984; Beven, 1997).

Initially, the experiments were designed to use the default model value of $m = 0.002$ for grassland (Beven et al., 1984). Both the Boscastle and Ryedale catchments are a mixture of agricultural pasture land, some sparse vegetation, and small urban settlements; but the dominant land cover is sparse vegetation or grassland, making the default $m = 0.002$ value seem most appropriate as a first approximation. Preliminary experimentation showed that the default value of $m = 0.002$ was adequate in reproducing the Boscastle hydrograph noted in an earlier study (HR Wallingford, 2005) (See also Figure 7.3), therefore no further detailed sensitivity analyses were carried out for Boscastle with respect to the m parameter.

For the Ryedale catchment, however, preliminary experimentation indicated that the hydrological response of the catchment was highly sensitive to the choice of m parameter. To assess the full range of sensitivity to the choice of m parameter in the Ryedale catchment, a series of simulations were carried out with a range of m values for both uniform and gridded (spatially variable) rainfall inputs. Simulations of the Ryedale flood event were carried out with the m values shown in Table 7.1. Each of the simulations was run with the model in hydrology-only mode, with no erosional process parameterisation switched on. To assess whether there was further sensitivity to the type of rainfall input (gridded or uniform), the sensitivity analyses were repeated with both types of rainfall input data.

7.3 Results

7.3.1 Model sensitivity to the m parameter

The model exhibited a strong sensitivity to the choice of the TOPMODEL m parameter. In the results presented in Figure 7.1 peak river discharge ranged from approximately $530 \text{ m}^3\text{s}^{-1}$ using an m value of 0.003 to $20 \text{ m}^3\text{s}^{-1}$ using an m value of 0.008 under uniform rainfall input conditions. Under spatially variable rainfall inputs, discharge was as high as $650 \text{ m}^3\text{s}^{-1}$ where $m = 0.003$. The measured peak discharge reported for the 2005 Ryedale storm at the Ness gauging station was $80 \text{ m}^3\text{s}^{-1}$ (Environment Agency, email communication), and a subsequent post event report estimated the peak discharge at $105 \text{ m}^3\text{s}^{-1}$ (Wass et al., 2008). In the sensitivity simulations, a value of $m = 0.005$ under uniform rainfall conditions produced a flood peak most closely matching the observed value, peaking at approximately $100 \text{ m}^3\text{s}^{-1}$, the choice of $m = 0.005$ for Ryedale also best approximated the timing in the rise and fall of the hydrograph. Under spatially variable conditions (Figure 7.2), a value of $0.007 < m < 0.008$ would appear to produce a hydrograph most likely to match the observed discharge rates in terms of the onset of flooding, but a value of $0.006 < m < 0.007$ would be likely to more closely match the magnitude of peak discharge. At a first approximation, the use of uniform rainfall inputs appeared to lead to better agreement of the model with measured discharges from the river gauging station data, in terms of agreement with both the timing and magnitude of the flood peak. It was decided therefore to use the calibration data from the uniform rainfall sensitivity analysis to choose the best value of m for the main set of simulations.

There were differences between the hydrographs of the observed and simulated discharges in terms of peak discharge timing and recession limb shape. The measured hydrograph overlaid in Figure 7.1 (black dashed line) showed a sharp rise at around 50 hours after the start of the simulation period. Lower m values ($m < 0.005$) resulted in the prediction of the flood peak being too early compared to the observed timing, with values > 0.005 predicting the flood peak timing too late. Most of the simulations failed to capture the extended duration of peak discharge, which lead to a ‘plateaued’ appearance of the measured hydrograph, lasting approximately 5–6 hours, before receding back to low flow levels. The simulation with $m = 0.006$ came closest

to predicting this plateaued hydrograph shape, but failed to predict the magnitude of water discharge correctly, underestimating the peak flow by almost 50%.

For Ryedale simulations, it was decided to use an m value of 0.005, providing the closest possible match to the flood peak discharge, although the model was unable to capture the true shape of the hydrograph and the receding limb. As the catchment simulations include a representation of erosion and sediment transport processes, which are often threshold dependent, it was felt necessary to match the discharge peak more closely over choosing to match the hydrograph shape precisely, therefore the value of 0.005 was used.

It was decided not to use different values of m for each of uniform and gridded simulations to limit the variability in parameter space in the ensemble of simulations. Although calibrating each rainfall input type with its own value of m may have produced better fitting hydrographs with the observations, the core aim of the thesis is to assess sensitivity to rainfall variability and erosion law parameterisation. Introducing variation of the m value between different simulations would have made comparing the water and sediment fluxes difficult, as they would have each been potentially controlled by m as well as either rainfall data resolution or erosion law. Using the same value of m for each catchment limits the number of variables to one in each simulation. A limitation of this approach is that most of the simulations for Ryedale actually achieved a better match with the observed hydrograph data when using the uniform rainfall inputs (Figure 7.4), rather than spatially variable rainfall inputs. However, since the primary purpose of the thesis was to assess the sensitivity of the model to rainfall spatial variability and erosion law, rather than improve the forecasting ability of such models, this was deemed an acceptable compromise. Further work could also explore varying the m parameter in tandem with other variables in the model, but this is beyond the scope of the present study.

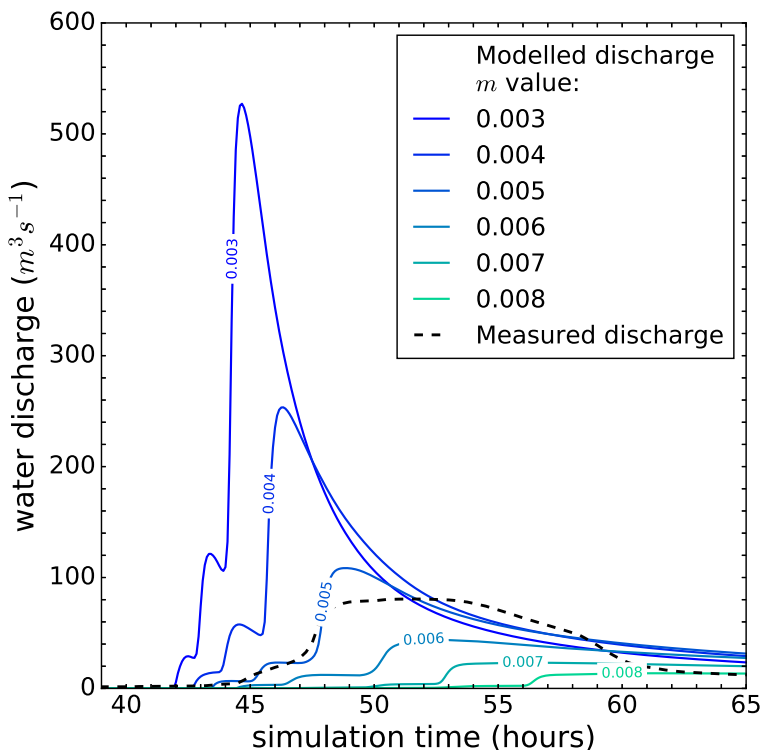


Figure 7.1: Hydrograph sensitivity to the m parameter under **uniform** rainfall inputs. Discharge over time at the Ryedale catchment outlet for varying values of the m parameter. The measured discharge at the catchment gauging station is overlaid in dashed line. The results from the simulations with $m > 0.008$ are omitted for clarity due to the low discharges they produced.

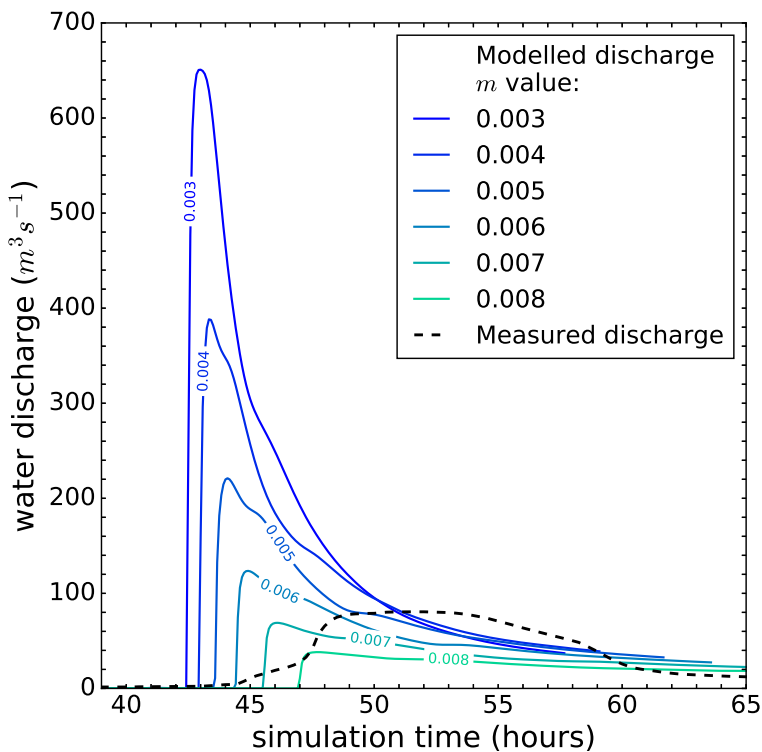


Figure 7.2: Hydrograph sensitivity to the m parameter under **gridded** rainfall inputs. Discharge over simulation time at the Ryedale catchment outlet for varying values of the m parameter. The measured discharge at the catchment gauging station is overlaid in dashed line. The results from the simulations with $m > 0.008$ are omitted for clarity due to the low discharges they produced.

7.3.2 Catchment hydrographs

General observations

At the catchment scale, hydrological response was sensitive to both the rainfall resolution and the choice of erosional model. For both catchments, higher resolution rainfall input data resulted in a greater maximum river discharge. In the Ryedale experiments, simulations using the gridded (spatially variable) rainfall input experienced a flashier hydrological response, reaching peak discharge several hours before the uniform rainfall input cases. This large difference in timing was not observed in any of the Boscastle simulations, with all simulations reaching peak discharge within 10 minutes of each other. Peak discharges and the timings of peak flow for each simulation are tabulated in Table 7.2.

The choice of erosion model also influenced the hydrological response. When catchment erosion was modelled using a transport-limited (TLIM) case, peak discharges were higher in all cases, but the timing of hydrograph peaks remained similar for each case. The difference in peak discharges was minimal when comparing the detachment-limited (DLIM) cases to the hydrology-only simulations.

Boscastle

The timing of peak discharge in the Boscastle catchment was similar for both the gridded and uniform rainfall simulations (Figure 7.3). In gridded rainfall simulations the discharge peaked 40 hours after the start of the simulation (1600 UTC) and for the uniform rainfall input simulations at 40 hours 10 minutes into the simulation (1610 UTC). The choice of erosional parameterisation did not appear to affect the timing of the peak discharge. However, it did result in small changes in the discharge rate at peak flow, of up to 14% difference in the uniform rainfall simulations, and 6% increase in the gridded rainfall simulations. The primary control on the amount of discharge at peak flow appeared to be the type of rainfall inputs into the model, with the gridded simulations predicting peak discharges up to 28% higher than their uniform counterparts.

Comparison with measured discharge is not possible in the Boscastle case, as the basin is ungauged. However, a number of methods exist for predicting runoff and river

flow in ungauged river basins (Sivapalan, 2003; Blöschl, 2013), and two estimations of discharge are presented here for comparison with the predictions from the HAIL-CAESAR model. Both estimations were derived in the HR Wallingford (2005) report and the hydrographs are overlaid on the model outputs from this study in Figure 7.3. The HR Wallingford report produced a simple hydrograph derived from eyewitness reports and water level marks, estimating a peak discharge of $180 \text{ m}^3\text{s}^{-1}$ at 1600 UTC, the same as the timing of peak flow in the HAIL-CAESAR simulations. A second estimation of the hydrograph during the Boscastle event was made in the report using a one-dimensional hydraulic model, InfoWorks RS, which also predicted a peak flow of approximately $178 \text{ m}^3\text{s}^{-1}$, but at the later time of 1700 UTC. The InfoWorks RS model uses a fixed representation of the river bed; in other words, it does not permit the topographic surface to change during the course of the model simulation.

The estimated flow from observations and the 1D hydraulic model was higher than any of the model predictions made in this study – a difference of 30–80 m^3s^{-1} was noted between the HAIL-CAESAR simulations and the two estimations from the HR Wallingford report. The rising and falling limbs of the hydrograph were also much shallower than the HAIL-CAESAR model predictions, which suggest a much more rapid rise and fall in water levels during the storm.

Ryedale

The hydrological response of the Ryedale catchment was more sensitive to the choice of rainfall input type, with marked differences in the timing and magnitude of the peak discharge between the uniform and gridded rainfall sets of simulations (Table 7.2, Figure 7.4). There is up to 83% increase in discharge in the gridded rainfall simulations when compared to the corresponding uniform rainfall input simulations. The hydrograph was less sensitive to the type of erosional parameterisation, with up to 40% difference observed in the uniform rainfall cases, and upto 25% difference in the gridded rainfall simulations.

The River Rye is gauged at several locations, and flow data was recorded during the 2005 flood, though the accuracy of gauging station data is uncertain during particularly high flow events (Shaw et al., 2010). The gauge data is measured at the River Rye

Ness gauging station¹. The outlet of the modelled catchment domain was set up to coincide (as near as possible) with the location of the Ness gauging station on the River Rye. The observed flow data from the gauging station is overlaid in Figure 7.4. The gauging station data most closely matches the hydrographs produced by the uniform rainfall inputs, though it is lower than all of the simulated hydrograph, peaking at approximately $81 \text{ m}^3\text{s}^{-1}$. A further value of peak discharge during the Ryedale flood was reported by Wass et al. (2008) as $105 \text{ m}^3\text{s}^{-1}$, derived from 1D flow modelling – the timing of this estimated peak flow was not available due to the type of model used. The value of peak discharge reported by Wass et al. (2008) is similar to that of the Environment Agency gauge data and the peak flows predicted by the uniform rainfall input simulations in this study.

The difference in timing of peak flow between the set of gridded rainfall input simulations and the uniform rainfall simulations is large; the gridded rainfall simulations predict the timing of peak flow being almost four hours earlier than the simulations using a uniform rainfall input. Observations reported in Wass et al. (2008) and the Environment Agency gauge support the predictions made by the uniform rainfall simulations in this case. However, this perhaps to be expected due to the fact the the TOPMODEL m value for Ryedale was calibrated using the uniform rainfall input data. The same value of m was then used with the gridded rainfall data (to ensure uniformity across simulations) though it is likely to be mis-calibrated in this case.

¹Environment Agency gauging station F2505 – British National Grid reference SE 69439 79196

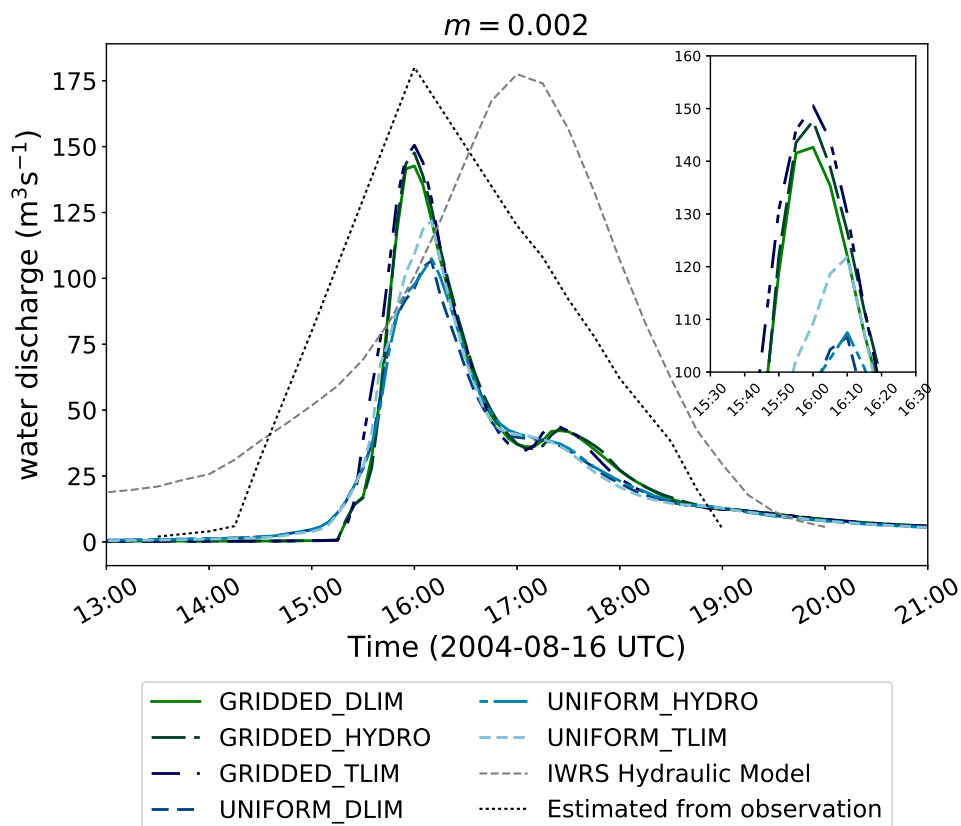


Figure 7.3: Boscastle hydrographs (discharge over time at catchment outlet) for each simulation of the 2004 Boscastle event listed in Table 6.2. Inset shows detail of main flood peaks around hour 40 of the simulation.

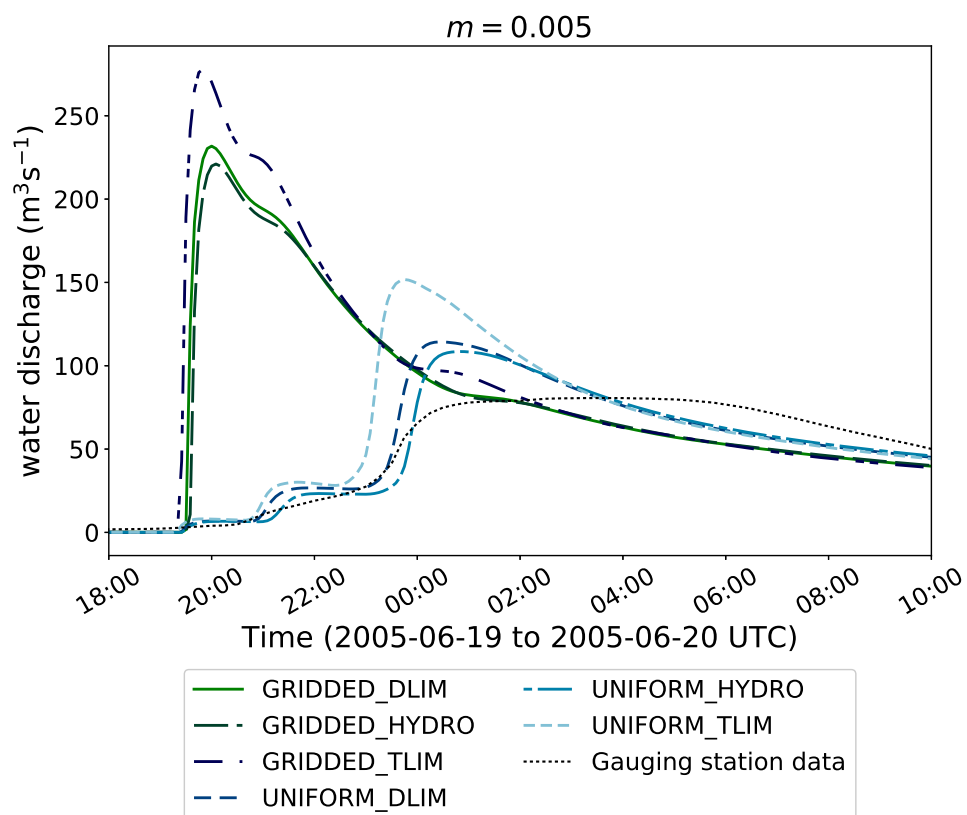


Figure 7.4: Ryedale hydrographs (discharge over time at catchment outlet) for each simulation of the 2005 Ryedale event listed in Table 6.2.

Table 7.2: Peak water discharges and corresponding times at peak flow for each of the simulation cases. Discharge is calculated at the outlet of the catchment model domain. Time is given in UTC on the day of the storm.

Simulation name	Peak discharge (m ³ s ⁻¹)	Time (UTC on storm day)
Boscastle: 2004-08-16		
GRIDDED_HYDRO	151	1600
GRIDDED_TLIM	148	1600
GRIDDED_DLIM	143	1600
UNIFORM_HYDRO	108	1610
UNIFORM_TLIM	122	1610
UNIFORM_DLIM	107	1610
Ryedale: 2005-06-19		
GRIDDED_HYDRO	221	2005
GRIDDED_TLIM	277	1950
GRIDDED_DLIM	232	2000
UNIFORM_HYDRO	108	0050†
UNIFORM_TLIM	151	2340
UNIFORM_DLIM	114	0025†

† – Time the following day.

7.3.3 Flood inundation and river levels

A series of flood inundation metrics are shown in Figures 7.5, 7.6, and 7.7, showing respectively:

1. Total area inundated by water
2. Mean water depth in the floodplain
3. Mean water depth in the main channel

The floodplain area is defined for the purpose of this analysis using the Clubb et al. (2017) floodplain delineation algorithm, a method which searches for statistically significant variation in terrain relief to identify and delineate floodplains in a catchment. The ‘main channel’ is herein defined as the mainstem channel with the highest stream order number (Strahler, 1957), removing any tributary channels in the headwaters. The mainstem channel is delineated using a simple channel network identification algorithm based on a contributing drainage area threshold (O’Callaghan and Mark, 1984; Tarboton et al., 1991). The inundation metrics were derived from water depth output files created every two hours of simulated time during the model runs.

As such, the absolute peak flood inundation may lie between two of the output file timesteps, but sufficient detail in spatial extents and dynamics of the floodwaters are still captured in the analysis and the resulting figures.

Generally, there is a tendency for the simulations with gridded rainfall input running in hydrology-only mode (`GRIDDED_HYDRO`) to predict the greatest extents of areal flood extent as well as floodwater depth across the floodplain and main river channel, behaviour observed in both case studies. Most simulations running in hydrology-only mode and uniform rainfall input (`UNIFORM_HYDRO`) also predict greater flood inundation extents and peak water levels, but this tendency is less prevalent in the Ryedale simulations. In fact, the Ryedale simulations appear to be marginally more sensitive to the type of rainfall input, with both the `GRIDDED` simulations producing slightly higher peak inundation levels, regardless of whether erosion parameterisation is switched on in the model.

The starker contrast observed was in the mean channel water depth of the Boscastle set of simulations; the difference in peak mean water depth was approximately 1 m between the hydrology-only and erosion-enabled simulations. In most of the other simulations, the differences in main channel mean water depth were smaller, on the order of tens of centimetres.

Total inundation area

Inundation area is defined here as the total area of the catchment grid cells that exceed the minimum discharge threshold at a given timestep. The minimum discharge threshold for all simulations was set as $0.03 \text{ m}^3\text{s}^{-1}$. The inundation amounts for the Boscastle and Ryedale simulations are presented in Figure 7.5. For clarity, only results from one type of the erosion-enabled simulations is presented in each case (transport-limited – `TLIM`). The predicted inundation areas for the detachment-limited erosion simulations were similar to the hydrology-only simulations, differing only by a few percentage points.

Boscastle Both of the hydrology-only simulations in the Boscastle case predicted the greatest peak in flood inundation area, with the gridded rainfall input simulations

predicting slightly higher peak inundation areas. The highest predicted flood inundation area resulted from the `GRIDDED_HYDRO` simulation, and the lowest peak from the `UNIFORM_TLIM` simulation. The rise and fall in the areal extent of the inundated flood area is rapid, peaking within hour 40 of the simulation (1600 UTC) and reducing by approximately 50% by the next output time step, two hours later at 1800 UTC.

Ryedale In the Ryedale simulations, predicted flood inundation area was again greatest in the `GRIDDED_HYDRO` simulation and lowest in the `UNIFORM_TLIM` simulation. In this set of simulations, both the gridded rainfall input experiments produce higher total inundation areas at the peak of the flood.

Floodplain mean water depth

Inundation area provides a general indication of the spatial extent of flooding within a catchment, but does not reveal as much about the distribution of water depths within the catchment, particularly the floodplain where many settlements are located in the Boscastle and Ryedale cases. Average floodplain water depths area presented in Figure 7.6 showing how water depths rise and fall on the floodplain over the course of each storm. The average depth is calculated for each output time step (two-hourly), by averaging the water depth in each model grid cell, limited to area delineated by the floodplain-finding algorithm (Clubb et al., 2017).

Boscastle Floodplain average water depths follow a similar pattern to that observed in the total inundation area timeseries: a sharp rise and peak corresponding to the time of maximum river discharge (1600 UTC), followed by a rapid drop-off by the time of the next model output timestep at 1800 UTC. Average water depths in the Boscastle floodplain peaked at just over 0.4 m for the `GRIDDED_HYDRO` simulations. Average floodplain water depths for the other simulations were approximately 0.35 m, and showed little variation from this value between the different simulation parameters.

Ryedale Water depths on the Ryedale floodplain were fast to reach their peak, but showed a more gradual recession after the flood peak than the Boscastle simulations. The highest mean floodplain water depths were predicted by the `GRIDDED_HYDRO` simulations at 0.16 m, though the difference between other simulations was minimal – the

lowest predicted mean depths of 0.14 m were observed in the `UNIFORM_TLIM` simulation, a difference of only 2 cm. The timings of peak water depth were slightly different between the gridded rainfall and uniform rainfall simulations, with uniform rainfall input simulations peaking 2–3 hours after the gridded rainfall input simulations, mirroring the pattern seen in the Ryedale hydrographs (Figure 7.4).

River channel water depth

Water depths in the river channel are determined by reporting the water depth along the channel midpoint, determined by a channel network extraction algorithm (Braun and Willett, 2013). Modification of the floodplain finding algorithm was considered to extract the entire channel footprint and average over the full channel width, but limitations in the algorithm’s ability to delineate the channel in the 5 m digital elevation model prevented this and so the channel midpoint was used as a representative sampling point of water depth. The channel section over which the average depth was taken was defined as the highest order channel in the catchment, i.e. the main channel stem into which all the other catchment tributaries flow.

Boscastle In the Boscastle catchment, (River Valency channel), peak mean channel water depths range from 2.4 m in the `GRIDDED_HYDRO` simulation to 1.2 m in the `GRIDDED_TLIM` simulations. There is a noticeable difference between the channel mean water depths at peak flow in the erosion-enabled simulations, which range between 1.2–1.4 m, and the mean depths in the hydrology-only simulations, both of which exceed 2 m. Modelling of river levels carried out by HR Wallingford (2005, figures 6.14, 6.15 in the report) using a one-dimensional hydraulic model predicted water levels in the Valency river channel ranging between 1–3 metres at the peak of the flood, within a similar range to the river channel levels predicted the HAIL-CAESAR simulations presented here.

Ryedale In the main channel of the River Rye, peak water depths range from approximately 1.2–1.5 m, a notably smaller range in depth than the Boscastle simulations. The highest mean water depths were predicted by the `GRIDDED_HYDRO` simulations. The other simulations predicted very similar peak mean channel water depths,

around 1.3 m. The lowest mean depths were predicted by the UNIFORM_TLIM simulation.

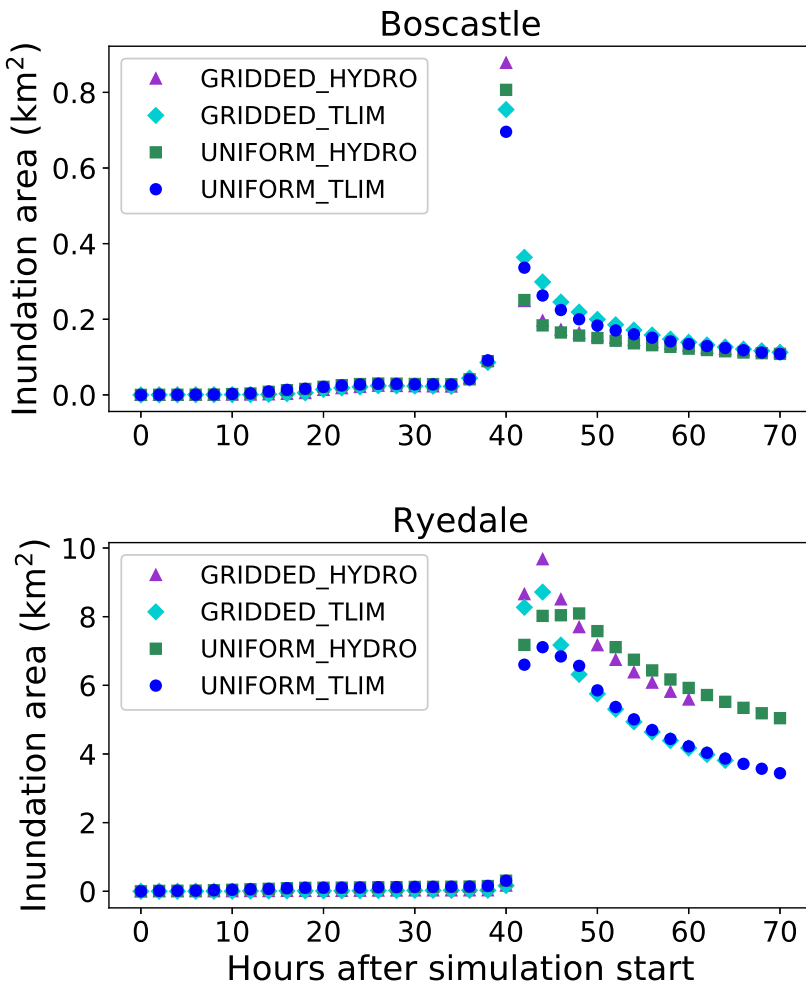


Figure 7.5: Total inundation area (km^2) covered by floodwaters in the Boscastle (top) and Ryedale (bottom) catchments throughout the duration of the each storm. Inundation area is shown for each combination of flood-only, erosion-enabled, gridded rainfall input, and uniform rainfall input simulation. The erosion-enabled simulations use the transport-limited erosion law (TLIM). Detachment limited erosion cases were omitted for clarity.

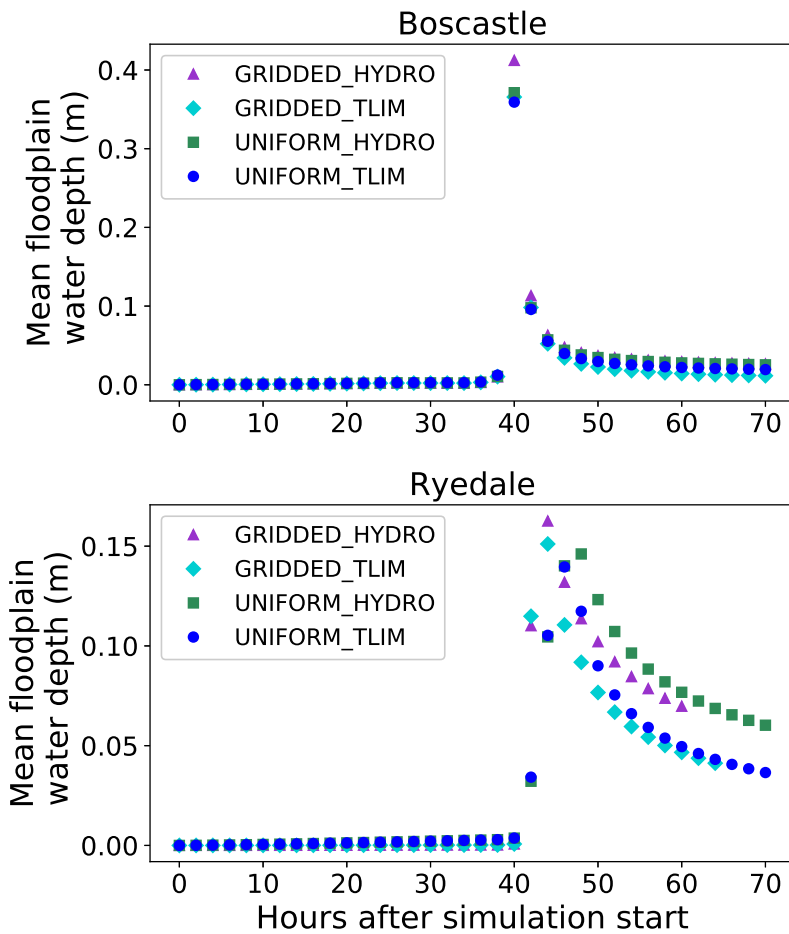


Figure 7.6: Mean floodplain water depth (metres) in the Boscastle (top) and Ryedale (bottom) catchments throughout the duration of the each storm. Floodplain is defined using the Clubb et al. (2017) floodplain delineation algorithm.) Water depth is shown for each combination of flood-only, erosion-enabled, gridded rainfall input, and uniform rainfall input simulation. The erosion-enabled simulations use the transport-limited erosion law (TLIM). Detachment limited erosion cases were omitted for clarity.

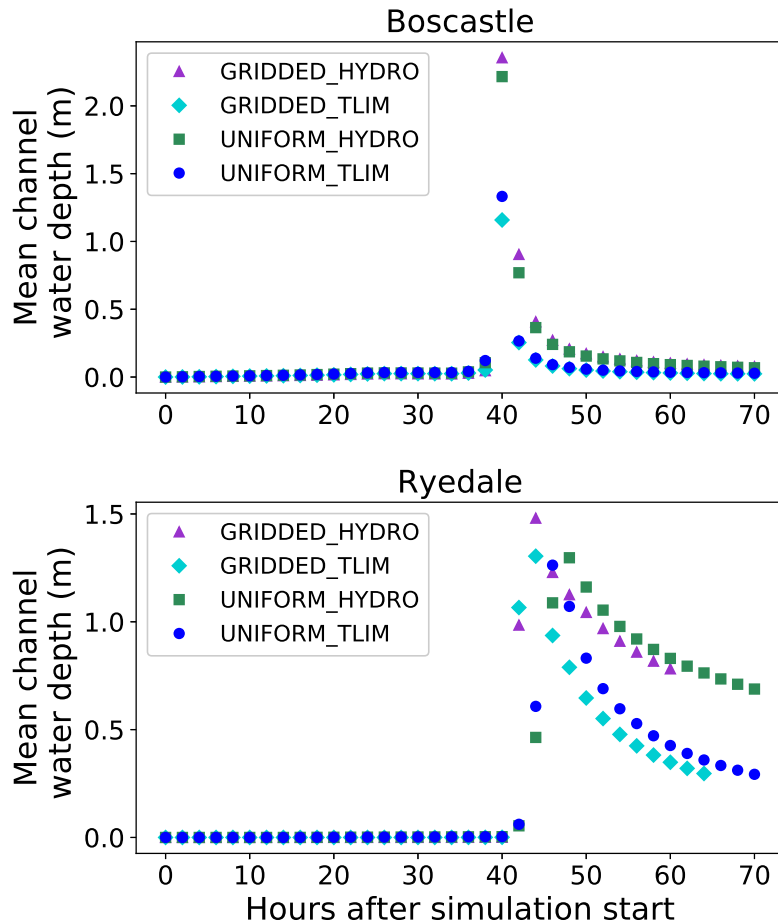


Figure 7.7: Main channel mean water depth (metres) in the Boscastle (top) and Ryedale (bottom) catchments throughout the duration of the each storm. The main channel is defined as the highest-order stream in each catchment (Strahler, 1957) and excludes all minor tributaries. Water depth is shown for each combination of flood-only, erosion-enabled, gridded rainfall input, and uniform rainfall input simulation. The erosion-enabled simulations use the transport-limited erosion law (TLIM). Detachment limited erosion cases were omitted for clarity.

7.3.4 Spatial variation in flood inundation

Thus far, the analysis of the model output has concerned catchment wide hydrological outputs and average water depths during flooding in the form of two-dimensional time series. The following section considers the spatial distribution of floodwaters across the catchments at the peak of each flood event. Comparisons between the spatial distribution of floodwaters under different model parameterisations are presented in Figures 7.9, 7.10 (Boscastle), and Figures 7.12, 7.13, 7.14 (Ryedale). An overview of the catchments and location of the main settlement in each is presented in Figure 7.8 and 7.11.

Boscastle

The Boscastle catchment simulations showed minimal variation in flood inundation extent. Simulations with gridded rainfall input did not result in substantially different predictions of floodwater inundation compared to those with uniform rainfall input. Both sets of simulations reflected the general extent of reported flood water extents (HR Wallingford, 2005). Simulations that allowed erosion to take place (**GRIDDED_TLIM** and **UNIFORM_TLIM**) showed a slight difference in the variation of floodwater depths in the floodplain area, particularly in the vicinity of Boscastle village, where Figure 7.9 is centred on. In hydrological-only simulations, the deepest water depths were predicted to occur in the confines of the river channel, whereas in erosion-enabled simulations, there appeared to be a ‘smoothing’ effect of water depths between the channel and the adjacent floodplain, suggesting that the channel geometry had altered during the flood event either by infilling from sediment from upstream or collapse of the adjacent river banks – this effect is particularly evident in Figure 7.10. Post-event reports of the Boscastle flood noted that the river channel in the Boscastle village area had indeed been inundated with debris during the storm, which had potentially contributed to the extent of the flooding within the village. The debris blockage of the river channel as it flowed under the road bridge in the centre of the village was also noted as a potential contributory factor to the pattern of flood inundation during the storm. Overall, the results from the Boscastle simulations indicate that although the general differences in flood extent are minimal, there are small localised variations in the distribution of flood water depths at key locations, which can be attributed to the parameterisation

of erosional processes in the simulations (Figure 7.9 and 7.10).

Ryedale

The Ryedale simulations showed less variation in flood extents between the gridded rainfall and uniform rainfall inputs. The flood extents were only slightly greater in the gridded rainfall input simulations, despite the much higher peak discharges predicted in these simulations (Figure 7.4). The main areas where flood extents were greater were in the floodplain area south of Helmsley (Figure 7.12) and in certain places around the settlement of Helmsley (Figure 7.13). The variation in water depths appeared to be less sensitive in comparison to the Boscastle simulations. In the lower reaches of the catchment (Figure 7.13), there appeared to be little indication that flood extents or water depths were sensitive to the erosion parameterisation, in contrast to the Boscastle simulations.

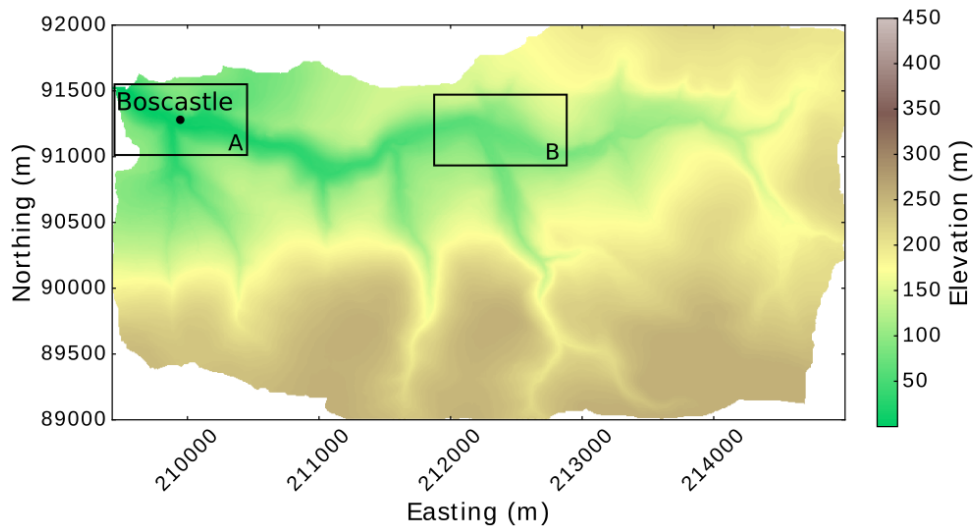


Figure 7.8: Location map of the Boscastle catchment and Valency river valley, with the village of Boscastle shown. Location of the zoom-in images in Figures 7.9 (A) and 7.10 (B) shown in rectangular outlines.

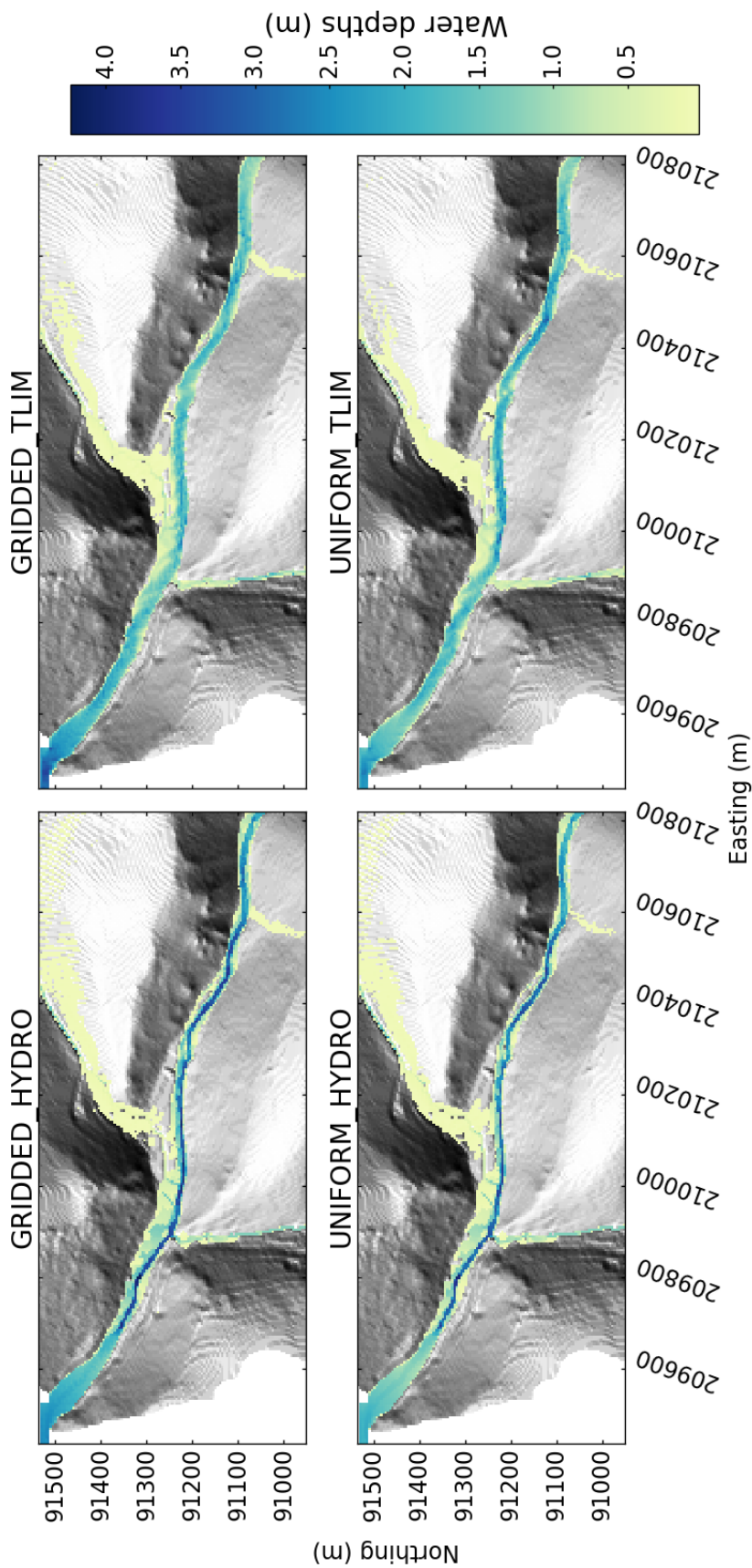


Figure 7.9: Flood extents in the Boscastle catchment around the village area (location A on the overview map in Figure 7.8) at the time of maximum river discharge for each simulation.

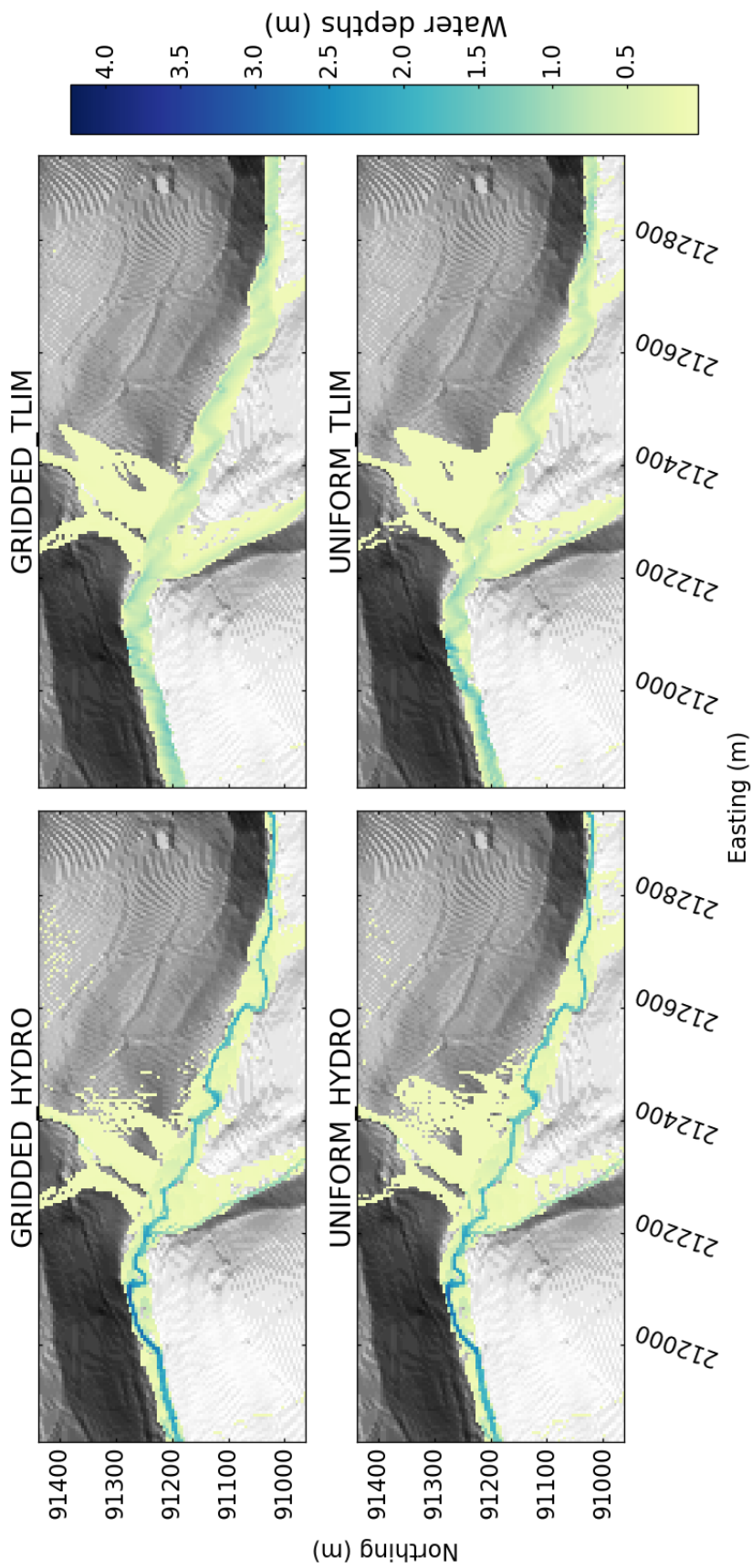


Figure 7.10: Flood extents in the Boscastle catchment around the upstream confluence area (location B on the overview map in Figure 7.8) at the time of maximum river discharge for each simulation.

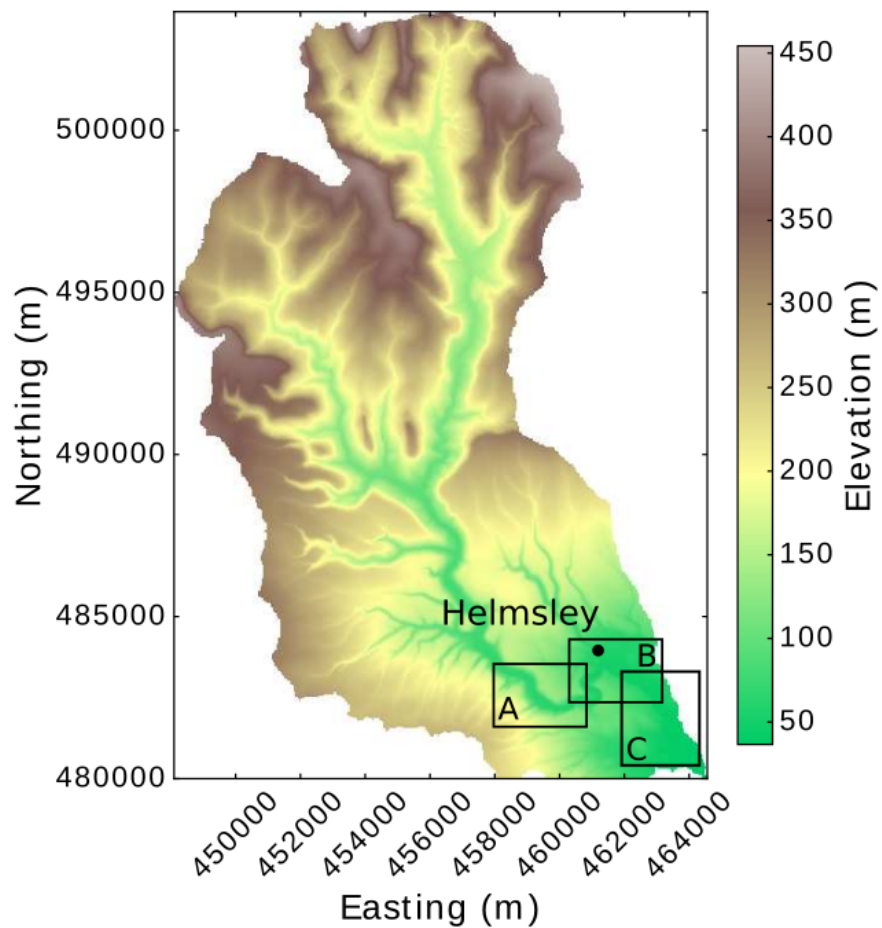


Figure 7.11: Location map of the Ryedale catchment and Rye river valley, with the village of Helmsley shown. Location of the zoom-in images in Figures 7.12 (A), 7.13 (B), and 7.14 (C) shown in rectangular outlines.

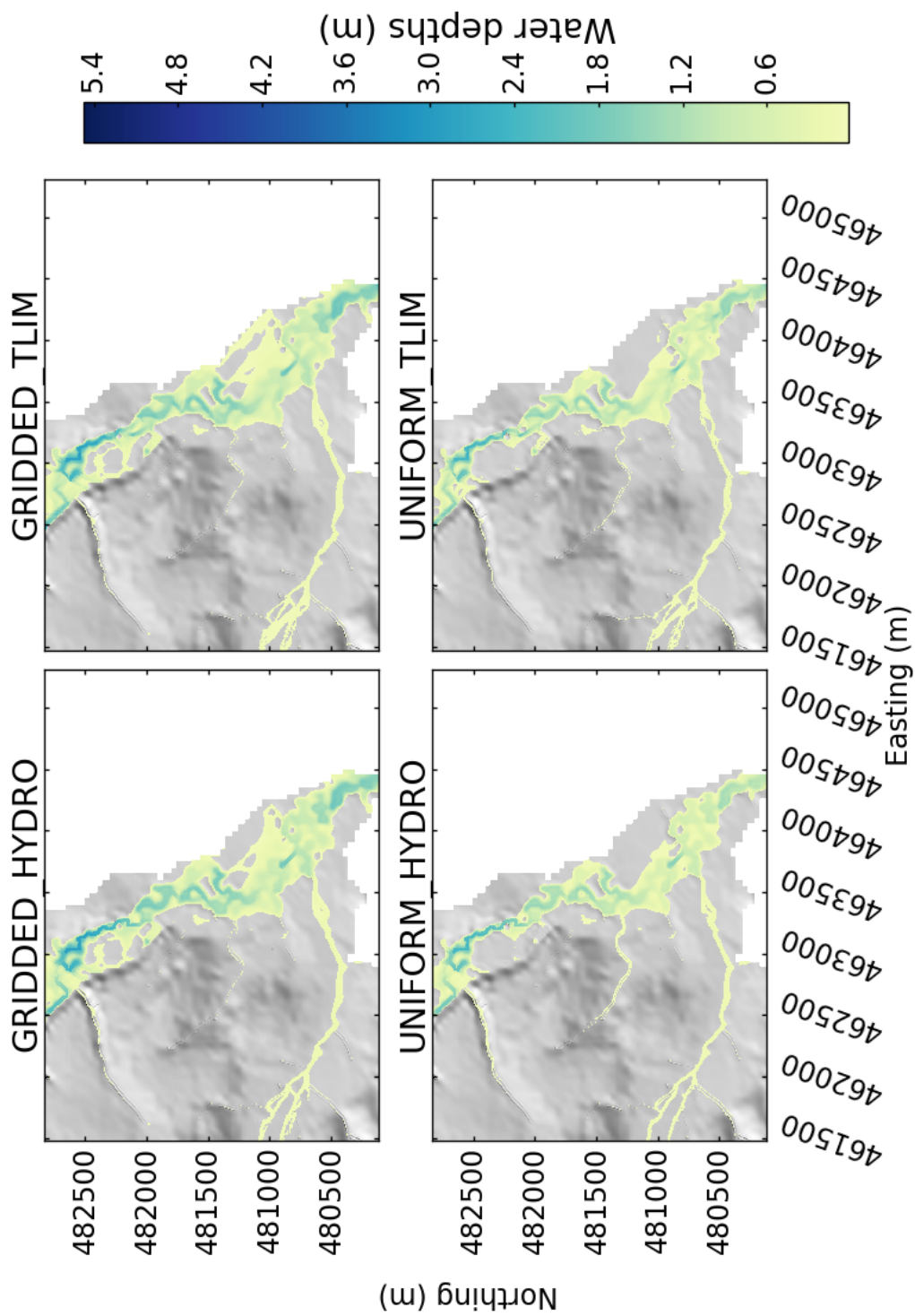


Figure 7.12: Flood extents in the Ryedale catchment in the floodplain area south of Helmsley (location C on the overview map in Figure 7.11) at the time of maximum river discharge for each simulation.

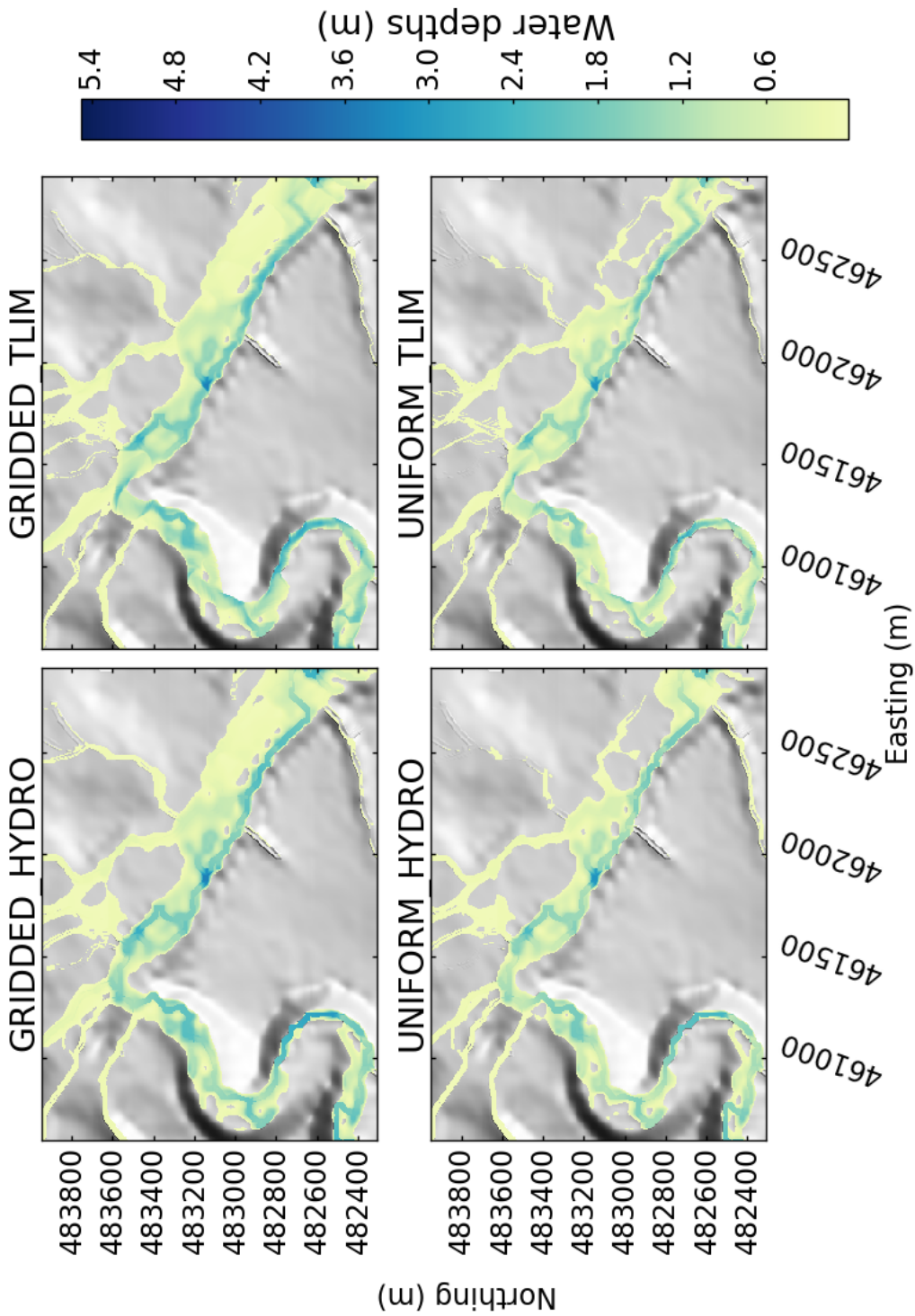


Figure 7.13: Flood extents in the Ryedale catchment in the area surrounding Helmsley village (location B on the overview map in Figure 7.11) at the time of maximum river discharge for each simulation.

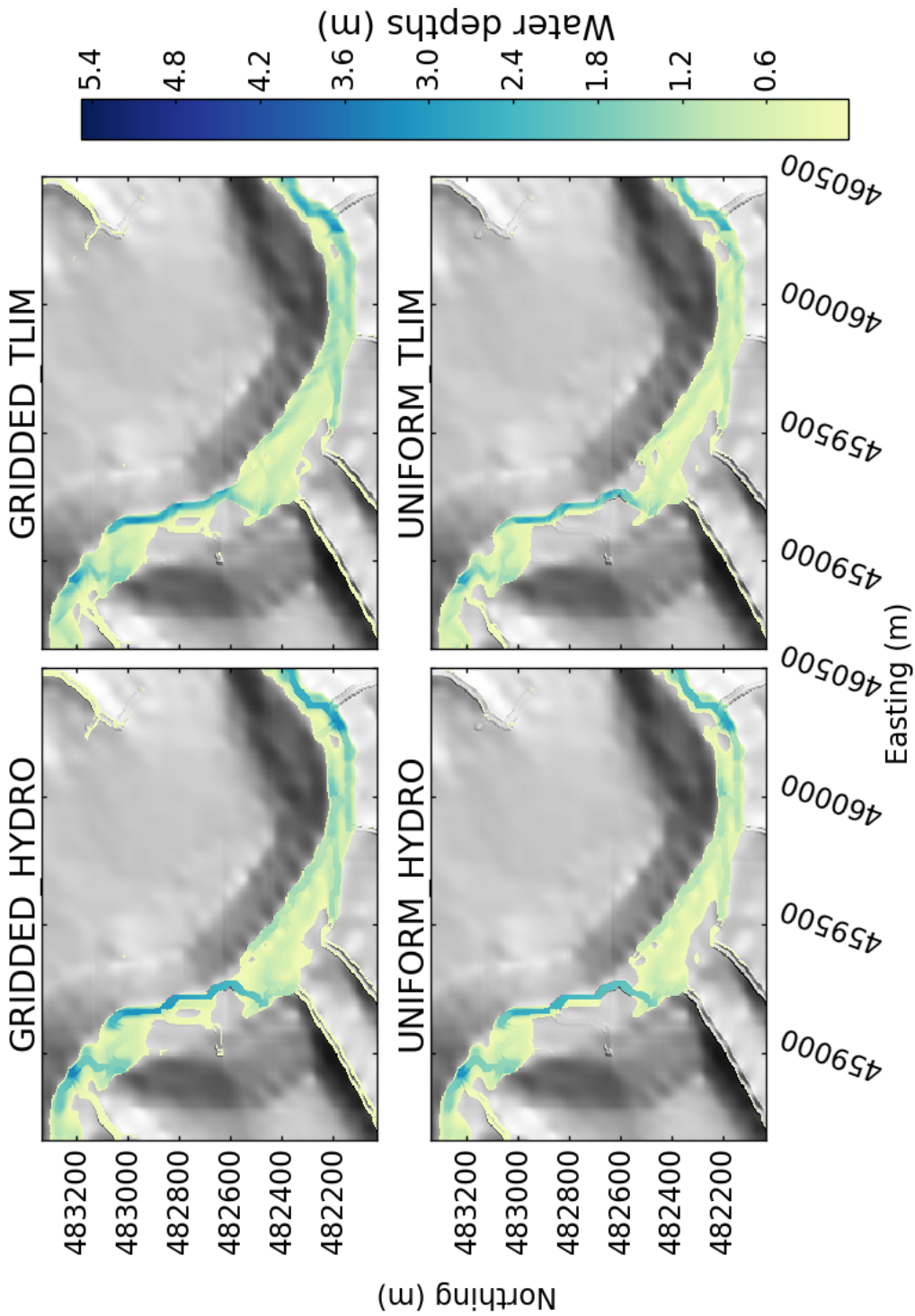


Figure 7.14: Flood extents in the Ryedale catchment in the gorge area west of Helmsley village (location A on the overview map in Figure 7.11) at the time of maximum river discharge for each simulation.

7.4 Discussion

The aim of this chapter was to explore how modelled flood hydrology and flood inundation extents are sensitive to two external factors: the spatial resolution of precipitation inputs and the parameterisation of erosional processes. An ensemble simulation approach was taken using a cellular automaton landscape evolution and hydrological model to simulate two historic case studies of flash flooding events in the UK, varying the parameterisations of erosion and rainfall spatial resolution in each simulation. The results paint a complex picture of the competing controls of 1) spatial resolution of rainfall input and 2) erosional processes representation within the catchment.

7.4.1 Rainfall spatial resolution

In comparison to erosional parameterisation, the spatial resolution of rainfall input to the catchment exhibits a first-order control on its hydrological response during the flash flood event in both of the case studies presented here. Hydrographs from the Ryedale simulations were noticeably different in the prediction of the magnitude and timing of peak discharges, although in the smaller Boscastle catchment the differences in hydrological response were smaller, both in terms of the difference in timing of the peak flow and the peak water discharge rate. There are size differences between the two catchments studied – the Ryedale catchment (270 km^2) is an order of magnitude larger in area than Boscastle (18 km^2) – and such differences in catchment size have previously (although not conclusively) been argued to control the sensitivity of catchments to spatial variability in rainfall inputs (Krajewski et al., 1991; Nicótina et al., 2008). Although it has been argued that smaller catchments up to around 3500 km^2 are largely insensitive to spatial variability in rainfall input due to a lack of heterogeneity in rainfall structures relative to the size of the catchment (Nicótina et al., 2008), the results in this study suggest catchments around 250 km^2 in size are sensitive to the spatial variability in rainfall inputs during intense rainfall events. For each simulation using gridded rainfall input, the cell width of the rainfall grid is 1 km. The relative amount of increase in rainfall detail between uniform and gridded simulations is potentially much greater in the larger Ryedale catchment than the Boscastle catchment. By using a 1 km gridded rainfall product as input data, the Ryedale simulation

potentially captures 15 times more rainfall heterogeneity compared to the respective Boscastle simulation, by virtue of it simply being a much larger catchment with a greater number of rainfall input cells.

The results from this study support the general consensus that there is some degree of sensitivity in catchment hydrology to rainfall spatial inputs, but in contrast to other studies, this sensitivity may be observed in much smaller catchments than previously thought. Furthermore, the flood inundation model used in this study appears to be more sensitive to spatial heterogeneity in rainfall inputs than it is to erosional parameterisation within the model, which may extend to hydrological modelling and flood forecasting in general. Further studies with different numerical models and different rainfall events would be needed to confirm this.

The findings here potentially offer some explanation to other other studies that have shown over longer timescales, hydrological outputs from catchments simulated with spatially variable rainfall input data can see significant increases in mean annual discharge (Coulthard and Skinner, 2016). If individual events can show notable differences in hydrological outputs, over time this will lead to larger differences in mean annual discharges. The general idea of catchment-size sensitivity to rainfall inputs is not challenged, but there is still a lack of consensus at what spatial scale this becomes a dominating factor. These findings suggest that catchments smaller than previously thought are also sensitive to rainfall spatial heterogeneity.

A secondary aim of this study was to investigate whether spatially detailed rainfall data leads to more accurate hydrological predictions, not merely *different* predictions. Where available, measurements of the timing, magnitude, and spatial distribution of flood inundation were compared with the predictions made by the numerical model. Both the Ryedale and Boscastle events were extensively studied and surveyed in their aftermath and comparisons with previous modelling studies of each event were made where these were available. With respect to the aim of improving the accuracy of flood inundation predictions with high-resolution rainfall data, the results were mixed. For the Boscastle case study, there was better agreement with the peak discharges published in the HR Wallingford (2005) report when using the gridded rainfall input to drive the numerical model, though a limitation of this comparison is that the hydrographs published in the HR Wallingford report were themselves based on

estimates from eyewitness observations, reconstructions from water-level marks, and one-dimensional hydraulic modelling. Nonetheless, the better agreement with other published findings is encouraging for the case of using high-resolution rainfall data in hydrological models.

In the Ryedale case study, using gridded rainfall input actually produced a less accurate prediction of the peak discharge during the flood, though the only comparison available was made with a single gauge station at the catchment outlet – gauging station data can be unreliable during extreme flows and this may partly explain the discrepancy. In this case, the uniform rainfall data actually gave a better hydrological prediction in terms of matching the timing and rate of peak discharge during the flood. The reasons for this are discussed in the next section.

7.4.2 Hydrograph calibration and choice of m parameter value

The poorer performance of the Ryedale hydrograph forecast using the gridded rainfall data is likely due to the use of the uniform rainfall data to calibrate the Ryedale simulations and arrive at the best value of the m parameter. The same value of $m = 0.005$ was then used in the Ryedale simulations using gridded rainfall input data, and this produces a less accurate prediction as a result (Figure 7.4). In future work, it would appear necessary to calibrate the value of m for different input data sources of rainfall, rather than relying on a single value of m across all simulations of the same catchment. The simplicity of using a single m value in this study was deemed necessary to allow for easier isolation of which factors caused the most sensitivity out of rainfall spatial variability or erosion law parameterisation. The resulting limitation of this approach is that it is difficult to robustly assess the forecasting potential of the model without a further set of simulations with re-calibrated m values.

Subsequent analysis showed that a separate sensitivity analyses using the gridded rainfall input revealed a different ‘best-fit’ value of $m = 0.0075$ when using the gridded rainfall input (Figure 7.2), leading to better hydrological predictions from the gridded rainfall input simulations. This raises the issue that the model can be configured with different parameters and arrive at the same or similar predictions – a concept referred to as equifinality and one which is often encountered in the hydrological modelling community (Beven, 1993; Beven and Freer, 2001b; Ebel and Loague, 2006) – which

somewhat limits the conclusions that can be drawn from the experiments comparing uniform rainfall inputs with gridded rainfall input. In this particular case, both choices of m value are within reasonable ranges for the types of environment simulated (Beven et al., 1984), but depending on the choice of m value, the case for using spatially variable rainfall inputs can be either strengthened or weakened. Does one chose to calibrate the model based on the type of rainfall spatial input as well, and if so, should it be calibrated further based on the type of erosional parameterisation enabled in the model? The size of the parameter space in the HAIL-CAESAR model is large, and a systematic exploration of every single combination of parameters would be time consuming if it were required for every case study to be simulated. Answering these questions of model calibration is beyond the scope of this study, but a recommendation can be made for future studies using the TOPMODEL-based runoff generation in models to assess the sensitivity to the m parameter as hydrological outputs may be highly sensitive to its value.

7.4.3 Erosional parameterisation

The results of the numerical modelling simulations suggested that choice of erosional parameterisation exerts a secondary control on the hydrological response of a catchment when compared to the effects of the choice in rainfall resolution input. Consistently across simulations, the enabling of a transport-limited (TLIM) erosional parameterisation in the HAIL-CAESAR model resulted in higher predicted peak discharges, evident in both the gridded rainfall and uniform rainfall sets of simulations. Again, the size of the catchment appears to be a factor in determining the degree of sensitivity, with the differences in hydrological output greater in the larger Ryedale catchment when using erosion-enabled simulations. The differences in discharge, however, are relatively smaller in both cases and any change in discharge from varying the choice of erosion law is surpassed by using a gridded rainfall input source over a spatially uniform one.

The same limited sensitivity to erosional parameterisation is noted by (Wong et al., 2015), using a similar hydraulic model to investigate flood inundation sensitivity to channel morphological change during flood events. The hydraulic model used in the Wong et al. (2015) study is based on the same two-dimensional flood inundation

model used in HAIL-CAESAR, coupled with a simple erosional model that allows the channel bed elevation to be eroded (but no sediment deposited) during the course of a flood. Wong et al. (2015) note that differences in hydrological response are minimal during erosion-enabled simulations, although there is a small increase of up to 5% in the simulated mean depth of floodwaters throughout the event they simulate. By contrast, the results presented here show that floodwater depths on average are lower in erosion-enabled simulations. The erosion-enabled simulations presented in this chapter address a limitation in the Wong et al. (2015) study in that they permit the redistribution of sediments within a catchment through depositional as well as erosional processes. In theory, such a model could capture channel blockage from sediment build up or infill during a flood, although this behaviour is not immediately apparent from the simulations carried out for these case studies. However, considering the sets of gridded-and uniform-rainfall input simulations separately, the predicted mean water depths in the main channel of each catchment (Figure 7.7) are lower in the erosion-enabled simulations indicating that sediment infill of the channels has taken place and reduced water depths in the channels. In the Boscastle simulations, the mean water depths are as much as 1 m lower in the transport-limited erosion-enabled simulations than the corresponding hydrology-only simulations where the morphology of the channel bed and floodplain are effectively fixed. Average floodplain water depths are also lower in the erosion-enabled Boscastle simulations (Figure 7.6). An alternative explanation for the lower water depths seen in the erosion-enabled simulations is that the coarse model output time step (two-hourly) simply did not capture the exact timing of peak flood water extent, and so the recorded depths for the erosion-enabled simulations are near to, but not quite, at the peak of flood inundation.

In models that permit the channel to be lowered through erosional processes, but no sediment deposition to take place, the channel and floodplain capacity to store or transport water can only be increased during the flood (e.g. Wong et al., 2015). The effect of this could either be to increase the rate of water transport downstream through the channels to the floodplains, or to increase the channel capacity to store water during the course of the flood. In Wong et al. (2015) the case seems to have been that water depths have increased on the floodplain when erosion was enabled in their model. In models that permit both channel erosion and sediment deposition, the possibility

arises that channel capacity is reduced during the flood through the deposition of sediments in the channel. However, detailed observational evidence recorded after the Boscastle event tends not to support this hypothesis as the amount of floodplain deposited sediments was on the order of centimetres, and most sections of the channel underwent net incision rather than deposition. In any case, a detailed analysis of the change in channel carrying capacity was beyond the scope of this study, but a change in channel capacity is a potential explanation for some of the differences seen between Wong et al. (2015) and the results of this analysis. A further explanation for the general lack of hydrological sensitivity to morphological changes to the channel and floodplain during large floods is that the channel and floodplain act as a single channel unit (Bates et al., 2005), and so localised changes to one hydromorphic feature are compensated for by the other, in effect dampening any potential hydrological sensitivity to erosional processes.

7.5 Conclusions

Considering the competing factors of spatial variation in rainfall inputs and erosional parameterisation in hydrological models, two main conclusions can be drawn from this investigation:

Rainfall resolution In distributed models of catchment hydrology, rainfall input data that is spatially variable is likely to lead to greater hydrological outputs during severe rainfall events. The probable cause of increased water outputs is that localised peaks in rainfall rate are captured by the use of high-resolution rainfall data, such as meteorological radar, that would otherwise be smoothed-out by spatially uniform rainfall inputs or coarser resolution rainfall data. This conclusion, however, assumes that rainfall structures themselves are spatially heterogeneous relative to the size of the catchment being modelled. Catchment size itself may be a controlling factor determining how sensitive the hydrological response is to spatially detailed rainfall input data, but another possible explanation is that it is the ratio of rainfall detail captured in input data, relative to the size of the catchment. A further systematic study investigating hydrological sensitivity to a range of rainfall structures of varying

structural complexity would be needed to assess this hypothesis.

Higher-resolution rainfall input data has the potential to improve the accuracy of hydrological predictions, but it is not conclusive that this is always the case based on the results of this study. For high-resolution rainfall data to be of use to hydrological modellers, the other parameters within the model must be well constrained, either through field study (where parameters can be constrained through field measurement), detailed exploration of parameter sensitivity and calibration of the model, or a combination of both.

Erosional parameterisation Hydrological simulations show some sensitivity to erosional parameterisation. The amount of change in hydrological outputs and spatial distribution of flood waters is small relative to the sensitivity to rainfall spatial heterogeneity. The conclusions in this respect are similar to that of Wong et al. (2015) in that getting an accurate representation of erosional process in hydrological models is likely to be of secondary importance compared to obtaining accurate inputs of rainfall intensity and distribution. Errors in the radar-derived rainfall rate and in the radar-derived spatial distribution of rainfall are more likely to have a larger impact on model performance compared to the nuances in flood dynamics predicted by erosion-enabled simulations. An often reported consequence of large flood events is that bridged channels and culverts can become blocked with mobilised debris (other than sediment), leading to localised changes in flood dynamics. A limitation of the HAIL-CAESAR model, and others like it, is that they cannot account for closed-channel flow and blockages from debris, but future model enhancements may enable this kind of localised change in flood hydraulics to be investigated further.

Summary

Hydrological modelling shows measurable sensitivity to the spatial variation in rainfall inputs using gridded rainfall data derived from meteorological radar. Sensitivity is more pronounced in larger catchments, though it is also noticeable in smaller catchments during extreme flood events, contrary to previously published studies. Whether or not high-resolution rainfall data can improve hydrological model performance depends on the constraint of other model parameters, notably the m parameter, that

can lead to large amounts of uncertainty in the hydrological response of a catchment to intense rainfall. It is also evident that the choice of rainfall input data resolution may require the m parameter to be re-calibrated, otherwise higher resolution rainfall data may actually produce a poorer hydrograph forecast (as evident in Figure 7.4). Erosional parameterisation within a hydrological model – the ability to represent changes in channel and floodplain morphology during a flash flood event – appears to be of only secondary importance in determining the hydrological response based on the studies carried out in this investigation. Nonetheless, both erosional parameterisation and spatial distribution of rainfall remain important factors to be considered in future models of flood inundation and catchment hydrology.

8

Hydrometeorological controls on landscape erosion modelling

8.1 Introduction

Landscape evolution is punctuated by intense erosive episodes driven by flood events triggered by intense rainfall (Wolman and Miller, 1960; Newson, 1980; Costa and O'Connor, 1995). Understanding the role rainfall plays in erosional processes is of importance to both long-term landscape evolution studies (e.g. Rinaldo et al., 1995; Tucker and Slingerland, 1997; Tucker and Bras, 2000), which have long sought effective ways of parameterising rainfall patterns within models (e.g Eagleson, 1978). Catchment sensitivity to rainfall variability is also important in the context of environmental prediction, such as predicting the likely geomorphological impacts of intense rainfall and flash flood events (e.g. Lane et al., 2007; De Luis et al., 2010; Milan, 2012). Given the possibility of changing hydro-meteorological conditions that may accompany climate change (Kendon et al., 2014), longer-term prediction of catchment sediment yields and erosion patterns has also seen an increased research effort in recent years (Coulthard et al., 2000; Coulthard et al., 2012a; Hancock et al., 2017). The drive to understand how landscapes respond to climatic conditions is aided greatly through the use of numerical landscape evolution models (Tucker and Hancock, 2010), which allow a wide range of scenarios to be tested, and quantify the sensitivity of particular processes to climatic boundary conditions, including rainfall distribution.

Investigation into infrequent but geomorphologically formative flash flooding events

has seen a resurgence by recent work such as Huang and Niemann (2006), looking at the long-term implications of different geomorphically effective event discharges on fluvial incision. Other studies have sought to quantify the amount of bedrock erosion during individual large flood events (e.g. Gupta et al., 2007; Lamb and Fonstad, 2010; Baynes et al., 2015), in an effort to better understand the role that low frequency, but high magnitude events have on landscape evolution. Still, our understanding of catchment-scale landscape evolution is far from complete – the role that rainfall plays in individual events appears to be highly variable from case to case. The behaviour of streams and rivers within catchments can vary in response to the same magnitude of flood event – some streams may erode during high flows, whereas others may deposit during high flows (Turowski et al., 2013). During small–medium flows, Turowski et al. (2013) also report that the dynamics of erosion are reversed, with some rivers acting as agents of deposition during floods, rather than being primarily erosional, depending on the preconditioning of the catchment by previous events. Further studies have reported that rapid gorge formation can be driven primarily by small to moderate sized floods (Anton et al., 2015), rather than rainfall events of much larger magnitude.

Temporal variability in rainfall patterns controls the evolution of landscapes over geological timescales, with the ability to influence the geomorphology of drainage basins and geometry of channel networks (Tucker and Bras, 2000; Sólyom and Tucker, 2004). The influence of spatial variability in rainfall patterns has affected the outcome of long-term topographic evolution, controlling morphology in landscapes subject to orographic rainfall gradients (Sólyom and Tucker, 2007; Han et al., 2014; Han et al., 2015). Sediment yields and morphological change are also sensitive to the resolution of rainfall inputs over decadal to millenial timescales (Coulthard and Skinner, 2016). However, no study has yet looked at the sensitivity of erosion to rainfall spatial patterns during single storm events – the goal of this chapter is to investigate the potential sensitivity of catchment-scale erosional processes to spatially distributed rainfall inputs.

8.1.1 Theory

The assumption of uniform rainfall over a river catchment is argued to hold true for small catchments (Sólyom and Tucker, 2004; Tucker and Hancock, 2010), but even

over small areas, mesoscale rainfall features, such as localised convective storm cells, can result in spatially and temporally uneven input of precipitation into the catchment (Peleg and Morin, 2014). In the case of intense convective precipitation, individual storm cells can be as small as 10km^2 in areal extent (Weisman and Klemp, 1986; Von Hardenberg et al., 2003). Over larger catchments, or those with steep topographic gradients, precipitation is likely to vary spatially, due to orographic enhancement of rainfall (Roe, 2003; Han et al., 2015). As such, rainfall-runoff generation, local river and tributary discharge, and erosion rates may vary considerably within individual drainage basins.

As discussed in Chapter 2, current numerical models of landscape evolution usually omit a realistic distribution of rainfall input in favour of uniform, homogenised precipitation across the landscape. When precipitation is ‘lumped’, either spatially or temporally in a catchment, local minima and maxima of precipitation are lost or smoothed-out. With discharge being a function of rainfall rate, this smoothing should therefore be expected to propagate through to local discharges and erosion rates. The uncertainty in erosion rates is potentially exacerbated by the non-linearity and threshold dependence of erosive processes (Coulthard et al., 1998; Phillips, 2003). The variability of precipitation is considered to be as important as total precipitation amount in determining erosional effectiveness (Tucker and Bras, 2000; Tucker and Hancock, 2010). As many geomorphic processes are threshold dependent (Schumm, 1979), such as fluvial incision into bedrock (Sklar and Dietrich, 2001; Snyder et al., 2003b), there is potential for the spatial distribution of rainfall to control local erosion rates within a catchment.

Rainfall resolution affects sediment yields over decadal and millennial timescales (Coulthard and Skinner, 2016). In a numerical modelling study of the River Swale catchment, UK, Coulthard and Skinner (2016) show that local distribution of erosion differed and catchment-wide sediment yields were predicted to increase by up to 100% as rainfall data resolution was increased. The study looked at the effects of rainfall input data grid-spacing as well the temporal resolution of rainfall data, showing both to have a control over sediment erosion within the catchment. The results were based on landscape evolution model simulations over a period of 1000 years, rather than individual storm events.

In numerical models of landscape evolution, resolving the precise temporal and spatial details of rain storms and the hydrological response is often computationally prohibitive, especially over long timescales, and as such modellers have taken to using simpler parameterisations of storm characteristics, such as using simple stochastic models to generate rainfall inputs and rainfall timeseries (Eagleson, 1978; Tucker et al., 2001a). In Chapter 5, an existing landscape-evolution model was redeveloped to address some of the computational issues and make it suitable for deployment on a high-performance computing service, enabling more effective use of higher-resolution digital topography data to initialise the terrain surface (Chapter 6) and finer-resolution rainfall input data to drive the model.

8.1.2 Objectives

The aim of this chapter is to assess how erosional processes are sensitive to the details of precipitation across a catchment during individual storms. The focus in this study is to quantify the sensitivity of erosional processes to the spatial distribution of rainfall during flood events, using the case studies outlined in Chapter 6.

The following questions are explored through the use of numerical modelling simulations:

1. Are fluvial erosion and sediment transport processes sensitive to the details of precipitation distribution at the catchment scale during single storm events?
2. Does the choice of erosional model operating within the catchment influence sensitivity to rainfall patterns?
3. What are the implications of this for longer-term landscape evolution?

To build upon the work done in previous studies (e.g. Han et al., 2015; Coulthard and Skinner, 2016), this chapter focuses on the sensitivity of sediment yield and erosion distribution to rainfall heterogeneity at timescales not previously investigated – single severe rain storms. Results from a series of numerical simulations set out in Chapter 6 are presented to assess how sensitive real landscapes are to the catchment-scale details of precipitation during intense rainfall events. The simulations are each based on

selected severe storms in the UK occurring in the past decade, which left significant flooding, damage, and geomorphological change in their wake (Chapter 6).

8.2 Results

Sediment flux predictions are presented at a catchment-wide scale, measured from the outlet of each catchment (Figures 8.2, 8.1). The spatial distribution of sediment deposition is presented in the form of 1D longitudinal profiles along the main channel (Figures 8.3, 8.4), as well as 2D planform maps of erosion and deposition distribution (Figures 8.8, 8.9, 8.5, 8.6, 8.7)

8.2.1 Catchment sediment flux

Sediment flux from both catchments was most sensitive to the sediment erosion parameterisation, rather than the spatial detail of rainfall inputs (Figures 8.2, 8.1). For both catchments simulated, sediment flux from each catchment was higher in the simulations using the transport-limited erosion law. The sediment flux increase observed in the Ryedale simulations ranged from 230% (gridded rainfall) to 600% (uniform rainfall) when switching from the detachment-limited to the transport-limited erosion law (Figure 8.1). In the Boscastle study, sediment flux was over an order of magnitude higher when using the transport-limited erosion law over the detachment-limited law (Figure 8.2). All detachment-limited simulations resulted in a much lower prediction in sediment flux.

The influence of rainfall input data spatial resolution played a secondary role in determining sediment yields. In almost all simulations, when the same erosion law parameterisation was used, sediment yields were greater with gridded rainfall data input. In Ryedale, using gridded rainfall input increased peak sediment flux by approximately 140% for transport-limited simulations, and 400% in the detachment-limited simulations. In the Boscastle transport-limited and detachment-limited simulations, peak sediment flux increased by approximately 50% in both cases. (Figure 8.2). The patterns of peak sediment discharge also mirrored that of water discharge (see Chapter 7, Section 7.3.2), with sediment flux peaking earlier in the simulations with higher resolution rainfall inputs.

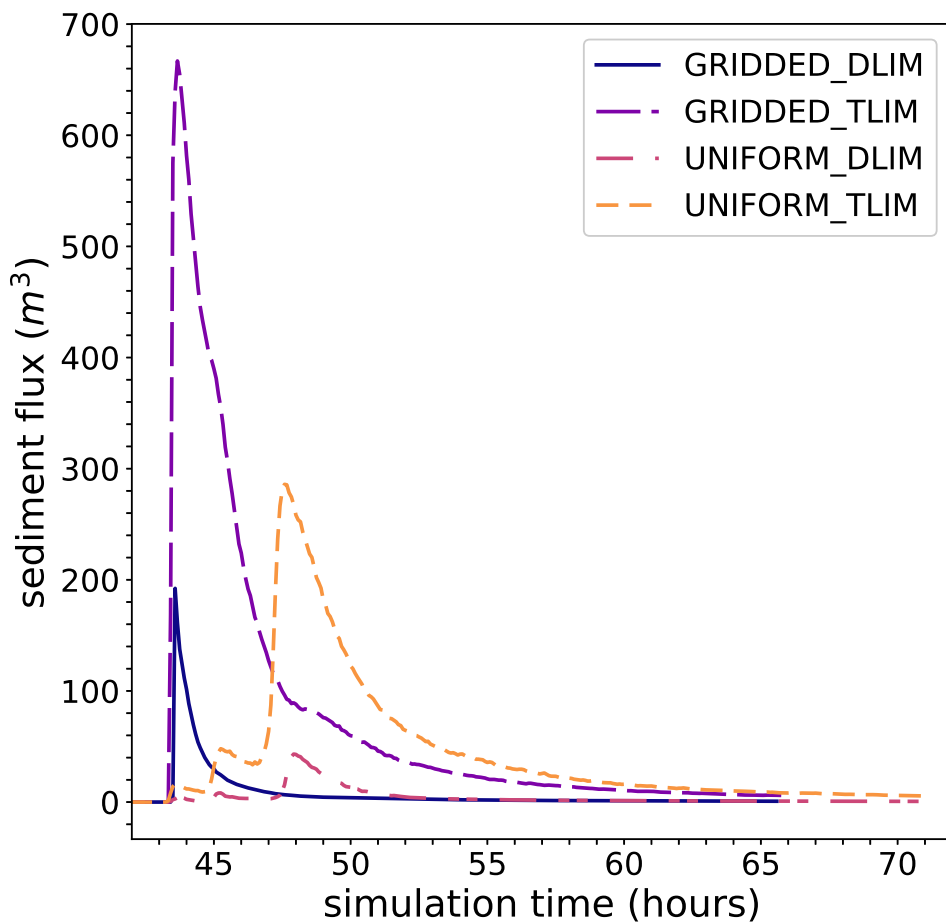


Figure 8.1: Ryedale sediment flux (Total sediment volume output per hour at catchment outlet) for each erosion-enabled simulation of the 2005 Ryedale event listed in Table 6.2.

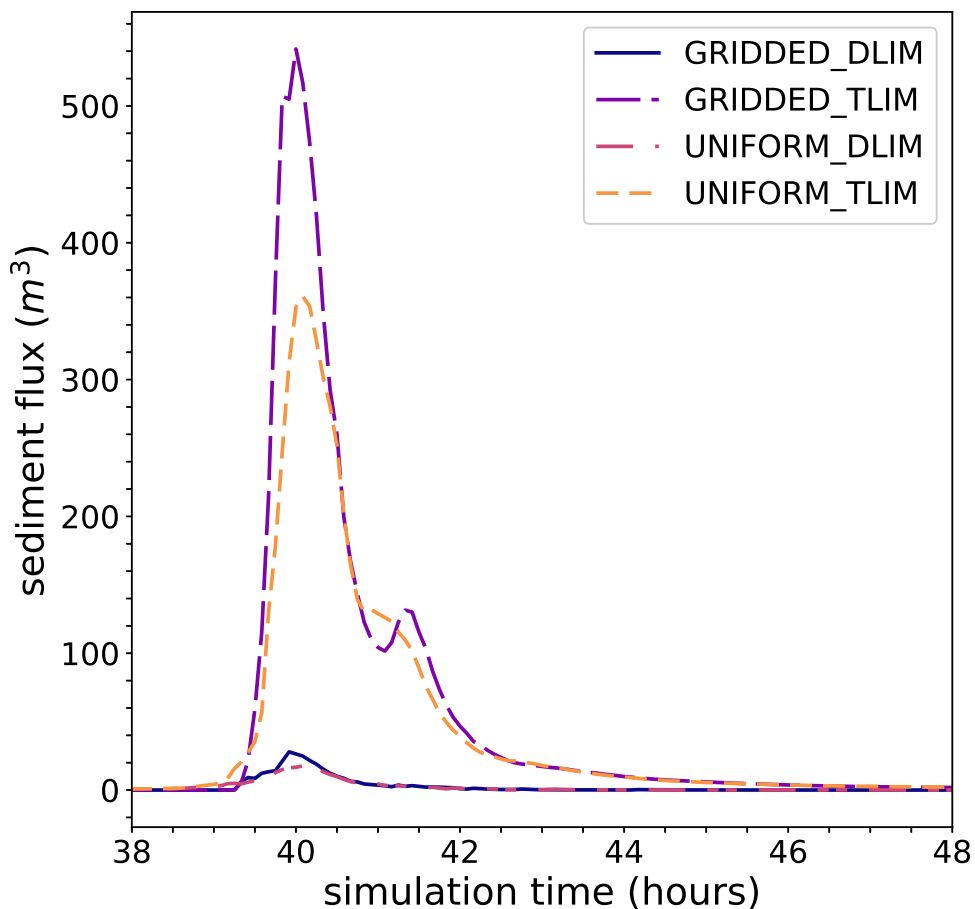


Figure 8.2: Boscastle sediment flux (total sediment volume output per hour at catchment outlet for each erosion-enabled simulation of the 2004 Boscastle event listed in Table 6.2.

8.2.2 Spatial variations in channel erosion

The main spatial variation in sediment erosion was within river channels. The amount of erosion in each simulation was highly sensitive to parameterisation choice of the sediment erosion and transport law, with the choice of rainfall input data (gridded vs uniform) being only a secondary controlling factor on the spatial distribution of erosion, all other factors being equal. This behaviour was exhibited in all simulations, shown in Figures 8.5 and 8.7. As differences between the GRIDDED and UNIFORM simulations were minimal, and erosion amounts in the detachment-limited simulations were small, only the profiles from the GRIDDED_TLIM simulations are shown for clarity.

To highlight the variation in erosion along the river channel, longitudinal channel profiles showing the average change in elevation after the storm are shown in Figures 8.3 and 8.4. The longitudinal profile shows the variation in erosion along the main channel within each catchment, averaged over a 10m wide channel cross-section centred on the midpoint of the channel. The longitudinal profiling technique is adapted from (Hergarten et al., 2014), where the resulting profiles are termed *swath* profiles. Originally the swath-profiling technique was written to calculate cross-sectional profiles across mountain ranges or basins, but here it has been adapted to create longitudinal profiles. To reduce the number of points plotted along the swath profile, erosion is also averaged longitudinally, using bins spaced every 200 m in the Rye river channel and every 50 m in the Valency river channel.

Swath profiling of the Valency river channel (Boscastle) shows overall net incision under transport-limited erosion parameterisation, with only small sections of the channel showing net sediment deposition (elevation increase) on average. Figure 8.3 shows most incision is predicted to occur in the mid to upper reaches of the channel (up to 1.8 m), with relatively little incision in the lowest reach of the catchment. The difference between gridded and uniform rainfall inputs shows a minimal difference along the main profile, though there is a slight tendency for the incision seen in the gridded rainfall input simulation to be higher in most places than the simulation using uniform input, with the difference in incision amounts between gridded and uniform rainfall inputs being of the order of tens of centimetres.

The swath profiling of the Rye river channel shows a large variation in incision and deposition rates within the catchment, although there is an overall tendency for

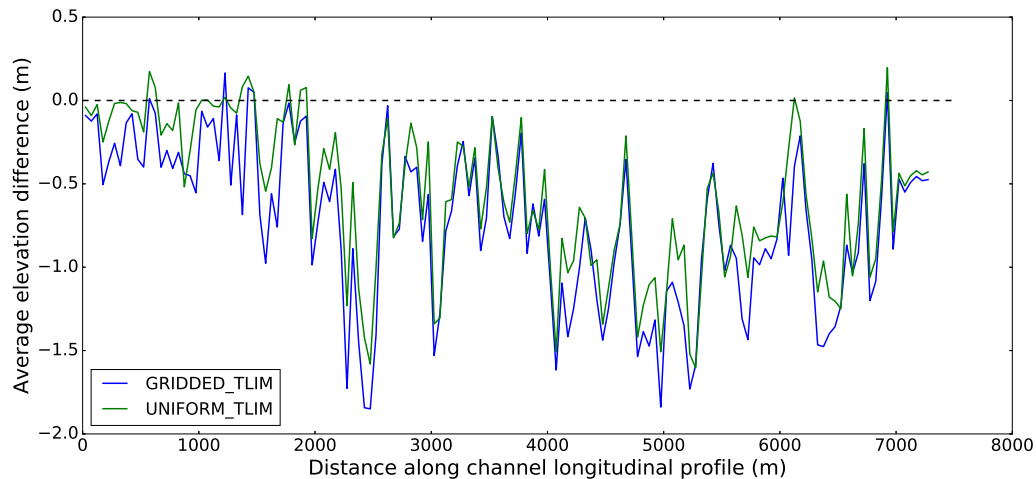


Figure 8.3: Channel averaged elevation difference along the main river channel in the Valency catchment. Simulation using the transport limited erosion parametrisation. Longitudinal profile is averaged over bins spaced every 50m. Transverse averaging (across the channel) is done over a 10m wide section centred on the channel midpoint. Results from the GRIDDED_TLIM simulation shown in blue and the UNIFORM_TLIM simulation shown in green.

net incision (Figure 8.4). The magnitude of both incision and deposition is higher in the mid to upper reaches of the Rye river channel, similar to the pattern observed in the Valency river. The differences in average elevation changes are not as clearly distinguishable between the gridded and uniform rainfall input parameterisations; magnitudes of erosional and depositional peaks are slightly higher in the lower reaches of the river channel, but in the mid to upper reaches the differences are more varied, with no clear signal emerging.

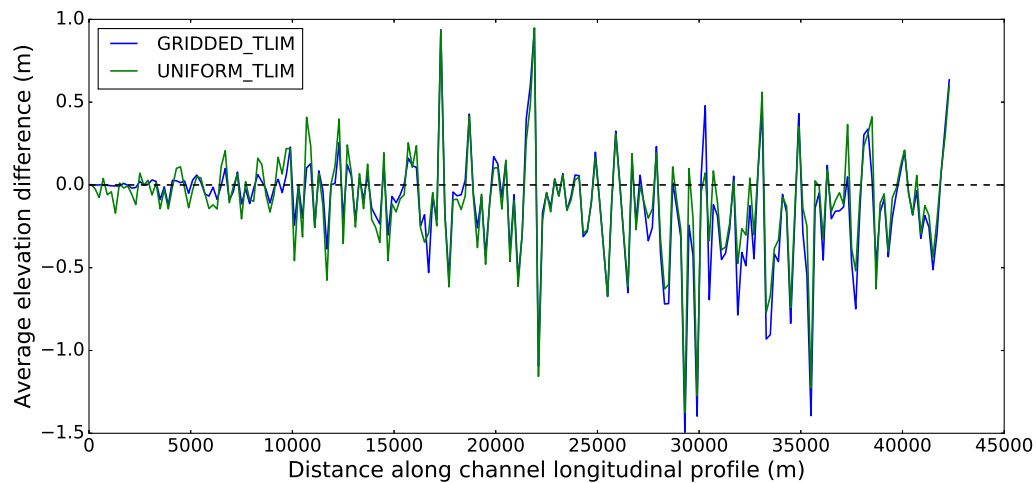


Figure 8.4: Channel averaged elevation difference along the main river channel in the Ryedale catchment. Simulation using the transport limited erosion parametrisation. Longitudinal profile is averaged over bins spaced every 200m. Transverse averaging (across the channel) is done over a 10m wide section centred on the channel mid-point. Results from the GRIDDED_TLIM erosion simulation shown in blue and the UNIFORM_TLIM simulation shown in green.

8.2.3 Local variation in erosion patterns

Boscastle

In the Boscastle catchment, there are slight differences in the spatial distribution of erosion between the gridded and uniform rainfall input simulations. In the area along the main channel of the Valency river around Boscastle village, gridded and uniform rainfall simulations appear to show very similar erosion and deposition amounts (Figure 8.5). The more obvious contrast lies in the choice of erosion law, with transport-limited erosion simulations predicting much higher amounts of elevation change.

In the south-eastern section of the catchment, the predicted amounts of erosion are notably higher in upper tributaries and adjacent hillslopes under the gridded rainfall simulation (Figure 8.8), when compared with the uniform rainfall input simulation (Figure 8.9). In the smaller tributaries of the catchment, detachment-limited simulations predicted little or no erosion. Figure 8.6 shows the Lesnewth stream and the erosion/deposition amounts in each simulation. The highest levels of erosion and deposition are predicted by the gridded rainfall, transport-limited erosion case, and in contrast there is almost no erosion predicted by the uniform rainfall, detachment-limited erosion case.

Ryedale

In the Ryedale catchment, the gridded rainfall input simulations predict slightly greater amounts of erosion and deposition in general, though it is difficult to pick out a particular area of the catchment where the differences are starkly contrasting. The spatial distribution of erosion and deposition in the Helmsley area is shown in Figure 8.7, for each of the four simulations. Small differences can be seen along the main floodplain and up into the gorge area of the river Rye, showing elevated levels of erosion and deposition in the gridded rainfall input simulations. In contrast to the Boscastle simulations, there was comparatively little sediment transport shown in any of the hillslope areas – compare the yellow shaded areas over the hillslopes in the Boscastle catchment erosion map (Figure 8.8) and their notable absence in the Ryedale catchment erosion map (Figure 8.8). As with the Boscastle simulations, the most obvious contrast in erosion amounts is seen between the different erosion law simulations.

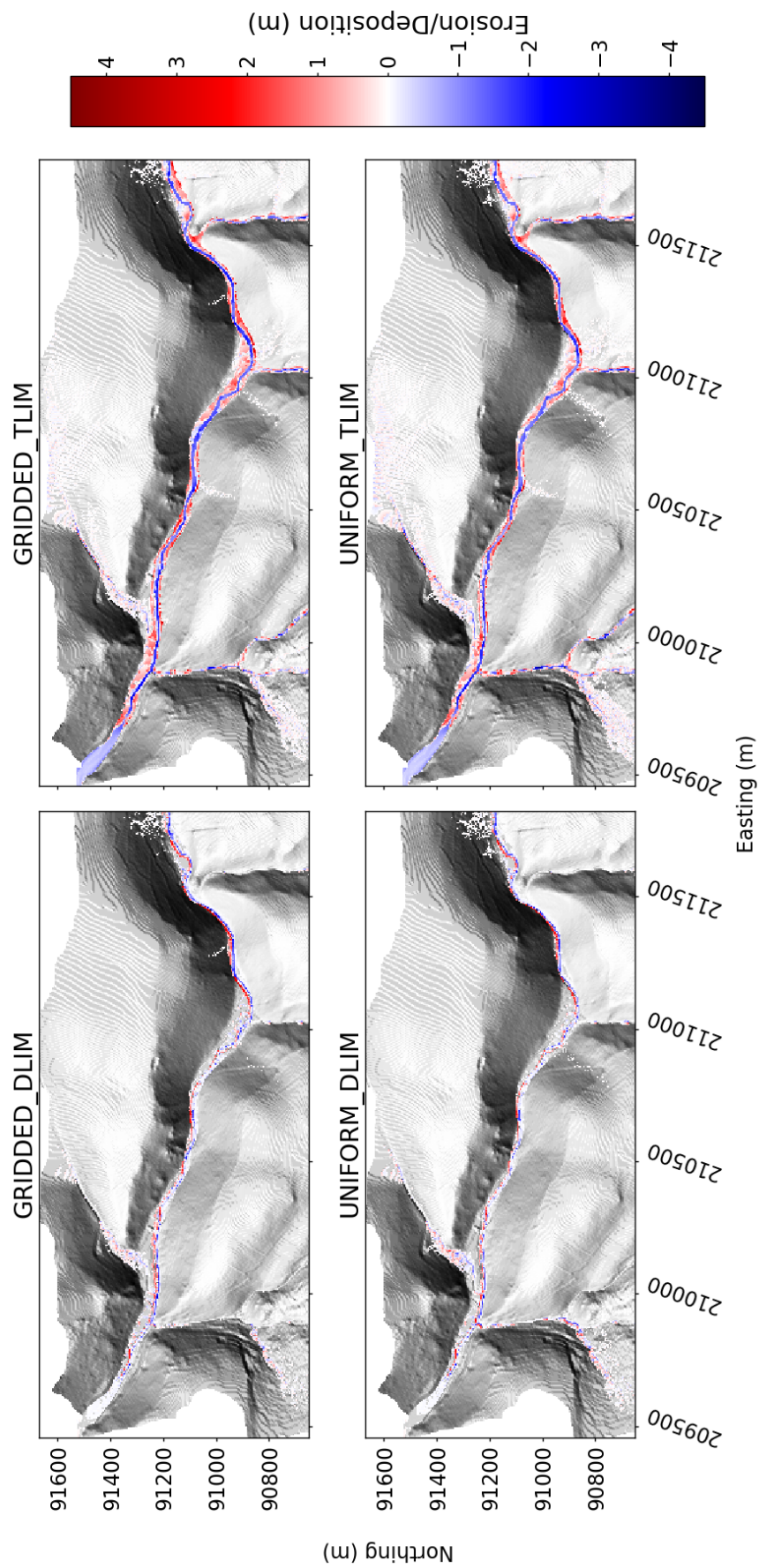


Figure 8.5: Boscastle. River Valency main channel in vicinity of Boscastle village. Net difference in elevation after 72 hours simulation, showing the gridded and uniform rainfall simulations, for each of the two erosion law end-members (transport-limited and detachment-limited). Elevation change smaller than $\pm 0.2\text{m}$ in magnitude is not shown for clarity. Boscastle harbour is located in the upper left corner of each figure.

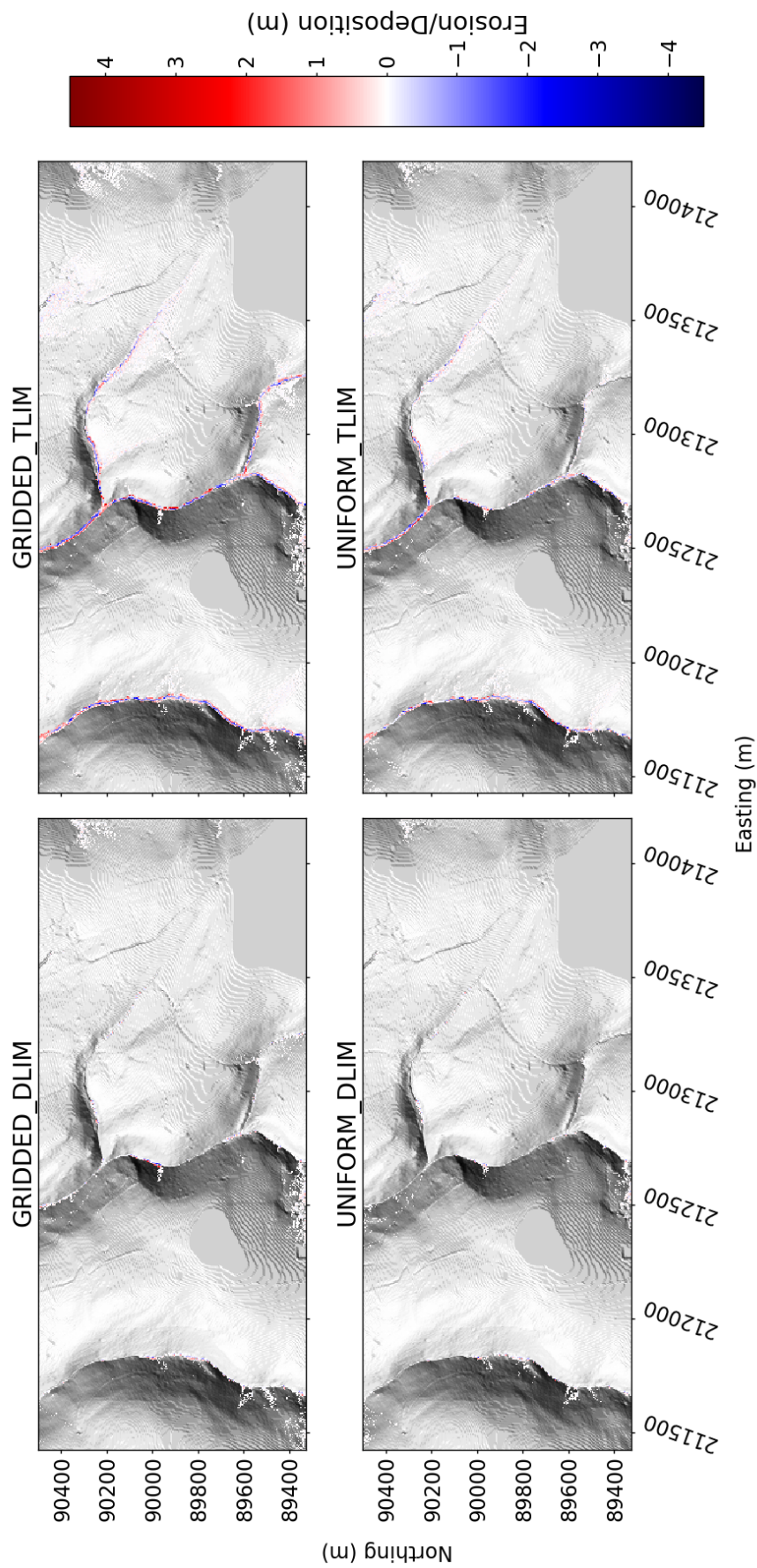


Figure 8.6: Boscastle. South-east section of catchment showing the Lesnewth Stream tributary channel. Net difference in elevation after 72 hours simulation, showing the gridded and uniform rainfall simulations, for each of the two erosion law end-members (transport-limited and detachment-limited). Elevation change smaller than $\pm 0.2\text{m}$ in magnitude is not shown for clarity.

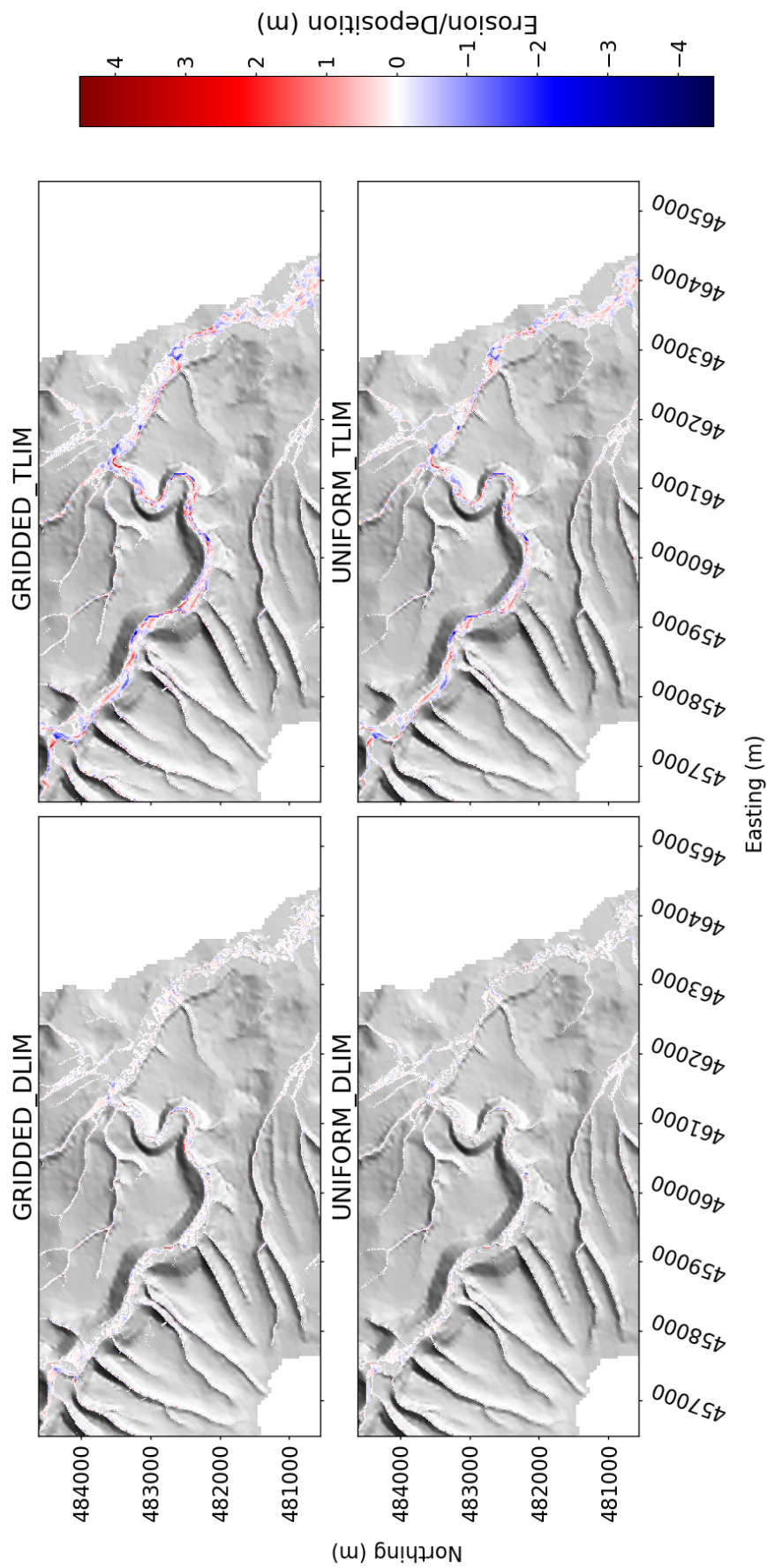


Figure 8.7: Ryedale. South-east section of Ryedale catchment showing the area around the village of Helmsley. Net difference in elevation after 72 hours simulation, showing the gridded and uniform rainfall simulations, for each of the two erosion law end-members (transport-limited and detachment-limited). Elevation change smaller than ± 0.2 m in magnitude is not shown for clarity.

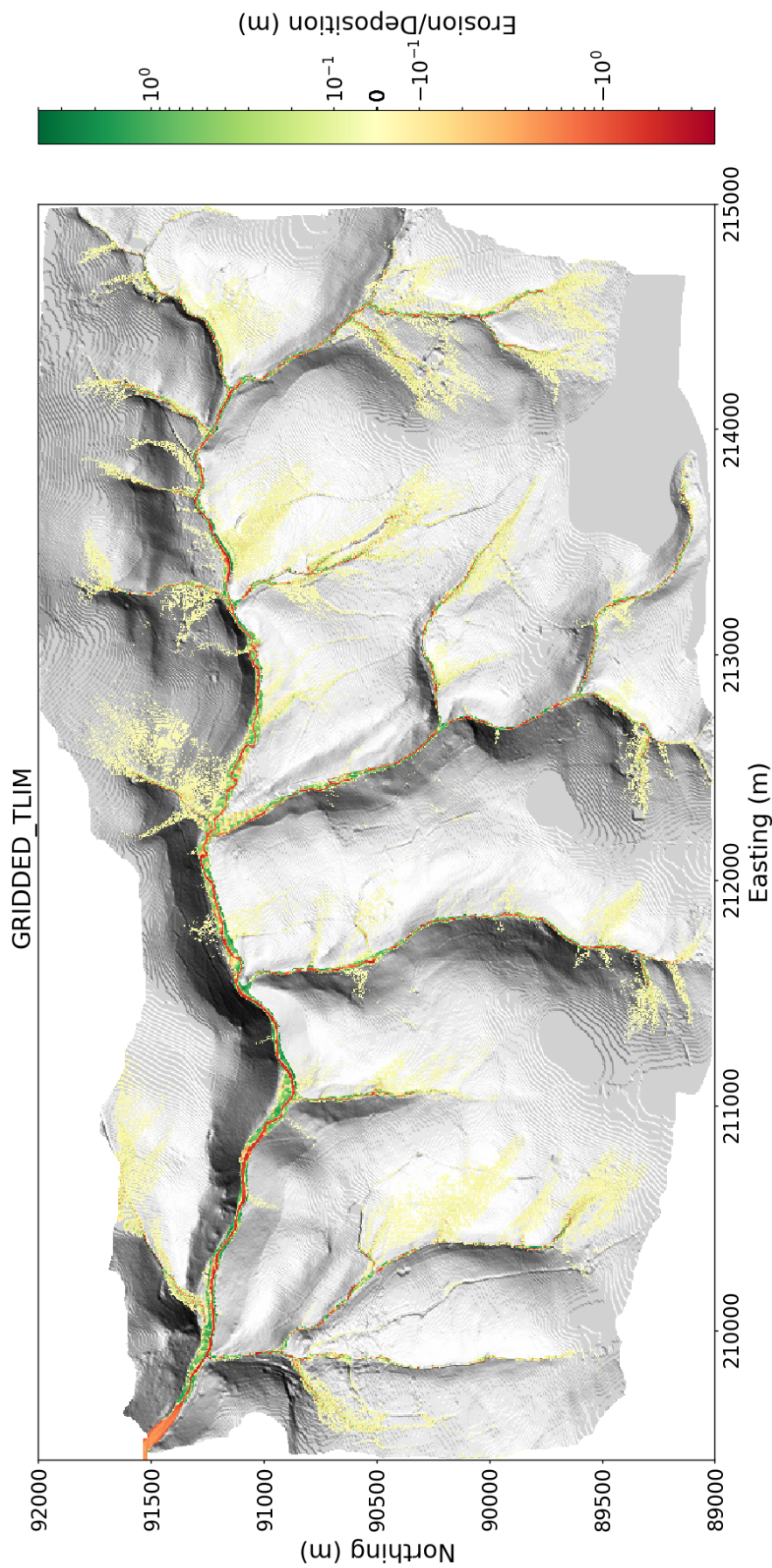


Figure 8.8: Boscastle. Map of extent of catchment change in elevation greater than 0.02m. Change in elevation shown after 72 hours of model simulation using gridded rainfall and the transport limited erosion law. Output from the gridded rainfall input, transport-limited erosion simulation (GRIDDED_TLIM). Logarithmic scale for erosion.

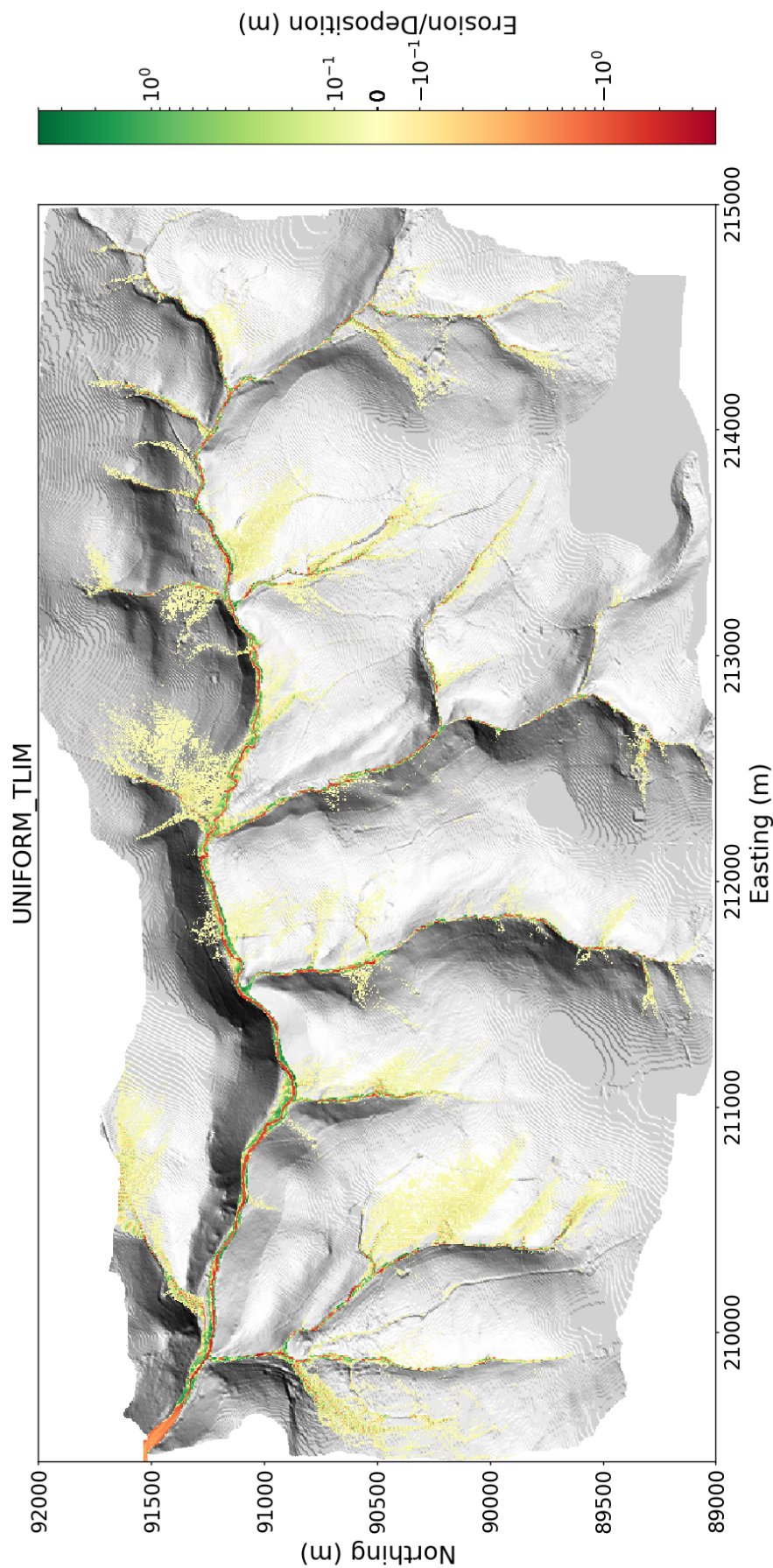


Figure 8.9: Boscastle. Map of extent of catchment change in elevation greater than 0.02m. Change in elevation shown after 72 hours of model simulation using uniform rainfall and the transport limited erosion law. Output from the uniform rainfall, transport-limited simulation (UNIFORM_TLIM). Logarithmic scale for erosion.

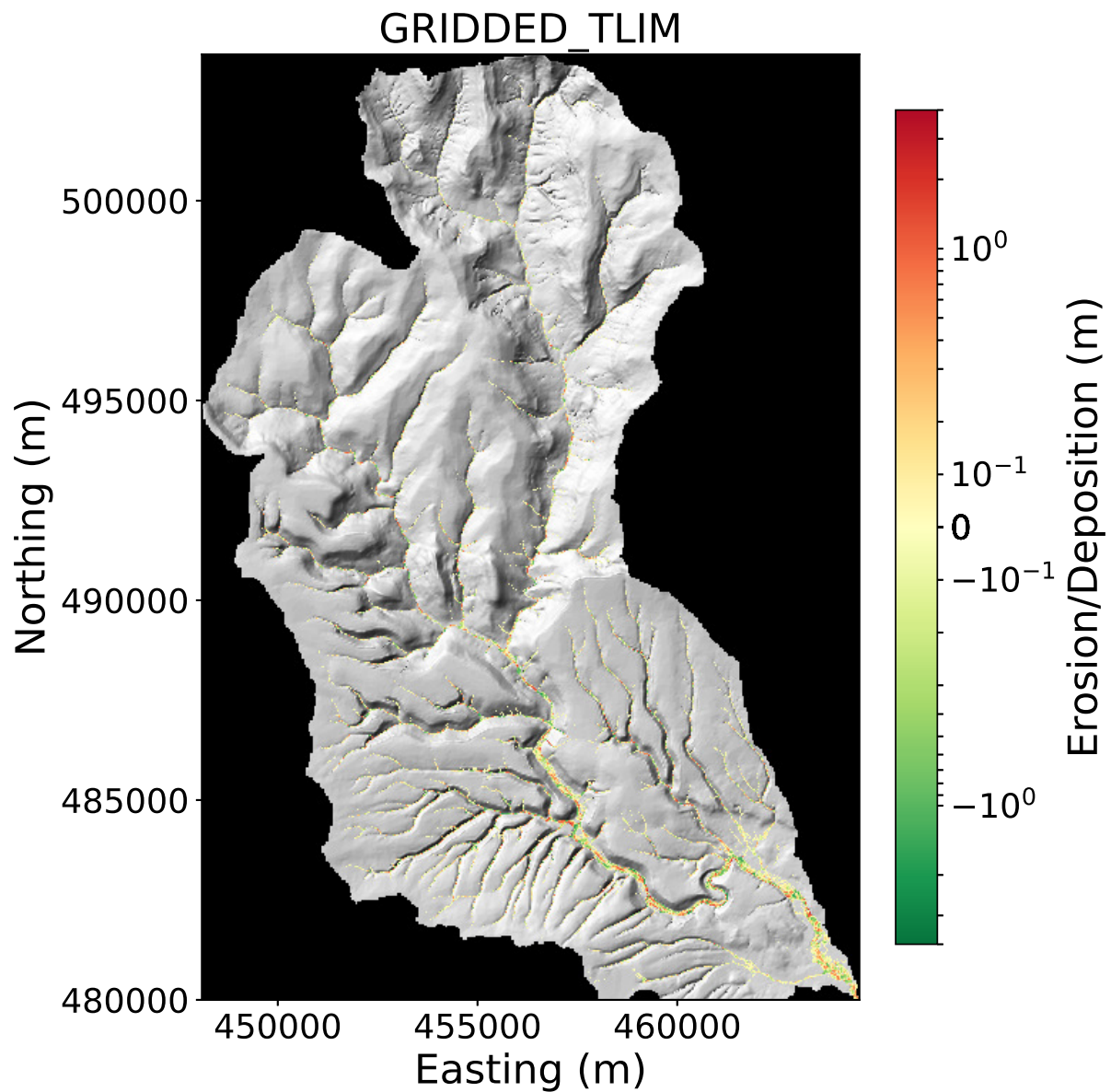


Figure 8.10: Ryedale. Map of extent of catchment change in elevation greater than 0.02m. Change in elevation shown after 72 hours of model simulation using uniform rainfall and the transport limited erosion law. Output from the uniform rainfall, transport-limited simulation (GRIDDED_TLIM). Logarithmic scale for erosion.

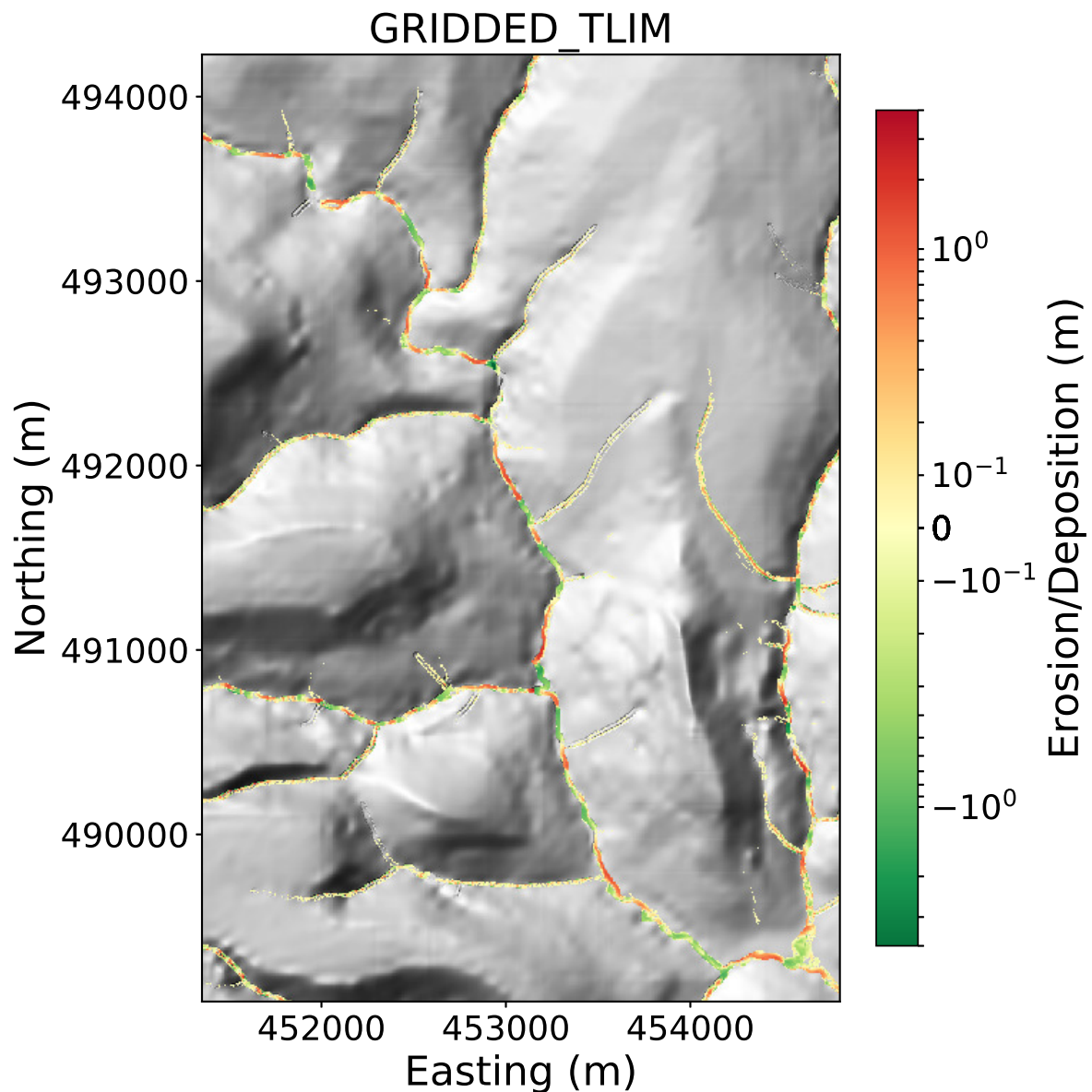


Figure 8.11: Ryedale, upper Rye channel. Map of extent of erosion and deposition greater than 0.02m in magnitude. Change in elevation shown after 72 hours of model simulation using gridded rainfall and the transport-limited erosion law (GRIDDED_TLIM). Logarithmic scale for erosion.

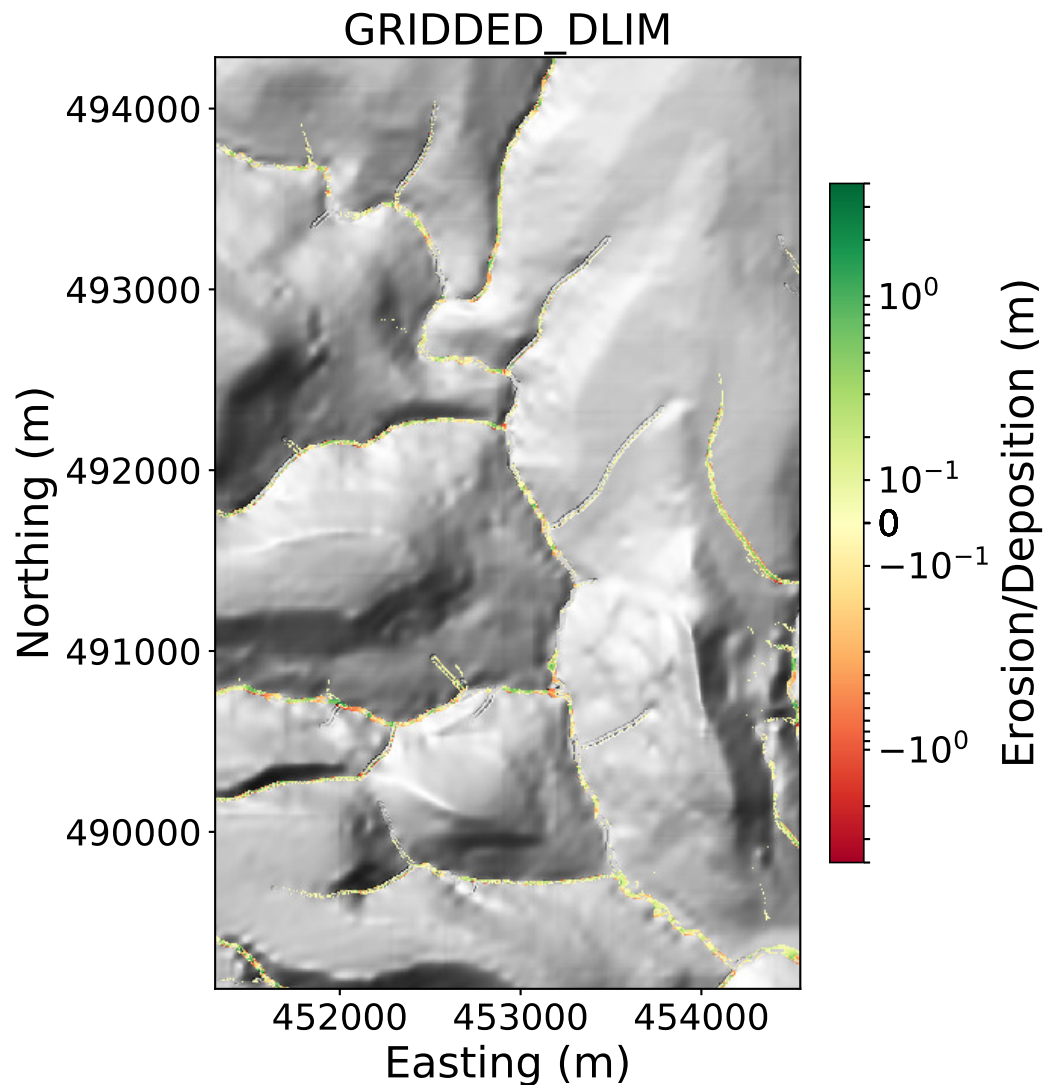


Figure 8.12: Ryedale, upper Rye channel. Map of extent of erosion and deposition greater than 0.02m in magnitude. Change in elevation shown after 72 hours of model simulation using gridded rainfall and the detachment-limited erosion law (GRIDDED_DLIM). Logarithmic scale for erosion.

8.3 Discussion

The analysis presented in this section discusses how erosional processes are sensitive to the spatial detail of precipitation in the context of flash flood events from intense rainfall. Improving our understanding of the relationship between rainfall patterns and erosional processes has two beneficiaries: 1) The short-term environmental forecasting community will be able to better assess the role that rainfall distribution has on sediment dynamics and erosion patterns. In the absence of spatially variable input data for environmental prediction, modellers will at least be able to gauge the potential uncertainty involved in sediment flux predictions and the distribution of erosion. 2) Within the context of longer-term landscape evolution, this study contributes to understanding the importance of individual storm events in driving landscape change over geological timescales. Current parameterisation of rainfall heterogeneity in long-term landscape evolution modelling is simplistic at best, and the results of this study can be used to guide rainfall parameterisation in landscape evolution model development.

The findings in this study are based on simulating historic flash flood events in upland catchments in the UK using a cellular automaton landscape evolution numerical model (HAIL-CAESAR, Chapter 5). As such, the conclusions drawn from these experiments will be influenced by the idiosyncrasies of the model itself and the individual characteristics of each catchment.

8.3.1 Sensitivity to erosion law and rainfall heterogeneity

One key finding from the experiments, exhibited in both case studies, is that erosion law choice in the model is a more dominant control on sediment flux, rather than the spatial detail of precipitation. The erosion-enabled simulations in these experiments represented two end-members of sediment transport and erosion laws (Table 6.2): transport-limited and detachment-limited erosion. The transport-limited law simulations predict much greater sediment flux and erosion than their detachment-limited counterparts, with up to an order of magnitude of difference in places. Compared to the erosion law parameterisation, the spatial resolution of rainfall input data played only a secondary role in determining erosion amounts. There was no clear evidence that the size of the catchment was important in this respect, with even the smaller

Boscastle catchment (18 km^2) showing a marked sensitivity to the choice of erosion law and slight sensitivity to rainfall distribution. The sediment flux output from each catchment during the storm showed an order of magnitude difference between detachment and transport-limited erosion parameterisations, given the same rainfall spatial inputs. In contrast, the difference in sediment flux between uniform and gridded rainfall simulations was much smaller in both sets of simulations.

Despite this study showing choice of erosion law being the dominant factor over rainfall spatial variability in controlling sediment flux, the study does confirm previous reports of increased sediment outputs from simulations using spatially heterogeneous rainfall data to drive simulations. Coulthard and Skinner (2016) reported that using finer-resolution rainfall data at 5 km grid spacing (also derived from meteorological radar) resulted in a doubling of sediment yields from a similar-sized upland catchment (415 km^2). The key difference in their findings was that the result was observed after a much longer simulation time of 1000 years, using a 10-year rainfall record looped over the course of the 1000 year simulation. While the rainfall data used in Coulthard and Skinner (2016) contain maximum rainfall intensities approaching those observed in the Boscastle and Ryedale storms used here, it is not clear whether these rainfall peaks were part of prolonged storms over catchment, or were merely brief, localised cloudbursts. In other words, it cannot be determined whether the increase in sediment output observed in the Coulthard and Skinner (2016) gridded rainfall simulations is due to a particular storm in the 10 year rainfall record, due to cumulative erosive effects of lower intensity but higher frequency rainfall events, or some combination of both. The work presented in this chapter suggests that rainfall spatial heterogeneity may partially account for higher sediment yields in individual storms as well as over longer simulations such as in Coulthard and Skinner (2016).

8.3.2 Comparison with observed geomorphic change post-flood

The resulting geomorphic change from the Boscastle 2004 flood, and to a lesser extent, the Ryedale flood of 2005 were extensively surveyed in the aftermath of each event. Both sets of simulations lacked a suitably high-resolution DEM representing the state of the catchment before the flood took place, so a detailed before-and-after assessment of the accuracy of the model predictions is not possible. However, comparison with

published reports on the erosion and deposition within each catchment allow us to make an assessment of whether the simulations were in broad agreement with the observations recorded after each flash flood event.

Boscastle

The geomorphological changes from the Boscastle flood were extensively mapped and recorded in an Environment Agency commissioned report carried out by HR Wallingford (2005). The amount of downcutting within the main Valency River channel was reported as 1–2 m in places. The transport-limited simulations predicted a similar magnitude of downcutting in places, but also tended to overestimate the amount of downcutting, predicting up to 4 m in places, which was not confirmed at any location by the HR Wallingford (2005) report. The detachment-limited simulations typically underestimated the amount of erosion and downcutting, particularly in the upper tributaries of the catchment, where little to no erosion was predicted, yet post-flood ground surveys reported substantial erosion within the channels.

Substantial channel widening of up to 3–4 m in places was reported in the HR Wallingford report. These simulations do not directly account for channel widening processes as there is no parameterisation of channel avulsion by lateral forces acting on the river bank within the HAIL-CAESAR model. The model allows indirect channel widening to take place through downcutting by water that has overtopped the channel banks, but this is not the primary mechanism through which channel widening occurs (Parker, 1976). Future enhancements to the HAIL-CAESAR model would be needed to allow lateral channel widening to be investigated in the typical sense, similar to the implementations in Murray and Paola (1997) and Coulthard et al. (2013). The simulations presented in this chapter therefore do not fully reflect the channel widening reported in the post-flood geomorphological survey. The over-prediction in downcutting may have occurred in compensation for the lack of a realistic channel widening mechanism in the model.

One area in which the gridded rainfall simulations performed better than the uniform rainfall inputs was in the tributaries in the south-east region of the catchment. The ground survey after the Boscastle flood noted significant amounts of erosion in the tributaries on the south side of the Valency River. The tributary shown in Figure 8.6

was observed as having up to 1–2 m of downcutting along its course. The gridded rainfall, transport-limited simulation GRIDDED_TLIM more accurately predicted this than the corresponding uniform rainfall input simulations. The regions of the catchment with the highest rainfall input – mainly the southern and eastern fringes of the catchment (Figure 6.2) – fed into the tributaries that experienced the channel downcutting. In this particular case high resolution rainfall input data can better resolve the pattern of erosion on the ground at a sub-catchment scale.

Deposition of sediment was observed along most sections of the lower reaches of the Valency floodplain. The transport-limited simulations predicted sediment deposition in the small floodplain areas immediately adjacent to the river channel, but substantially overpredicted the amount of sediment deposition in places, predicting as much as 2–3 m of deposition. Ground surveys, while noting deposition of sediment in many places, reported sediment deposition on the order of centimetres, not metres. A similar overestimation of deposition was present in both the gridded and uniform rainfall simulations, reinforcing the conclusion that the choice and parameterisation of erosion law is a stronger controlling factor than the spatial heterogeneity of rainfall.

Large sediment deposits were noted after the event in the harbour area of Boscastle village (HR Wallingford, 2005).¹ Notably, all simulations failed to predict this correctly, in fact predicting net sediment erosion in the harbour area (Figure 8.5, north-west corner). The discord between observations and model predictions in the harbour area may arise from the poor parameterisation of the interface where the catchment drains out into the sea in this location. The sea and tide in the harbour act as a natural dampener to water flow velocities, which would be expected to encourage deposition of sediments here.

Ryedale

Geomorphic change in the aftermath of the Ryedale flood was not as extensively surveyed compared to the Boscastle event. However, several studies made qualitative and some quantitative observations regarding the geomorphic impact of the event (Dong, 2006; Wass et al., 2008; Hopkins, 2012). Channel downcutting was substantial, with 2–3 m reported in the upper tributaries of the Rye catchment (Wass et al.,

¹Although the exact depths were not quantified in the report.

2008; Hopkins, 2012). This pattern of channel incision was generally captured in the transport-limited simulations of the Ryedale flood, but not in the detachment-limited simulations which tended to underpredict channel incision in the upper reaches of the catchment, which is shown in Figures 8.12 and 8.11). Sediment deposition was reported in the lower reaches of the catchment, particularly in the village of Helmsley, but was not mapped extensively, unlike the Boscastle survey. The simulations show areas of sediment deposition and erosion on the order of 0.5–3 m around the Helmsley area and the surrounding flood plain. Photographic evidence (Dong, 2006; Hopkins, 2012) however, suggests these predictions are somewhat over-estimates of the amount of incision and deposition in the floodplain area around Helmsley.

The Ryedale storm was noted for its triggering of over 100 shallow landslides within the catchment (Galiatsatos et al., 2007; Dong, 2006; Wass et al., 2008). The treatment of landsliding in the HAIL-CAESAR model is simplistic, based on a simple critical slope threshold required to trigger landslides, and as a result the reported landslides went largely unpredicted by all of the simulations. More complex models of landsliding are able to account for the role of soil saturation and pore water pressure in triggering of shallow landslides (e.g. Iverson, 2000; Crosta and Frattini, 2003) and could be incorporated into future development of the model.

8.3.3 Implications for longer-term landscape evolution

The experiments presented in this chapter have focused on the hydrogeomorphic response to single severe storm events, events which produced 3-hour rainfall totals with return periods of 1 in 330 years (Ryedale) and 1 in 1300 years (Boscastle). The amounts of river channel incision predicted as a result of these storms is comparable to that predicted by studies of landscape evolution on scales of 1000 years; for example, a study of a similar upland river basin by Coulthard and Skinner (2016) predicted channel incision amounts of 0.5–5m over a 1000 year simulation. Ground surveys after both events (HR Wallingford, 2005; Dong, 2006) revealed somewhat lower channel incision amounts, though of the same order of magnitude (1–3 m). The transport-limited erosion law experiments presented here, using the same sediment transport law in the Coulthard and Skinner (2016) study, predict comparable amounts of channel incision during a single storm event. Previous studies of upland catchments in the

UK that have experienced similar flash flood events have responded in a similar fashion (Johnson and Warburton, 2002b; Milan, 2012), showing catchment sediment fluxes far higher than typical background levels for similar sized catchments (e.g. Johnson and Warburton, 2002a). If the flood return periods are assumed to be broadly correct, these simulations, along with previously published field studies, support the view that the majority of sediment erosion occurs during infrequent but high-magnitude flood events, rather than through gradual erosion or more frequent but lower-magnitude events.

8.4 Conclusion

This study was designed to test whether erosional processes in river catchments are sensitive to the spatial distribution of rainfall inputs, within the timeframe of an individual severe storm. In the context of erosion law versus rainfall spatial resolution, these experiments have shown that it is the choice of erosional parameterisation in the model, and not necessarily the spatial detail of rainfall input data, that exerts a first-order control on the total sediment yields and the magnitude of river incision.

A further conclusion can also be made that rainfall spatial distribution does have an impact on sediment outputs and distribution of erosion in a catchment during an intense rainfall event, but in the cases shown here, it is a secondary control when compared to the choice and parameterisation of the erosion or sediment transport law. Where there is notable rainfall heterogeneity in a storm, spatially distributed rainfall data can be used to more accurately predict local variations in channel incision within the catchment, as was evident in the observed and predicted erosion patterns in the Boscastle catchment.

The study has touched upon whether landscape evolution models may be used for shorter-term forecasting tools to predict the impact of flash floods on the landscape, such as predicting local areas of channel erosion and deposition. There are still a number of limitations in current landscape erosion models that prevent them being used as tools of detailed predictive ability, notably the sensitivity from the choice of erosion laws as highlighted above. Using rainfall radar data as input to the model also introduces a further source of potential error (Chapter 4), which further compounds

the uncertainty in predictions made by using a landscape evolution model in such a way to provide forecasts of landscape erosion in a single severe rainfall event.

The importance of high-magnitude, low-frequency storm events as drivers of longer-term landscape evolution is reinforced by this study. The amounts of channel incision predicted by the simulations, and confirmed in previously published geomorphological surveys of Boscastle (HR Wallingford, 2005) and Ryedale (Dong, 2006; Wass et al., 2008), shows that a single storm can have as much erosive impact as centuries of higher-frequency, lower-magnitude events. If one were to extrapolate the differences in predictions between uniform and gridded rainfall inputs based on this study, the effect of rainfall spatial detail could be argued to play a secondary role in longer-term landscape evolution. Cumulatively the small differences observed in erosion between uniform and gridded rainfall inputs to the model may become more pronounced over longer-term landscape evolution simulations, reconciling this study with previously published work. These findings are made in the context of two catchments in the UK during heavy convective rainfall events. Other factors and feedbacks may come into play over longer timescales, in different catchments, or under different meteorological conditions. Nonetheless, the analysis of the numerical simulations presented in this chapter suggest that hydro-geomorphic processes are at least partly sensitive to the spatial distribution of rainfall during intense storms.

9

Conclusions

9.1 Review of aims and overview of results

I set out to investigate the sensitivity of hydrogeomorphic processes to rainfall spatial variability during intense rainfall events. The aims of the thesis presented in Chapter 1 consisted of two scientific aims and one technological aim to support them. The scientific aims were to investigate the influence of using spatially variable rainfall input data on a) flood inundation predictions and b) sediment flux and distribution of erosion and deposition; both aims addressed within the context of flash flooding events from intense rainfall. To address these questions, a hydrodynamic landscape evolution model was developed based on an existing model, capable of carrying out ensemble-style simulations on high-performance computing (HPC) services (Chapter 5). To build on previous studies that have investigated the role of rainfall spatial resolution in isolation, or with other competing factors, a secondary variable was introduced: the choice of erosional process parameterisation in the model. This study is believed to be the first to investigate the sensitivity of rainfall resolution and erosional process parameterisation in tandem, and to assess which has the greater control on hydrogeomorphic processes in river catchments. It is also one of few studies to investigate the role of these two competing factors within the context of an individual flash flooding event from intense rainfall.

The two core scientific hypotheses (presented in detail in Chapter 6, Section 6.4) stated:

1. Flood inundation modelling is sensitive to the spatial detail of precipitation

inputs.

2. Erosional processes in river catchments are sensitive to the spatial distribution of rainfall inputs.

These results from the testing of these hypotheses are discussed in the conclusions made in Chapters 7 and 8 and are summarised in the following sections:

9.1.1 Flood-inundation model sensitivity

Flood inundation model predictions are sensitive to spatial distribution of rainfall inputs, specifically the use of 1km gridded rainfall data, when compared to using uniform averaged data as model input. Predicted hydrological discharge is higher using gridded rainfall inputs, though not necessarily more accurate when compared to measured discharges during the respective flood events simulated. In the Boscastle case study, river discharges more closely matched the observed data, whereas in the Ryedale event, uniform rainfall inputs into the model actually produced a better match to observed data. The choice of erosional process parameterisation plays only a secondary role in hydrological response.

9.1.2 Erosion and sediment flux sensitivity

Fluvial erosional processes in river catchments are somewhat sensitive to the use of spatially variable rainfall input data to the model, though it is only of secondary importance when compared to the sensitivity observed in the use of different erosional process law parametrisations. The difference in sediment outputs were much greater under a transport-limited type erosion law, compared to a detachment-limited one. The effects from using spatially variable rainfall input data on sediment fluxes were less noticeable in comparison, but still had a measurable effect on sediment fluxes. Using spatially variable rainfall data increased sediment yields in both case studies and under both types of erosional parameterisation.

9.2 Key themes and synthesis

It was set out to determine whether hydrogeomorphic processes in river catchments were sensitive to the spatial detail of rainfall input data. Numerical simulations using a hydrodynamic landscape evolution model have indicated that resolving the spatial detail in rainfall structure during severe storms has a demonstrable effect on both hydrological and sediment fluxes. (e.g. Figures 7.3, 8.2, 7.4, 8.1). Though the magnitude of the sensitivity varied between experiments, there was a general increase in peak discharge and peak sediment flux in simulations with gridded rainfall data used as the rainfall input, compared to simulations that used a single, spatially uniform value for rainfall. Existing studies investigating landscape evolution model sensitivity to rainfall resolution (Coulthard and Skinner, 2016) have noted similar increases in water discharge and sediment yields when using spatially heterogeneous rainfall data. The results from the experiments presented in this chapter are broadly in agreement with the general findings of Coulthard and Skinner (2016) although the timescales simulated in this study are on the order of hours, rather than decades. The results presented here suggest that the effect of rainfall resolution sensitivity applies to hydrogeomorphic processes at the single storm event timescale, as well as landscape evolution over periods of decades to hundreds of years.

Opting to use spatially variable rainfall data at 1 km resolution was sufficient to observe sediment flux sensitivity to rainfall variability in a catchment as small as 12 km². However, rainfall features equal to or greater in size than the catchment over which they rain upon may well be homogeneous enough in spatial extent and rainfall rate that a ‘uniform’ approximation of their intensity is sufficient to represent the rainfall rate at all points in the catchment. From a hydrological perspective, as seen in the Boscastle catchment simulations, using a spatially variable rainfall input data source did not notably alter the outcome of the hydrological predictions (Figures 7.9, 7.13). However, in the Ryedale catchment simulations, the hydrological predictions were notably different based on the choice of rainfall input data resolution, affecting both the timing and magnitude of the resulting flood peak. It is possible that hydrological processes are less sensitive to rainfall spatial variability in smaller catchments than erosional processes are, although further systematic study would be necessary to

determine exactly what the threshold catchment size might be where rainfall spatial variability becomes an issue in hydrological models.

9.3 Technical advances

The numerical simulation work in this project has been made possible by the development of a numerical landscape evolution model suitable for deployment on HPC services (Chapter 5). The porting and development of landscape erosion and evolution models for HPC has thus far been under-exploited in the geomorphological modelling community. The development and parallelisation of the HAIL-CAESAR model as part of this thesis is an advancement of existing methods in computational modelling for hydro-geomorphology:

Firstly, the model's basis as a redevelopment of an existing model (CAESAR-Lisflood) provides a continuity and familiarity with the existing user base. Core functionality is preserved, which will hopefully encourage an uptake in use of the model amongst existing users of the CAESAR-Lisflood model. The translation of the original model's code, preserving the algorithms as closely as possible in a different programming language, ensures there is comparability between the original and redeveloped version of the model presented here.

Secondly, in addition to the speed-up in simulation runtimes achieved, the ability to now use HPC facilities to conduct hydrogeomorphological modelling studies allows large-scale sensitivity analyses to be done, with multiple member 'ensemble-style' simulations, in a similar fashion to numerical weather prediction model ensembles (Sivillo et al., 1997; Klein et al., 2015). In this study, six-member simulations per case study are used for the main set of experiments (Table 6.2), with ten member simulations used for the parameter sensitivity analysis in Chapter 7 (Table 7.1). With sufficient computing resources, much larger ensemble simulations would be possible using the HAIL-CAESAR model.

9.4 Future research and applications

This study has touched upon the potential for using large ensemble-style simulations to assess sensitivity in landscape evolution modelling studies. Since numerical landscape evolution models typically contain a large number of parameters, particularly as they often combine multiple-process sub-models such as erosion, hydrology, hillslope processes, and other surface processes, a thorough exploration of parameter space is usually beyond the scope of many studies. Current applications of landscape erosion and evolution models rarely make use of multiple-member ensemble simulations, whereas this practice is more commonly found in hydrological modelling (Cloke and Pappenberger, 2009; Wong et al., 2015) and numerical weather prediction (Sivillo et al., 1997). Hydrogeomorphic and landscape evolution modelling studies have been late adopters of ensemble simulations, but this thesis as well as other projects (e.g. Schaake et al., 2007; Skinner et al., 2017) highlight the timely applicability of ensemble-style simulations for future hydrogeomorphic research. The HAIL-CAESAR model could be used in this way in future studies to more rigorously assess model sensitivity to user-defined parameters in landscape evolution modelling. Taking advantage of the increase in computing power in recent decades with the HAIL-CAESAR model presented in this thesis would enable a rigorous exploration of model sensitivity to parameter-space, initial model conditions, input data quality, model resolution, and many other sources of potential uncertainty (Pelletier et al., 2015).

Further development of the model would allow it to tackle large catchments at regional to continental scale, or very high resolution studies of smaller river catchments. High resolution topographic data already exists at resolutions of 0.2 to 0.5 m, primarily sourced from LiDAR-derived topographic data. At this resolution, river channel and other geomorphological features can be resolved in great detail within the model domain. Although the data is readily available now, few modelling studies have yet made use of such high resolution data, partly because of limitations in computational resources and appropriately designed software. Notwithstanding, the HAIL-CAESAR model would require further development to address the scaling issues highlighted in Chapter 5, in order to tackle model domains containing tens of millions of grid cells.

Predicting catchment response to intense rainfall events is a pressing societal issue. Current flood forecasting applications tend to focus primarily on the hydrological response of catchments without taking into account geomorphological change during such events. Future development of models in the flood-forecasting community could expand them to be more holistic simulators of catchment processes, including sediment erosion and transport, in addition to their core functionally of predicting flood inundation extents.

9.5 Future development of HAIL-CAESAR

A number of interested parties have expressed interest in using HAIL-CAESAR for further landscape evolution and hydrological modelling. Future development work is outlined here.

Reach mode

Development of the model in future would include the development of a ‘reach-mode’ in addition to the ‘whole-catchment’ mode currently implemented in the model. Reach-mode would be a configuration of the model that allows it to simulate localised sections of a river channel and surrounding area. Reach-mode is also feature of the progenitor to the HAIL-CAESAR model, CAESAR-Lisflood, and has applications where detailed simulations are required of particular sections of river channel, but not of the entire catchment. Reach mode (as part of CAESAR-Lisflood) has been employed in a number of studies to date (CITE) and would be a useful addition to the CAESAR modelling community.

Process representation

A number of processes in the CAESAR and CAESAR-Lisflood models were omitted in the HAIL-CAESAR development process because of time constraints and applicability to the research questions posed in this thesis. Additional process representation in the HAIL-CAESAR model could be facilitated by the implementation of the following additional subroutines in the model code:

- **Lateral channel erosion.** Currently only downcutting erosion and deposition is represented in the model. The lack of lateral erosion mechanisms was highlighted as a possible limitation in the HAIL-CAESAR model’s ability to fully predict the amount and distribution in the Boscastle event documented in Chapter 8
- **Slope processes.** Slope processes in HAIL-CAESAR as well as CAESAR-Lisflood have very simple representations based on simple threshold gradients to initiate redistribution of slope material between adjacent cells. A number of more physically realistic slope process models exist that could be incorporated into the HAIL-CAESAR model.
- **Groundwater.** Interest has been expressed by the developers of the British Geological Survey’s CLiDE model in using HAIL-CAESAR as a basis for the development of a coupled groundwater–catchment hydrology and erosion model for use on HPC services. The groundwater components would be based on the algorithms in the existing CLiDE model, another CAESAR-based model with applications in environmental modelling and prediction (e.g. Barkwith et al., 2015).
- **MPI parallelisation.** HAIL-CAESAR was parallelised in a way to facilitate the use of multi-member ensemble simulations on shared-memory compute nodes. This method of parallelisation lends itself well to sensitivity analyses as demonstrated in this thesis, and moderately large domains and high-resolution data. However, to fully exploit the highest resolution datasets available, or to conduct regional to continental scale modelling studies, a different parallelisation strategy would have to be employed using what is termed ‘distributed-memory’ parallelism, whereby the model domain is decomposed across multiple computing nodes. The most common approach to this is to use a parallelisation standard known as MPI – the Message Passing Interface. Initial plans for the implementation of HAIL-CAESAR with the MPI software libraries are currently under development. Such work would require a considerable development effort but there are precedents for purely hydrological models being parallelised in this way before (Vivoni et al., 2011), and many of the techniques could be applied to landscape evolution models such as HAIL-CAESAR.

There has also been an interest expressed in using part of the HAIL-CAESAR model as an educational tool for teaching MPI parallelisation, in part due to the cellular automaton modelling framework being a relatively straightforward modelling technique to parallelise over a 2D domain (Edinburgh Parallel Computing Centre – personal communication).

9.6 Summary

This thesis has presented a novel method for simulating hydrological and geomorphological processes at the catchment scale using high-performance computing systems. This method was then applied to investigating the sensitivity of hydrogeomorphic processes to the spatial resolution of rainfall input data and erosional process parameterisation. It was found that while spatial variability in rainfall input data to models can affect the hydrological outputs of numerical models, predictions are not necessarily more accurate in all cases when using spatially variable rainfall input data. In terms of predicting sediment fluxes and erosion distribution, the choice of erosion law had a more pronounced effect on sediment fluxes compared to spatially variable rainfall input data. Notwithstanding, the use of spatially variable rainfall data in hydrodynamic landscape evolution models can in some cases better predict localised distribution of erosion within a river catchment. The findings and methodological developments pose a useful contribution to the future of hydrogeomorphological modelling and its applications in environmental prediction and forecasting.

Bibliography

- Adams, J. M., N. M. Gasparini, D. E. Hobley, G. E. Tucker, E. W. Hutton, S. S. Nudurupati, and E. Istanbulluoglu (2017). ‘The Landlab v1. 0 OverlandFlow component: a Python tool for computing shallow-water flow across watersheds.’ In: *Geoscientific Model Development* 10.4.
- Ahnert, F. (1976). ‘Brief description of a comprehensive three-dimensional process-response model of landform development’. In: *Z. Geomorphol. Suppl* 25, pp. 29–49.
- Aitken, M. J. (1998). *An introduction to optical dating: the dating of Quaternary sediments by the use of photon-stimulated luminescence*. Oxford University Press.
- Amdahl, G. M. (1967). ‘Validity of the single processor approach to achieving large scale computing capabilities’. In: *Proceedings of the April 18-20, 1967, spring joint computer conference*. ACM, pp. 483–485.
- Anderson, R. S., J. L. Repka, and G. S. Dick (1996). ‘Explicit treatment of inheritance in dating depositional surfaces using in situ ^{10}Be and ^{26}Al ’. In: *Geology* 1, pp. 47–51.
- Anton, L., A. Mather, M. Stokes, A. Muñoz-Martin, and G. De Vicente (2015). ‘Exceptional river gorge formation from unexceptional floods’. In: *Nature communications* 6.
- Attal, M., G. E. Tucker, A. C. Whittaker, P. A. Cowie, and G. P. Roberts (2008). ‘Modeling fluvial incision and transient landscape evolution: Influence of dynamic channel adjustment’. In: *Journal of Geophysical Research* 113.F3, F03013. ISSN: 0148-0227. DOI: 10.1029/2007JF000893. URL: <http://www.agu.org/pubs/crossref/2008/2007JF000893.shtml>.
- Attal, M., P. A. Cowie, A. C. Whittaker, D. Hobley, G. E. Tucker, and G. P. Roberts (2011). ‘Testing fluvial erosion models using the transient response of bedrock rivers

- to tectonic forcing in the Apennines, Italy'. In: *Journal of Geophysical Research* 116.F2, F02005. ISSN: 0148-0227. DOI: 10.1029/2010JF001875. URL: <http://doi.wiley.com/10.1029/2010JF001875>.
- Axelsson, P. (1999). 'Processing of laser scanner data—algorithms and applications'. In: *ISPRS Journal of Photogrammetry and Remote Sensing* 54.2, pp. 138–147.
- Aycock, J. (2003). 'A brief history of just-in-time'. In: *ACM Computing Surveys (CSUR)* 35.2, pp. 97–113.
- Baartman, J. E. M., A. J. A. M. Temme, J. M. Schoorl, M. H. A. Braakhekke, and T. A. Veldkamp (2012a). 'Did tillage erosion play a role in millennial scale landscape development?' In: *Earth Surface Processes and Landforms* 37.15, pp. 1615–1626. ISSN: 01979337. DOI: 10.1002/esp.3262.
- Baartman, J. E. M., W. Van Gorp, A. J. A. M. Temme, and J. M. Schoorl (2012b). 'Modelling sediment dynamics due to hillslope-river interactions: Incorporating fluvial behaviour in landscape evolution model LAPSUS'. In: *Earth Surface Processes and Landforms* 37.9, pp. 923–935. ISSN: 01979337. DOI: 10.1002/esp.3208.
- Barnhart, K. R. and R. S. Anderson (2014). 'Chilly Hilly-coupling models of landscape evolution and subsurface thermal processes'. In: *AGU Fall Meeting Abstracts*. Vol. 1, p. 3.
- Barkwith, A., M. D. Hurst, C. R. Jackson, L. Wang, M. A. Ellis, and T. J. Coulthard (2015). 'Simulating the influences of groundwater on regional geomorphology using a distributed, dynamic, landscape evolution modelling platform'. In: *Environmental Modelling and Software* 74, pp. 1–20. ISSN: 13648152. DOI: 10.1016/j.envsoft.2015.09.001. URL: <http://dx.doi.org/10.1016/j.envsoft.2015.09.001>.
- Barros, A. P. and D. P. Lettenmaier (1994). 'Dynamic modeling of orographically induced precipitation'. In: *Reviews of Geophysics* 32.94, pp. 265–284.
- Barredo, J. I. (2009). 'Normalised flood losses in Europe: 1970–2006'. In: *Natural Hazards and Earth System Sciences* 9.1, pp. 97–104.
- Bates, P. D. and A. De Roo (2000). 'A simple raster-based model for flood inundation simulation'. In: *Journal of hydrology* 236.1, pp. 54–77.
- Bates, P., K. Marks, and M. Horritt (2003). 'Optimal use of high-resolution topographic data in flood inundation models'. In: *Hydrological Processes* 17.3, pp. 537–557.

- Bates, P. D., M. Horritt, N. Hunter, D. Mason, and D. Cobby (2005). ‘Numerical modelling of floodplain flow’. In: *Computational Fluid Dynamics*. John Wiley and Sons Ltd.: Chichester, UK.
- Bates, P. D., M. S. Horritt, and T. J. Fewtrell (2010). ‘A simple inertial formulation of the shallow water equations for efficient two-dimensional flood inundation modelling’. In: *Journal of Hydrology* 387.1, pp. 33–45.
- Bates, P. and S. Lane (1998). ‘Preface : High resolution flow modelling in hydrology and geomorphology’. In: *Hydrological Processes* 12, pp. 1129–1130. ISSN: 08856087. DOI: 10.1002/(SICI)1099-1085(19980630)12:8<1129::AID-HYP697>3.0.CO;2-8.
- Baynes, E. R., M. Attal, S. Niedermann, L. A. Kirstein, A. J. Dugmore, and M. Naylor (2015). ‘Erosion during extreme flood events dominates Holocene canyon evolution in northeast Iceland’. In: *Proceedings of the National Academy of Sciences* 112.8, pp. 2355–2360.
- Beer, A. R., J. M. Turowski, B. Fritschi, and D. H. Rieke-Zapp (2015). ‘Field instrumentation for high-resolution parallel monitoring of bedrock erosion and bedload transport’. In: *Earth Surface Processes and Landforms* 40.4, pp. 530–541. ISSN: 10969837. DOI: 10.1002/esp.3652.
- Bell, V. and R. Moore (2000). ‘The sensitivity of catchment runoff models to rainfall data at different spatial scales’. In: *Hydrology and Earth System Sciences Discussions* 4.4, pp. 653–667.
- Bennett, O. (2014). *House of Commons Library Standard Note: Flood defense spending in England*. Tech. rep. SN/SC/755. House of Commons Library.
- Berne, A., G. Delrieu, J.-D. Creutin, and C. Obled (2004). ‘Temporal and spatial resolution of rainfall measurements required for urban hydrology’. In: *Journal of Hydrology* 299.3, pp. 166–179.
- Beven, K. and J. Freer (2001a). ‘A dynamic topmodel’. In: *Hydrological processes* 15.10, pp. 1993–2011.
- (2001b). ‘Equifinality, data assimilation, and uncertainty estimation in mechanistic modelling of complex environmental systems using the GLUE methodology’. In: *Journal of hydrology* 249.1, pp. 11–29.

- Beven, K. and M. J. Kirkby (1979). 'A physically based, variable contributing area model of basin hydrology/Un modèle à base physique de zone d'appel variable de l'hydrologie du bassin versant'. In: *Hydrological Sciences Journal* 24.1, pp. 43–69.
- Beven, K., M. Kirkby, N. Schofield, and A. Tagg (1984). 'Testing a physically-based flood forecasting model (TOPMODEL) for three UK catchments'. In: *Journal of Hydrology* 69.1-4, pp. 119–143.
- Beven, K. and P. Carling (1989). *Floods: hydrological, sedimentological and geomorphological implications*. John Wiley and Sons Ltd.
- Beven, K. (2011). *Rainfall-runoff modelling: the primer*. John Wiley & Sons.
- (1993). 'Prophecy, reality and uncertainty in distributed hydrological modelling'. In: *Advances in water resources* 16.1, pp. 41–51.
- (1996). 'Equifinality and uncertainty in geomorphological modelling'. In: *The scientific nature of geomorphology. Proceeding of the 27th Binghamton Symposium in Geomorphology held 27-29 September 1996* September 1996, pp. 289–314.
- (1997). 'TOPMODEL: a critique'. In: *Hydrological processes* 11.9, pp. 1069–1085.
- Biswas, A. K. (1970). *History of hydrology*. North-Holland Amsterdam.
- Blackburn, M., J. Methven, and N. Roberts (2008). 'Large-scale context for the UK floods in summer 2007'. In: *Weather* 63.9, p. 280.
- Blöschl, G. (2013). *Runoff prediction in ungauged basins: synthesis across processes, places and scales*. Cambridge University Press.
- Bonnet, S. and A. Crave (2006). 'Macroscale dynamics of experimental landscapes'. In: *Geological Society, London, Special Publications* 253.1, pp. 327–339. ISSN: 0305-8719. DOI: 10.1144/GSL.SP.2006.253.01.17. URL: <http://sp.lyellcollection.org/cgi/doi/10.1144/GSL.SP.2006.253.01.17>.
- Bonnet, S. (2009). 'Shrinking and splitting of drainage basins in orogenic landscapes from the migration of the main drainage divide'. In: *Nature Geoscience* 2.11, pp. 766–771. ISSN: 1752-0894. DOI: 10.1038/ngeo666. URL: <http://dx.doi.org/10.1038/ngeo666>.
- Borga, M., E. N. Anagnostou, and E. Frank (2000). 'On the use of real-time radar rainfall estimates for flood prediction in mountainous basins'. In: *Journal of Geophysical Research: Atmospheres* 105.D2, pp. 2269–2280.

- Bras, R. L., G. E. Tucker, and V. Teles (2003). ‘Six myths about mathematical modeling in geomorphology’. In: *Prediction in geomorphology*, pp. 63–79.
- Braun, J. and S. D. Willett (2013). ‘A very efficient O(n), implicit and parallel method to solve the stream power equation governing fluvial incision and landscape evolution’. In: *Geomorphology* 180–181, pp. 170–179. ISSN: 0169555X. DOI: 10.1016/j.geomorph.2012.10.008. URL: <http://linkinghub.elsevier.com/retrieve/pii/S0169555X12004618>.
- Braun, J. and F. Guillocheau (2014). ‘Journal of Geophysical Research Solid Earth’. In: pp. 6093–6112. DOI: 10.1002/2014JB010998. Received. URL: <http://onlinelibrary.wiley.com/doi/10.1002/jgrb.50332/abstract>.
- Braun, J. and M. Sambridge (1997). ‘Modelling landscape evolution on geological time scales: a new method based on irregular spatial discretization’. In: *Basin Research* 9.1, pp. 27–52. ISSN: 0950-091X. DOI: 10.1046/j.1365-2117.1997.00030.x. URL: <http://doi.wiley.com/10.1046/j.1365-2117.1997.00030.x>.
- Braun, J., D. Zwart, and J. H. Tomkin (1999). ‘A new surface-processes model combining glacial and fluvial erosion’. In: *Annals of Glaciology* 28, pp. 282–290. ISSN: 0260-3055. DOI: doi:10.3189/172756499781821797. URL: <http://dx.doi.org/10.3189/172756499781821797>.
- Brazier, R. (2004). ‘Quantifying soil erosion by water in the UK: a review of monitoring and modelling approaches’. In: *Progress in Physical Geography* 28.3, pp. 340–365.
- Brocklehurst, S. H. and K. X. Whipple (2004). ‘Hypsometry of glaciated landscapes’. In: *Earth Surface Processes and Landforms* 29.7, pp. 907–926.
- Browning, K. A., C. J. Morcrette, J. Nicol, A. M. Blyth, L. J. Bennett, B. J. Brooks, J. Marsham, S. D. Mobbs, D. J. Parker, F. Perry, P. A. Clark, S. P. Ballard, M. A. Dixon, R. M. Forbes, H. W. Lean, Z. Li, N. M. Roberts, U. Corsmeier, C. Barthlott, B. Deny, N. Kalthoff, S. Khodayar, M. Kohler, C. Kottmeier, S. Kraut, M. Kunz, J. Lenfant, A. Wieser, J. L. Agnew, D. Bamber, J. McGregor, K. M. Beswick, M. D. Gray, E. Norton, H. M. A. Ricketts, A. Russell, G. Vaughan, A. R. Webb, M. Bitter, T. Feuerle, R. Hankers, H. Schulz, K. E. Bozier, C. G. Collier, F. Davies, C. Gaffard, T. J. Hewison, D. N. Ladd, E. C. Slack, J. Waight, M. Ramatschi, D. P. Wareing, and R. J. Watson (2007). ‘The Convective Storm Initiation Project’. In:

- Bulletin of the American Meteorological Society* 88.12, pp. 1939–1955. ISSN: 0003-0007. DOI: 10.1175/BAMS-88-12-1939. URL: <http://journals.ametsoc.org/doi/abs/10.1175/BAMS-88-12-1939>.
- Browning, K. (2003). ‘Quantitative precipitation forecasting’. In: *Weather* 58.3, pp. 126–127.
- Bunte, K., S. R. Abt, J. P. Potyondy, and S. E. Ryan (2004). ‘Measurement of Coarse Gravel and Cobble Transport Using Portable Bedload Traps’. In: *Journal of Hydraulic Engineering* 130.9, pp. 879–893. ISSN: 0733-9429. DOI: 10.1061/(ASCE)0733-9429(2004)130:9(879).
- Burbank, D. W. and R. S. Anderson (2011). *Tectonic Geomorphology*. 2nd. Wiley-Blackwell, p. 472.
- Burt, S. (2005). ‘Cloudburst upon Hendraburnick Down: The Boscastle storm of 16 August 2004’. In: *Weather* 60.8, pp. 219–227.
- Casas, A., G. Benito, V. Thorndycraft, and M. Rico (2006). ‘The topographic data source of digital terrain models as a key element in the accuracy of hydraulic flood modelling’. In: *Earth Surface Processes and Landforms* 31.4, pp. 444–456.
- Castelltort, S., L. Goren, S. D. Willett, J.-D. Champagnac, F. Herman, and J. Braun (2012). ‘River drainage patterns in the New Zealand Alps primarily controlled by plate tectonic strain’. In: *Nature Geoscience* 5.10, pp. 744–748. ISSN: 1752-0894. DOI: 10.1038/ngeo1582. URL: <http://www.nature.com/doifinder/10.1038/ngeo1582>.
- Chapuis, M., S. Dufour, M. Provansal, B. Couvert, and M. De Linares (2015). ‘Coupling channel evolution monitoring and RFID tracking in a large, wandering, gravel-bed river: Insights into sediment routing on geomorphic continuity through a riffle–pool sequence’. In: *Geomorphology* 231, pp. 258–269.
- Chang, K.-t. and B.-w. Tsai (1991). ‘The effect of DEM resolution on slope and aspect mapping’. In: *Cartography and geographic information systems* 18.1, pp. 69–77.
- Chappell, C. F. (1986). ‘Quasi-stationary convective events’. In: *Mesoscale meteorology and forecasting*. Springer, pp. 289–310.
- Church, M. (2003). ‘What is a geomorphological prediction?’ In: *Prediction in Geomorphology*, pp. 183–194.

- Ciach, G. J. (2003). ‘Local random errors in tipping-bucket rain gauge measurements’. In: *Journal of Atmospheric and Oceanic Technology* 20.5, pp. 752–759.
- Cinderey, M. (2005). ‘North York Moors storms–19 June 2005’. In: *Weather* 60.9, pp. 273–273.
- Clevis, Q., G. E. Tucker, S. T. Lancaster, A. Desitter, N. Gasparini, and G. Lock (2006a). ‘A simple algorithm for the mapping of TIN data onto a static grid: applied to the stratigraphic simulation of river meander deposits’. In: *Computers & geosciences* 32.6, pp. 749–766.
- Clevis, Q., G. E. Tucker, G. Lock, S. T. Lancaster, N. Gasparini, A. Desitter, and R. L. Bras (2006b). ‘Geoarchaeological Simulation of Meandering River Deposits and Settlement Distributions: A Three-Dimensional Approach’. In: *Geoarcheology* 21.8, pp. 843–874. DOI: DOI:10.1002/gea.20142.
- Cloke, H. and F. Pappenberger (2009). ‘Ensemble flood forecasting: a review’. In: *Journal of Hydrology* 375.3, pp. 613–626.
- Clubb, F. J., S. M. Mudd, D. T. Milodowski, M. D. Hurst, and L. J. Slater (2014). ‘Objective extraction of channel heads from high-resolution topographic data’. In: *Water Resources Research* 50.5, pp. 4283–4304.
- Clubb, F., S. Mudd, D. Milodowski, D. Valters, L. Slater, M. Hurst, and A. Limaye (2017). ‘Geomorphometric delineation of floodplains and terraces from slope and channel relief thresholds’. In: *Earth Surface Dynamics*.
- Cohen, S., G. Willgoose, and G. Hancock (2008). ‘A methodology for calculating the spatial distribution of the area-slope equation and the hypsometric integral within a catchment’. In: *Journal of Geophysical Research: Earth Surface* 113.F3.
- Collins, D. B. G. and R. L. Bras (2004). ‘Modeling the effects of vegetation-erosion coupling on landscape evolution’. In: *Journal of Geophysical Research* 109.F3, pp. 1–11. ISSN: 0148-0227. DOI: 10.1029/2003JF000028.
- Cole, S. J. and R. J. Moore (2008). ‘Hydrological modelling using raingauge-and radar-based estimators of areal rainfall’. In: *Journal of Hydrology* 358.3, pp. 159–181.
- Colwell, R. (2013). ‘The chip design game at the end of Moore’s law’. In: *2013 IEEE Hot Chips 25 Symposium (HCS)*. IEEE, pp. 1–16.
- Costa, J. E. and J. E. O’Connor (1995). ‘Geomorphically Effective Floods’. In: *Natural and Anthropogenic Influences in Fluvial Geomorphology; Geophysical Monograph*

- Series; vol. 89.* Vol. 18. Natural and Anthropogenic Influences in Fluvial Geomorphology, pp. 45–56.
- Coulthard, T., M. Kirkby, and M. Macklin (2000). ‘Modelling geomorphic response to environmental change in an upland catchment’. In: *Hydrological Processes* 14.11-12, pp. 2031–2045.
- Coulthard, T., M. Macklin, and M. Kirkby (2002). ‘A cellular model of Holocene upland river basin and alluvial fan evolution’. In: *Earth Surface Processes and Landforms* 27.3, pp. 269–288.
- Coulthard, T. J. and M. J. V. D. Wiel (2006). ‘A cellular model of river meandering’. In: *Earth Surface Processes and Landforms* 31.1, pp. 123–132. ISSN: 0197-9337. DOI: 10.1002/esp.1315. URL: <http://doi.wiley.com/10.1002/esp.1315>.
- Coulthard, T. J., J. Ramirez, H. J. Fowler, and V. Glenis (2012a). ‘Using the UKCP09 probabilistic scenarios to model the amplified impact of climate change on drainage basin sediment yield’. In: *Hydrology and Earth System Sciences* 16.11, pp. 4401–4416. ISSN: 1607-7938. DOI: 10.5194/hess-16-4401-2012. URL: <http://www.hydrol-earth-syst-sci.net/16/4401/2012/>.
- Coulthard, T. J., G. R. Hancock, and J. B. C. Lowry (2012b). ‘Modelling soil erosion with a downscaled landscape evolution model’. In: *Earth Surface Processes and Landforms* 37.10, pp. 1046–1055. ISSN: 01979337. DOI: 10.1002/esp.3226. URL: <http://doi.wiley.com/10.1002/esp.3226>.
- Coulthard, T. J., J. C. Neal, P. D. Bates, J. Ramirez, G. A. M. de Almeida, and G. R. Hancock (2013). ‘Integrating the LISFLOOD-FP 2D hydrodynamic model with the CAESAR model: implications for modelling landscape evolution’. In: *Earth Surface Processes and Landforms* 38.15, pp. 1897–1906. ISSN: 01979337. DOI: 10.1002/esp.3478. URL: <http://doi.wiley.com/10.1002/esp.3478>.
- Coulthard, T. J. and C. J. Skinner (2016). ‘The sensitivity of landscape evolution models to spatial and temporal rainfall resolution’. In: *Earth Surface Dynamics* 4.3, p. 757.
- Coulthard, T., M. Kirkby, and M. Macklin (1996). ‘A cellular automaton landscape evolution model’. In: *Proceedings of the First International Conference on Geo-Computation*. Vol. 1, pp. 248–281.

- Coulthard, T. J., M. J. Kirkby, and M. G. Macklin (1998). ‘Non-linearity and spatial resolution in a cellular automaton model of a small upland basin’. In: *Hydrology and Earth System Sciences* 2.2/3, pp. 257–264.
- Coulthard, T. J. (2001). ‘Landscape Evolution Models: a software review’. In: *Hydrological Processes* 17.3.15, pp. 165–173.
- Coulthard, T. (2017). *CAESAR-Lisflood 1.9b*. DOI: 10.5281/zenodo.321820. URL: <https://doi.org/10.5281/zenodo.321820>.
- Coulthard, T. J. (1999). ‘Modelling upland catchment response to Holocene environmental change.’ Doctoral dissertation. University of Leeds.
- Crosta, G. and P. Frattini (2003). ‘Distributed modelling of shallow landslides triggered by intense rainfall’. In: *Natural Hazards and Earth System Science* 3.1/2, pp. 81–93.
- Croissant, T. and J. Braun (2014). ‘Constraining the stream power law: a novel approach combining a landscape evolution model and an inversion method’. In: *Earth Surface Dynamics* 2.1, pp. 155–166. ISSN: 2196-632X. DOI: 10.5194/esurf-2-155-2014. URL: <http://www.earth-surf-dynam.net/2/155/2014/>.
- Culling, W. E. H. (1960). ‘Analytical Theory of Erosion’. In: *The Journal of Geology* 68.3, pp. 336–344.
- Dagum, L. and R. Menon (1998). ‘OpenMP: an industry standard API for shared-memory programming’. In: *IEEE computational science and engineering* 5.1, pp. 46–55.
- Dana, J. D. (1882). ‘The flood of the Connecticut River valley from the melting of the Quaternary glacier’. In: *American Journal of Science* 135, pp. 179–202.
- Darby, S. E., J. Leyland, M. Kummu, T. a. Räsänen, and H. Lauri (2013). ‘Decoding the drivers of bank erosion on the Mekong river: The roles of the Asian monsoon, tropical storms, and snowmelt.’ In: *Water resources research* 49.4, pp. 2146–2163. ISSN: 0043-1397. DOI: 10.1002/wrcr.20205. URL: <http://www.ncbi.nlm.nih.gov/articlerender.fcgi?artid=3709126%7B%5C%7Dtool=pmcentrez%7B%5C%7Drendertype=abstract>.
- De Luis, M., J. González-Hidalgo, and L. Longares (2010). ‘Is rainfall erosivity increasing in the Mediterranean Iberian Peninsula?’ In: *Land Degradation & Development* 21.2, pp. 139–144.

- Dietrich, W. E., D. G. Bellugi, L. S. Sklar, J. D. Stock, A. M. Heimsath, and J. J. Roering (2003). ‘Geomorphic transport laws for predicting landscape form and dynamics’. In: *Prediction in geomorphology*, pp. 103–132.
- Dietze, M. (2014). ‘RCHILD-an R-package for flexible use of the landscape evolution model CHILD’. In: *EGU General Assembly Conference Abstracts*. Vol. 16, p. 2155.
- Dong, L. (2006). ‘Evaluation of high quality topographic data for geomorphological and flood impact studies in upland area: North York Moors, UK’. Master’s thesis. Durham University.
- Doswell, C. A., H. E. Brooks, and R. A. Maddox (1996). ‘Flash Flood Forecasting : An Ingredients-Based Methodology’. In: *Weather and Forecasting* 11.December 96, pp. 560–581.
- Doswell, C. A. (1993). ‘Flash flood-producing convective storms: current understanding and research’. In: *Proceedings, Spain-US Joint Workshop on Natural Hazards 8-11 June 1993, Barcelona, Spain*.
- Dunai, T. J. (2010). *Cosmogenic Nuclides: Principles, concepts and applications in the Earth surface sciences*. Cambridge University Press.
- Eagleson, P. S. (1978). ‘Climate, Soil, and Vegetation: Introduction to Water Balance Dynamics’. In: *Water Resources Research* 14.5, pp. 705–712.
- Ebel, B. A. and K. Loague (2006). ‘Physics-based hydrologic-response simulation: Seeing through the fog of equifinality’. In: *Hydrological Processes* 20.13, pp. 2887–2900.
- Ebert, E. E. (2007). ‘Methods for verifying satellite precipitation estimates’. In: *Measuring precipitation from space*. Springer, pp. 345–356.
- Egholm, D. L., M. F. Knudsen, C. D. Clark, and J. E. Lesemann (2011). ‘Modeling the flow of glaciers in steep terrains: The integrated second-order shallow ice approximation (iSOSIA)’. In: *Journal of Geophysical Research* 116.F2, F02012. ISSN: 0148-0227. DOI: 10.1029/2010JF001900. URL: <http://doi.wiley.com/10.1029/2010JF001900>.
- Egholm, D. L., V. K. Pedersen, M. F. Knudsen, and N. K. Larsen (2012). ‘Coupling the flow of ice, water, and sediment in a glacial landscape evolution model’. In: *Geomorphology* 141-142, pp. 47–66. ISSN: 0169555X. DOI: 10.1016/j.geomorph.2011.12.019. URL: <http://linkinghub.elsevier.com/retrieve/pii/S0169555X11006325>.

- Einfalt, T., K. Arnbjerg-Nielsen, C. Golz, N.-E. Jensen, M. Quirmbach, G. Vaes, and B. Vieux (2004). ‘Towards a roadmap for use of radar rainfall data in urban drainage’. In: *Journal of Hydrology* 299.3, pp. 186–202.
- Fabry, F. (2015). *Radar Meteorology: Principles and Practice*. Cambridge University Press.
- Fewtrell, T. J., J. C. Neal, P. D. Bates, and P. J. Harrison (2011). ‘Geometric and structural river channel complexity and the prediction of urban inundation’. In: *Hydrological Processes* 25.20, pp. 3173–3186.
- Fowler, H. and R. Wilby (2010). ‘Detecting changes in seasonal precipitation extremes using regional climate model projections: Implications for managing fluvial flood risk’. In: *Water Resources Research* 46.3.
- Gabellani, S., G. Boni, L. Ferraris, J. Von Hardenberg, and A. Provenzale (2007). ‘Propagation of uncertainty from rainfall to runoff: A case study with a stochastic rainfall generator’. In: *Advances in water resources* 30.10, pp. 2061–2071.
- Galiatsatos, N., D. Donoghue, and L. Warburton (2007). ‘Assessment of sediment delivery from shallow landslides in upland terrain using 3D remote sensing’. In: *RSPSoc2007: Challenges for earth observation-scientific, technical and commercial, Newcastle, UK*.
- Galland, J.-C., N. Goutal, and J.-M. Hervouet (1991). ‘TELEMAC: A new numerical model for solving shallow water equations’. In: *Advances in Water Resources* 14.3, pp. 138–148.
- Gallay, M. (2013). ‘Direct acquisition of data: airborne laser scanning’. In: *Geomorphological techniques* 2.1.4, pp. 1–17.
- Gasparini, N. M., G. E. Tucker, and R. L. Bras (2004). ‘Network-scale dynamics of grain-size sorting: Implications for downstream fining, stream-profile concavity, and drainage basin morphology’. In: *Earth Surface Processes and Landforms* 29.4, pp. 401–421. ISSN: 01979337. DOI: 10.1002/esp.1031.
- Germann, U., G. Galli, M. Bosacchi, and M. Bolliger (2006). ‘Radar precipitation measurement in a mountainous region’. In: *Quarterly Journal of the Royal Meteorological Society* 132.618, pp. 1669–1692.

- Gesch, D., M. Oimoen, S. Greenlee, C. Nelson, M. Steuck, and D. Tyler (2002). ‘The national elevation dataset’. In: *Photogrammetric engineering and remote sensing* 68.1, pp. 5–32.
- Gilbert, G. K. and C. E. Dutton (1877). *Report on the Geology of the Henry Mountains*. Tech. rep. Washington: US Geographical and Geological Survey of the Rocky Mountain Region.
- Golding, B., P. Clark, and B. May (2005). ‘The Boscastle flood: Meteorological analysis of the conditions leading to flooding on 16 August 2004’. In: *Weather* 60.8, pp. 230–235.
- Golding, B. (2000). ‘Quantitative precipitation forecasting in the UK’. In: *Journal of Hydrology* 239.1, pp. 286–305.
- Goldberg, D. (1991). ‘What every computer scientist should know about floating-point arithmetic’. In: *ACM Computing Surveys (CSUR)* 23.1, pp. 5–48.
- Gomez-Gesteira, M., B. D. Rogers, A. J. C. Crespo, R. A. Dalrymple, M. Narayanaswamy, and J. M. Domínguez (2012). ‘SPHysics—development of a free-surface fluid solver—Part 1: Theory and formulations’. In: *Computers & Geosciences* 48, pp. 289–299. ISSN: 0098-3004. DOI: 10.1016/j.cageo.2012.02.029. URL: <http://www.sciencedirect.com/science/article/pii/S0098300412000854>.
- Goren, L., S. D. Willett, F. Herman, and J. Braun (2014). ‘Coupled numerical-analytical approach to landscape evolution modeling’. In: *Earth Surface Processes and Landforms* 39.4, pp. 522–545. ISSN: 01979337. DOI: 10.1002/esp.3514. URL: <http://doi.wiley.com/10.1002/esp.3514>.
- Graham, S. L., P. B. Kessler, and M. K. McKusick (1982). ‘Gprof: A call graph execution profiler’. In: *ACM Sigplan Notices*. Vol. 17. 6. ACM, pp. 120–126.
- Gray, M. and C. Marshall (1998). ‘Mesoscale convective systems over the UK, 1981–97’. In: *Weather* 53.11, pp. 388–396.
- Gunn, R. and G. D. Kinzer (1949). ‘The terminal velocity of fall for water droplets in stagnant air’. In: *Journal of Meteorology* 6.4, pp. 243–248.
- Gupta, S., J. S. Collier, A. Palmer-Felgate, and G. Potter (2007). ‘Catastrophic flooding origin of shelf valley systems in the English Channel’. In: *Nature* 448.7151, pp. 342–345.

- Gustafson, J. L. (1988). 'Reevaluating Amdahl's law'. In: *Communications of the ACM* 31.5, pp. 532–533.
- Habib, E., W. F. Krajewski, and A. Kruger (2001). 'Sampling errors of tipping-bucket rain gauge measurements'. In: *Journal of Hydrologic Engineering* 6.2, pp. 159–166.
- Hackney, C., S. E. Darby, and J. Leyland (2013). 'Modelling the response of soft cliffs to climate change: A statistical, process-response model using accumulated excess energy'. In: *Geomorphology* 187, pp. 108–121. ISSN: 0169555X. DOI: 10.1016/j.geomorph.2013.01.005. URL: <http://linkinghub.elsevier.com/retrieve/pii/S0169555X13000214>.
- Haile, A. T. and T. Rientjes (2005). 'Effects of LiDAR DEM resolution in flood modelling: a model sensitivity study for the city of Tegucigalpa, Honduras'. In: *Workshop on Laser scanning 2005, Enschede, the Netherlands, September 12-14, 2005* 3.
- Hancock, G. and G. Willgoose (2001). 'Use of a landscape simulator in the validation of the SIBERIA catchment evolution model: Declining equilibrium landforms'. In: *Water resources research* 37.7, pp. 1981–1992.
- Hancock, G., G. Willgoose, and K. Evans (2002). 'Testing of the SIBERIA landscape evolution model using the Tin Camp Creek, Northern Territory, Australia, field catchment'. In: *Earth Surface Processes and Landforms* 27.2, pp. 125–143.
- Hancock, G. R. and G. R. Willgoose (2004). 'An experimental and computer simulation study of erosion on a mine tailings dam wall'. In: *Earth Surface Processes and Landforms* 29.4, pp. 457–475. ISSN: 01979337. DOI: 10.1002/esp.1045.
- Han, J., N. M. Gasparini, J. P. Johnson, and B. P. Murphy (2014). 'Modeling the influence of rainfall gradients on discharge, bedrock erodibility, and river profile evolution, with application to the Big Island, Hawai'i'. In: *Journal of Geophysical Research: Earth Surface* 119.6, pp. 1418–1440.
- Han, J., N. M. Gasparini, and J. P. Johnson (2015). 'Measuring the imprint of orographic rainfall gradients on the morphology of steady-state numerical fluvial landscapes'. In: *Earth Surface Processes and Landforms* 40.10, pp. 1334–1350.
- Hancock, G., T. Coulthard, and J. Lowry (2015). 'Predicting uncertainty in sediment transport and landscape evolution – the influence of initial surface conditions'. In: *Computers & Geosciences*, pp. 1–14. ISSN: 00983004. DOI: 10.1016/j.cageo.

- 2015.08.014. URL: <http://www.sciencedirect.com/science/article/pii/S0098300415300406>.
- Hancock, G., D. Verdon-Kidd, and J. Lowry (2017). ‘Sediment output from a post-mining catchment—Centennial impacts using stochastically generated rainfall’. In: *Journal of Hydrology* 544, pp. 180–194.
- Hancock, G. R. (2003). ‘Effect of catchment aspect ratio on geomorphological descriptors’. In: *Prediction in Geomorphology*, pp. 217–230.
- Hannaford, J. (2004). ‘Development of a strategic data management system for a national hydrological database, the UK national river flow archive’. In: *Proceeding of 6th International Conference on Hydroinformatics, Singapore*, pp. 21–24.
- Harrison, D., S. Driscoll, and M. Kitchen (2000). ‘Improving precipitation estimates from weather radar using quality control and correction techniques’. In: *Meteorological Applications* 7.2, pp. 135–144.
- Harrison, D. L., R. W. Scovell, and M. Kitchen (2009). ‘High-resolution precipitation estimates for hydrological uses’. In: *Proceedings of the Institution of Civil Engineers-Water Management*. Vol. 162. 2. Thomas Telford Ltd, pp. 125–135.
- Harrison, D. L., K. Norman, C. Pierce, and N. Gaussiat (2012). ‘Radar products for hydrological applications in the UK’. In: *Proceedings of the Institution of Civil Engineers-Water Management*. Vol. 165. 2. Thomas Telford Ltd, pp. 89–103.
- Hasbargen, L. E. and C. Paola (2003). ‘How Predictable is Local Erosion Rate in Eroding Landscapes?’ In: *Prediction in Geomorphology*, pp. 231–240. DOI: 10.1029/135GM16. URL: <http://dx.doi.org/10.1029/135GM16>.
- Hay, L., M. Clark, M. Pagowski, G. Leavesley, and W. Gutowski Jr (2006). ‘One-way coupling of an atmospheric and a hydrologic model in Colorado’. In: *Journal of Hydrometeorology* 7.4, pp. 569–589.
- Herman, F. and J. Braun (2008). ‘Evolution of the glacial landscape of the Southern Alps of New Zealand: Insights from a glacial erosion model’. In: *Journal of Geophysical Research* 113.F2, F02009. ISSN: 0148-0227. DOI: 10.1029/2007JF000807. URL: <http://doi.wiley.com/10.1029/2007JF000807>.
- Hergarten, S., J. Robl, and K. Stüwe (2014). ‘Extracting topographic swath profiles across curved geomorphic features’. In: *Earth Surface Dynamics* 2.1, p. 97.

- Hergarten, S., J. Robl, and K. Stüwe (2015). ‘Tectonic geomorphology at small catchment sizes – extensions of the stream-power approach and the χ method’. In: *Earth Surf. Dynam. Discuss.* pp. 689–714. DOI: 10.5194/esurfd-3-689-2015.
- Hill, M. D. and M. R. Marty (2008). ‘Amdahl’s Law in the Multicore Era’. In: *Computer* 41.7, pp. 33–38.
- Hobley, D. E., G. E. Tucker, J. M. Adams, N. M. Gasparini, E. Hutton, E. Istanbulluoglu, and S. Nudurupati (2013). ‘Modeling impact cratering as a geomorphic process using the novel landscape evolution model Landlab’. In: *AGU Fall Meeting Abstracts*. Vol. 1, p. 868.
- Hobley, D. E., J. M. Adams, S. S. Nudurupati, E. W. Hutton, N. M. Gasparini, E. Istanbulluoglu, and G. E. Tucker (2016). ‘Creative computing with Landlab: an open-source toolkit for building, coupling, and exploring two-dimensional numerical models of Earth-surface dynamics, Earth Surf’. In: *Earth Surface Dynam. Discuss.* 10.
- (2017). ‘Creative computing with Landlab: an open-source toolkit for building, coupling, and exploring two-dimensional numerical models of Earth-surface dynamics’. In: *Earth Surface Dynamics* 5.1, p. 21.
- Hoey, T. B., P. Bishop, and R. I. Ferguson (2003). ‘Testing numerical models in geomorphology: how can we ensure critical use of model predictions?’ In: *Prediction in Geomorphology*, pp. 241–256.
- Hong, S.-Y., M.-S. Koo, J. Jang, J.-E. Esther Kim, H. Park, M.-S. Joh, J.-H. Kang, and T.-J. Oh (2013). ‘An evaluation of the software system dependency of a global atmospheric model’. In: *Monthly Weather Review* 141.11, pp. 4165–4172.
- Hooke, R. L. (2003). ‘Predictive modeling in geomorphology: An oxymoron?’ In: *Prediction in geomorphology*, pp. 51–61.
- Hopkins, J. (2012). ‘Knowledge of, and response to, upland flash flooding: a case study of flood risk management of the 2005 flash flood in upper Ryedale, North Yorkshire, UK’. Doctoral dissertation. Durham University.
- Hou, A. Y., R. K. Kakar, S. Neeck, A. A. Azarbarzin, C. D. Kummerow, M. Kojima, R. Oki, K. Nakamura, and T. Iguchi (2014). ‘The global precipitation measurement mission’. In: *Bulletin of the American Meteorological Society* 95.5, pp. 701–722.

- Houze, R. A. (2012). 'Orographic Effects on Precipitating Clouds'. In: *Reviews of Geophysics* 50, pp. 1–47. DOI: 10.1029/2011RG000365.1. INTRODUCTION.
- Hovius, N., C. P. Stark, and P. A. Allen (1997). 'Sediment flux from a mountain belt derived by landslide mapping'. In: *Geology* 25.3, pp. 231–234. ISSN: 00917613. DOI: 10.1130/0091-7613(1997)025<0231:SFFAMB>2.3.CO;2.
- Howard, A. D. and G. Kerby (1983). 'Channel changes in badlands'. In: *Geological Society of America Bulletin* 94.6, pp. 739–752.
- Howard, A. D. (1994). 'A detachment-limited model of drainage basin evolution'. In: *Water resources research* 30.7, pp. 2261–2285.
- (1998). 'Long profile development of bedrock channels: Interaction of weathering, mass wasting, bed erosion, and sediment transport'. In: *Rivers over rock: Fluvial processes in bedrock channels*, pp. 297–319.
- HR Wallingford (2005). *Flooding in Boscastle and North Cornwall, August 2004. Phase 2 studies report*. HR Wallingford.
- Huang, X. and J. D. Niemann (2006). 'Modelling the potential impacts of groundwater hydrology on long-term drainage basin evolution'. In: *Earth Surface Processes and Landforms* 31, pp. 1802–1823. DOI: 10.1002/esp.
- Ivanov, V. Y., E. R. Vivoni, R. L. Bras, and D. Entekhabi (2004). 'Catchment hydrologic response with a fully distributed triangulated irregular network model'. In: *Water Resources Research* 40.11.
- Iverson, R. M. (2000). 'Landslide triggering by rain infiltration'. In: *Water resources research* 36.7, pp. 1897–1910.
- Jackson, D. W. T., M. C. Bourke, and T. A. G. Smyth (2015). 'The dune effect on sand-transporting winds on Mars'. In: *Nature Communications* 6, p. 8796. ISSN: 2041-1723. DOI: 10.1038/ncomms9796. URL: <http://www.nature.com/doifinder/10.1038/ncomms9796>.
- Jasak, H., A. Jemcov, and Z. Tukovic (2007). 'OpenFOAM : A C++ Library for Complex Physics Simulations'. In: *International Workshop on Coupled Methods in Numerical Dynamics* m, pp. 1–20.
- Johnson, R. M. and J. Warburton (2002a). 'Annual sediment budget of a UK mountain torrent'. In: *Geografiska Annaler: Series A, Physical Geography* 84.2, pp. 73–88.

- Johnson, R. M. and J. Warburton (2002b). 'Flooding and geomorphic impacts in a mountain torrent: Raise Beck, Central Lake District, England'. In: *Earth Surface Processes and Landforms* 27.9, pp. 945–969.
- Jones, M. R., S. Blenkinsop, H. J. Fowler, and C. G. Kilsby (2014). 'Objective classification of extreme rainfall regions for the UK and updated estimates of trends in regional extreme rainfall'. In: *International Journal of Climatology* 34.3, pp. 751–765.
- Joss, J. and A. Waldvogel (1969). 'Raindrop size distribution and sampling size errors'. In: *Journal of the Atmospheric Sciences* 26.3, pp. 566–569.
- Kendon, E. J., N. M. Roberts, H. J. Fowler, M. J. Roberts, S. C. Chan, and C. A. Senior (2014). 'Heavier summer downpours with climate change revealed by weather forecast resolution model'. In: *Nature Climate Change* June, pp. 1–7. DOI: 10.1038/NCLIMATE2258.
- Kleinhans, M. G., R. I. Ferguson, S. N. Lane, and R. J. Hardy (2013). 'Splitting rivers at their seams: bifurcations and avulsion'. In: *Earth Surface Processes and Landforms* 38.1, pp. 47–61.
- Klein, C., D. Heinzeller, J. Bliefernicht, and H. Kunstmann (2015). 'Variability of West African monsoon patterns generated by a WRF multi-physics ensemble'. In: *Climate Dynamics* 45.9–10, pp. 2733–2755.
- Knebl, M., Z.-L. Yang, K. Hutchison, and D. Maidment (2005). 'Regional scale flood modeling using NEXRAD rainfall, GIS, and HEC-HMS/RAS: a case study for the San Antonio River Basin Summer 2002 storm event'. In: *Journal of Environmental Management* 75.4, pp. 325–336.
- Kollet, S. J., R. M. Maxwell, C. S. Woodward, S. Smith, J. Vanderborght, H. Vereecken, and C. Simmer (2010). 'Proof of concept of regional scale hydrologic simulations at hydrologic resolution utilizing massively parallel computer resources'. In: *Water resources research* 46.4.
- Krajewski, W. F., V. Lakshmi, K. P. Georgakakos, and S. C. Jain (1991). 'A Monte Carlo study of rainfall sampling effect on a distributed catchment model'. In: *Water resources research* 27.1, pp. 119–128.
- Krishnan, S., C. Crosby, V. Nandigam, M. Phan, C. Cowart, C. Baru, and R. Arrowsmith (2011). 'OpenTopography: a services oriented architecture for community

- access to LIDAR topography'. In: *Proceedings of the 2nd International Conference on Computing for Geospatial Research & Applications*. ACM, p. 7.
- Lague, D. (2005). 'Discharge, discharge variability, and the bedrock channel profile'. In: *Journal of Geophysical Research* 110.F4, F04006. ISSN: 0148-0227. DOI: 10.1029/2004JF000259. URL: <http://doi.wiley.com/10.1029/2004JF000259>.
- (2013). 'The stream power river incision model: evidence, theory and beyond'. In: *Earth Surface Processes and Landforms*, n/a–n/a. ISSN: 01979337. DOI: 10.1002/esp.3462. URL: <http://doi.wiley.com/10.1002/esp.3462>.
- Lamb, M. P. and M. A. Fonstad (2010). 'Rapid formation of a modern bedrock canyon by a single flood event'. In: *Nature Geoscience* 3.7, pp. 477–481.
- Lancaster, S. T. and G. E. Grant (2003). 'You want me to predict what?' In: *Prediction in geomorphology*, pp. 41–50.
- Lancaster, S. T., S. K. Hayes, and G. E. Grant (2003). 'Effects of wood on debris flow runout in small mountain watersheds'. In: *Water Resources Research* 39.6. DOI: 10.1029/2001.
- Lane, S., V. Tayefi, S. Reid, D. Yu, and R. Hardy (2007). 'Interactions between sediment delivery, channel change, climate change and flood risk in a temperate upland environment'. In: *Earth Surface Processes and Landforms* 32.3, pp. 429–446.
- Lane, S., S. Reid, V. Tayefi, D. Yu, and R. Hardy (2008). 'Reconceptualising coarse sediment delivery problems in rivers as catchment-scale and diffuse'. In: *Geomorphology* 98.3, pp. 227–249.
- Lane, S. N. (2008). 'Climate change and the summer 2007 floods in the UK'. In: *Geography* 93.2, p. 91.
- Lemmens, M. (2011). 'Terrestrial laser scanning'. In: *Geo-information*. Springer, pp. 101–121.
- Liang, Q. and L. S. Smith (2015). 'A high-performance integrated hydrodynamic modelling system for urban flood simulations'. In: *Journal of Hydroinformatics* 17.4, pp. 518–533.
- Loague, K., C. S. Heppner, B. B. Mirus, B. A. Ebel, Q. Ran, A. E. Carr, S. H. BeVille, and J. E. VanderKwaak (2006). 'Physics-based hydrologic-response simulation: Foundation for hydroecology and hydrogeomorphology'. In: *Hydrological Processes* 20.5, pp. 1231–1237.

- Luk, S. (1979). 'Effect of soil properties on erosion by wash and splash'. In: *Earth Surface Processes* 4.3, pp. 241–255.
- Luyckx, G., P. Willems, and J. Berlamont (1998). 'Influence of the spatial variability of rainfall on sewer system design'. In: *Hydrology in a changing environment*. Vol. 3. John Wiley & sons, pp. 339–349.
- Manning, R., J. P. Griffith, T. F. Pigot, and L. F. Vernon-Harcourt (1890). *On the flow of water in open channels and pipes*.
- Mann, C. C. (2000). 'The end of Moores law'. In: *Technology Review* 103.3, pp. 42–48.
- Martin, Y. and M. Church (2004). 'Numerical modelling of landscape evolution: geomorphological perspectives'. In: *Progress in Physical Geography* 28.3, pp. 317–339.
- Marshall, J., R. Langille, and W. M. K. Palmer (1947). 'Measurement of rainfall by radar'. In: *Journal of Meteorology* 4.6, pp. 186–192.
- McCulloch, J. S. and M. Robinson (1993). 'History of forest hydrology'. In: *Journal of Hydrology* 150.2-4, pp. 189–216.
- Met Office (2003). *1 km Resolution UK Composite Rainfall Data from the Met Office Nimrod System*. <http://catalogue.ceda.ac.uk/>.
- Meyer-Peter, E. and R. Müller (1948). 'Formulas for bed-load transport'. In: IAHR.
- Meyer, L. (1981). 'How rain intensity affects interrill erosion'. In: *Trans. ASAE* 24.6, pp. 1472–1475.
- (1994). 'Rainfall simulators for soil erosion research'. In: *Soil erosion research methods* 3, pp. 83–103.
- Micheletti, N., J. H. Chandler, and S. N. Lane (2015). 'Structure from motion (SFM) photogrammetry'. In:
- Milan, D. J. (2012). 'Geomorphic impact and system recovery following an extreme flood in an upland stream: Thinhope Burn, northern England, UK'. In: *Geomorphology* 138.1, pp. 319–328.
- Molnar, P. and P. England (1990). 'Late Cenozoic uplift of mountain ranges and global climate change: chicken or egg?' In: *Nature* 346, pp. 29–34.
- Molnar, P. (2001). 'Climate change, flooding in arid environments, and erosion rates'. In: *Geology* 29.12, p. 1071. ISSN: 0091-7613. DOI: 10.1130/0091-7613(2001)029<1071:CCFIAE>2.0.CO;2.

- Monniaux, D. (2008). ‘The pitfalls of verifying floating-point computations’. In: *ACM Transactions on Programming Languages and Systems (TOPLAS)* 30.3, p. 12.
- Moore, G. E. (1998). ‘Cramming More Components onto Integrated Circuits’. In: *Proceedings of the IEEE* 86.1.
- Morgan, R., J. Quinton, R. Smith, G. Govers, J. Poesen, K. Auerswald, G. Chisci, D. Torri, and M. Styczen (1998). ‘The European Soil Erosion Model (EUROSEM): a dynamic approach for predicting sediment transport from fields and small catchments’. In: *Earth surface processes and landforms* 23.6, pp. 527–544.
- Morgan, R. (1978). ‘Field studies of rainsplash erosion’. In: *Earth Surface Processes* 3.3, pp. 295–299.
- Mudd, S. M., M. Attal, D. T. Milodowski, S. W. D. Grieve, and D. a. Valters (2014). ‘A statistical framework to quantify spatial variation in channel gradients using the integral method of channel profile analysis’. In: *Journal of Geophysical Research: Earth Surface* 119.2, pp. 138–152. ISSN: 21699003. DOI: 10.1002/2013JF002981. URL: <http://doi.wiley.com/10.1002/2013JF002981>.
- Mudd, S. M. (2017). ‘Detection of transience in eroding landscapes’. In: *Earth Surface Processes and Landforms* 42.1, pp. 24–41.
- Mulvaney, T. (1851). ‘On the use of self-registering rain and flood gauges in making observations of the relations of rainfall and flood discharges in a given catchment’. In: *Proceedings of the institution of Civil Engineers of Ireland* 4.2, pp. 18–33.
- Murray, A. S. and A. G. Wintle (2000). ‘Luminescence dating of quartz using an improved single-aliquot regenerative-dose protocol’. In: *Radiation Measurements* 32.1, pp. 57–73. ISSN: 13504487. DOI: 10.1016/S1350-4487(99)00253-X.
- Murray, A. B. and C. Paola (1997). ‘Properties of a cellular braided-stream model’. In: *Earth Surface Processes and Landforms* 22.11, pp. 1001–1025.
- National River Flow Archive (2016). <https://nrfa.ceh.ac.uk/>. Accessed: 2016-05-01.
- Neal, J., T. Fewtrell, and M. Trigg (2009). ‘Parallelisation of storage cell flood models using OpenMP’. In: *Environmental Modelling & Software* 24.7, pp. 872–877.
- Nearing, M. and P. Hairsine (2010). ‘The Future of Soil Erosion Modelling’. In: *Handbook of Erosion Modelling*, pp. 389–397. DOI: 10.1002/9781444328455.ch20.

- Neuhold, C., P. Stanzel, and H. Nachtnebel (2009). ‘Incorporating river morphological changes to flood risk assessment: uncertainties, methodology and application’. In: *Natural Hazards and Earth System Sciences* 9.3, pp. 789–799.
- Newson, M. (1979). ‘The results of ten years’ experimental study on Plynlimon, mid-Wales, and their importance for the water industry’. In: *Journal of Institution of Water Engineers and Scientists* 33.4, pp. 321–333.
- Newson, M. (1980). ‘The geomorphological effectiveness of floods—a contribution stimulated by two recent events in mid-wales’. In: *Earth Surface Processes* 5.1, pp. 1–16.
- Nicótina, L., E. Alessi Celegon, A. Rinaldo, and M. Marani (2008). ‘On the impact of rainfall patterns on the hydrologic response’. In: *Water Resources Research* 44.12.
- O’Callaghan, J. F. and D. M. Mark (1984). ‘The extraction of drainage networks from digital elevation data’. In: *Computer vision, graphics, and image processing* 28.3, pp. 323–344.
- Olivier, S. L., A. K. Porterfield, K. B. Wheeler, M. Spiegel, and J. F. Prins (2012). ‘OpenMP task scheduling strategies for multicore NUMA systems’. In: *International Journal of High Performance Computing Applications*, p. 1094342011434065.
- Oreskes, N., K. Shrader-Frechette, and K. Belitz (1994). ‘Verification, validation, and confirmation of numerical models in the earth sciences’. In: *Science* 263.5147, pp. 641–646.
- Owen, J. J., R. Amundson, W. E. Dietrich, K. Nishiizumi, B. Sutter, and G. Chong (2011). ‘The sensitivity of hillslope bedrock erosion to precipitation’. In: *Earth Surface Processes and Landforms* 36.1, pp. 117–135. ISSN: 01979337. DOI: 10.1002/esp.2083. URL: <http://doi.wiley.com/10.1002/esp.2083>.
- Park, S., J. Mitchell, and G. Bubenzer (1983). ‘Rainfall characteristics and their relation to splash erosion’. In: *Trans. ASAE* 26.3, pp. 795–804.
- Parker, G. (1976). ‘On the cause and characteristic scales of meandering and braiding in rivers’. In: *Journal of fluid mechanics* 76.03, pp. 457–480.
- Passalacqua, P., T. Do Trung, E. Foufoula-Georgiou, G. Sapiro, and W. E. Dietrich (2010). ‘A geometric framework for channel network extraction from lidar: Non-linear diffusion and geodesic paths’. In: *Journal of Geophysical Research: Earth Surface* 115.F1.

- Pasculli, A. and C. Audisio (2015). ‘Cellular Automata Modelling of Fluvial Evolution: Real and Parametric Numerical Results Comparison Along River Pellice (NW Italy)’. In: *Environmental Modeling & Assessment*, pp. 1–17.
- Pazzaglia, F. J. (2003). ‘Landscape evolution models’. In: *Development of Quaternary Science* 1, pp. 247–274. DOI: 10.1016/S1571-0866(03)01012-1.
- Pedersen, H. S. and B. Hasholt (1995). ‘Influence of wind speed on rainsplash erosion’. In: *Catena* 24.1, pp. 39–54.
- Pellarin, T., G. Delrieu, G.-M. Saulnier, H. Andrieu, B. Vignal, and J.-D. Creutin (2002). ‘Hydrologic visibility of weather radar systems operating in mountainous regions: Case study for the Ardeche catchment (France)’. In: *Journal of Hydrometeorology* 3.5, pp. 539–555.
- Peleg, N. and E. Morin (2014). ‘Stochastic convective rain-field simulation using a high-resolution synoptically conditioned weather generator (HiReS-WG)’. In: *Water Resources Research* 50.3, pp. 2124–2139.
- Pelletier, J. D., A. Brad Murray, J. L. Pierce, P. R. Bierman, D. D. Breshears, B. T. Crosby, M. Ellis, E. Foufoula-Georgiou, A. M. Heimsath, and C. Houser (2015). ‘Forecasting the response of Earth’s surface to future climatic and land use changes: A review of methods and research needs’. In: *Earth’s Future* 3.7, pp. 220–251.
- Pelletier, J. D. (2012). ‘Fluvial and slope-wash erosion of soil-mantled landscapes: detachment- or transport-limited?’ In: *Earth Surface Processes and Landforms* 37.1, pp. 37–51. ISSN: 01979337. DOI: 10.1002/esp.2187. URL: <http://doi.wiley.com/10.1002/esp.2187>.
- Perrault, P. (1674). ‘De l’origine des fontaines’. In: Carbonnel J.-P. (éd.), *Textes fondateurs de l’hydrologie, Asnières, CNFSH, Commission de terminologie*.
- Peura, M. and J. Koistinen (2007). ‘Using radar data quality in computing composites and nowcasting products’. In: *33rd Conference on Radar Meteorology*.
- Phillips, J. D. (2003). ‘Sources of nonlinearity and complexity in geomorphic systems’. In: *Progress in Physical Geography* 27.1, pp. 1–23.
- Pitt, M. (2008). ‘The Pitt Review: Lessons learned from the 2007 floods’. In: *Cabinet Office, London* 505.4.
- Plate, E. J. (2002). ‘Flood risk and flood management’. In: *Journal of Hydrology* 267.1, pp. 2–11.

- Rabus, B., M. Eineder, A. Roth, and R. Bamler (2003). ‘The shuttle radar topography mission—a new class of digital elevation models acquired by spaceborne radar’. In: *ISPRS journal of photogrammetry and remote sensing* 57.4, pp. 241–262.
- Raymo, M. E. and W. F. Ruddiman (1992). ‘Tectonic forcing of Cenozoic climate’. In: *Nature* 359, pp. 117–122.
- Rickenmann, D. and B. W. McArdell (2007). ‘Continuous measurement of sediment transport in the Erlenbach stream using piezoelectric bedload impact sensors’. In: *Earth Surface Processes and Landforms* 32.9, pp. 1362–1378.
- Rico-Ramirez, M. A. and I. D. Cluckie (2008). ‘Classification of ground clutter and anomalous propagation using dual-polarization weather radar’. In: *IEEE Transactions on Geoscience and Remote Sensing* 46.7, pp. 1892–1904.
- Rinaldo, A., W. E. Dietrich, R. Rigon, G. K. Vogel, and I. Rodriguez-Iturbe (1995). ‘Geomorphological signatures of varying climate’. In: *Nature* 374.6523, p. 632.
- Roe, G. H., D. R. Montgomery, and B. Hallet (2002). ‘Effects of orographic precipitation variations on the concavity of steady-state river profiles’. In: *Geology* 30, pp. 143–146. DOI: 10.1130/0091-7613(2002)030<0143.
- Roe, G. H. (2003). ‘Orographic precipitation and the relief of mountain ranges’. In: *Journal of Geophysical Research* 108.B6, p. 2315. ISSN: 0148-0227. DOI: 10.1029/2001JB001521. URL: <http://doi.wiley.com/10.1029/2001JB001521>.
- (2005). ‘Orographic Precipitation’. In: *Annual Review of Earth and Planetary Sciences* 33.1, pp. 645–671. ISSN: 0084-6597. DOI: 10.1146/annurev.earth.33.092203.122541. URL: <http://www.annualreviews.org/doi/abs/10.1146/annurev.earth.33.092203.122541>.
- Rosser, N. J., D. N. Petley, M. Lim, S. A. Dunning, and R. J. Allison (2005). ‘Terrestrial laser scanning for monitoring the process of hard rock coastal cliff erosion’. In: *Quarterly Journal of Engineering Geology and Hydrogeology* 38.4, pp. 363–375.
- Sakellariou, R. (1996). ‘On the quest for perfect load balance in loop-based parallel computations’. Doctoral dissertation. University of Manchester.
- Schoorl, J., M. Sonneveld, and A. Veldkamp (2000). ‘Three-dimensional landscape process modelling: the effect of DEM resolution’. In: *Earth Surface Processes and Landforms* 25.9, pp. 1025–1034.

- Schoorl, J. M. and A. Veldkamp (2001). ‘Linking land use and landscape process modelling: A case study for the Álora region (South Spain)’. In: *Agriculture, Ecosystems and Environment* 85.1-3, pp. 281–292. ISSN: 01678809. DOI: 10.1016/S0167-8809(01)00194-3.
- Schaake, J. C., T. M. Hamill, R. Buizza, and M. Clark (2007). ‘HEPEX: the hydrological ensemble prediction experiment’. In: *Bulletin of the American Meteorological Society* 88.10, pp. 1541–1547.
- Schäuble, H., O. Marinoni, and M. Hinderer (2008). ‘A GIS-based method to calculate flow accumulation by considering dams and their specific operation time’. In: 34, pp. 635–646. DOI: 10.1016/j.cageo.2007.05.023.
- Schoorl, J. M., A. J. A. M. Temme, and T. Veldkamp (2014). ‘Modelling centennial sediment waves in an eroding landscape - catchment complexity’. In: *Earth Surface Processes and Landforms* 39.11, pp. 1526–1537. ISSN: 10969837. DOI: 10.1002/esp.3605.
- Schumm, S. A. (1979). ‘Geomorphic thresholds: the concept and its applications’. In: *Transactions of the Institute of British Geographers*, pp. 485–515.
- Schaller, R. R. (1997). ‘Moore’s law: past, present and future’. In: *IEEE spectrum* 34.6, pp. 52–59.
- Sear, D. A., M. D. Newson, and C. R. Thorne (2010). *Guidebook of applied fluvial geomorphology*. Thomas Telford Ltd.
- Segond, M.-L., N. Neokleous, C. Makropoulos, C. Onof, and C. Maksimovic (2007). ‘Simulation and spatio-temporal disaggregation of multi-site rainfall data for urban drainage applications’. In: *Hydrological Sciences Journal* 52.5, pp. 917–935.
- Seidl, M. and W. Dietrich (1992). ‘The problem of channel erosion into bedrock’. In: *Functional geomorphology* 23, pp. 101–124.
- Shaw, E. M., K. Beven, N. A. Chappell, and R. Lamb (2010). *Hydrology in practice*. CRC Press.
- Shah, S., P. O’connell, and J. Hosking (1996a). ‘Modelling the effects of spatial variability in rainfall on catchment response. 1. Formulation and calibration of a stochastic rainfall field model’. In: *Journal of Hydrology* 175.1-4, pp. 67–88.

- Shah, S., P. O'connell, and J. Hosking (1996b). 'Modelling the effects of spatial variability in rainfall on catchment response. 2. Experiments with distributed and lumped models'. In: *Journal of Hydrology* 175.1-4, pp. 89–111.
- Sibley, A. M. (2009). 'Analysis of the North York Moors storms—19 June 2005'. In: *Weather* 64.2, pp. 39–42.
- Sidle, R. C. and Y. Onda (2004). 'Hydrogeomorphology: overview of an emerging science'. In: *Hydrological Processes* 18.4, pp. 597–602.
- Simpson, J., R. F. Adler, and G. R. North (1988). 'A proposed tropical rainfall measuring mission (TRMM) satellite'. In: *Bulletin of the American meteorological Society* 69.3, pp. 278–295.
- Sivillo, J. K., J. E. Ahlquist, and Z. Toth (1997). 'An ensemble forecasting primer'. In: *Weather and Forecasting* 12.4, pp. 809–818.
- Sivapalan, M. (2003). 'Prediction in ungauged basins: a grand challenge for theoretical hydrology'. In: *Hydrological Processes* 17.15, pp. 3163–3170.
- Skinner, C., T. J. Coulthard, and D. Parsons (2015). 'Simulating tidal and storm surge hydraulics with a simple 2D inertia based model, in the Humber Estuary, U.K.' In: *Estuaries, Coasts and Shelf Science* 155, pp. 126–136. ISSN: 0272-7714. DOI: \url{http://dx.doi.org/10.1016/j.ecss.2015.01.019}. URL: <http://dx.doi.org/10.1016/j.ecss.2015.01.019>.
- Skinner, C., T. Coulthard, W. Schwanghart, and M. Van De Wiel (2017). 'The Landscape Evolution Model Sensitivity Investigation'. In: *EGU General Assembly Conference Abstracts*. Vol. 19.
- Sklar, L. S. and W. E. Dietrich (2001). 'Sediment and rock strength controls on river incision into bedrock'. In: *Geology* 29.12, pp. 1087–1090.
- (2006). 'The role of sediment in controlling steady-state bedrock channel slope: Implications of the saltation–abrasion incision model'. In: *Geomorphology* 82.1, pp. 58–83.
- Slater, L. J. (2016). 'To what extent have changes in channel capacity contributed to flood hazard trends in England and Wales?' In: *Earth Surface Processes and Landforms* 41.8, pp. 1115–1128.
- Smith, R. B. and I. Barstad (2004). 'A linear theory of orographic precipitation'. In: *Journal of the Atmospheric Sciences* 61.12, pp. 1377–1391.

- Smith, J. A., M. L. Baeck, K. L. Meierdiercks, P. A. Nelson, A. J. Miller, and E. J. Holland (2005). ‘Field studies of the storm event hydrologic response in an urbanizing watershed’. In: *Water Resources Research* 41.10.
- Smith, L. S. and Q. Liang (2013). ‘Towards a generalised GPU/CPU shallow-flow modelling tool’. In: *Computers & Fluids* 88, pp. 334–343.
- Smith, L. S., Q. Liang, and P. F. Quinn (2015). ‘Towards a hydrodynamic modelling framework appropriate for applications in urban flood assessment and mitigation using heterogeneous computing’. In: *Urban Water Journal* 12.1, pp. 67–78.
- Snyder, N. P., G. E. Tucker, and D. J. Merritts (2003a). ‘Importance of a stochastic distribution of floods and erosion thresholds in the bedrock river incision problem’. In: *Journal of Geophysical Research* 108.B2, p. 2117. ISSN: 0148-0227. DOI: 10.1029/2001JB001655. URL: <http://doi.wiley.com/10.1029/2001JB001655>.
- Snyder, N. P., K. X. Whipple, G. E. Tucker, and D. J. Merritts (2003b). ‘Importance of a stochastic distribution of floods and erosion thresholds in the bedrock river incision problem’. In: *Journal of Geophysical Research: Solid Earth* 108.B2.
- Sólyom, P. B. and G. E. Tucker (2004). ‘Effect of limited storm duration on landscape evolution, drainage basin geometry, and hydrograph shapes’. In: *Journal of Geophysical Research* 109.F3, F03012. ISSN: 0148-0227. DOI: 10.1029/2003JF000032. URL: <http://doi.wiley.com/10.1029/2003JF000032>.
- Sólyom, P. B. and G. E. Tucker (2007). ‘The importance of the catchment area-length relationship in governing non-steady state hydrology, optimal junction angles and drainage network pattern’. In: *Geomorphology* 88.1, pp. 84–108.
- Stover, S. and D. Montgomery (2001). ‘Channel change and flooding, Skokomish River, Washington’. In: *Journal of Hydrology* 243.3, pp. 272–286.
- Stock, J. D. and W. E. Dietrich (2003). ‘Valley Incision by Debris Flows: Evidence of a Topographic Signature’. In: *Water Resour. Res.* 39.4, pp. 1089–1113. ISSN: 0043-1397. DOI: 10.1029/2001WR001057.
- Stock, J. D. and D. R. Montgomery (1999). ‘Geologic constraints on bedrock river incision using the stream power law’. In: *Journal of Geophysical Research. B* 104, pp. 4983–4993.

- Stokes, S. (1999). ‘Luminescence dating applications in geomorphological research’. In: *Geomorphology* 29.1-2, pp. 153–171. ISSN: 0169555X. DOI: 10.1016/S0169-555X(99)00012-4.
- Strangeways, I. (2010). ‘A history of rain gauges’. In: *Weather* 65.5, pp. 133–138.
- Strahler, A. N. (1957). ‘Quantitative analysis of watershed geomorphology’. In: *Eos, Transactions American Geophysical Union* 38.6, pp. 913–920.
- Sun, X.-H. and Y. Chen (2010). ‘Reevaluating Amdahl’s law in the multicore era’. In: *Journal of Parallel and Distributed Computing* 70.2, pp. 183–188.
- Sweeney, K. E., J. J. Roering, and C. Ellis (2015). ‘Experimental evidence for hillslope control of landscape scale’. In: 349.6243, pp. 51–53.
- Tarolli, P., J. R. Arrowsmith, and E. R. Vivoni (2009). ‘Understanding earth surface processes from remotely sensed digital terrain models’. In: *Geomorphology* 113.1, pp. 1–3.
- Tarboton, D. G., R. L. Bras, and I. Rodriguez-Iturbe (1991). ‘On the extraction of channel networks from digital elevation data’. In: *Hydrological processes* 5.1, pp. 81–100.
- Tarboton, D. G. (1997). ‘A new method for the determination of flow directions and upslope areas in grid digital elevation models’. In: *Water Resources Research* 33.2, p. 309. ISSN: 0043-1397. DOI: 10.1029/96WR03137.
- Temme, A. J. A. M. and A. Veldkamp (2009). ‘Multi-process Late Quaternary landscape evolution modelling reveals lags in climate response over small spatial scales’. In: *Earth Surface Processes and Landforms* 34.January, pp. 573–889. URL: <http://www3.interscience.wiley.com/journal/121517813/abstract>.
- Temme, A. J. A. M., L. Claessens, A. Veldkamp, and J. M. Schoorl (2011). ‘Evaluating choices in multi-process landscape evolution models’. In: *Geomorphology* 125.2, pp. 271–281. ISSN: 0169555X. DOI: 10.1016/j.geomorph.2010.10.007. URL: <http://dx.doi.org/10.1016/j.geomorph.2010.10.007>.
- Temme, A., J. Schoorl, L. Claessens, A. Veldkamp, and F. Shroder (2013). ‘Quantitative modeling of landscape evolution, treatise on geomorphology’. In: *Quantitative Modeling of Geomorphology*. 2.13. Academic Press, pp. 180–200.

- Thorndahl, S., J. A. Smith, M. L. Baeck, and W. F. Krajewski (2014). ‘Analyses of the temporal and spatial structures of heavy rainfall from a catalog of high-resolution radar rainfall fields’. In: *Atmospheric Research* 144, pp. 111–125.
- Tomkin, J. H. (2007). ‘Coupling glacial erosion and tectonics at active orogens: A numerical modeling study’. In: *Journal of Geophysical Research: Earth Surface* 112.2, pp. 1–14. ISSN: 21699011. DOI: 10.1029/2005JF000332.
- Trucano, T. and L. Swiler (2006). ‘Calibration, Validation, and Sensitivity Analysis: What’s What’. In: *Reliability Engineering and System Safety* 91.10, pp. 1331–1357.
- Tucker, G. E. and R. L. Bras (2000). ‘A stochastic approach to modeling the role of rainfall variability in drainage basin evolution’. In: *Water Resources Research* 36.7, pp. 1953–1964.
- Tucker, G. E., S. T. Lancaster, N. M. Gasparini, R. L. Bras, and S. M. Rybarczyk (2001a). ‘An object-oriented framework for distributed hydrologic and geomorphic modeling using triangulated irregular networks’. In: *Computers & Geosciences* 27.8, pp. 959–973. ISSN: 00983004. DOI: 10.1016/S0098-3004(00)00134-5. URL: <http://linkinghub.elsevier.com/retrieve/pii/S0098300400001345>.
- Tucker, G., S. Lancaster, N. Gasparini, and R. Bras (2001b). ‘The channel-hillslope integrated landscape development model (CHILD)’. In: *Landscape erosion and evolution modeling*. Springer, pp. 349–388.
- Tucker, G. E. and G. R. Hancock (2010). ‘Modelling Landscape Evolution’. In: *Earth Surface Processes and Landforms* 50, pp. 28–50. DOI: 10.1002/esp.
- Tucker, G. E., D. E. J. Hobley, E. Hutton, N. M. Gasparini, E. Istanbulluoglu, J. M. Adams, and S. S. Nudurupati (2015). ‘CellLab-CTS 2015: a Python library for continuous-time stochastic cellular automaton modeling using Landlab’. In: *Geoscientific Model Development Discussions* 8.11, pp. 9507–9552. ISSN: 1991-962X. DOI: 10.5194/gmdd-8-9507-2015. URL: <http://www.geosci-model-dev-discuss.net/8/9507/2015/>.
- Tucker, G. E. and R. Slingerland (1997). ‘Drainage basin responses to climate change’. In: *Water Resources Research* 33.8, pp. 2031–2047.
- Tucker, G. E. (2004). ‘Drainage basin sensitivity to tectonic and climatic forcing: Implications of a stochastic model for the role of entrainment and erosion thresholds’. In: *Earth Surface Processes and Landforms* 29.2, pp. 185–205.

- Turowski, J. M., D. Rickenmann, and S. J. Dadson (2010). ‘The partitioning of the total sediment load of a river into suspended load and bedload: a review of empirical data’. In: *Sedimentology* 57.4, pp. 1126–1146.
- Turowski, J. M., A. Badoux, J. Leuzinger, and R. Hegglin (2013). ‘Large floods, alluvial overprint, and bedrock erosion’. In: *Earth Surface Processes and Landforms* 38.9, pp. 947–958.
- Tye, A. M., M. D. Hurst, and A. Barkwith (2013). ‘Nene phosphate in sediment investigation’. In: *Environment Agency Project, Ref. 30258*.
- Vaaja, M., J. Hyppä, A. Kukko, H. Kaartinen, H. Hyppä, and P. Alho (2011). ‘Mapping topography changes and elevation accuracies using a mobile laser scanner’. In: *Remote Sensing* 3.3, pp. 587–600.
- Valters, D. A. (2016). ‘Modelling Geomorphic Systems: Landscape Evolution’. In: *Geomorphological Techniques*. Vol. 6. British Society for Geomorphology, pp. 5–12.
- Van De Wiel, M. J., T. J. Coulthard, M. G. Macklin, and J. Lewin (2007). ‘Embedding reach-scale fluvial dynamics within the CAESAR cellular automaton landscape evolution model’. In: *Geomorphology* 90.3, pp. 283–301.
- (2011). ‘Modelling the response of river systems to environmental change: progress, problems and prospects for palaeo-environmental reconstructions’. In: *Earth-Science Reviews* 104.1, pp. 167–185.
- van Gorp, W., A. Temme, and J. Schoorl (2015). ‘LAPSUS: soil erosion-landscape evolution model’. In: *EGU General Assembly Conference Abstracts*. Vol. 17, p. 15915.
- Vivoni, E. R., G. Mascaro, S. Mniszewski, P. Fasel, E. P. Springer, V. Y. Ivanov, and R. L. Bras (2011). ‘Real-world hydrologic assessment of a fully-distributed hydrological model in a parallel computing environment’. In: *Journal of Hydrology* 409.1, pp. 483–496.
- Von Hardenberg, J., L. Ferraris, and A. Provenzale (2003). ‘The shape of convective rain cells’. In: *Geophysical research letters* 30.24.
- von Ruette, J., P. Lehmann, and D. Or (2013). ‘Rainfall-triggered shallow landslides at catchment scale: Threshold mechanics-based modeling for abruptness and localization’. In: *Water Resources Research* 49.10, pp. 6266–6285.

- von Ruette, J., P. Lehmann, and D. Or (2014). ‘Effects of rainfall spatial variability and intermittency on shallow landslide triggering patterns at a catchment scale’. In: *Water Resources Research* 50.10, pp. 7780–7799.
- Warburton, J., J. Holden, and A. J. Mills (2004). ‘Hydrological controls of surficial mass movements in peat’. In: *Earth-Science Reviews* 67.1, pp. 139–156.
- Warren, R. A., D. J. Kirshbaum, R. S. Plant, and H. W. Lean (2014). ‘A ‘Boscastle-type’ quasi-stationary convective system over the UK Southwest Peninsula’. In: *Quarterly Journal of the Royal Meteorological Society* 140.678, pp. 240–257.
- Wass, P., D. Faulkner, and A. Curini (2008). ‘An investigation into the North Yorkshire floods of June 2005’. In: *JBA Consulting, Skipton*.
- Weisman, M. L. and J. B. Klemp (1986). ‘Characteristics of isolated convective storms’. In: *Mesoscale meteorology and forecasting*. Springer, pp. 331–358.
- Welsh, K., J. Dearing, R. Chiverrell, and T. Coulthard (2009). ‘Testing a cellular modelling approach to simulating late-Holocene sediment and water transfer from catchment to lake in the French Alps since 1826’. In: *The Holocene* 19.5, pp. 785–798.
- Whipple, K. X. and B. J. Meade (2006). ‘Orogen response to changes in climatic and tectonic forcing’. In: *Earth and Planetary Science Letters* 243.1, pp. 218–228.
- Whipple, K. X. and G. E. Tucker (1999). ‘Dynamics of the stream-power river incision model: Implications for height limits of mountain ranges, landscape response timescales, and research needs’. In: *Journal of Geophysical Research: Solid Earth* 104.B8, pp. 17661–17674.
- Wilcock, P. R. and J. C. Crowe (2003). ‘Surface-based transport model for mixed-size sediment’. In: *Journal of Hydraulic Engineering* 129.2, pp. 120–128.
- Wilby, R. L., K. Beven, and N. Reynard (2008). ‘Climate change and fluvial flood risk in the UK: more of the same?’ In: *Hydrological processes* 22.14, pp. 2511–2523.
- Wilson, J., G. Aggett, Y. Deng, and C. Lam (2008). ‘Water in the Landscape: A Review of Contemporary Flow Routing Algorithms’. In: December 2015, p. 461. DOI: 10.1007/978-3-540-77800-4.
- Willgoose, G. and G. Hancock (2011). ‘18 Applications of Long-Term Erosion and Landscape Evolution Models’. In: *Handbook of Erosion Modelling*, p. 339.

- Wilson, G., D. Aruliah, C. T. Brown, N. P. C. Hong, M. Davis, R. T. Guy, S. H. Haddock, K. D. Huff, I. M. Mitchell, and M. D. Plumbley (2014). ‘Best practices for scientific computing’. In: *PLoS Biol* 12.1, e1001745.
- Wilson, C. B., J. B. Valdes, and I. Rodriguez-Iturbe (1979). ‘On the influence of the spatial distribution of rainfall on storm runoff’. In: *Water Resources Research* 15.2, pp. 321–328.
- Wilson, J. W. and E. A. Brandes (1979). ‘Radar measurement of rainfall—A summary’. In: *Bulletin of the American Meteorological Society* 60.9, pp. 1048–1058.
- Willgoose, G., R. L. Bras, and I. R.-. Turbe (1991). ‘A Coupled Channel Network Growth and Hillslope Evolution Model 1.’ In: *Water Resources Research* 27.7, pp. 1671–1684.
- Willebeek-LeMair, M. H. and A. P. Reeves (1993). ‘Strategies for dynamic load balancing on highly parallel computers’. In: *IEEE Transactions on parallel and distributed systems* 4.9, pp. 979–993.
- Willgoose, G., R. L. Bras, and I. Rodriguez-Iturbe (1994). ‘Hydrogeomorphology modelling with a physically based river basin evolution model’. In: *Process models and theoretical geomorphology*, pp. 271–294.
- Willems, P. (2001). ‘A spatial rainfall generator for small spatial scales’. In: *Journal of Hydrology* 252.1, pp. 126–144.
- Willgoose, G. (2005). ‘Mathematical Modeling of Whole Landscape Evolution’. In: *Annual Review of Earth and Planetary Sciences* 33.1, pp. 443–459. ISSN: 0084-6597. DOI: 10.1146/annurev.earth.33.092203.122610. URL: <http://www.annualreviews.org/doi/abs/10.1146/annurev.earth.33.092203.122610>.
- Willett, S. D. (1999). ‘Orogeny and orography: The effects of erosion on the structure of mountain belts’. In: *Journal of Geophysical Research* 104.B12, pp. 28957–28981.
- Wobus, C., K. X. Whipple, E. Kirby, N. Snyder, J. Johnson, K. Spyropolou, B. Crosby, and D. Sheehan (2006). ‘Tectonics from topography: Procedures, promise, and pitfalls’. In: *Geological Society of America Special Papers* 398, pp. 55–74.
- Wobus, C. W., G. E. Tucker, and R. S. Anderson (2010). ‘Does climate change create distinctive patterns of landscape incision?’ In: *Journal of Geophysical Research* 115.F4, F04008. ISSN: 0148-0227. DOI: 10.1029/2009JF001562. URL: <http://doi.wiley.com/10.1029/2009JF001562>.

- Wolman, M. G. and J. P. Miller (1960). ‘Magnitude and Frequency of Forces in Geomorphic Processes’. In: *The Journal of Geology* 68.1, pp. 54–74.
- Wong, J. S., J. E. Freer, P. D. Bates, D. A. Sear, and E. M. Stephens (2015). ‘Sensitivity of a hydraulic model to channel erosion uncertainty during extreme flooding’. In: *Hydrological Processes* 29.2, pp. 261–279.
- Wong, W. E., J. R. Horgan, S. London, and H. Agrawal (1997). ‘A study of effective regression testing in practice’. In: *Software Reliability Engineering, 1997. Proceedings., The Eighth International Symposium on*. IEEE, pp. 264–274.
- Yang, R., S. D. Willett, and L. Goren (2015). ‘In situ low-relief landscape formation as a result of river network disruption.’ In: *Nature* 520.7548, pp. 526–9. ISSN: 1476-4687. DOI: 10.1038/nature14354. URL: <http://www.ncbi.nlm.nih.gov/pubmed/25903633>.
- Younger, P. M., A. Gadian, C.-G. Wang, J. Freer, and K. Beven (2008). ‘The usability of 250 m resolution data from the UK Meteorological Office Unified Model as input data for a hydrological model’. In: *Meteorological Applications* 15.2, pp. 207–217.
- Zhang, J. X., K.-T. Chang, and J. Q. Wu (2008). ‘Effects of DEM resolution and source on soil erosion modelling: a case study using the WEPP model’. In: *International Journal of Geographical Information Science* 22.8, pp. 925–942.

Appendix A

Software availability

A.1 Radar data processing code

The software for the radar data extraction and re-gridding for use in the HAIL-CAESAR/CAESAR-Lisflood models is available at the online software repository GitHub at: <https://github.com/dvalters/nimrod-toolbox/releases/tag/0.2>

A.2 HAIL-CAESAR landscape evolution model code

The HAIL-CAESAR landscape evolution modelling software is available at the online software repository GitHub at: <https://github.com/dvalters/HAIL-CAESAR/releases/tag/v0.9>

A.3 Figure plotting software

The code used to plot figures from the model simulation output in this thesis was part of the *LSDMappingTools* package and can be found here: <https://github.com/LSDtopotools/LSDMappingTools>. The author contributed to a significant part of the LSDMappingTools software development during the course of the PhD.

Appendix B

Paper reprint

Modelling Geomorphic Systems: Landscape Evolution

The content of Chapter 2 was adapted for an article in the British Society for Geomorphology's *Geomorphological Techniques* article series. A reprint is included in this appendix.

5.6.12 Modelling Geomorphic Systems: Landscape Evolution

Declan A. Valters¹

¹School of Earth, Atmospheric and Environmental Sciences, University of Manchester
(declan.valters@manchester.ac.uk)



Landscape evolution models (LEMs) present the geomorphologist with a means of investigating how landscapes evolve in response to external forcings, such as climate and tectonics, as well as internal process laws. LEMs typically incorporate a range of different geomorphic transport laws integrated in a way that simulates the evolution of a 3D terrain surface forward through time. The strengths of LEMs as research tools lie in their ability to rapidly test many different hypotheses of landscape evolution, to investigate the importance of particular processes by isolating them within a model, and to make quantitative predictions of geomorphic change within landscapes. LEMs can be applied to situations lasting from days to millions of years in real time, but reduce this to minutes or hours in model run-time. This chapter presents a brief introduction to the underlying principles of landscape evolution modelling, followed by an overview of the features of currently available, commonly-used models, and example applications from recent literature. Suggestions for dealing with common pitfalls in landscape evolution modelling, calibration, and confirming model predictions are also discussed.

KEYWORDS: numerical modelling, landscape evolution, fluvial, hillslope

Introduction

Landscape evolution models (LEMs) are quantitative tools used to simulate Earth surface processes and the evolution of the land surface. LEMs can be used to deduce whether hypotheses about landscape evolution are likely to be valid, by making quantitative predictions about their development. The earliest LEMs were conceptual and largely qualitative, such as the early pictorial landscape evolution diagrams by Gilbert (1880), Figure 1a. Gilbert's model contains many of the key components in a modern LEM. The background schematic depicts the effect of an uplift field alone on the landscape, and the foreground depicts the combined effects of uplift and erosion. Gilbert also recognised the important concept of boundary conditions in LEMs, stating that the base of the diagram represents a fixed sea-level in this case. These early models offered insight into the potential course of landscape evolution, and sowed the seeds

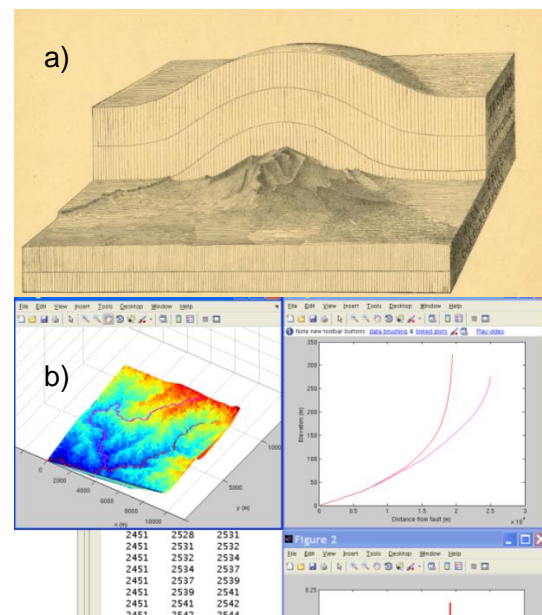


Figure 1. The evolution of LEMs. (a) The diagrammatic LEM of Gilbert (1880) compared to (b) a computer numerical model (CHILD, Tucker et al. 2001).

for the later development of LEMs that abound today. In Figure 1b, a computer-based LEM (CHILD, Tucker et al. 2001) is shown, with the components of boundary conditions, uplift, and other process representations that are still core concepts in modern LEMs. The advent of computerised, numerical LEMs, such as those in Figure 1b, along with high-resolution digital topographic data provide important quantitative tools for investigating landscape process and form.

Scope

This chapter provides a practical guide to the usage of numerical LEMs. Readers interested in more theoretical aspects of landscape evolution modelling should refer to other detailed literature reviews, such as those by Pazzaglia (2003), Martin and Church (2004), Willgoose (2005), Tucker and Hancock (2010), and Pelletier (2013). Other reviews focus on the use and application of LEMs, such as Van De Wiel et al. (2011); Willgoose and Hancock (2011); Temme et al. (2013). This chapter is not solely a software-type review of different LEMs (e.g. Coulthard, 2001), though comparisons between the features of various LEMs will be made to aid the prospective landscape evolution modeller. In short, the chapter aims to provide an overview of the usage, theoretical background, example applications, and software features of mainstream LEMs at the present time.

The application of physical analogue models is not discussed here, but readers can refer to Chapter 5.3 of this book: Green (2014). Numerical LEMs have not replaced their analogue counterparts – nor are they intended to. Physical models are actively used in landscape evolution studies (e.g. Hancock and Willgoose, 2002; Bonnet and Crave, 2006; Bonnet, 2009; Sweeney et al., 2015), but such experiments are usually custom-designed to meet the particular needs of a specific research question, and the materials available to construct the analogue model. In numerical landscape evolution modelling, there is more of a collective move (perhaps subconsciously) towards using a small number of community-developed numerical models, which are freely available to the modelling community.

The LEMs discussed in this chapter (see Appendix A) are primarily designed to simulate

processes in humid–temperate sub-aerial environments. The role of glacial or aeolian processes are undoubtedly important in landscape evolution, but are frequently overlooked by the current range of available models. Glacial system modelling is covered in greater detail in Chapter 5.6.5 of this book (Rowan, 2011), and features discussion on LEMs that simulate glacial erosion processes (e.g. Braun et al., 1999; Egholm et al., 2011, 2012; Herman and Braun, 2008; Tomkin, 2007). Coastal, glacial, and aeolian processes are currently better catered for in environment-specific models (see the other sub-chapters in Part 5.6 of the book, *Environment Specific Models*, e.g. Rowan (2011), Grenfell (2015)). However, the range of geomorphic process representation in LEMs continues to expand and develop.

Fundamentals of Landscape Evolution Modelling

Governing Equations

LEMs are ultimately driven by a set of mathematical equations – the geomorphic transport functions, often termed ‘laws’ (Dietrich et al., 2003; Tucker and Hancock, 2010). These laws may be derived from physical first principles, empirical evidence, or sometimes a combination of both. When implemented in a model, these laws are applied to a series of discretised cells or nodes representing the landscape. Conservation of mass is applied when calculating the fluxes in and out of neighbouring cells or nodes. (See Chapter 5.2 (Hutton, 2012) in this book for a more detailed description of mass continuity in numerical models.) The most common assumption made in most LEMs with respect to conservation of mass is that each column of rock or regolith has discrete boundaries between layers of different densities (Figure 2), i.e. there is no allowance for a dynamic variation of density throughout the each column in the model. Some models may further assume a uniform layer of substrate with no separate regolith layer. With these assumptions in mind, the majority of LEMs use a mass balance equation of the form:

$$\frac{\partial \eta}{\partial t} = B - \nabla \cdot \mathbf{q}_s$$

where η is the surface elevation, t is time, B is a source such as the rate of sediment production, uplift or subsidence rate, and $\nabla \cdot \mathbf{q}_s$

is the divergence of flux of material – what comes in minus what goes out – in the x and y directions (after Tucker, 2010, eq. (3).) Further discussion of continuity of mass in LEMs can be found in Tucker (2010) and in Hutton (2012).

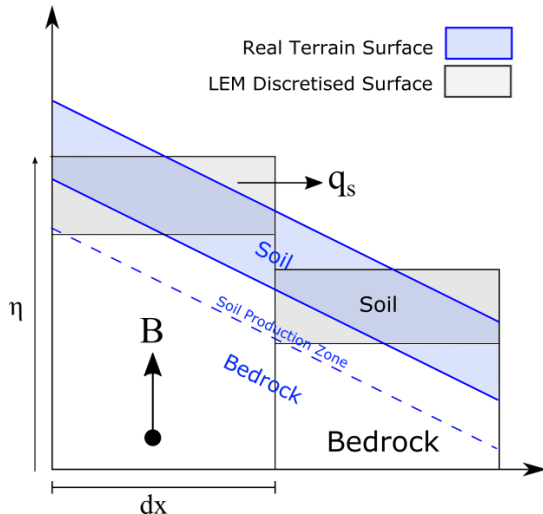


Figure 2. Conservation of mass in a soil mantled landscape or sediment covered channel (after Dietrich et al., 2003; and Tucker, 2010). η is the surface elevation, B is the boundary (base-level) change, q_s the sediment transport term, and dx the grid cell size in a discretised landscape (assuming regular grid-spacing in this example).

The modeller must be aware of which equations are implemented in the chosen LEM. Simpler models may be based on a single equation for each process represented, or even a single geomorphic transport function representing bulk processes, such as the hillslope diffusion equation (Culling, 1960). More complex models offer the user a wide range of governing equations to select from – this allows comparisons to be made from using different theoretical models of sediment erosion and transport. The Channel-Hillslope Integrated Landscape Development (CHILD) model (Tucker et al., 2001b), for example, allows the user to select from several different governing equations for sediment transport, fluvial incision, and hillslope erosion.

Each of these laws is based on a set of assumptions about the environments that they represent. The selection of the appropriate geomorphic transport law may be scale dependent. The basic stream power law, for example, does not scale well when applied to

drainage basins below around 1 km² in area (Hergarten et al., 2015; Stock and Dietrich, 2003). The LEM user should consult the appropriate literature to understand the basis limitations of specific geomorphic transport functions.

Realism and Prediction

An important question to ask in the selection of an LEM is what degree of physical realism is sufficient and appropriate for the hypothesis being tested. Models with a strong physical basis, for example those based on computational fluid dynamics (CFD) such as OpenFOAM (Jasak et al., 2007), or SPHysics (Gomez-Gesteira et al., 2012), may be appropriate for studying landscape evolution on very small scales, at the level where forces from multi-directional fluid flow and particle motion form part of the hypothesis (e.g. Bates and Lane, 1998; Jackson et al., 2015). The trade-off in using such models is the increased computational expense, which is why they are infrequently used in studies of landscape evolution beyond small scales.

Simpler representations of geomorphic processes in landscape evolution are often sufficient in lieu of fully physics-based models. Again, the appropriateness depends on the scale and complexity of the problem being studied. The value in using reduced-complexity models as exploratory tools is discussed in detail by Murray (2007).

The question is often posed whether LEMs can be used as truly predictive tools (Hooke, 2003) to make quantitative, accurate, and confirmable predictions about how landscapes will respond to future environmental changes at human timescales (Pelletier et al., 2015). Recently, however, some authors have used LEMs to make quantitative forecasts about the evolution of landscapes in very specific environments, such as the response of coastal cliff erosion to climate change over the next century (Hackney et al., 2013), and the evolution and remediation of former quarries and tailings from mining operations (Hancock and Willgoose, 2004; Hancock et al., 2015b).

Technical Implementation

LEMs are designed to simulate the evolution of topography over a discretised x , y , z landscape surface, as shown in Figure 3. Usually this type of model is referred to as a

3D or ‘whole-landscape’ model (Willgoose, 2005). The term ‘2.5D’ is sometimes used as most LEMs do not explicitly use a vertical coordinate *sensu stricto*. Instead, the vertical dimension is modelled implicitly as a variable for each (x, y) grid cell. LEMs are implemented over a fixed spatial extent (the model domain), with pre-defined boundaries, as denoted by the x and y directions in Figure 3.

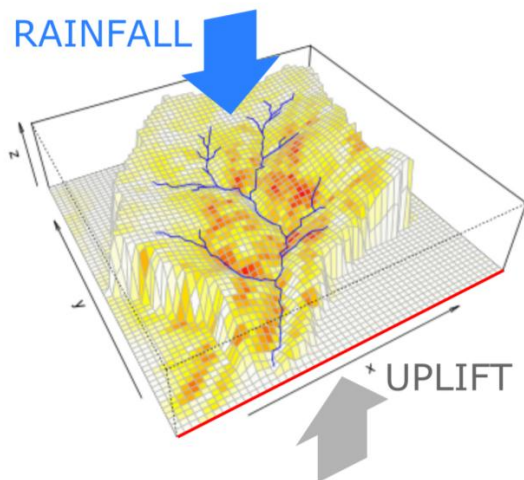


Figure 3. Main components and boundary conditions of a landscape evolution model. Boundary conditions include the climatic, tectonic and base-level conditions (rainfall and uplift), as well as the conditions specified on the model domain edges, such as where water and sediment can leave the model domain (shown by the red line). Channel network shown by blue lines. Erosion rate (red-yellow) is shown as a grid cell variable in this example.

Grid and Discretisation

The grid or mesh representing the land surface may be regular (rectilinear cells) or irregular, such as a triangular irregular network (TIN). The discretisation method of the terrain, and for rectilinear gridded domains the grid-cell size, dictates the length scale of landscape features that can be resolved in the model. Figure 4a depicts a typical regular gridded model domain. In this case, the maximum resolution of the river channel (in blue) is limited to the grid cell size of the model domain, or digital elevation model (DEM) used to initialise the model. Consideration should be given to whether the input data and model domain are of fine enough grid-spacing to resolve geomorphic features of interest.

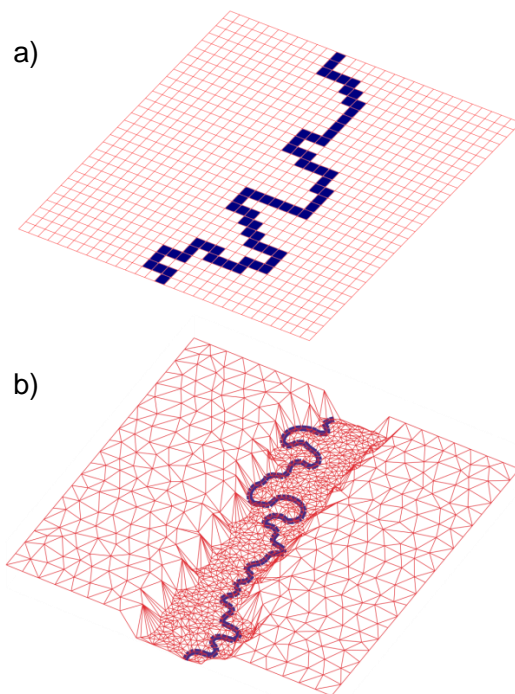


Figure 4. A comparison of two terrain-discretisation approaches. a) Regular, rectangular gridded discretisation. b) TIN, (Triangulated Irregular Network), with adaptive re-meshing. (Figure 4b re-drawn from Tucker, et al. 2001b).

The advantage of irregular gridded models is that they allow adaptive re-meshing to finer grid-spacing (Figure 4b) where detailed resolution of certain geomorphic features is advantageous, such as in river channels or gullies (Braun and Sambridge, 1997; Tucker et al., 2001a). Triangular irregular networks also have advantages for the representation of drainage networks – flow routing is not restricted to 45 degree increments as it is in regular, square-gridded models (Figure 5) (Tucker et al., 2001b).

In regular gridded LEMs, the grid cell size is uniform across the entire model domain. Regular gridded models dominate the current range of models, being computationally less expensive, and having a source code structure that is often easier to understand, if modifications need to be made. Regular gridded models are more easily compatible with the common raster formats of DEMs, such as TIFF and ASCII raster data, as well as other data inputs derived from remote sensing such as land-use, soil moisture, and vegetation cover.

Surface Flow Routing

In real landscapes surface water may flow in multiple directions over terrain, but in LEMs flow direction is limited by a flow-routing algorithm and the discretisation scheme representing the land surface. The simplest square-gridded models route water from a single cell into one of either 4 or 8 adjacent cells, based on the path of steepest descent (Figure 5), known as the D4 or D8 algorithms (e.g. O'Callaghan and Mark, 1984). D8 algorithms, though simple, tend to be too convergent – resulting in a channel network with each stream the width of a single grid-cell (Wilson et al., 2008). More complex algorithms use a scheme where water can be routed in multiple flow directions (MFD) and the total water flux can be apportioned over multiple cells (Figure 5). However, this class of algorithm tends to be overly dispersive in water flow routing (Wilson et al., 2008).

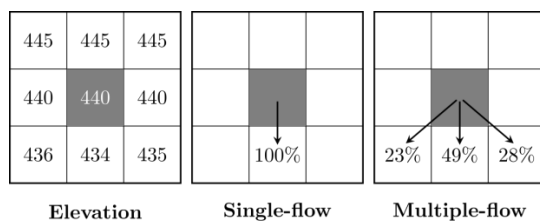


Figure 5. Comparison of single- and multiple flow direction routing methods. (Re-drawn from Schäuble et al., 2008).

The D-infinity scheme (Tarboton, 1997) is a single flow direction method aimed at addressing some of the limitations of the standard D8 algorithm. For detailed reviews of flow routing schemes see the works of Wilson et al. (2008) and (Schäuble et al., 2008). The appropriate scheme depends on the level of realism required for the hypothesis being tested. Simulations of complex riverine processes, incorporating braided channel networks, for example, would require a model with a multiple-direction flow-routing model. Flow routing models, with the notable exception of the FastScape algorithm (Braun and Willett, 2013), are typically the most computationally expensive part of a landscape evolution model, involving many iterative calculations per grid cell or node.

Data Input Sources

For modelling of real landscapes, thought must be given to the source data used to

initialise the landscape surface in the model. In simulations of large-scale landscape evolution (model domains of tens to hundreds of kilometres), input data resolution can be relatively coarse, such as a 90m SRTM-derived (Shuttle Radar Topography Mission) DEM. Even this resolution may be higher than necessary and DEMs may be coarsened through resampling with GIS software in order to reduce the total number of grid cells and hence computational expense. Higher resolution DEMs are necessary for modelling small-scale features, such as gully formation or hillslope erosion (Nearing and Hairsine, 2010). It may be necessary to acquire sufficiently high resolution data, on the order of metres to centimetres, from sources such as airborne LiDAR (see Chapter 2.1.4, Gallay, 2013), terrestrial laser scanning (see Chapter 2.1.5., Smith, 2015), or structure from motion techniques (SfM, see Chapter 2.2.2, Micheletti et al., (2015)). In short, the appropriate resolution of input data is dictated by the length scales at which the geomorphic processes of interest operate.

Boundary Conditions

Thought must also be given to the boundary conditions of the model domain. Boundary conditions refer to any input or constraint on the x , y , z minima and maxima of the model domain (Figure 3), including tectonic or base-level change, and climatic input, such as precipitation. Most models will operate on the principle of having at least one open boundary where water or sediment can flow out. In some models the placement of boundary outlets is customisable by the user (e.g. CHILD, FastScape). The LEM user should also consider the possibility that these boundary conditions may not be fixed over time, such as variation in rainfall rate or uplift rate. In some situations, the boundary conditions may exhibit some kind of feedback with the internal processes of the model domain (e.g. Raymo and Ruddiman, 1992; Willett, 1999).

Current Models

LEM development has bloomed in the previous two decades, in part due to significant and continued computational advancement, and there is now a wide variety of models to choose from. (See Appendix B for a systematic overview of the different LEMs available and their features and process

representation). The range of models available vary in their complexity, applicability to different timescales, and different process representation. In this section, some of the existing LEMs currently in common use are briefly reviewed.

CAESAR-Lisflood

A family of related models have developed from the original CAESAR LEM (Coulthard et al., 1996, 2002). The original CAESAR model is a cellular automaton model that simulates water flow across the landscape, fluvial erosion, sediment deposition, and hillslope processes. CAESAR-Lisflood (Coulthard et al., 2013), the current iteration of the model, uses a more physical-based surface water flow component based on a simplified numerical solution to the shallow water equations (LISFLOOD-FP, Bates et al., 2010). The non-steady hydrological component of the model allows effects such as tidal flows, lake filling, and the blocking of valley floors by alluvial fans to be represented in LEMs (Coulthard et al., 2013).

CAESAR-Lisflood is suited to simulation of entire drainage basins (in catchment mode) or sections of a river channel (in reach mode, e.g. Coulthard and van de Wiel, 2006; van de Wiel et al., 2007). CAESAR-Lisflood is an appropriate tool for timescales ranging from modelling the effects of a single storm over a few hours, through seasonal, to annual, and millennial time scales of landscape evolution. Process representation in CAESAR-Lisflood is focussed primarily on hydrodynamics and sediment transport, including the simulation of multiple-sized grain fractions.

Though there is theoretically no upper limit to the time periods that can be simulated with CAESAR-Lisflood, existing studies have focused on shorter scales from decades up to thousands of years, such as simulating sediment output of a small basin under short term climate predictions (Coulthard et al., 2012a), simulating storm and tidal surge dynamics on coastal environments (Skinner et al., 2015), forecasting the short term geomorphic evolution of former mine-workings and excavations (Pascullo and Audisio, 2015), amongst others.

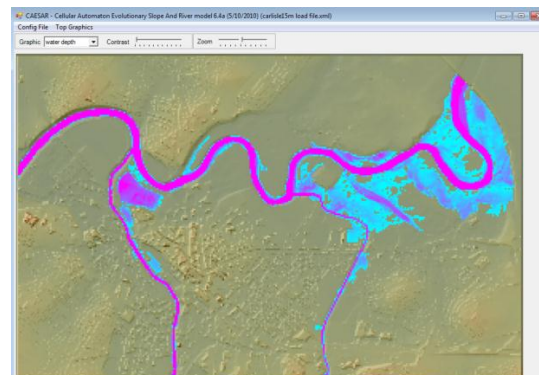


Figure 6. CAESAR-Lisflood simulating the flooding of Carlisle, UK, 2005. Hydrogeomorphic effects of single floods can be simulated in this LEM due to the implementation of a non-steady flow hydrological component (Bates et al., 2010). Blue to pink colouring represents water depth, with pink indicating the deepest water depths. Model domain 5 km across.

CAESAR-Lisflood uses a graphical user interface (GUI) to set model parameters and display output (Figure 6). The GUI makes model set-up quick and easier for users with less familiarity with command-line operations or code modification. The current version is limited to running in a Windows-only environment. The integration of visualisation with the core model code also allows the user to view model output as the simulation progresses (Figure 6), this has the advantage of letting the user monitor output without having to wait for a full simulation to complete and visualise the output in a separate step.

CHILD

The Channel Hillslope Integrated Landscape Development model (CHILD, Tucker et al., 2001b) is another widely used model for investigating landscape evolution in a variety of environments, on temporal scales from decades to millions of years. The modular design of the LEM has facilitated its expansion over recent years and it now supports various types of geomorphic process representation. CHILD supports initialisation of the terrain surface from DEM data or generating synthetic topographies from scratch. A wide range of fluvial incision processes can be simulated with CHILD, including both detachment- and transport-limited erosion models, sediment transport, and a range of hydrological and rainfall-runoff generation routines. Recent development of modules has extended

process representation to include, for example, modules of dynamic vegetation growth (Collins and Bras, 2004), floodplain evolution (Clevis et al., 2006), dynamic adjustment of channel width (Attal et al., 2008), representation of sediment grain size (Gasparini et al., 2004), debris flows (Lancaster et al., 2003), and stochastic rainfall generation (Tucker and Bras, 2000).

CHILD differs from many of the other models described in this section, as it eschews a traditional grid-based spatial discretisation in favour of a triangular mesh, or TIN. As previously discussed in the *Technical Implementation* section, this allows the model resolution to vary spatially across the domain, becoming higher in regions where smaller scale features and processes operate, such as river meanders, and coarser where features are much larger in spatial extent, such as floodplains and hillslopes (Tucker et al., 2001a).

The CHILD model's TIN-based approach is advantageous in its flexibility at representing different scale features within a landscape (Braun and Sambridge, 1997; Tucker et al., 2001b), but adds an extra layer of complexity when working with typical raster data formats, requiring conversion between raster and TIN data at the input and output stages of the modelling workflow. A series of MATLAB scripts are provided with the model for visualising output. The open-source *RCHILD* package is also available for output visualisation with the R programming language (Dietze, 2014). The CHILD model is platform-independent.

FastScape-based LEMs

FastScape is an algorithm based on an efficient implicit numerical scheme to solve variants of the stream power law for modelling large scale landscape evolution (Braun and Willett, 2013). The major advance made by the FastScape algorithm was to increase the efficiency of the flow routing calculation – a bottleneck in most LEMs – and hence the model is useful for rapidly testing hypotheses of landscape evolution. Several related LEMs have been based on an implementation of the FastScape algorithm, including:

- The 'original' FastScape LEM (Braun and Willett, 2013)

- DAC – the Divide and Capture model (Castelltort et al., 2012; Goren et al., 2014)
- LSDTopoTools: Raster Model (<http://lsdtopotools.github.io>), e.g. Mudd, 2016)

Recent applications of FastScape-based LEMs have focused on the simulation of synthetic landscapes under differing tectonic, lithological, and climatic boundary conditions (e.g Braun and Willett, 2013; Braun et al., 2014; Castelltort et al., 2012; Goren et al., 2014; Yang et al., 2015). The FastScape LEM also allows for the use of DEM data to set the initial surface topography in the model. An optional GUI interface is also included with the FastScape LEM, though this is currently only functional in Linux-based environments. The underlying FastScape algorithm is generic, and not necessarily tied to any particular LEM – users may choose to implement the algorithm in other open source models.

LAPSUS

The LAPSUS model (Landscape Modelling at Multi-dimensions and Scales) is a modular, multi-process model suited to studying catchment-scale erosional processes and landscape evolution at a range of temporal scales from years to hundreds of thousands of years (van Gorp et al., 2015; Schoorl et al., 2000). LAPSUS is strongly suited to studying landscape evolution by means of soil and sediment redistribution through processes of fluvial erosion, surface wash, landsliding, tillage, creep, and tectonics. Applications include studying the interaction of non-linear processes in landscape evolution (Schoorl et al., 2014; Temme and Veldkamp, 2009), the role of tillage and changing land-use in decadal to millennial scale landscape evolution (Baartman et al., 2012b; Schoorl and Veldkamp, 2001), the sensitivity of soil erosion to rainfall intensity (Baartman et al., 2012a), and exploring uncertainty and parameter choice in landscape evolution modelling (Temme et al., 2011). LAPSUS features a graphical user interface similar in appearance to the CAESAR interface in Figure 6, allowing a similar visual monitoring of model outputs to take place without further post-processing required.

Other LEMs

Landscape evolution modellers have a vast choice of models at their disposal: the organisation CSDMS (Community Surface Dynamics Modelling System: <http://csdms.colorado.edu>) operates as a *de facto* model repository for developers and users of LEMs. The terrestrial model section lists well over one hundred different models that have been published to the site. CSDMS is a useful starting place for potential modellers to select an LEM based on their own requirements. A summary of some of the more commonly used models over the last decade is presented in Appendix B, showing the key features of each model for comparison.

Some LEMs extend the functionality (and often complexity) of existing models. For example, the CAESAR-Lisflood-DESC model (Barkwith et al., 2015) features, in addition to the core components of CAESAR-Lisflood, modules for distributed surface and soil hydrology, groundwater hydrology and a more physically realistic representation of landsliding. Applications of CLiDE have included the prediction of geomorphic and environmental hazards over human timescales (e.g. Barkwith et al., 2015; Tye et al., 2013).

The current range of LEMs includes well established software packages such as the SIBERIA and CASCADE models. SIBERIA (Willgoose et al., 1991b) is a square gridded model originally developed to investigate the feedbacks between hydrology, catchment form, and tectonics (Willgoose et al., 1991a, 1994). CASCADE (Braun and Sambridge, 1997) was an early implementation of a TIN-based model designed to simulate long-term landscape evolution as a function of fluvial and hillslope processes. Though the deployment of these two models has declined in recent years somewhat, they continue to be used as a benchmark in some studies (e.g. Hancock et al., 2015).

Recent developments within the modelling community have extended traditional modelling functionality with other elements of geomorphic analysis. The LSDTopoTools software (<http://lsdtopotools.github.io>), for example, features an LEM based on the FastScape algorithm, integrated within a set of powerful topographic analysis tools. This

allows easy transition between modelling and analysis of the results using common and novel topographic metrics.

Another recent development is the *Landlab* software package (<http://landlab.github.io/>), which takes a highly modular approach to numerical modelling of landscapes. The user can rapidly create their own bespoke LEM from a set of existing components. This results in a high degree of user control over the complexity of the model configuration, not only in terms of process representation, but also the effect that technical aspects, such as grid type and flow routing algorithm have on model performance and output. The modular design avoids the usual expenditure of re-writing commonly used codes for process representation, model gridding, and standardised file input and output. A key strength of Landlab is its accessibility to users who do not have significant prior experience in designing and implementing numerical codes, but wish to embark on model development. Examples of Landlab's applications include the study of impact cratering on landscape evolution (Hobley et al., 2013), the impacts of wildfires on hydrologic response (Adams et al., 2014), quantifying the link between regolith production and subsurface temperatures (Barnhart and Anderson, 2014), investigating the response of landscape evolution under non-steady state hydrology (Adams 2015), and as a basis for developing a stochastic cellular automaton model (Tucker et al., 2015).

The selection of LEMs discussed here range from those that have already established a wide user-base in landscape evolution research (e.g. CHILD, CAESAR, LAPSUS), to newer developments that offer novel functionality or process representation for modellers (e.g. Landlab, CLiDE, DAC, LSDTopoTools). Neither this section, nor the list in Appendix B is exhaustive, and some previously popular models have been omitted as it was felt they have been superseded or subsumed by newer offerings. The range of LEMs discussed here should nevertheless provide a starting point for tackling a wide range of modelling endeavours.

Applications and Examples

This section presents a short discussion of three recent studies using landscape evolution models. The selection was chosen to represent a broad selection of timescales,

landscape types, and conceptual models. The reader should refer to the table in Appendix A for an expanded list of examples for further reading.

Testing Fluvial Erosion Laws (CHILD, Attal et al. 2008)

Several laws of fluvial erosion have been proposed to describe the evolution of river profiles (e.g. Seidl and Dietrich, 1992; Howard, 1994; Dietrich et al., 2003), and discriminating between which law is appropriate for a given landscape is challenging. Attal et al. (2008) tackle this by selecting river basins believed to be undergoing a transient response to base level change along an active fault (setting depicted in Figure 7). They use an LEM to test two of the common end-member models of fluvial incision: a transport-limited and detachment-limited case. The underlying process models are parameterised and calibrated using field data collected from the basins. Starting from a steady-state form of each basin's topography, the CHILD model simulations are run with fault throw accelerations programmed at known intervals, which are well documented from previous studies.

An inverse problem is set up, using an ensemble of model simulations to determine which combination of fluvial incision model and parameters produce the closest match to the observed topography. The study also benefits from careful selection of field sites with uniform lithologies, which helps constrain the range of variables.

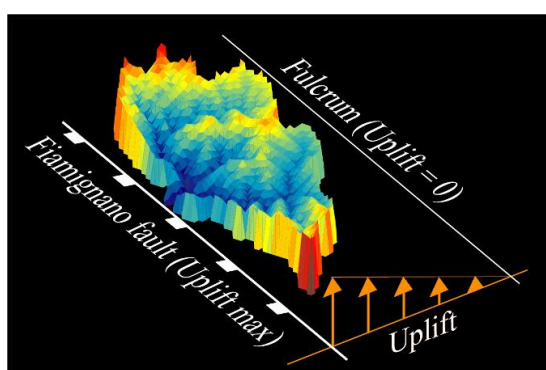


Figure 7. Example output from the CHILD model used in Attal et al. (2008). Landscape response to tectonic perturbation (fault throw acceleration) is shown. Example using real topography in the Italian Apennines.

Climate, Tectonics or Morphology in Sediment Yields (CAESAR, Coulthard and Van De Wiel, 2013)

Landscape evolution covers a range of temporal scales – this study by Coulthard and Van De Wiel (2013) focuses on landscape evolution over short time periods of c. 100–1000 years. The study uses a forward modelling approach to predict the relative importance of different perturbations to a river catchment of approximately 500 km² in the North of England. The CAESAR model was set up to run a series of 100 year and 1000 year experiments, each with a single different tectonic or climatic perturbation introduced to each experiment, with all other conditions remaining the same.

From the results of the experiments, the authors are able to predict the relative impacts of climatic versus tectonic perturbations on the catchment. For a transport-limited environment, the authors discover climatic changes have the greater effect on sediment yields at shorter timescales, with sediment signals from increased rates of uplift being lost in the internal storage of the basin.

The study shows that LEMs may be used to make useful predictions about sediment yields in order to assess the *relative* importance of external perturbations, rather than to precisely predict the amounts of sediment output. Furthermore, landscape evolution is the result of a complex interaction of several competing processes, and by carefully isolating each process or potential perturbation in separate experiments, it is possible to explore which factors have the most significant impact on drainage basin evolution.

Coupled Numerical-Analytical Approach to Landscape Evolution Modelling (DAC-FastScape, Goren et al. 2014)

This study tackles a shortcoming in previous LEMs where the form and processes associated with drainage divides were under-represented in models, and investigates the implications on landscape evolution at the range scale, with an LEM that can accurately represent drainage divides. The authors propose a hybrid numerical-analytical model called 'Divide and Capture' (DAC, based on the FastScape algorithm of Braun and Willett, 2013), which calculates the positioning of drainage divides based on a sub-grid scale

parametrisation of divide migration. Their precise analytical description of water divides is found to alter the dynamics of basins either side of the divide. Using a synthetic landscape (Figure 8), they find that the time taken for landscapes to reach steady state is longer due to the dynamic reorganisation and basin capture that persists about drainage divides, long after traditional LEMs would have reached steady state.

The study tackles the problem using a range of synthetic topographies, and is an example

of using LEMs in an exploratory way to make general predictions about landscape form. The latter half of the study shows that ‘real’ topographies can be simulated in general terms, using a model set-up that simulates the key features of the New Zealand Southern Alps. A real DEM is not used, but by carefully choosing the initial conditions, parameters, and tectonic boundary conditions the authors show that this simplified version of a landscape is sufficient to represent the key characteristics of their study area (Figure 8).

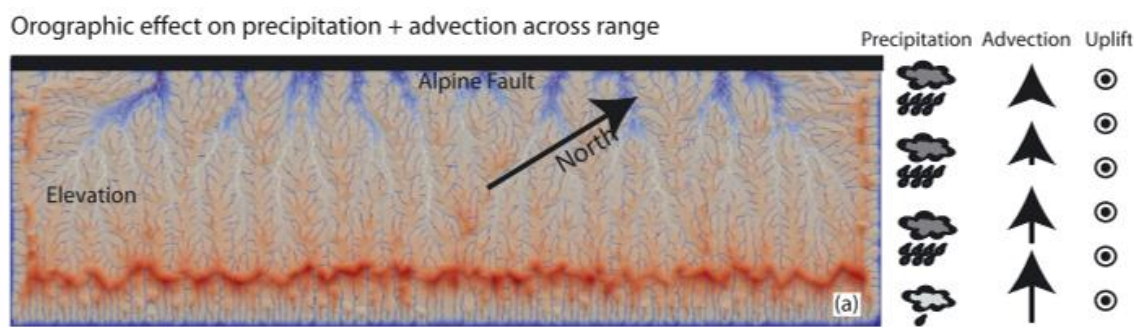


Figure 8. Goren et al. (2014) show how LEMs can use a terrain of reduced complexity, while still maintaining the essential features of the real-world landscape it represents. Here, the New Zealand Southern Alps are represented within the DAC model.

Uncertainty, Sensitivity, and Calibration

Uncertainty

Uncertainty in modelling describes our inability to know precisely the initial conditions of a model, to represent in a model all the processes that govern landscape evolution, and ultimately to know with certainty the accuracy of the predicted outcome (Beven, 1996; Pelletier et al., 2015). All LEMs make simplifications regarding process representation, partly due to a lack of detailed knowledge in how certain processes work, and partly due to limitations about how these processes can be represented in computer models. Uncertainty may also stem from inaccuracies in input data sources, the choice of model parameters, and the boundary conditions of the model (and whether these parameters and boundary conditions might change through time). Uncertainty in LEMs may lead to errors that propagate through the simulation and increase in magnitude as a

simulation progresses.

Ideally, one should address uncertainty by first assessing which parameters the model is most sensitive to – it may be that large uncertainties in one parameter have relatively little effect on the model outcome, whereas small uncertainties in a different parameter produce unexpectedly large variation in the model outcome (Pelletier et al., 2015).

Methods such as ensemble analysis should be considered, whereby multiple instances of the same simulation are run, with a range of parameters chosen from a probability distribution to assess the most likely outcomes from a model. While uncertainty cannot be removed entirely from modelling studies, it is useful to be able to state the most probable outcome(s), based on a probabilistic distribution of input conditions.

Uncertainty is a particular challenge in landscape evolution modelling as many processes are threshold dependent, or scale non-linearly (Schumm, 1979). In choosing

parameter values, guidance should be taken from reported values of such parameters in the published literature. Readers are referred to Chapter 5.2, *Numerical Modelling*, (Hutton, 2012) for further discussion of uncertainty, as well as the review by (Pelletier et al., 2015), and LEM studies that have explored uncertainty in more detail (Hancock et al., 2015a; Mudd et al., 2014; Temme et al., 2011).

Sensitivity and Calibration

Following earlier definitions, (Oreskes et al., 1994; Trucano and Swiler, 2006) calibration is defined here as the selection and modification of input parameters of a model in order that they maximise agreement with observed data in real landscapes. Such parameters in LEMs might include the coefficient terms in fluvial erosion laws, for example the K , m , and n parameters in the stream power law (Seidl and Dietrich, 1992), hydrological parameters such as Manning's n (Manning et al., 1890), or the threshold shear stresses required to initiate erosion (Snyder et al., 2003). Many such parameters are not directly quantifiable by field measurement, and model users should consult similar studies for recommended values, or conduct their own sensitivity analyses to constrain uncertainty in parameter choice. Other parameters may lend themselves to more rigorous methods of calibration, where they link directly or indirectly to measurable values in the field. Examples would include the calibration of hydrological parameters to produce a 'best fit' with observed discharge values at river gauging stations (e.g. Coulthard et al., 2013; Wong et al., 2015), constraining stream power law parameters using statistical models and sensitivity analyses (Croissant and Braun, 2014; Mudd et al., 2014), or the field measurement of sediment shear strength to assist in setting erosion threshold parameters (see Chapter 1.3.1, Grabowski, 2014).

Validation & Confirmation

Validation is the process of assessing the legitimacy of a model set-up. Results from a model may or may not be valid depending on the quality of input data and model parameter choice (Oreskes et al., 1994). Moreover, (as noted by Oreskes et al., 1994) validation does not necessarily establish the truth or accuracy of model predictions, only that the model is internally consistent. In practice, it can be

thought of as a 'sanity check' on the input to the LEM before beginning the simulation. For example, is the input DEM of sufficient resolution to represent the scale of geomorphic features expected to be formed? Do the input parameters conform to observed or realistic ranges? (See *Calibration* in previous section). If the answers to these types of question are 'no', the model predictions will be invalid.

Geomorphologists use LEMs to deduce whether hypotheses about landscape evolution are likely to be valid, which requires a method for assessing how the model output supports the hypothesis. *Confirmation* refers to the assessment of how model predictions – after selecting suitable input parameters – match observations in nature (Oreskes et al., 1994). Directly observing landscape evolution is challenging at human timescales, as whole-landscape change occurs at slow pace, making direct confirmation of model predictions difficult in many situations (Hasbargen and Paola, 2003; Hoey et al., 2003). Some predictions made by LEMs, however, can be directly or indirectly confirmed to a certain extent with field observations. This includes short term phenomena such as gully formation, coastal erosion, and river bank incision. At short timescales, direct monitoring and quantification of erosion rates, particularly in rapidly eroding fluvial settings, becomes feasible.

Field Confirmation

Techniques to indirectly measure the rates of landscape change are wide-ranging, and include measuring sediment flux at catchment outlets, using traps to measure bedload erosion and deposition (e.g. Bunte et al., 2004), bedload impact sensors (e.g. Raven et al., 2010; Rickenmann and Mc Ardell, 2007; Turowski et al., 2010), suspended sediment measurements at gauging stations (Brazier, 2004), and the use of radio frequency identification-tagged sediment particles to track sediment movement (e.g. Beer et al., 2015; Chapuis et al., 2015). Further information on such measurement techniques can be found in Parts 3.3 (fluvial) and 3.4 (glacial) of this book.

Through the rise of digital photogrammetric techniques, such as airborne and terrestrial

laser scanning, direct measurement of whole-landscape morphological change is now possible at high enough resolutions to quantify small differences in topographic features, particularly in rapidly evolving landscapes (e.g. Rosser et al., 2005; Vaaja et al., 2011). Using these methods to aid model confirmation would be limited to small scale studies, as processing of point cloud data from these sources can be highly computationally expensive (Axelsson, 1999). Parts 2.1 (Direct acquisition of elevation data) and 2.2 (Photogrammetric techniques) provide more information on related measurement techniques. Chapter 2.3.2 (Williams, 2012) covers the use of DEMs of difference to quantify landscape change over discrete time periods. Despite their availability, there are as of yet few examples that employ these direct methods of landscape quantification in the confirmation of predictions made by LEMs.

At longer, geomorphologically significant timescales, a range of techniques becomes available to assist in the calibration of LEMs and confirmation of hypotheses. Two popular techniques are mentioned here, but other suitable techniques may be found in relevant reviews and textbooks (e.g. Anderson and Anderson, 2010; Burbank and Anderson, 2011).

Optically stimulated luminescence dating uses a property of quartz and feldspar minerals that records the amount of time they have sat in a sedimentary or soil deposit, which can be used for dating landforms (Aitken, 1998; Murray and Wintle, 2000; Stokes and Clark, 1999). The applicability of this technique to different temporal scales is site-specific and ranges from years to upwards of hundreds of thousands of years (Madsen and Murray, 2009). A more comprehensive overview is provided in Chapter 4.2.6 of this book (Mellett, 2013).

Cosmogenic radionuclide (CRN) dating is a technique based on the interaction of cosmic rays with certain isotopes in minerals in the Earth's surface (Anderson et al., 1996; Dunai, 2010). The production rate of certain isotopes can then be used to determine absolute ages and erosion rates in the landscape. Chapter 4.2.10 of this book (Darvill, 2013) also provides an overview and example applications of this technique. A recent application combining an LEM with a model of CRN production rates is found in Mudd (2016),

where it is used to explore the detection of transience in landscapes. The method is suitable for determining ages up to c. 4 million years (Burbank and Anderson, 2011).

Topographic Metrics

In the past, looser forms of qualitative assessment have been used where LEMs are applied in an exploratory manner, such as to test mathematical models of geomorphic processes, or make speculative predictions of landscape evolution. In this sense, topographies generated by LEMs can be compared to real landscapes that they are intended to represent. Visual inspection of real versus simulated terrains can provide some degree of hypothesis confirmation (Bras et al., 2003; Hooke, 2003). However, it is recommended that this approach be extended to quantitative analysis by using a range of topographic metrics to compare simulated topographies with their natural counterparts. Such metrics include: mean relief, slope, river profile concavity, channel steepness indices (e.g Wobus et al., 2006), terrain curvature, hypsometry, and roughness. A similar technique of comparing LEM output to physical analogue models has also been implemented by Hancock and Willgoose, (2002).

A range of techniques is available to assist the modeller in assessing model predictions and confirming hypotheses of landscape evolution. The most appropriate methods will depend on the time-scale of the study, and the type of predictions made by the hypothesis.

Limitations

Landscape evolution models are based on a body of existing theoretical models describing geomorphic processes. Arguably, one of the greatest limitations in landscape evolution modelling is the lack of unified theories describing key processes in the landscape, such as fluvial incision or hillslope form (Dietrich et al., 2003). This forces the user to select from an often wide (and still expanding) range of geomorphic transport laws, without sufficient knowledge of the particular landscape equation in question to select the most appropriate law. Sensitivity analyses may help to quantify the uncertainty stemming from this issue.

Long term landscape evolution modelling (on the order of thousands to millions of years)

suffers from the issue of how to upscale micro-scale geomorphic processes to the macro-scale. The extent to which quasi-random fluctuations in geomorphic processes, such as turbulent flow in rivers and small-scale heterogeneity in soil or bedrock composition, should be incorporated into long-term laws of landscape evolution laws is not yet fully developed (Tucker and Hancock, 2010). Many LEMs have relied on statistical approaches to deal with this issue (e.g. Hovius et al., 1997; Lague, 2005, 2013). However, the scaling exponents and statistical distributions in these parameterisations are often based on limited empirical evidence from field observation.

Numerical landscape evolution modelling is also bound by limitations of computing power available to the user. Considerations have to be made when designing LEM experiments in order that the simulations can be carried out in reasonable compute time. Higher grid resolutions and less parameterisation of key processes may lead to more physically realistic simulations, but at increased computational expense. Recent releases of some LEMs have begun to tackle this by incorporating parallelisation techniques into the model code (see Appendix B), taking advantage of multi-core processors that have now proliferated into most personal computers as well as supercomputers.

Conclusions

When considering the use of landscape evolution models in geomorphological research, the modeller must make key decisions at certain stages of the modelling process. The modelling process can be summarised as follows:

- 1) Definition of the research aim and purpose of the model.
- 2) Selection of appropriate model and components.
- 3) Choice of input data if applicable.
- 4) Selection and calibration of model parameters, possibly including sensitivity analysis to address uncertainty.

- 5) Validation of model set-up – is the choice of parameters and input data logical and internally consistent?
- 6) Confirmation of model predictions against observed data.
- 7) Interpretation of model predictions.

There are two factors that should be considered at each of these stages: scale and process representation. The intended scale of the experiment, both temporal and spatial, has implications for LEM selection (e.g. is the model suitable for the time-scale of interest?). Process representation should also strongly guide decisions at each stage. The user needs to know which laws are implemented in their chosen LEM, and what parameters are associated with them that need to be selected and calibrated. If the model offers a choice of geomorphic process laws to choose from, which is the most appropriate for the environment that the experiment is intended to emulate?

Landscape evolution models are powerful tools for the geomorphologist. Like all powerful tools, however, care must be used to avoid unintended consequences from misuse. Numerical LEMs have heralded a new era in geomorphic research, and are increasingly used to address important research questions in geomorphology. They aid both our understanding of how geomorphic processes work, and our ability to make quantitative predictions about landscape change in the future.

Acknowledgements

The author wishes to thank Martin Hurst and Marco Van De Wiel for constructive and detailed reviews of the initial manuscript, which improved the content of this chapter significantly. The Editor, Simon Cook, also provided suggestions that refined the final version of the chapter. Useful feedback and discussion on an initial draft was also provided by Simon Brocklehurst, David Schultz, and Geraint Vaughan.

Appendix A: Recent Applications of Landscape Evolution Models

Author	Year	LEM	Application
Coulthard et al.	2000	CAESAR	Catchment sensitivity to land use and climate change (100-1000 years)
Schoorl and Veldkamp	2001	LAPSUS	Modelling the effects of changing land use over decadal times scales on landscape evolution
Tucker and Whipple	2002	CHILD	Modelling topographic outcomes of fluvial incision laws.
Simpson and Schlunegger	2003	<i>unnamed/study-specific</i>	Co-evolution of hillslope and channel morphology
Tucker	2004	CHILD	Topographic outcomes of fluvial incision laws
Collins and Bras	2004	CHILD	Coupled vegetation growth erosion model
Hancock and Willgoose	2004	SIBERIA	Sediment runoff and gully formation in mining tailings
Sólyom and Tucker	2004	CHILD	Landscape morphological dependence on storm duration
Pelletier	2004	<i>unnamed/study-specific</i>	Effect of flow routing algorithm on drainage divide migration
Brocklehurst and Whipple	2006	GOLEM	Comparing glacial vs fluvial erosional effectiveness
Passalacqua et al.	2006	<i>unnamed/study-specific</i>	Grid scale resolution control on LEM output
Attal et al.	2008	CHILD	Channel geometry adjustment to tectonic perturbations
Anders et al.	2008	CASCADE	Influence of precipitation phase on mountain range morphology
Temme and Veldkamp	2009	LAPSUS	Integration of multiple landscape processes to predict evolution of a quaternary landscape
Attal et al.	2011	CHILD	Applicability of fluvial erosion laws in transient landscapes
Pelletier	2012	<i>unnamed/study-specific</i>	Transport vs detachment limited erosion in soil-mantled landscape evolution
Coulthard et al.	2012	CAESAR	Assessing geomorphic response to climate model prediction
Baartman et al.	2012	LAPSUS	Determining the role of tillage in millennial scale landscape evolution
Coulthard and Van De Wiel	2013	CAESAR	Geomorphic response to climate change in upland river catchments
Braun et al.	2013	FastScape	Fluvial erosion in dynamic topography (mantle upwelling)
Booth et al.	2013	<i>unnamed/study-specific</i>	Deep seated landsliding in landscape evolution models
Croissant and Braun	2013	FastScape	Constraint of stream power law parameters
Colberg and Anders	2014	CASCADE	Evolution of passive margin escarpments under orographic rainfall
Braun et al.	2014	FastScape	Rock density controls on erosion
Willett et al.	2014	DAC	Dynamic reorganisation of river networks
Han et al.	2014	CHILD	Influence of rainfall gradients on river profile evolution
Mudd et al.	2014	CHILD	Testing statistical method for identifying channel segments and stream power law parameters
Schoorl et al.	2014	LAPSUS	Modelling the dynamics of centennial scale sediment waves in an eroding catchment
Han et al.	2015	CHILD [#]	Role of orographic rainfall in controlling landscape morphology

15

Declan A. Valters

Braun et al.	2015	FastScape	Landscape evolution under cyclic rainfall variations
Yang et al.	2015	DAC	<i>In situ</i> formation of peneplains due to river network reorganisation
Skinner et al.	2015	CAESAR-Lisflood	Simulating tidal and storm surge dynamics on coastal evolution
Hancock et al.	2015	CAESAR-Lisflood SIBERIA	Erosional stability of rehabilitated mine landscape
Mudd	2016	LSDTopoTools	Detecting transience in eroding landscapes

[†] Referring to LEMs custom written for a specific study and not released as a standalone model.

[‡] Modified version of CHILD, not in official release as of 2016.

Model	Time scale applicability (years)	Input types	Landscape Type	Grid type	Language	Fluvial – TL†	Fluvial – DL‡	Rainfall-runoff	Flooding	Non-steady flow	Hillslope creep	Soil formation	Landslide - Shallow	Landslide - Deep	Grain size	Tectonics - Vertical	Tectonics – Horiz.	Climatic variability	Rainfall distribution**	Weathering	Stratigraphy	Groundwater	Bedrock variation	Vegetation	GUI	Parallelisation	Open Source
CHILD	$10^3 - 10^7$	DEM/Synth*	Basin/Range	TIN	C++																						
FastScape	$10^4 - 10^7$	DEM/Synth.	Range	Square	Fortran																					#	
CAESAR-Lisflood	$10^2 - 10^4$	DEM	Basin/Reach	Square	C#																						
CLIDE§	$10^2 - 10^4$	DEM	Basin	Square	C#																						
SIBERIA	$10^3 - 10^7$	DEM/Synth.	Range	Square	Fortran																						
LSDTopoTools¶	$10^2 - 10^7$	Synth.	Range/Basin	Square	C++																						
Landlab	$10^3 - 10^7$	DEM/Synth.	Range	TIN/Sqr.	Python																						
LAPSUS	$10^{-1} - 10^5$	DEM	Basin	Square	C#																					#	

Appendix B: Model process representation and technical comparison.

* – 'Synthetic' DEM. I.e. the model will initialise itself to a synthetic terrain based on certain initial conditions without an external DEM file.

† – Transport limited

‡ – Detachment limited

§ – Based on the CAESAR-Lisflood model, with further coupled components for groundwater.

¶ – Contains a FastScape-based landscape evolution model, and a CAESAR-based hydrodynamic model.

– On request of the authors.

|| – Range: multiple basins, mountain range evolution; Basin: singular drainage basin/river catchment; Reach: sections of river catchment

** – Spatial distribution of rainfall/climate input

■	Featured/Yes
■	Caveat
□	Not featured/Unknown

References

- Adams JM, Rengers FK, Gasparini NM, Tucker GE, Nudurupati SS, Hobley DEJ, Istanbulluoglu E, Hutton EWH. 2014. Exploring Post-Wildfire Hydrologic Response in Central Colorado Using Field Observations and the Landlab Modeling Framework. *AGU Fall Meeting Abstracts 2014*.
- Aitken MJ. 1998. *An introduction to optical dating: the dating of Quaternary sediments by the use of photon-stimulated luminescence*. Oxford University Press.
- Anders AM, Roe GH, Montgomery DR, Hallet B. 2008. Influence of precipitation phase on the form of mountain ranges. *Geology* **36**: 479. DOI: 10.1130/G24821A.1
- Anderson RS, Anderson SP. 2010. *Geomorphology: The Mechanics and Chemistry of Landscapes*. Cambridge University Press: Cambridge.
- Anderson RS, Repka JL, Dick GS. 1996. Explicit treatment of inheritance in dating depositional surfaces using in situ ^{10}Be and ^{26}Al . *Geology*: 47–51.
- Attal M, Cowie PA, Whittaker AC, Hobley D, Tucker GE, Roberts GP. 2011. Testing fluvial erosion models using the transient response of bedrock rivers to tectonic forcing in the Apennines, Italy. *Journal of Geophysical Research* **116**: F02005. DOI: 10.1029/2010JF001875
- Attal M, Tucker GE, Whittaker AC, Cowie PA, Roberts GP. 2008. Modeling fluvial incision and transient landscape evolution: Influence of dynamic channel adjustment. *Journal of Geophysical Research* **113**: F03013. DOI: 10.1029/2007JF000893
- Axelsson P. 1999. Processing of laser scanner data—algorithms and applications. *ISPRS Journal of Photogrammetry and Remote Sensing* **54**: 138–147.
- Baartman JEM, Jetten VG, Ritsema CJ, de Vente J. 2012a. Exploring effects of rainfall intensity and duration on soil erosion at the catchment scale using openLISEM: Prado catchment, SE Spain. *Hydrological Processes* **26**: 1034–1049. DOI: 10.1002/hyp.8196
- Baartman JEM, Temme AJAM, Schoorl JM, Braakhekke MHA, Veldkamp TA. 2012b. Did tillage erosion play a role in millennial scale landscape development? *Earth Surface Processes and Landforms* **37**: 1615–1626. DOI: 10.1002/esp.3262
- Barkwith A, Hurst MD, Jackson CR, Wang L, Ellis MA, Coulthard TJ. 2015. Simulating the influences of groundwater on regional geomorphology using a distributed, dynamic, landscape evolution modelling platform. *Environmental Modelling and Software* **74**: 1–20. DOI: 10.1016/j.envsoft.2015.09.001
- Barnhart KR, Anderson RS. 2014. Chilly Hilly-coupling models of landscape evolution and subsurface thermal processes. 3 pp. *AGU Fall Meeting Abstracts 2014*.
- Bates P, Lane S. 1998. Preface : High resolution flow modelling in hydrology and geomorphology. *Hydrological Processes* **12**: 1129–1130. DOI: 10.1002/(SICI)1099-1085(19980630)12:8<1129::AID-HYP697>3.0.CO;2-8
- Bates PD, Horritt MS, Fewtrell TJ. 2010. A simple inertial formulation of the shallow water equations for efficient two-dimensional flood inundation modelling. *Journal of Hydrology* **387**: 33–45. DOI: 10.1016/j.jhydrol.2010.03.027
- Beer AR, Turowski JM, Fritschi B, Rieke-Zapp DH. 2015. Field instrumentation for high-resolution parallel monitoring of bedrock erosion and bedload transport. *Earth Surface Processes and Landforms* **40**: 530–541. DOI: 10.1002/esp.3652
- Beven K. 1996. Equifinality and uncertainty in geomorphological modelling. The scientific nature of geomorphology. *Proceeding of the 27th Binghamton Symposium in Geomorphology held 27-29 September 1996*: 289–314.
- Bonnet S. 2009. Shrinking and splitting of drainage basins in orogenic landscapes from the migration of the main drainage divide. *Nature Geoscience* **2**: 766–771. DOI: 10.1038/ngeo666

 Modelling Geomorphic Systems: Landscape Evolution 18

- Bonnet S, Crave A. 2006. *Macroscale dynamics of experimental landscapes*. Geological Society, London, Special Publications **253**: 327–339. DOI: 10.1144/GSL.SP.2006.253.01.17
- Booth AM, Roering JJ, Rempel AW. 2013. Topographic signatures and a general transport law for deep-seated landslides in a landscape evolution model. *Journal of Geophysical Research: Earth Surface* **118**: 603–624. DOI: 10.1002/jgrf.20051
- Bras RL, Tucker GE, Teles V. 2003. Six myths about mathematical modeling in geomorphology. In *Prediction in geomorphology*, Wiley-Blackwell.
- Braun J, Robert X, Simon-Labréteau T. 2013. Eroding dynamic topography. *Geophysical Research Letters* **40**: 1494–1499. DOI: 10.1002/grl.50310
- Braun J, Cambridge M. 1997. Modelling landscape evolution on geological time scales: a new method based on irregular spatial discretization. *Basin Research* **9**: 27–52. DOI: 10.1046/j.1365-2117.1997.00030.x
- Braun J, Simon-Labréteau T, Murray KE, Reiners PW. 2014. Topographic relief driven by variations in surface rock density. *Nature Geoscience* **7**: 534–540. DOI: 10.1038/ngeo2171
- Braun J, Voisin C, Gourlan AT, Chauvel C. 2015. Erosional response of an actively uplifting mountain belt to cyclic rainfall variations. *Earth Surface Dynamics* **3**: 1–14. DOI: 10.5194/esurf-3-1-2015
- Braun J, Willett SD. 2013. A very efficient O(n), implicit and parallel method to solve the stream power equation governing fluvial incision and landscape evolution. *Geomorphology* **180–181**: 170–179. DOI: 10.1016/j.geomorph.2012.10.008
- Braun J, Zwart D, Tomkin JH. 1999. A new surface-processes model combining glacial and fluvial erosion. *Annals of Glaciology* **28**: 282–290. DOI: doi:10.3189/172756499781821797
- Brazier R. 2004. Quantifying soil erosion by water in the UK: a review of monitoring and modelling approaches. *Progress in Physical Geography* **28**: 340–365.
- Brocklehurst SH, Whipple KX. 2006. Assessing the relative efficiency of fluvial and glacial erosion through simulation of fluvial landscapes. *Geomorphology* **75**: 283–299. DOI: 10.1016/j.geomorph.2005.07.028
- Bunte K, Abt SR, Potyondy JP, Ryan SE. 2004. Measurement of Coarse Gravel and Cobble Transport Using Portable Bedload Traps. *Journal of Hydraulic Engineering* **130**: 879–893. DOI: 10.1061/(ASCE)0733-9429(2004)130:9(879)
- Burbank DW, Anderson RS. 2011. *Tectonic Geomorphology*. 2nd ed. Wiley-Blackwell.
- Castelltort S, Goren L, Willett SD, Champagnac J-D, Herman F, Braun J. 2012. River drainage patterns in the New Zealand Alps primarily controlled by plate tectonic strain. *Nature Geoscience* **5**: 744–748. DOI: 10.1038/ngeo1582
- Chapuis M, Dufour S, Provansal M, Couvert B, De Linares M. 2015. Coupling channel evolution monitoring and RFID tracking in a large, wandering, gravel-bed river: Insights into sediment routing on geomorphic continuity through a riffle–pool sequence. *Geomorphology* **231**: 258–269.
- Clevis Q, Tucker GE, Lock G, Lancaster ST, Gasparini N, Desitter A, Bras RL. 2006. Geoarchaeological Simulation of Meandering River Deposits and Settlement Distributions: A Three-Dimensional Approach. *Geoarchaeology* **21**: 843–874. DOI: DOI:10.1002/gea.20142
- Colberg JS, Anders AM. 2013. Numerical modeling of spatially-variable precipitation and passive margin escarpment evolution. *Geomorphology* **207**: 203–212. DOI: 10.1016/j.geomorph.2013.11.006
- Collins DBG, Bras RL. 2004. Modeling the effects of vegetation-erosion coupling on landscape evolution. *Journal of Geophysical Research* **109**: 1–11. DOI: 10.1029/2003JF000028
- Coulthard T, Kirkby M, Macklin M. 1996. A cellular automaton landscape evolution model. *Proceedings of the 1st International Conference on Geocomputation*, University of Leeds.
- Coulthard TJ. 2001. Landscape Evolution Models: a software review. *Hydrological Processes* **173**: 165–173.

- Coulthard TJ, Hancock GR, Lowry JBC. 2012a. Modelling soil erosion with a downscaled landscape evolution model. *Earth Surface Processes and Landforms* **37**: 1046–1055. DOI: 10.1002/esp.3226
- Coulthard TJ, Kirkby MJ, Macklin MG. 2000. Modelling geomorphic response to environmental change in an upland catchment. *Hydrological Processes* **14**: 1920–1934.
- Coulthard TJ, Macklin MG, Kirkby MJ. 2002. A cellular model of Holocene upland river basin and alluvial fan evolution. *Earth Surface Processes and Landforms* **27**: 269–288. DOI: 10.1002/esp.318
- Coulthard TJ, Neal JC, Bates PD, Ramirez J, de Almeida GAM, Hancock GR. 2013. Integrating the LISFLOOD-FP 2D hydrodynamic model with the CAESAR model: implications for modelling landscape evolution. *Earth Surface Processes and Landforms* **38**: 1897–1906. DOI: 10.1002/esp.3478
- Coulthard TJ, Ramirez J, Fowler HJ, Glenis V. 2012b. Using the UKCP09 probabilistic scenarios to model the amplified impact of climate change on drainage basin sediment yield. *Hydrology and Earth System Sciences* **16**: 4401–4416. DOI: 10.5194/hess-16-4401-2012
- Coulthard TJ, Wiel MJ Van De. 2006. A cellular model of river meandering. *Earth Surface Processes and Landforms* **31**: 123–132. DOI: 10.1002/esp.1315
- Coulthard TJ, Van De Wiel MJ. 2013. Climate, tectonics or morphology: What signals can we see in drainage basin sediment yields? *Earth Surface Dynamics* **1**: 13–27. DOI: 10.5194/esurf-1-13-2013
- Croissant T, Braun J. 2014. Constraining the stream power law: a novel approach combining a landscape evolution model and an inversion method. *Earth Surface Dynamics* **2**: 155–166. DOI: 10.5194/esurf-2-155-2014
- Culling WEH. 1960. Analytical Theory of Erosion. *The Journal of Geology* **68**: 336–344.
- Darvill CM. 2013. Cosmogenic nuclide analysis. In Cook SJ, Clark LE, and Nield JM (eds), *Geomorphological Techniques*.
- Dietrich WE, Bellugi DG, Heimsath AM, Roering JJ, Sklar LS, Stock JD. 2003. Geomorphic Transport Laws for Predicting Landscape Form and Dynamics. *Geophysical Monograph* **135**: 1–30. DOI: 10.1029/135GM09
- Dietze M. 2014. RCHILD-an R-package for flexible use of the landscape evolution model CHILD. *EGU General Assembly Conference Abstracts* **16**.
- Dunai TJ. 2010. *Cosmogenic Nuclides: Principles, concepts and applications in the Earth surface sciences*. Cambridge University Press.
- Egholm DL, Knudsen MF, Clark CD, Lesemann JE. 2011. Modeling the flow of glaciers in steep terrains: The integrated second-order shallow ice approximation (iSOSIA). *Journal of Geophysical Research* **116**: F02012. DOI: 10.1029/2010JF001900
- Egholm DL, Pedersen VK, Knudsen MF, Larsen NK. 2012. Coupling the flow of ice, water, and sediment in a glacial landscape evolution model. *Geomorphology* **141-142**: 47–66. DOI: 10.1016/j.geomorph.2011.12.019
- Gallay M. 2013. Direct Acquisition of Data: Airborne laser scanning. In Cook SJ, Clark LE, and Nield JM (eds), *Geomorphological Techniques*. British Society for Geomorphology.
- Gasparini NM, Tucker GE, Bras RL. 2004. Network-scale dynamics of grain-size sorting: Implications for downstream fining, stream-profile concavity, and drainage basin morphology. *Earth Surface Processes and Landforms* **29**: 401–421. DOI: 10.1002/esp.1031
- Gilbert GK. 1880. *Geology of the Henry Mountains*. US Geographical and Geological Survey, Washington, D.C.
- Gomez-Gesteira M, Rogers BD, Crespo AJC, Dalrymple R a., Narayanaswamy M, Domínguez JM. 2012. SPHysics—development of a free-surface fluid solver—Part 1: Theory and formulations. *Computers & Geosciences* **48**: 289–299. DOI: 10.1016/j.cageo.2012.02.029
- Goren L, Willett SD, Herman F, Braun J. 2014. Coupled numerical-analytical approach to landscape evolution modeling. *Earth*

Modelling Geomorphic Systems: Landscape Evolution	20
---	----

- Surface Processes and Landforms* **39**: 522–545. DOI: 10.1002/esp.3514
- van Gorp W, Temme A, Schoorl J. 2015. LAPSUS: soil erosion-landscape evolution model. *EGU General Assembly Conference Abstracts*. **17**.
- Grabowski RC. 2014. Measuring the shear strength of cohesive sediment in the field. In Cook SJ, Clark LE, and Nield JM (eds), *Geomorphological Techniques*. British Society for Geomorphology.
- Green DL. 2014. Modelling Geomorphic Systems: Scaled Physical Models. In Cook SJ, Clark LE, and Nield JM (eds), *Geomorphological Techniques*. British Society for Geomorphology.
- Grenfell MC. 2015. Modelling Geomorphic Systems: Fluvial. In Cook SJ, Clark LE, and Nield JM (eds), *Geomorphological Techniques*. British Society for Geomorphology.
- Hackney C, Darby SE, Leyland J. 2013. Modelling the response of soft cliffs to climate change: A statistical, process-response model using accumulated excess energy. *Geomorphology* **187**: 108–121. DOI: 10.1016/j.geomorph.2013.01.005
- Han J, Gasparini NM, Johnson JPL. 2015. Measuring the imprint of orographic rainfall gradients on the morphology of steady-state numerical fluvial landscapes. *Earth Surface Processes and Landforms* **40**: 1334–1350. DOI: 10.1002/esp.3723
- Han J, Gasparini NM, Johnson JPL, Murphy BP. 2014. Modeling the influence of rainfall gradients on discharge, bedrock erodibility, and river profile evolution, with application to the Big Island, Hawai'i. *Journal of Geophysical Research: Earth Surface* **119**: 1418–1440. DOI: 10.1002/2013JF002961
- Hancock GR, Coulthard TJ, Lowry JBC. 2015a. Predicting uncertainty in sediment transport and landscape evolution – the influence of initial surface conditions. *Computers & Geosciences*: 1–14. DOI: 10.1016/j.cageo.2015.08.014
- Hancock GR, J.B.C. L, Coulthard TJ. 2015b. Catchment reconstruction — erosional stability at millennial time scales using landscape evolution models. *Geomorphology* **231**: 15–27. DOI: 10.1016/j.geomorph.2014.10.034
- Hancock GR, Willgoose GR. 2002. The use of a landscape simulator in the validation of the Siberia landscape evolution model: Transient landforms. *Earth Surface Processes and Landforms* **27**: 1321–1334. DOI: 10.1002/esp.414
- Hancock GR, Willgoose GR. 2004. An experimental and computer simulation study of erosion on a mine tailings dam wall. *Earth Surface Processes and Landforms* **29**: 457–475. DOI: 10.1002/esp.1045
- Hasbargen LE, Paola C. 2003. How Predictable is Local Erosion Rate in Eroding Landscapes? *Prediction in Geomorphology*: 231–240. DOI: 10.1029/135GM16
- Hergarten S, Robl J, Stüwe K. 2015. Tectonic geomorphology at small catchment sizes – extensions of the stream-power approach and the χ method. *Earth Surf. Dynam. Discuss.*: 689–714. DOI: 10.5194/esurfd-3-689-2015
- Herman F, Braun J. 2008. Evolution of the glacial landscape of the Southern Alps of New Zealand: Insights from a glacial erosion model. *Journal of Geophysical Research* **113**: F02009. DOI: 10.1029/2007JF000807
- Hobley DE, Tucker GE, Adams JM, Gasparini NM, Hutton E, Istanbulluoglu E, Nudurupati S. 2013. Modeling impact cratering as a geomorphic process using the novel landscape evolution model Landlab. 868 pp. *AGU Fall Meeting Abstracts*.
- Hoey TB, Bishop P, Ferguson RI. 2003. Testing numerical models in geomorphology: how can we ensure critical use of model predictions? *Prediction in Geomorphology*: 241–256.
- Hooke RL. 2003. Predictive modeling in geomorphology: An oxymoron? *Prediction in geomorphology*: 51–61. American Geophysical Union.
- Hovius N, Stark CP, Allen PA. 1997. Sediment flux from a mountain belt derived by landslide mapping. *Geology* **25**: 231–234. DOI: 10.1130/0091-7613(1997)025<0231:SFFAMB>2.3.CO;2
- Howard AD. 1994. A detachment limited model of drainage basin evolution. *Water Resource Research* **30**: 2261–2285.
- Hutton CJ. 2012. Modelling Geomorphic Systems: Numerical Modelling. In Cook SJ, Clark LE, and Nield JM (eds), *Geomorphological Techniques*, Chap. 5, Sec. 6.12 (2016)

- Geomorphological Techniques*. British Society for Geomorphology.
- Jackson DWT, Bourke MC, Smyth TAG. 2015. The dune effect on sand-transporting winds on Mars. *Nature Communications* **6**: 8796. DOI: 10.1038/ncomms9796
- Jasak H, Jemcov A, Tukovic Z. 2007. OpenFOAM : A C++ Library for Complex Physics Simulations. *International Workshop on Coupled Methods in Numerical Dynamics* **m**: 1–20.
- Lague D. 2005. Discharge, discharge variability, and the bedrock channel profile. *Journal of Geophysical Research* **110**: F04006. DOI: 10.1029/2004JF000259
- Lague D. 2013. The stream power river incision model: evidence, theory and beyond. *Earth Surface Processes and Landforms*: **39**(1), 38–61. DOI: 10.1002/esp.3462
- Lancaster ST, Hayes SK, Grant GE. 2003. Effects of wood on debris flow runout in small mountain watersheds. *Water Resources Research* **39**. DOI: 10.1029/2001
- Madsen AT, Murray AS. 2009. Optically stimulated luminescence dating of young sediments: A review. *Geomorphology* **109**: 3–16. DOI: 10.1016/j.geomorph.2008.08.020
- Manning R, Griffith JP, Pigot TF, Vernon-Harcourt LF. 1890. *On the flow of water in open channels and pipes*.
- Martin Y, Church M. 2004. Numerical modelling of landscape evolution: geomorphological perspectives. *Progress in Physical Geography* **28**: 317–339. DOI: 10.1191/0309133304pp412ra
- Mellett CL. 2013. Luminescence Dating. In Cook SJ, Clark LE, and Nield JM (eds), *Geomorphological Techniques*. British Society for Geomorphology.
- Micheletti N, Chandler JH, Lane SN. 2015. Structure from Motion (SfM) Photogrammetry. In *Geomorphological Techniques*, Cook SJ, Clark LE, and Nield JM (eds). British Society for Geomorphology;
- Mudd SM. 2016. Detection of transience in eroding landscapes. *Earth Surface Processes and Landforms*. DOI: 10.1002/esp.3923
- Mudd SM, Attal M, Milodowski DT, Grieve SWD, Valters DA. 2014. A statistical framework to quantify spatial variation in channel gradients using the integral method of channel profile analysis. *Journal of Geophysical Research: Earth Surface* **119**: 138–152. DOI: 10.1002/2013JF002981
- Murray AB. 2007. Reducing model complexity for explanation and prediction. *Geomorphology* **90**: 178–191. DOI: 10.1016/j.geomorph.2006.10.020
- Murray AS, Wintle AG. 2000. Luminescence dating of quartz using an improved single-aliquot regenerative-dose protocol. *Radiation Measurements* **32**: 57–73. DOI: 10.1016/S1350-4487(99)00253-X
- Nearing M, Hairsine P. 2010. The Future of Soil Erosion Modelling. *Handbook of Erosion Modelling*: 389–397. DOI: 10.1002/9781444328455.ch20
- O'Callaghan JF, Mark DM. 1984. The extraction of drainage networks from digital elevation data. *Computer Vision, Graphics, and Image Processing* **27**: 247. DOI: 10.1016/S0734-189X(84)80047-X
- Oreskes N, Shrader-frechette K, Belitz K. 1994. Verification, Validation, in *Models Numerical and the Confirmation of Earth Sciences*. American Association for the Advancement of Science **263**: 641–646.
- Pasculli A, Audisio C. 2015. Cellular Automata Modelling of Fluvial Evolution: Real and Parametric Numerical Results Comparison Along River Pellice (NW Italy). *Environmental Modeling & Assessment*: 1–17.
- Passalacqua P, Porte-Agel F, Foufoula-Georgiou E, Paola C. 2006. Application of dynamic subgrid-scale concepts from large-eddy simulation to modeling landscape evolution. *Water Resources Research* **42**: 1–11. DOI: 10.1029/2006WR004879
- Pazzaglia FJ. 2003. Landscape evolution models. *Development of Quaternary Science* **1**: 247–274. DOI: 10.1016/S1571-0866(03)01012-1
- Pelletier J. 2013. Fundamental Principles and Techniques of Landscape Evolution Modeling. In *Treatise in Geomorphology*, Elsevier.
- Pelletier JD. 2004. Persistent drainage migration in a numerical landscape evolution model. *Geophysical Research Letters* **31**: 4–7. DOI: 10.1029/2004GL020802

 Modelling Geomorphic Systems: Landscape Evolution 22

- Pelletier JD. 2012. Fluvial and slope-wash erosion of soil-mantled landscapes: detachment- or transport-limited? *Earth Surface Processes and Landforms* **37**: 37–51. DOI: 10.1002/esp.2187
- Pelletier JD et al. 2015. Forecasting the response of Earth's surface to future climatic and land use changes: A review of methods and research needs. *Earth Future* **3**: 220–251. DOI: 10.1002/2014EF000290
- Raven EK, Lane SN, Ferguson R. 2010. Using sediment impact sensors to improve the morphological sediment budget approach for estimating bedload transport rates. *Geomorphology* **119**: 125–134.
- Raymo ME, Ruddiman WF. 1992. Tectonic forcing of Cenozoic climate. *Nature* **359**: 117–122.
- Rickenmann D, McArdell BW. 2007. Continuous measurement of sediment transport in the Erlenbach stream using piezoelectric bedload impact sensors. *Earth Surface Processes and Landforms* **32**: 1362–1378.
- Rosser NJ, Petley DN, Lim M, Dunning SA, Allison RJ. 2005. Terrestrial laser scanning for monitoring the process of hard rock coastal cliff erosion. *Quarterly Journal of Engineering Geology and Hydrogeology* **38**: 363–375.
- Rowan A V. 2011. Modelling Geomorphic Systems: Glacial. In Cook SJ, Clark LE, and Nield JM (eds), *Geomorphological Techniques*. British Society for Geomorphology.
- Schäuble H, Marinoni O, Hinderer M. 2008. A GIS-based method to calculate flow accumulation by considering dams and their specific operation time. *Computers & Geosciences*, **34**: 635–646. DOI: 10.1016/j.cageo.2007.05.023
- Schoorl JM, Sonneveld MPW, Veldkamp a. 2000. Three-dimensional landscape process modelling: the effect of DEM resolution. *Earth Surf. Process. Landforms* **25**: 1025–1034. DOI: 10.1002/1096-9837(200008)25:9<1025::AID-ESP116>3.0.CO;2-Z
- Schoorl JM, Temme AJAM, Veldkamp T. 2014. Modelling centennial sediment waves in an eroding landscape - catchment complexity. *Earth Surface Processes and Landforms* **39**: 1526–1537. DOI: 10.1002/esp.3605
- Schoorl JM, Veldkamp A. 2001. Linking land use and landscape process modelling: A case study for the Álora region (South Spain). *Agriculture, Ecosystems and Environment* **85**: 281–292. DOI: 10.1016/S0167-8809(01)00194-3
- Schumm SA. 1979. Geomorphic thresholds: the concept and its applications. *Transactions of the Institute of British Geographers*: 485–515.
- Seidl MA, Dietrich WE. 1992. The Problem of Channel Erosion into Bedrock. In *Functional Geomorphology*, Schmidt KH and de Ploey J (eds). Cremlingen-Destedt, Germany; 101–124.
- Simpson G, Schlunegger F. 2003. Topographic evolution and morphology of surfaces evolving in response to coupled fluvial and hillslope sediment transport. *Journal of Geophysical Research* **108**: 1–16. DOI: 10.1029/2002JB002162
- Skinner C, Coulthard TJ, Parsons D. 2015. Simulating tidal and storm surge hydraulics with a simple 2D inertia based model, in the Humber Estuary, U.K. *Estuaries, Coasts and Shelf Science* **155**: 126–136. DOI: <http://dx.doi.org/10.1016/j.ecss.2015.01.019>
- Smith MW. 2015. Direct acquisition of elevation data: Terrestrial Laser Scanning. In Cook SJ, Clark LE, and Nield JM (eds), *Geomorphological Techniques*. British Society for Geomorphology.
- Snyder NP, Whipple KX, Tucker GE, Merritts DJ. 2003. Channel response to tectonic forcing: field analysis of stream morphology and hydrology in the Mendocino triple junction region, northern California. *Geomorphology* **53**: 97–127. DOI: 10.1016/S0169-555X(02)00349-5
- Sólyom PB, Tucker GE. 2004. Effect of limited storm duration on landscape evolution, drainage basin geometry, and hydrograph shapes. *Journal of Geophysical Research* **109**: F03012. DOI: 10.1029/2003JF000032
- Stock JD, Dietrich WE. 2003. Valley Incision by Debris Flows: Evidence of a Topographic Signature. *Water Resour. Res.* **39**: 1089–1113. DOI: 10.1029/2001WR001057
- Stokes CR, Clark CD. 1999.

- Geomorphological criteria for identifying Pleistocene ice streams. *Annals of Glaciology* **28**: 67–74.
- Sweeney KE, Roering JJ, Ellis C. 2015. Experimental evidence for hillslope control of landscape scale. *Science*, **349**: 51–53.
- Tarboton DG. 1997. A new method for the determination of flow directions and upslope areas in grid digital elevation models. *Water Resources Research* **33**: 309. DOI: 10.1029/96WR03137
- Temme A, Schoorl JM, Claessens LFG, Veldkamp A, Shroder FS. 2013. Quantitative Modeling of Landscape Evolution. In *Quantitative Modeling of Geomorphology*, Elsevier; 180–200.
- Temme AJAM, Claessens L, Veldkamp A, Schoorl JM. 2011. Evaluating choices in multi-process landscape evolution models. *Geomorphology* **125**: 271–281. DOI: 10.1016/j.geomorph.2010.10.007
- Temme AJAM, Veldkamp A. 2009. Multi-process Late Quaternary landscape evolution modelling reveals lags in climate response over small spatial scales. *Earth Surface Processes and Landforms* **34**: 573–889.
- Tomkin JH. 2007. Coupling glacial erosion and tectonics at active orogens: A numerical modeling study. *Journal of Geophysical Research: Earth Surface* **112**: 1–14. DOI: 10.1029/2005JF000332
- Trucano T., Swiler L. 2006. Calibration, Validation, and Sensitivity Analysis: What's What. *Reliability Engineering and System Safety* **91**: 1331–1357.
- Tucker GE. 2004. Drainage Basin Sensitivity To Tectonic and Climatic Forcing : Implications of a Stochastic Model for the Role of Entrainment and Erosion Thresholds. *Earth Surface Processes and Landforms* **205**: 185–205. DOI: 10.1002/esp.1020
- Tucker GE, Bras RL. 2000. A stochastic approach to modeling the role of rainfall variability in drainage basin evolution. *Water Resources Research* **36**: 1953–1964.
- Tucker GE, Hancock GR. 2010. Modelling Landscape Evolution. *Earth Surface Processes and Landforms* **50**: 28–50. DOI: 10.1002/esp
- Tucker GE, Hobley DEJ, Hutton E, Gasparini NM, Istanbulluoglu E, Adams JM, Nudurupati SS. 2015. CellLab-CTS 2015: a Python library for continuous-time stochastic cellular automaton modeling using Landlab. *Geoscientific Model Development Discussions* **8**: 9507–9552. DOI: 10.5194/gmdd-8-9507-2015
- Tucker GE, Lancaster ST, Gasparini NM, Bras RL, Rybarczyk SM. 2001a. An object-oriented framework for distributed hydrologic and geomorphic modeling using triangulated irregular networks. *Computers & Geosciences* **27**: 959–973. DOI: 10.1016/S0098-3004(00)00134-5
- Tucker GE, Lancaster ST, Gasparini NM, Rafael L. 2001b. The Channel-Hillslope Integrated Landscape Development Model (CHILD). In *Landscape Erosion and Evolution Modelling*, Harmon RS and Doe WW (eds). Kluwer Academic - Plenum Publishers; 349–388.
- Tucker GE, Whipple KX. 2002. Topographic outcomes predicted by stream erosion models: Sensitivity analysis and intermodel comparison. *Journal of Geophysical Research* **107**: 2179. DOI: 10.1029/2001JB000162
- Turowski JM, Rickenmann D, Dadson SJ. 2010. The partitioning of the total sediment load of a river into suspended load and bedload: a review of empirical data. *Sedimentology* **57**: 1126–1146.
- Tye AM, Hurst MD, Barkwith A. 2013. Nene phosphate in sediment investigation. British Geological Survey, Nottingham.
- Vaaja M, Hyppä J, Kukko A, Kaartinen H, Hyppä H, Alho P. 2011. Mapping topography changes and elevation accuracies using a mobile laser scanner. *Remote Sensing* **3**: 587–600.
- Van De Wiel MJ, Coulthard TJ, Macklin MG, Lewin J. 2007. Embedding reach-scale fluvial dynamics within the CAESAR cellular automaton landscape evolution model. *Geomorphology* **90**: 283–301. DOI: 10.1016/j.geomorph.2006.10.024
- Van De Wiel MJ, Coulthard TJ, Macklin MG, Lewin J. 2011. Modelling the response of river systems to environmental change: Progress, problems and prospects for palaeoenvironmental reconstructions. *Earth-Science Reviews* **104**: 167–185. DOI:

- 10.1016/j.earscirev.2010.10.004
- Willett SD. 1999. Orogeny and orography: The effects of erosion on the structure of mountain belts. *Journal of Geophysical Research* **104**: 28957–28981.
- Willett SD, McCoy SW, Perron JT, Goren L, Chen C-Y. 2014. Dynamic reorganization of river basins. *Science* **343**: 1248765. DOI: 10.1126/science.1248765
- Willgoose G. 2005. Mathematical Modeling of Whole Landscape Evolution. *Annual Review of Earth and Planetary Sciences* **33**: 443–459. DOI: 10.1146/annurev.earth.33.092203.122610
- Willgoose G, Bras RL, Rodriguez-Iturbe I. 1994. Hydrogeomorphology modelling with a physically based river basin evolution model. *Process models and theoretical geomorphology*: 271–294.
- Willgoose G, Bras RL, Turbe IR-. 1991a. A Coupled Channel Network Growth and Hillslope Evolution Model 1. *Water Resources Research* **27**: 1671–1684.
- Willgoose GR, Bras RL, Rodriguez-Iturbe I. 1991b. Results from a new model of river basin evolution. *Earth Surface Processes and Landforms* **16**: 237–254.
- Willgoose GR, Hancock GR. 2011. Applications of Long-Term Erosion and Landscape Evolution Models. In *Handbook of Erosion Modelling*, John Wiley & Sons; 339.
- Williams RD. 2012. DEMs of Difference. In Cook SJ, Clark LE, and Nield JM (eds), *Geomorphological Techniques*. British Society for Geomorphology.
- Wilson J, Aggett G, Deng Y, Lam C. 2008. *Water in the Landscape: A Review of Contemporary Flow Routing Algorithms*. 213–236. Springer Berlin Heidelberg. DOI: 10.1007/978-3-540-77800-4
- Wobus C, Whipple KX, Kirby E, Snyder NP, Johnson J, Spyropoulos K, Crosby B, Sheehan D. 2006. Tectonics from Topography: Procedures, promise, and pitfalls. In *Tectonics, Climate, and Landscape Evolution: Geological Society of America Special Paper 218*, Willett SD, Hovius N, Brandon MT, and Fisher DM (eds). Penrose Conference Series; 55–74.
- Wong JS, Freer JE, Bates PD, Sear DA, Stephens EM. 2015. Sensitivity of a hydraulic model to channel erosion uncertainty during extreme flooding. *Hydrological Processes* **29**: 261–279. DOI: 10.1002/hyp.10148
- Yang R, Willett SD, Goren L. 2015. In situ low-relief landscape formation as a result of river network disruption. *Nature* **520**: 526–9. DOI: 10.1038/nature14354